

Copyright Warning & Restrictions

The copyright law of the United States (Title 17, United States Code) governs the making of photocopies or other reproductions of copyrighted material.

Under certain conditions specified in the law, libraries and archives are authorized to furnish a photocopy or other reproduction. One of these specified conditions is that the photocopy or reproduction is not to be “used for any purpose other than private study, scholarship, or research.” If a user makes a request for, or later uses, a photocopy or reproduction for purposes in excess of “fair use” that user may be liable for copyright infringement,

This institution reserves the right to refuse to accept a copying order if, in its judgment, fulfillment of the order would involve violation of copyright law.

Please Note: The author retains the copyright while the New Jersey Institute of Technology reserves the right to distribute this thesis or dissertation

Printing note: If you do not wish to print this page, then select “Pages from: first page # to: last page #” on the print dialog screen

The Van Houten library has removed some of the personal information and all signatures from the approval page and biographical sketches of theses and dissertations in order to protect the identity of NJIT graduates and faculty.

INFORMATION TO USERS

This manuscript has been reproduced from the microfilm master. UMI films the text directly from the original or copy submitted. Thus, some thesis and dissertation copies are in typewriter face, while others may be from any type of computer printer.

The quality of this reproduction is dependent upon the quality of the copy submitted. Broken or indistinct print, colored or poor quality illustrations and photographs, print bleedthrough, substandard margins, and improper alignment can adversely affect reproduction.

In the unlikely event that the author did not send UMI a complete manuscript and there are missing pages, these will be noted. Also, if unauthorized copyright material had to be removed, a note will indicate the deletion.

Oversize materials (e.g., maps, drawings, charts) are reproduced by sectioning the original, beginning at the upper left-hand corner and continuing from left to right in equal sections with small overlaps. Each original is also photographed in one exposure and is included in reduced form at the back of the book.

Photographs included in the original manuscript have been reproduced xerographically in this copy. Higher quality 6" x 9" black and white photographic prints are available for any photographs or illustrations appearing in this copy for an additional charge. Contact UMI directly to order.

UMI

A Bell & Howell Information Company
300 North Zeeb Road, Ann Arbor MI 48106-1346 USA
313/761-4700 800/521-0600

UMI Number: 9635194

**Copyright 1996 by
Mukherjee, Sudhi Ranjan**

All rights reserved.

**UMI Microform 9635194
Copyright 1996, by UMI Company. All rights reserved.**

**This microform edition is protected against unauthorized
copying under Title 17, United States Code.**

UMI
300 North Zeeb Road
Ann Arbor, MI 48103

ABSTRACT

DEVELOPMENT OF A MULTIVARIATE QSAR MODEL TO PREDICT DESORPTION OF HALOGENATED ALIPHATIC HYDROCARBONS FROM ACTIVATED SLUDGE SOLIDS

**by
Sudhi Ranjan Mukherjee**

Data collected from different wastewater treatment processes have provided statistically significant evidence that many toxic organic contaminants on EPA's list of priority pollutants concentrate several orders of magnitude greater than influent concentrations in industrial and municipal wastewater sludges. Because of the reversibility of sorption processes, it is possible for sorbed organic compounds to desorb at a later time, hence making disposal of these sludges a potential problem. Although a number of models have been developed to predict sorption parameters, they have all been based on empirically derived descriptors whose validity is seriously compromised by the variation in available data for these parameters. In this research study a reliable QSAR model based on theoretically derived molecular connectivity indexes has been developed to predict the release of halogenated aliphatic hydrocarbon compounds from activated sludge solids. Model development was conducted using a statistically designed training set of compounds. Sorption of halogenated aliphatics was observed to be a totally reversible process, which was modeled by a QSAR model based on the first order molecular connectivity index for activated sludge solids fractionated at a Relative Centrifugal Force (RCF) of 5000 x g.

**DEVELOPMENT OF A MULTIVARIATE QSAR MODEL TO PREDICT
DESORPTION OF HALOGENATED ALIPHATIC HYDROCARBONS FROM
ACTIVATED SLUDGE SOLIDS**

**by
Sudhi Ranjan Mukherjee**

**A Dissertation
Submitted to the Faculty of
New Jersey Institute of Technology
in Partial Fulfillment of the Requirements for the Degree of
Doctor of Philosophy**

Department of Civil and Environmental Engineering

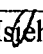
May 1996

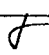
Copyright © 1996 by Sudhi Ranjan Mukherjee
ALL RIGHTS RESERVED

APPROVAL PAGE

DEVELOPMENT OF A MULTIVARIATE QSAR MODEL TO PREDICT DESORPTION OF HALOGENATED ALIPHATIC HYDROCARBONS FROM ACTIVATED SLUDGE SOLIDS


Sudhi Ranjan Mukherjee

Dr. Hsin-Neng Hsieh, Dissertation Advisor  Date _____
Professor of Civil and Environmental Engineering

Dr. Su Ling Cheng, Committee Member  Date _____
Professor of Civil and Environmental Engineering

Dr. Robert Dresnack, Committee Member _____ Date _____
Professor of Civil and Environmental Engineering

Dr. Somenath Mitra, Committee Member _____ Date _____
Assistant Professor of Chemical Engineering, Chemistry and Environmental Science

Dr. Dorairaja Raghu, Committee Member  Date _____
Professor of Civil and Environmental Engineering

BIOGRAPHICAL SKETCH

Author: Sudhi Ranjan Mukherjee
Degree: Doctor of Philosophy
Date: May 1996

Undergraduate and Graduate Education:

- Doctor of Philosophy in Civil Engineering
New Jersey Institute of Technology
Newark, New Jersey, 1996
- Master of Science in Civil Engineering
Iowa State University
Ames, Iowa, 1992
- Bachelor of Engineering in Civil Engineering
Osmania University
Hyderabad, India, 1990

Major: Civil Engineering

Presentations and Publications:

Mukherjee, S. R., Levine, A. D. and Barot, M. (1995). "Enumeration of Petroleum Hydrocarbon Utilizing Bacteria," Proceedings of the 50th Purdue Industrial Waste Conference, Purdue, USA.

Mukherjee, S. R. and Levine, A. D. (1993). "Evaluation Of Chemical Pretreatment Methods For Solubilization Of Particulate Organics," New Jersey Water Environment Association Conference, Atlantic City, New Jersey, USA.

Mukherjee, S. R. and Levine, A. D. (1992). "Chemical Solubilization Of Particulate Organics As A Pretreatment Approach," Water Science and Technology, vol. 5, pp. 2289-2292.

This dissertation is dedicated to my parents

ACKNOWLEDGMENT

At the very outset I would like to acknowledge my most sincere gratitude and appreciation for Dr. Hsieh's support and guidance through the most critical and trying times of this research study. Dr. Raghu's help in letting me use the Geo-Environmental Laboratory facilities for my research, and his faith in me served as an immense source of inspiration in carrying this work through to completion. I am grateful to Dr. Dresnack for his support, guidance and flexibility. I would also like to express sincere appreciation for the support extended to me by Dr. Cheng and Dr. Mitra. I would like to thank Ms. Wu for setting me up in the initial stages of this research and her continuing support. The moral support extended to me by our very witty and very adorable Chairperson, "Bill" Spillers - especially at a time when I was without an advisor, helped me in good measure. I would like to thank Dr. Levine for her foresight and guidance in developing this research study, and also for the many things I learned from her through my few years of association with her. I would like to acknowledge the help I received from Dr. Robert Boethling of the U.S. EPA who provided me with the software for calculating the molecular connectivity indexes. I would like to thank Mr. Eimess who fabricated the reactor and helped me on innumerable occasions. Also, Ms. Link and Ms. Hartlaub at the Civil Engineering offices who hold the whole act together, and all my fellow students from whom I learned so much. I would like to thank the university for supporting me with a research assistantship and partially funding this research. I would like to acknowledge the support from my family, and finally I thank my wife for her support and for bearing with me through this endeavor.

TABLE OF CONTENTS

Chapter	Page
1 INTRODUCTION.....	1
1.1 Research Objectives	4
2 BACKGROUND	6
2.1 Distribution of Priority Pollutants in Wastewater Solids	7
2.2 Sorption Processes in Wastewater Solids.....	10
2.3 Desorption Processes in Wastewater Solids.....	21
2.4 Measurement of Sorption-Desorption in Wastewater Solids	24
3 QUANTITATIVE STRUCTURE ACTIVITY RELATIONSHIPS (QSAR).....	31
3.1 Molecular Connectivity	33
3.2 Applications of Molecular Connectivity Indexes in QSAR Analysis	46
4 MODELING TECHNIQUES	53
4.1 Free Energy Models.....	54
4.2 Free Wilson Mathematical Model	57
4.3 Discriminant Analysis	59
4.4 Cluster Analysis.....	60
4.5 Principal Components and Factor Analysis.....	60
4.6 Pattern Recognition	62
4.7 Combined Multivariate Statistical Analysis	64
4.8 Selection of Training Set of Compounds	65

TABLE OF CONTENTS (Continued)

Chapter	Page
5 MATERIALS AND METHODS	84
5.1 Sources of Activated Sludge Solids.....	84
5.1.1 Laboratory Scale Activated Sludge Reactor with Recycle	85
5.1.2 Aerobic Sequencing Batch Reactor (ASBR).....	92
5.1.3 Pure Oxygen Process Activated Sludge	95
5.2 Centrifugal Fractionation of Activated Sludge Solids.....	97
5.3 Characterization of Activated Sludge Solids.....	100
5.4 Sorption-Desorption Experiments	105
5.5 Phase Separation at Higher RCFs.....	120
5.6 Calculation of Molecular Connectivity Indexes using GRAPHIII®	122
6 RESULTS AND DISCUSSION	123
6.1 Effect of RCF on Phase Separation Efficiency.....	123
6.2 Sorption Experiments	134
6.3 Desorption experiments.....	139
6.4 Model Development and Validation.....	142
6.5 Comparison with Other Models and Studies.....	150
6.6 Application of QSAR Model to a Secondary Wastewater Treatment Process.....	158
7 CONCLUSIONS AND RECOMMENDATIONS	165
APPENDIX A SORPTION AND DESORPTION ISOTHERMS	169

TABLE OF CONTENTS **(Continued)**

Chapter	Page
APPENDIX B SORPTION AND DESORPTION EXPERIMENTAL DATA	199
APPENDIX C SORPTION ISOTHERMS USING AZO DYE 151	229
APPENDIX D CONNECTIVITY INDEXES OF THE AX CLASS	233
REFERENCES	236

LIST OF TABLES

Table	Page
2.1.1. Concentration factors of some commonly occurring priority pollutants in municipal wastewater sludges.....	8
3.1. Some characteristics of QSAR in drug design and environmental sciences.....	33
3.1.1. Valence delta values for neutral third quantum level atoms and halogens.	43
3.2.1. QSAR models relating molecular connectivity indexes to biodegradation rates and extent of chemical compounds	51
4.8.1. Distribution of environmental organic chemicals into four major classes	71
4.8.2. Descriptor variables for a selected set of aliphatic hydrocarbons (AX Class)...80	80
4.8.3. Descriptor variables for selected halogenated aliphatic compounds	82
5.1.1.1. Composition of feed substrate used for the activated sludge process.....	89
5.1.1.2. Operational details of 20 L activated sludge reactor with recycle at equilibrium.	90
5.1.2.1 Operational characteristics of the Aerobic Sequencing Batch Reactor (ASBR.).....	95
5.3.1. Characterization of activated sludge solids before centrifugal fractionation of biosolids from different processes.....	104
5.3.2. Characterization of activated sludge solids prepared for sorption-desorption experiments.	104
5.3.3. Characteristics of organic material fractionated using filtration techniques.....	105
5.4.1. Frequency and methodology for different analytical determinations during the sorption and desorption studies.	119
5.4.2. Gas chromatographic conditions used for determination of target compounds.	120
6.2.1. Freundlich isotherms showing sorption behavior of compounds in the training set using biomass from two different unit operations.....	137

LIST OF TABLES (Continued)

Table	Page
6.2.2. Sorption capacities calculated using data from Freundlich isotherms for each compound in the training set of compounds.	138
6.3.1. Ratio of target compound initially present in the biomass to the aqueous phase concentration at the end of the experiment.	141
6.4.1. Statistical analysis of sorption data using multiple linear regression techniques.	143
6.4.2. Multiple linear regression analysis using molecular connectivity indexes and the partition coefficient, log K _p	147
6.4.3. Comparison of experimental biomass partition coefficients to estimated values.	148
6.4.4. Model validation by comparing predicted sorption capacities for dichloroethane and tribromofluoromethane to experimental values.....	149
6.4.5. Freundlich isotherms showing sorption behavior of compounds in the training set using biomass from different unit operations.....	149
6.5.1. Comparison of experimental and predicted biomass partition coefficient using biomass from a pure oxygen activated sludge treatment system.....	151
6.5.2. Freundlich isotherms showing sorption behavior of compounds in the training set using biomass from a pure oxygen treatment process.....	153
6.5.3. Comparison of estimated sorption coefficients for some halogenated aliphatics on activated sludge solids.	154
B.1. Sorption and desorption data for methylene chloride with biomass from activated sludge reactor with recycle.	199
B.2. Sorption and desorption data for methylene chloride with biomass from ASBR.	200
B.3. Sorption and desorption data for methylene chloride with biomass from pure oxygen activated sludge process.	201
B.4. Sorption and desorption data for trichloromethane with biomass from activated sludge reactor with recycle.	202

LIST OF TABLES (Continued)

Table	Page
B.5. Sorption and desorption data for trichloromethane with biomass from ASBR.	203
B.6. Sorption and desorption data for trichloromethane with biomass from pure oxygen activated sludge process.	204
B.7. Sorption and desorption data for trichlorofluoromethane with biomass from activated sludge reactor with recycle.	205
B.8. Sorption and desorption data for trichlorofluoromethane with biomass from ASBR.	206
B.9. Sorption and desorption data for trichlorofluoromethane with biomass from pure oxygen activated sludge process.	207
B.10. Sorption and desorption data for dichloroethane with biomass from activatedsludge reactor with recycle.	208
B.11. Sorption and desorption data for dichloroethane with biomass from ASBR....	209
B.12. Sorption and desorption data for dichloroethane with biomass from pure oxygen activated sludge process.	210
B.13. Sorption and desorption data for tetrachloroethane with biomass from activated sludge reactor with recycle.	211
B.14. Sorption and desorption data for tetrachloroethane with biomass from ASBR.	212
B.15. Sorption and desorption data for tetrachloroethane with biomass from pure oxygen activated sludge process.	213
B.16. Sorption and desorption data for bromoethane with biomass from activated sludge reactor with recycle.	214
B.17. Sorption and desorption data for bromoethane with biomass from ASBR.....	215
B.18. Sorption and desorption data for bromoethane with biomass from pure oxygen activated sludge process.	216
B.19. Sorption and desorption data for dibromoethane with biomass from activated sludge reactor with recycle.	217

LIST OF TABLES (Continued)

Table	Page
B.20. Sorption and desorption data for dibromoethane with biomass from ASBR. ...	218
B.21. Sorption and desorption data for dibromoethane with biomass from pure oxygen activated sludge process.	219
B.22. Sorption and desorption data for tribromofluoromethane with biomass from activated sludge reactor with recycle.	220
B.23. Sorption and desorption data for tribromofluoromethane with biomass from ASBR.	221
B.24. Sorption and desorption data for tribromofluoromethane with biomass from pure oxygen activated sludge process.	222
B.25. Sorption and desorption data for chloropropane with biomass from activated sludge reactor with recycle.	223
B.26. Sorption and desorption data for chloropropane with biomass from ASBR. ...	224
B.27. Sorption and desorption data for chloropropane with biomass from pure oxygen activated sludge process.	225
B.28. Sorption and desorption data for bromobutane with biomass from activated sludge reactor with recycle.	226
B.29. Sorption and desorption data for bromobutane with biomass from ASBR.	227
B.30. Sorption and desorption data for bromobutane with biomass from pure oxygen activated sludge process.	228
C.1. Adsorption isotherm for azo dye 151 using biomass from laboratory scale activated sludge reactor with recycle, dye concentration varied.	229
C.2. Adsorption isotherm for azo dye 151 using biomass from laboratory scale activated sludge reactor with recycle, dye concentration varied.	229
C.3. Adsorption isotherm for azo dye 151 using biomass from laboratory scale activated sludge reactor with recycle, dye concentration varied.	
C.4. Adsorption isotherm for azo dye 151 using biomass from laboratory scale activated sludge reactor with recycle, dye concentration varied.	230

LIST OF TABLES (Continued)

Table	Page
C.5. Adsorption isotherm for azo dye 151 using biomass from laboratory scale activated sludge reactor with recycle, dye concentration varied.	230
C.6. Adsorption isotherm for azo dye 151 using biomass from laboratory scale activated sludge reactor with recycle, dye concentration varied.	230
C.7. Adsorption isotherm for azo dye 151 using biomass from laboratory scale activated sludge reactor with recycle, solids concentration varied.	230
C.8. Adsorption isotherm for azo dye 151 using biomass from laboratory scale activated sludge reactor with recycle, solids concentration varied.	230
C.9. Adsorption isotherm for azo dye 151 using biomass from laboratory scale activated sludge reactor with recycle, solids concentration varied.	231
C.10. Adsorption isotherm for azo dye 151 using biomass from laboratory scale activated sludge reactor with recycle, solids concentration varied.	231
C.11. Adsorption isotherm for azo dye 151 using biomass from laboratory scale activated sludge reactor with recycle, solids concentration varied.	231
C.12. Adsorption isotherm for azo dye 151 using biomass from laboratory scale activated sludge reactor with recycle, solids concentration varied.	232
D.1. Molecular connectivity indexes calculated using GRAPH III©.	233

LIST OF FIGURES

Figure	Page
3.1.1. Structural formulae, graphs and connection matrices for different molecules. ..	35
3.1.3. Two bond fragmentation of the isopentane molecular skeleton.	39
3.1.4. Dissection of a molecule into different path fragments.	40
3.1.5. Assignment of δ values based on count of adjacent bonds.	41
3.2.1. Principle of QSAR analysis.	47
4.8.1. (a) Full factorial Design (FD) in three variables, 2^3 factorial design. (b) Fractional Factorial Design (FFD) in three variables, 2^{3-1} fractional factorial design.	70
4.8.2. Score plot of principal component 1 (t_1) against principal component 2 (t_2). ...	74
4.8.3. Score plot of principal component 1 (t_1) against principal component 3 (t_3). ...	75
4.8.4. Score plot of principal component 1 (t_4) against principal component 3 (t_3). ...	76
4.8.5. Loading plot of loading vector 1 (p_1) against loading vector 2 (p_2).	77
4.8.6. Loading plot of loading vector 1 (p_1) against loading vector 3 (p_3).	78
4.8.7. Loading plot of loading vector 4 (p_4) against loading vector 3 (p_3).	79
5.1.1.1. Schematic of 20 L activated sludge reactor with recycle.	87
5.1.2.1. Schematic showing the Aerobic Sequencing Batch Reactor (ASBR) setup.	93
5.1.3.1. Schematic of the pure oxygen activated sludge treatment facility operated by the Passaic Valley Sewerage Commissioners (PVSC).	96
5.2.1. Experimental protocol used for the centrifugal fractionation of biosolids from waste activated sludge.	98
5.3.1. Dissolved oxygen uptake rates measured for activated sludge solids as received from the different activated sludge processes at 20°C.	101

LIST OF FIGURES (Continued)

Figure	Page
5.3.2. Dissolved oxygen uptake rates measured for activated sludge solids from the different activated sludge processes at pH 3.0 and temperature 20°C.	102
5.3.3. Experimental protocol used for quantification of particle size distribution in WAS using filtration techniques.	103
5.4.1. Centrifugal separation of activated sludge solids at different RCFs at 20°C, water density=998.2 kg/m ³ , density of biomass=1050kg/m ³ , dynamic viscosity=0.001002 N.s/m ² , and settling velocity = 0.0012 m/s.	107
5.4.2. Freundlich isotherm developed for varying concentrations of substrate biosolids, azo dye concentration remaining constant.	111
5.4.3. Freundlich isotherm developed for varying concentrations of azo dye 151, substrate biosolids concentration remaining constant.	112
5.4.4. Kinetics of sorption of azo dye 151 on activated sludge solids. Concentration of azo dye is constant, biomass solids concentration varied.	114
5.4.5. Kinetics of sorption of azo dye 151 on activated sludge solids. Concentration of biomass solids is constant, azo dye concentration varied.	115
5.4.6. Experimental protocol used for quantifying sorption-desorption processes in activated sludge solids.	116
5.5.1. Experimental protocol used to evaluate the effect of using higher RCFs for phase separation on the determination of sorption-desorption parameters.	121
6.1.1. Effect of varying RCFs on the phase separation efficiency of a biosolids suspension at 20°C from a laboratory scale activated sludge reactor with recycle.	126
6.1.2. Effect of varying RCFs on the phase separation efficiency of a biosolids suspension at 20°C from an ASBR.	127
6.1.3. Effect of varying RCFs on the phase separation efficiency of a biosolids suspension at 20°C from a pure oxygen activated sludge process.	128

LIST OF FIGURES (Continued)

Figure	Page
6.1.4. Sorption of azo dye 151 onto activated sludge solids (PVSC) fractionated at 2000 x g. Biomass was collected from a pure oxygen activated sludge treatment system.	129
6.1.5. Sorption of azo dye 151 onto activated sludge solids (PVSC) fractionated at 20000 x g. Biomass was collected from a pure oxygen activated sludge treatment system.	130
6.2.1. Comparison of estimated sorption isotherms for the compounds in the training set using sorption capacities in Table 6.2.2 estimated at aqueous phase equilibrium concentrations of 2.5, 5, 10 and 20 mg/L, slope $n = 1$	136
6.4.1. Correlation between first order molecular connectivity index ($^1\chi$) and biomass partition coefficient ($\log K_p$).	145
6.4.2. Comparison between experimentally determined values and predicted value for the biomass partition coefficient.	146
6.5.1. Comparison between experimental and predicted biomass partition coefficient using biomass from a pure oxygen activated sludge treatment system (PVSC).	152
6.5.2. Correlation of experimentally determined biomass partition coefficient with soil sorption coefficient estimated from the Sabljic model.	155
6.5.3. Correlation of predicted biomass partition coefficient with biomass coefficient estimated from soil sorption coefficients for the AX class of halogenated aliphatic hydrocarbons.	156
6.6.1. Schematic showing potential use of QSAR models based on molecular connectivity indexes to predict the fate of halogenated aliphatic hydrocarbon compounds in a wastewater treatment plant.	160
A.1. Sorption isotherm for Methylene Chloride with biomass from activated sludge reactor with recycle. Desorbed concentrations of methylene chloride could not be determined.	169
A.2. Sorption isotherm for Methylene Chloride with biomass from ASBR. Desorbed concentrations of methylene chloride could not be determined.	170

LIST OF FIGURES (Continued)

Figure	Page
A.3. Sorption isotherm for Methylene Chloride with biomass from pure oxygen activated sludge process. Desorbed concentrations of methylene chloride could not be determined.....	171
A.4. Sorption and desorption isotherms for Trichloromethane with biomass from activated sludge reactor with recycle. Circles represent sorbed concentrations and crosses represent desorbed concentrations.....	172
A.5. Sorption and desorption isotherms for Trichloromethane with biomass from ASBR. Circles represent sorbed concentrations and crosses represent desorbed concentrations.	173
A.6. Sorption and desorption isotherms for Trichloromethane with biomass from pure oxygen activated sludge process (PVSC). Circles represent sorbed concentrations and crosses represent desorbed concentrations.	174
A.7. Sorption and desorption isotherms for Trichlorofluoromethane with biomass from activated sludge reactor with recycle. Circles represent sorbed concentrations and crosses represent desorbed concentrations.....	175
A.8. Sorption and desorption isotherms for Trichlorofluoromethane with biomass from ASBR. Circles represent sorbed concentrations and crosses represent desorbed concentrations.	176
A.9. Sorption and desorption isotherms for Trichlorofluoromethane with biomass from pure oxygen activated sludge process (PVSC). Circles represent sorbed concentrations and crosses represent desorbed concentrations.	177
A.10. Sorption and desorption isotherms for Dichloroethane with biomass from activated sludge reactor with recycle. Circles represent sorbed concentrations and crosses represent desorbed concentrations.....	178
A.11. Sorption and desorption isotherms for Dichloroethane with biomass from ASBR. Circles represent sorbed concentrations and crosses represent desorbed concentrations.	179
A.12. Sorption and desorption isotherms for Dichloroethane with biomass from pure oxygen activated sludge process (PVSC). Circles represent sorbed concentrations and crosses represent desorbed concentrations.	180

LIST OF FIGURES (Continued)

Figure	Page
A.13. Sorption and desorption isotherms for Tetrachloroethane with biomass from activated sludge reactor with recycle. Circles represent sorbed concentrations and crosses represent desorbed concentrations.....	181
A.14. Sorption and desorption isotherms for Tetrachloroethane with biomass from ASBR. Circles represent sorbed concentrations and crosses represent desorbed concentrations.	182
A.15. Sorption and desorption isotherms for Tetrachloroethane with biomass from pure oxygen activated sludge process (PVSC). Circles represent sorbed concentrations and crosses represent desorbed concentrations.	183
A.16. Sorption and desorption isotherms for Bromoethane with biomass from activated sludge reactor with recycle. Circles represent sorbed concentrations and crosses represent desorbed concentrations.....	184
A.17. Sorption and desorption isotherms for Bromoethane with biomass from ASBR. Circles represent sorbed concentrations and crosses represent desorbed concentrations.	185
A.18. Sorption and desorption isotherms for Bromoethane with biomass from pure oxygen activated sludge process (PVSC). Circles represent sorbed concentrations and crosses represent desorbed concentrations.	186
A.19. Sorption and desorption isotherms for Dibromoethane with biomass from activated sludge reactor with recycle. Circles represent sorbed concentrations and crosses represent desorbed concentrations.....	187
A.20. Sorption and desorption isotherms for Dibromoethane with biomass from ASBR. Circles represent sorbed concentrations and crosses represent desorbed concentrations.	188
A.21. Sorption and desorption isotherms for Dibromoethane with biomass from pure oxygen activated sludge process (PVSC). Circles represent sorbed concentrations and crosses represent desorbed concentrations.....	189
A.22. Sorption isotherm for Tribromofluoromethane with biomass from activated sludge reactor with recycle. Desorption concentrations could not be measured..	190

LIST OF FIGURES (Continued)

Figure	Page
A.23. Sorption isotherm for Tribromofluoromethane with biomass from ASBR. Desorption concentrations could not be measured.	191
A.24. Sorption isotherm for Tribromofluoromethane with biomass from pure oxygen activated sludge process (PVSC). Desorption concentrations could not be measured.	192
A.25. Sorption and desorption isotherms for Chloropropane with biomass from activated sludge reactor with recycle. Circles represent sorbed concentrations and crosses represent desorbed concentrations.....	193
A.26. Sorption and desorption isotherms for Chloropropane with biomass from ASBR. Circles represent sorbed concentrations and crosses represent desorbed concentrations.	194
A.27. Sorption and desorption isotherms for Chloropropane with biomass from pure oxygen activated sludge process (PVSC). Circles represent sorbed concentrations and crosses represent desorbed concentrations.....	195
A.28. Sorption and desorption isotherms for Bromobutane with biomass from activated sludge reactor with recycle. Circles represent sorbed concentrations and crosses represent desorbed concentrations.....	196
A.29. Sorption and desorption isotherms for Bromobutane with biomass from ASBR. Circles represent sorbed concentrations and crosses represent desorbed concentrations.....	197
A.30. Sorption and desorption isotherms for Bromobutane with biomass from pure oxygen activated sludge process (PVSC). Circles represent sorbed concentrations and crosses represent desorbed concentrations.....	198

CHAPTER 1

INTRODUCTION

Many toxic organic pollutants are present in influent municipal wastewater as a result of discharge from either industries or through the domestic discharge of consumer products. Toxic organic compounds have been detected in influents, effluents and sludges from many wastewater treatment facilities (Bell and Tsezos, 1988). Data collected from different wastewater treatment processes have provided statistically significant evidence that many of the toxic organic contaminants on the United States Environmental Protection Agency's (U.S. EPA) list of priority pollutants are concentrated several orders of magnitude greater than influent concentrations in municipal wastewater sludges (Petrasek *et al.*, 1983, U.S. EPA, 1984, Bell and Tsezos, 1988 and Dobbs *et al.*, 1986, 1989). Because of the reversibility of sorption processes, it is possible for organic compounds sorbed on to biological solids, to be desorbed under appropriate conditions at a later time, hence making disposal of these sludges a potential problem (Bell, 1987).

Estimates of the concentration of toxic organic compounds in sludge, and the rates and extent of release allow assessment of the impact of toxic organic compounds on sludge disposal options such as anaerobic digestion, land application, incineration and beneficial reuse. Sorption and desorption parameters are important properties of organic chemicals that are required in many scientific studies and engineering applications. From an environmental perspective, sorption and desorption processes are directly related to the steady state concentration of a chemical pollutant in its resident phase, which in turn would control the pollutant's toxicity, biosorption, bioavailability, etc., and transfer to

other phases. From an engineering point of view, knowledge of sorption and desorption parameters is a vital input in process and reactor design, plant operation, pollution control and management, and decision making (Govind *et al.*, 1991). In spite of such wide and critical applications, accurate partitioning data are scarce at best, and when available are inconsistent from one source to the other (Sabljić, 1989, 1992). In many instances, reported data are contradictory even for commonly occurring chemicals (Nirmalakhandan and Speece, 1989). Predictive models that have been developed in the past have related partitioning phenomena to other empirically measured or estimated parameters such as aqueous solubility, octanol-water partition coefficient, lipophilicity, etc. Since these empirically measured parameters on which these models are based are themselves very inconsistent, the reliability of partitioning coefficients calculated from such models is low (Sabljić, 1989, 1992). There is thus a need to develop predictive models based on parameters that are either consistent, or theoretically derivable. Models based on theoretically derivable parameters are desirable as they have zero intrinsic error, an important consideration in good model building.

Quantitative Structure Activity Relationship (QSAR) models based on molecular connectivity indexes are investigated in this study as a tool to estimate sorptive and desorptive processes in biological wastewater treatment. Mathematical models that relate physical, chemical, biological or environmental activity to quantitative structural descriptors or physicochemical properties are collectively known as QSAR models (Reddy and Locke, 1994). QSAR models are usually developed for groups of compounds with similar structure, based on the premise that the variations in the activity within a series of similar structures can be correlated with changes in parameters which reflect

molecular properties. The primary objective is to predict the activities of untested, structurally similar compounds using statistically derived multivariate models. Thus far, molecular connectivity indexes have been shown to be the most successful structural property for describing and predicting soil sorption coefficients, association coefficients with dissolved humic substances, Henry's law constants, solubility constants, bioconcentration factors in aquatic organisms and vegetation, biodegradation rates and fish acute toxicity (Sabljic, 1992). The development of highly accurate and reliable predictive relationships between environmental behavior and structural data of xenobiotics makes possible accurate assessments on environmental profiles of chemicals that are proven, potentially hazardous, or even chemicals that are in the conceptual stages of design and development from solely structural information.

This research study is directed towards developing a predictive QSAR model using molecular connectivity indexes and a statistically designed training set of halogenated aliphatic hydrocarbon compounds. Halogenated aliphatic hydrocarbon compounds were chosen for this proposed study as they are widely used in industrial processes, and are known to be a serious problem in wastewater treatment and sludge disposal. The ability to estimate rapidly and accurately the environmental fate and transport of a large number and variety of chemicals based on models developed by testing only statistically designed training sets of representative compounds promises enormous savings of material and human resources. The use of a statistically designed training set of compounds for model development reflects an innovative method of experimental design, and promises immense efficiency in developing statistically reliable models. The sorption-desorption model(s) developed through this proposed study will

provide a scientific basis for regulatory agencies, industries, municipalities, and other facilities involved in wastewater treatment (municipal or industrial) and sludge disposal to better evaluate the potential for concentration and subsequent release of contaminants from activated sludge solids.

1.1 Research Objectives

A review of the literature indicates that there is only limited data available relevant to the behavior of priority pollutants, especially aliphatic hydrocarbons in water pollution control systems. This research study aims at providing information relevant to the experimental determination and model development for the prediction of sorption and desorption processes observed in different secondary treatment plant activated sludge solids. The objective of the present work is to examine the sorptive and desorptive capacity of a statistically selected training set of halogenated aliphatic hydrocarbons using solids from different activated sludge unit processes under controlled experimental conditions. The specific objectives of this research study include

1. Quantifying the sorption-desorption processes for halogenated aliphatic hydrocarbon compounds using activated sludge solids from two different laboratory scale activated sludge unit processes. The data collected from this study will be validated using activated sludge collected from a municipal wastewater treatment plant. The use of sludge from these treatment systems which have different physical, chemical and

biological characteristics, primarily influenced by the nature of operation of the treatment systems, provides a strong basis for model building and statistical validity.

2. Development of a statistically robust predictive model to estimate contaminant desorption using multivariate QSAR techniques to relate sorptive and desorptive behavior of halogenated aliphatic hydrocarbons to molecular connectivity indexes. Molecular connectivity indexes provide structural information about the topology and three dimensional aspects of a molecule. Since these indexes are theoretically derived based on specific atoms, their arrangement in space, and bonding, they form a very fundamental basis for model development.
3. Exploring possible ways of integration with other QSAR models and/or databases to predict fate processes such as solubility, volatilization, biodegradation, etc. This research study aims at augmenting a variety of highly successful QSAR models based on molecular connectivity indexes that have already been developed to estimate fate parameters in soil and sediment matrices. Cross correlations, if any, between models developed for soil and sediment and those obtained from this experimental study for biological sludges could potentially help estimation of behavior of contaminants in activated sludge solids based on already available soil and sediment data.

CHAPTER 2

BACKGROUND

Partitioning of toxic organic compounds influence the steady state concentration of a chemical pollutant and its fate and transport in the environment. Since interphase partitioning phenomena influence the removal of organics from the bulk aqueous flow in wastewater treatment plants, quantitative and qualitative information about the sorption and desorption processes would enable the prediction of accumulation and subsequent release of toxic organic compounds, provide a basis for modeling the process, and correlate sorption-desorption evidenced to other physical, chemical and microbiological processes. Present laws in the United States, and in an increasing number of countries globally, require that all chemicals be assessed for their environmental behavior and potential hazards. Human and material resources currently are insufficient to obtain and verify experimentally even basic information about the fate and transport of these chemicals in the environment. Hence, it is necessary to develop quantitative models that will accurately and rapidly predict environmental behavior for large sets of compounds.

In recent years there has been increased interest in the behavior and fate of organic contaminants during wastewater treatment processes. The release of toxic and potentially hazardous organic compounds, especially from the 114 organic compounds identified by the U.S. EPA as priority pollutants, to the environment has become an issue of concern in the past few years. The biorefractory nature of such pollutants, their toxicity and consequent need for the implementation of hazardous substances control have prompted many researchers to investigate the fate of toxic organic compounds in the environment.

It has been shown that many of the toxic organic compounds that enter a conventional biological wastewater treatment system with domestic and industrial wastewater inflow, accumulate several orders in magnitude as compared to the initial influent wastewater concentration in the microbial biomass without significant biodegradation occurring (Tsezos and Seto, 1986). Studies have also shown that microbial cells tend to concentrate pollutants from their aquatic environment and release these organic compounds at a later point in time (Rogers *et al.*, 1989, Petrasek *et al.* 1983, Patterson and Kodukala, 1981, Tsezos 1983, 1986).

2.1 Distribution of Priority Pollutants in Wastewater Solids

Limited information is available on the occurrence, concentration or distribution of halogenated aliphatic hydrocarbons in biological sludges from wastewater treatment plants in the United States. Most of the organic pollutants are present in municipal wastewaters at relatively low concentrations of less than 10 µg/L, although certain compounds have been detected at much higher concentrations (Petrasek *et al.*, 1983). A comprehensive study was conducted by the U.S. EPA in 1984 to study the fate of priority toxic pollutants in Publicly Owned Treatment Works (POTWs) (U.S. EPA, 1984). While other studies have been conducted to study the fate of toxic organics in POTWs, this particular study by the U.S. EPA appears to be the most comprehensive, and a good resource for information related to a wide range of priority pollutants and treatment processes (U.S. EPA, 1984, Petrasek *et al.*, 1983, Rogers *et al.*, 1989, Dobbs *et al.*, 1986,

Tsezos 1989). A review of this research study clearly indicates that contaminants concentrate several orders of magnitude greater than their influent concentrations in biological sludges. In many instances it was observed that even though concentrations of some priority pollutants was below the detection limit in the effluent wastewater, their concentrations in biological sludges was far greater than permissible values (U.S. EPA, 1984). The concentration factors of some commonly occurring priority pollutants are summarized in Table 2.1.1.

Table 2.1.1. Concentration factors of some commonly occurring priority pollutants in municipal wastewater sludges (U.S. EPA, 1984).

Pollutant	Avg. Inflow Conc.	Avg. Sludge Conc.	Conc. Factor ¹
1,2-Trans-Dichloroethylene	7 µg/L	984 µg/L	140.6
Di-n-butyl-phthalate	9 µg/L	608 µg/L	67.6
Butyl benzyl phthalate	12 µg/L	809 µg/L	67.4
Naphthalene	7 µg/L	373 µg/L	53.3
Ethylbenzene	22 µg/L	418 µg/L	19.0
Phenol	54 µg/L	899 µg/L	16.7
Benzene	20 µg/L	131 µg/L	6.6

¹ Concentration Factor = Average sludge conc. (µg/L)/ Average inflow conc. (µg/L)

A number of different mechanisms have been proposed as being potentially responsible for the accumulation of organics by microbial biomass (Patterson and Kodukala, 1981, Tsezos, 1986). Adsorption has, however, been shown to be the primary mechanism through which organic compounds are accumulated by microbial biomass (Tsezos, 1986). Unlike heavy metals, relatively little is known about the range and concentration of synthetic organic chemicals that enter sewage treatment works, the efficiency with which they are degraded or removed during treatment, or their typical concentration in sewage sludge and treated effluent (Rogers *et al.*, 1989). The uptake or

accumulation of chemicals by microbial biomass has been termed biosorption, although a variety of other terms have also been used in the literature. The mechanism responsible for biosorption has been shown to be complex and among others involves sorption (adsorption and absorption) into various components of the microbial cell and subsequent partitioning (Tsezos and Bell, 1989).

Organic chemicals in sewage may be present in true solution, in colloidal fractions, or sorbed onto particulate material. During different unit operations in a sewage treatment facility, some organic contaminants that are resistant to physical, chemical or microbial degradation during their contact period with a particular treatment scheme, partition onto sludge solids as a consequence of their hydrophobic or lipophilic character (Rogers *et al.*, 1989, Petrasek *et al.*, 1983). Knowledge of the subsequent fate of these organic contaminants following disposal of contaminated sludge solids is important if a balanced view of their overall impact on the environment is to be gained. The sorption of hazardous organic pollutants by microbial biomass may complicate the management and disposal of waste sludge from municipal or industrial wastewater biological treatment plants. Sludge that may have accumulated hazardous organics could potentially release them back into the environment depending on the sludge disposal option implemented. On the other hand, sorptive processes could be viewed as being potentially beneficial in the concentration and removal of trace organics from the aqueous phase, making the aqueous phase amenable to other treatment schemes or reuse. Whichever way one likes to look at the sorptive-desorptive processes, it is important to quantify the process so that an engineered sludge and wastewater management process can be successfully implemented.

2.2 Sorption Processes in Wastewater Solids

Sorption of hydrophobic compounds on biomass is one of the fundamental processes controlling the transfer of toxic organic compounds from the aqueous phase to the solid phase. The extent of accumulation of toxic organic compounds through biosorption onto wastewater solids not only affects the efficiency of the treatment system, but also impacts the management of residual wastewater solids and sludges. However, the understanding of sorption processes in wastewater treatment remains poor. Information in the literature remains scant on the mechanisms of uptake of toxic organic compounds by wastewater solids (Wang and Govind, 1993). Most published reports on sorption of toxic organic compounds on wastewater solids only correlate the experimental data using empirical equations such as the Freundlich or the Langmuir equations. Few authors address the mechanistic aspects of sorption-desorption processes, and whenever information is available in the literature there appears to be no consensus regarding the exact mechanism of uptake of toxic organic compounds by microbial biomass. Little effort has been made to relate sorptive properties to the nature of wastewater solids, and even fewer studies address the desorption issue.

Sorption and desorption processes not only affect a chemical's mobility, but also are dominant factors in other fate related processes such as bioconcentration, bioavailability and biodegradation, etc. A review of the literature shows that there is ambiguity in the way biosorption is defined and measured. Adsorption, partitioning,

sorption and biosorption have been most commonly used in the literature to describe the uptake of target compounds by biomass (U.S. EPA, 1984, Petrasek *et al.*, 1983, Rogers *et al.* 1989, Dobbs *et al.*, 1986, Tsezos, 1989). This ambiguity can be attributed primarily to the lack of complete understanding of the actual process of uptake observed in biological wastewater treatment systems. Since uptake by biomass is a complex process involving many different mechanisms, in this research study sorption or biosorption will be used interchangeably to describe this process.

The current state of the understanding of sorption processes in biological wastewater treatment systems is that sorption of toxic organic compounds on wastewater solids consists primarily of two processes: (i) sorption of the toxic organic compound(s) from the bulk liquid onto the sludge surface, and (ii) partitioning of the toxic organic compound (s) between the aqueous phase and the organic matter in the sludge (Wang and Govind, 1993). Wastewater solids, particularly activated sludge, contain a high percentage of organic matter (50 - 85%) in a relatively loose physical form (Wang and Govind, 1993, Wang, 1993). It is generally believed that the organic matter in activated sludge solids is a complex mixture of live and dead microorganisms which can be represented by a simple cell. A typical procaryotic cell is composed of the cell wall, cell membrane, nucleus, nucleolus, ribosomes, etc., which are basically different forms of fats, proteins and carbohydrates that may sometimes resemble organic solvents (Wang and Govind, 1993). This permits the molecules of toxic organic compounds to dissolve and penetrate into the cell and distribute in the cell wall and the interior. Essentially, the uptake of toxic organic compounds by biological sludge through dissolution into the cells can be viewed as a partitioning process in which the target compounds are distributed

between two phases: the aqueous solution and the organic matter of the cell. A similar approach has been reported in the literature for describing partitioning phenomenon of toxic organic compounds onto other bacteria, soil and sediment (Wang and Govind, 1993). Tsezos and Bell showed that the majority of the pollutant uptake by biomass is located in the cell interiors, although an appreciable amount of the uptake was found in the cell wall and cell membrane (Tsezos and Bell, 1989).

It is understood that the greatest extent of sorption occurs on the cell wall and the cell membrane (Tsezos and Bell, 1989). The cell wall is a rigid structure outside the cell membrane which provides support and protection to the cell. The cell wall is usually a mono layer which is responsible for the strength of the cell wall, although some bacteria may have multiple layers. The cell wall is essentially made up of a layer of peptidoglycan composed of two sugar derivatives: *N-acetylglucosamine*, and *N-acetylmuramic acid*, and a small group of other amino acids. These constituents are connected to form a repeating structure (Brock and Madigan, 1991). Unlike the cell membrane, the cell wall is relatively permeable to small molecules. Proteins called *porins* are present in the cell wall which serve as membrane channels for the entrance and exit of low molecular weight substances. The largest *porins* allow entry of substances up to molecular weight 5000 (Brock and Madigan, 1991).

The cell membrane, sometimes called the plasma membrane, is a thin structure that completely surrounds the cell. This membrane is 8 nm thick, and serves as a critical barrier separating the inside of the cell (the cytoplasm) from its environment. If the membrane is broken, the integrity of the cell is destroyed, the internal contents of the cell leak into the environment, and the cell dies. The cell membrane is also a highly selective

barrier, enabling a cell to concentrate specific metabolites and excrete waste materials. An analysis of the structure of the cell membrane for a typical procaryotic cell shows that the matrix is composed of phospholipids, with the hydrophobic groups directed inwards and the hydrophilic groups towards the outside where they interact with the aqueous surroundings. Embedded in the matrix are hydrophobic proteins, while the hydrophilic proteins and other charged species such as metal ions are attached to the hydrophilic surfaces.

In a study conducted by Wang and Govind, the mechanism of partitioning was investigated by comparing the calculated surface area on activated carbon and activated sludge (Wang and Govind, 1993). It was shown that partitioning appears to be a part of the mechanism, while sorption onto sludge surface constitutes the other part. Since the majority of biological sludges is microorganisms which consist of cell walls and cell membrane encapsulating the inner components of the cell, molecules of toxic organic compounds must first permeate through the cell membrane to partition with the organic matter of the cell interior. In a membrane permeation process, the permeating molecules first sorb on the membrane surface then partition into and diffuse across the membrane (Wang and Govind, 1993). Similar mechanisms have also been reported by other researchers, describing sorption on bacteria as a rapid sorption process accompanied by slower diffusive penetration into the bacteria (Sugiura *et al.* 1975). The theory of sorption being a two stage process which consists of a rapid adsorption phase followed by a slower partitioning process described by the “two-box” model has been expressed by other researchers as well (Tsezos *et al.*, 1986, 1988, 1989, 1991, Wang, 1991). Hence the uptake of an organic pollutant by sludge is thought to be through a combination of

sorption and partitioning. When equilibrium is attained, the relative contribution to the overall uptake by sorption and partitioning depends on several factors such as surface area and affinity between pollutants and the organic matter in the biomass.

In a study conducted by Tsezos and Bell, sorption onto microbial cell walls isolated from *R. arrhizius* and activated sludge biomass was studied to understand the mechanism of biosorption (Tsezos and Bell, 1989). The basic premise of this study is that if the fraction of the total cell mass consisting of cell walls is known, the fraction of the biosorptive uptake attributed to cell walls can be determined from experimental uptake data for cell walls and whole cells. The fraction of the total uptake attributed to sorption onto the cell walls is given by (Tsezos and Bell, 1989):

$$F = \frac{U_w C_w}{U_t} \times 100 \quad (2.2.1)$$

where

F = fraction of total uptake attributed to sorption by cell walls, (%)

U_w = uptake by cell walls per unit mass of sorbent, (mg/g)

U_t = uptake by whole cells, (mg/g)

C_w = fraction of cells consisting of cell walls

The cell wall fraction in activated sludge has been determined experimentally to be 67.5% of the mass of the activated sludge cells (Tsezos and Bell, 1989). These values were found to be consistent with reported values for other types of cells. It was argued by the authors, Tsezos and Bell, that if the dominant mechanism for biosorption was sorption

onto the cell walls, as is the case for the biosorption of metal ions, the cell walls would be expected to display higher uptake capacity than whole cells (Tsezos and Bell, 1989). It was observed however that cell walls showed lower uptake than the respective dead cells. It was observed that for live activated sludge biomass cell walls, about 50% of the total uptake by the cell was attributed to uptake by cell walls, as estimated by equation (2.2.1). It was found that the fraction of pollutant accumulated by the cell walls was less than that expected if the cell walls were responsible for biosorption alone, suggesting that other parts of the cell are responsible for a substantial part of the observed uptake (Tsezos and Bell, 1989). The fraction of the total uptake attributed to the sorption on cell walls was found to be greater in activated sludge (~ 50%) than in other types of cell walls (~ 20%).

There is no agreement among different researchers however on the effect of lipids concentration on the biosorptive uptake capacities of different cell types. While researchers such as Canton *et al.* have demonstrated that 13% of the uptake of α -hexachlorocyclohexane (α -HCH) occurred in the cell walls and 87% in the lipid fraction of algal cell, Tsezos and Seto have reported that the lipid contents of cells are not related to the biosorptive capacity of cells (Canton *et al.*, 1977, Tsezos and Seto, 1986). Based on the examination of results reported in the literature, it can be inferred that the uptake, biosorption, involves both uptake by the cell walls and by other cellular components (Canton *et al.*, 1977, Tsezos and Seto, 1986, Wang and Govind , 1993).

Sorption of organic chemicals in aquatic systems may be described by a sorption isotherm, which gives the relationship between a chemical's concentration in the particulate phase and in the aqueous phase. Sorption coefficients are often determined in batch experiments. A known amount of biomass (sorbent medium) is added to an

aqueous solution containing the target compound, and shaken for a period of time under controlled environmental conditions. Subsequently the sorption coefficients are determined from the ratio of the concentrations of the target compound in the solid and liquid phases (Scharp *et al.*, 1994). A review of the literature shows that Langmuir and Freundlich adsorption isotherm models have been widely used to fit organic uptake data by biosolids with success, while BET isotherms seldom seem to explain sorption phenomena in biomass adequately (Dobbs *et al.* 1986, Tsezos 1989). The Freundlich isotherm may be described as

$$\frac{x}{m} = K C_e^{\frac{1}{n}} \quad (2.2.2)$$

$$\log \left(\frac{x}{m} \right) = \log (K) + \frac{1}{n} \log C_e \quad (2.2.3)$$

where

$x = C_0 - C_e$, Concentration of target compound sorbed onto biomass, mg/L

C_0 = Initial concentration of target compound in aqueous phase, mg/L

m = Weight of sorbent material (biomass), g

K = Sorption coefficient

C_e = Equilibrium concentration of the target compound in the aqueous phase, mg/L

n = Empirical constant, slope of the linear isotherm

In Equation (2.2.2), both the value of K and $1/n$ give the sorption capacity as a function of the effluent concentration in the linearized form of this equation. Within a range, the sorption capacity is related to K and $1/n$, with higher K and $1/n$ indicative of greater sorption capacity. It should be noted here that while K is a linear function of the concentration, $1/n$ is an exponential function. That means, if the value of K is small and that $1/n$ is large (> 1), the sorption capacity is dependent on the equilibrium concentration. Conversely if K is large and $1/n$ is small (< 1), the sorption capacity is favored by a lower effluent concentration. In most wastewater situations encountered in the environment, the exponential coefficient is close to 1.

A theoretical adsorption model based on the assumption that the adsorbent surface is saturated when a monolayer of the target compound has been sorbed was developed by Langmuir (Tchobanoglous and Schroeder, 1985). The Langmuir isotherm may be described as

$$\frac{x}{m} = \frac{a b C_e}{1 + b C_e} \quad (2.2.4)$$

where

a = empirical constant

b = saturation coefficient, m^3/g .

x , m and C_e are as defined above

Selection of an appropriate adsorption model is made by fitting the adsorption isotherms to experimental data. Most researchers indicate that the Freundlich model

presents a better fit to observed sorption data than the Langmuir model (Wang, 1993). Sorption in biological systems has frequently been represented by the Freundlich equation or a linearized form as shown by Equation (2.2.3). In dilute systems typical of most environmental aquatic situations, the partition coefficient, sometimes also called as the “distribution coefficient”, K_p for sorption on wastewater solids can be defined as

$$K_p = \frac{C_a}{C_s} \quad (2.2.5)$$

where

C_a = concentration of contaminant in aqueous phase, mg/L

C_s = concentration of contaminant in solid phase, mg/L

It has been observed that the extent to which an organic compound partitions itself between the solid and aqueous phases is largely independent of the properties of the solids, especially when dealing with sorption processes evidenced in complex solids, such as biological wastewater sludges, soils and sediment (Dobbs *et al.*, 1986, Wang, 1993). Some researchers have used Total Organic Carbon (TOC) to normalize the sorption coefficient K_p . Once the sorption coefficient K_p has been determined for a particular kind of solids, it is divided by the percent organic carbon contained in the solids and multiplied by 100 to obtain K_{oc} . K_{oc} can be expressed as

$$K_{oc} = \frac{K_p}{\% \text{ TOC}} \times 100 \quad (2.2.6)$$

where

K_{oc} = sorption coefficient based organic carbon concentration, mg/g

As can be seen from the nature of the equations discussed above, the magnitude of calculated sorption coefficients would depend on the basis of their determination. Since there is no agreement about which basis should be used to express sorption capacities, the use of suspended solids is still a common practice (Wang, 1993). In his doctoral dissertation Wang states that the use of suspended solids is justified since suspended solids in biomass is directly proportional to the organic carbon content (Wang, 1993). However, that is not the case, and a review of the literature and practical experience shows that the ratio of TOC to Total Suspended Solids (TSS) can vary over a wide range depending on the biological unit process and influent wastewater characteristics (Tchobanoglous, 1991). Total Organic Carbon was used exclusively to express sorption and desorption capacities throughout this research study.

A wide variety of relationships and equations have been reported in the literature on prediction of partition coefficients of various compounds based on their octanol-water partition coefficients, combination of different expressions relating partition coefficients, molar volume, melting point, entropy of fusion and molecular structure-activity (Lyman and Rosenblatt, 1982). However, the utility of most methods is limited as they use experimentally or empirically established relationships based on statistically unreliable data as a basis for developing predictive models. This is evidenced in the wide variation in data available on partitioning coefficients reported for soil, sediment and biological sludge matrices (Dobbs *et al.*, 1986, Tsezos, 1989, Wang *et al.*, 1993). Dobbs *et al.* concluded that one correlation between K_{oc} and K_{ow} is valid for all types of wastewater

solids, i.e., primary, secondary, and digested sludge, even from different plants (Dobbs *et al.* 1986). From a study conducted on wastewater solids obtained from different treatment processes and different wastewater treatment plants, it was concluded that the correlation between K_{oc} (soil sorption coefficient) and K_{ow} (octanol-water partition coefficient) is valid for all types of wastewater solids, with a correlation coefficient $r = 0.99$ (Dobbs *et al.* 1986). The following relationship was obtained on wastewater solids and octanol-water partition coefficient :

$$\log K_p' = 1.14 + 0.58 \log K_{ow} \quad (2.2.7)$$

where

$$K_p' = \frac{K_{oc}}{C_e / 1000} \quad (2.2.8)$$

K_{oc} = soil sorption coefficient normalized for the TOC, mg/g

C_e = aqueous phase equilibrium concentration, mg/L

However the utility of such models are limited due to the lack of consistent data on octanol water partition coefficients. A similar inadequacy is observed in other models that have been developed using empirically derived parameters such as lipophilicity, bioconcentration factors, etc. There is need to develop quantitative relationships that can accurately predict sorption parameters based on information that is theoretically derivable and not subject to variation from one research study to the other. The objective of this research study is to develop such a relationship using theoretically derived parameters

called molecular connectivity indexes to predict the sorption and desorption potential of halogenated aliphatic hydrocarbons from activated sludge solids.

2.3 Desorption Processes in Wastewater Solids

Desorption may be defined as the reverse process of biosorption during which the sorbed compound establishes an equilibrium relationship with the aqueous phase (Wang, 1993). If the sorption process was completely reversible, then the isotherms of sorption and desorption would have the same coefficients and slopes. However, biosorption is sometimes not a completely reversible process as some organic molecules are irreversibly bound and are not available for release even though an externally oriented concentration gradient might exist. Thermodynamic parameters such as the sorption coefficients K_d (distribution coefficient) or K_{oc} are useful to fate models to the extent that sorption is reversible on a time scale that is short compared to the fate process under consideration (Pignatello, 1990). Although a major portion of the sorbate appears to react in a rapidly reversible manner, it is becoming increasingly clear that more complex non-equilibrium behavior is possible for a significant portion of the sorbed organic compounds. Certain compounds have long been known to exhibit hysteric isotherms which cannot always be attributed to experimental artifacts (Pignatello, 1990). In virtually all such cases, the sorbate appears to have a higher affinity for the solids (greater K_d) in the reverse direction (desorptive), than in the forward direction (sorptive) (Pignatello, 1990). In some cases the

desorption isotherm extrapolates to nonzero sorbed concentrations, implying an irreversible fraction (Pignatello, 1990).

Review of the literature shows that the desorption of toxic organic chemicals from biomass is a poorly understood phenomenon with conflicting reports on the reversibility of the process, experimental conditions, biomass characteristics, and methodology (Tsezos 1989, Wang *et al.*, 1993). In a study conducted by Wang *et al.*, it was concluded that the desorption of pentachlorobiphenyl (PCB) and tetrachlorobiphenyl from algae depended on the time of sorption exposure: desorption after one hour of exposure resulted in release of 96% of the contaminant, while desorption after 48 hours exposure released only 74% (Wang *et al.* 1993). Research into the sorption-desorption behavior of PCBs on sediment have indicated that sorption was wholly reversible (Gschwend and Wu, 1985). Similar conclusions were drawn by Tsezos and Bell using dead activated sludge biomass and *R. arrhizus* for certain pesticides (Tsezos and Bell, 1987, 1988). There is evidence to suggest that malathion may have been irreversibly sorbed on to microbial biomass in an experimental study conducted by Tsezos and Bell, although the authors state in later works that the mechanisms may not have been entirely biosorption (Tsezos and Bell, 1991). However, it has been pointed out by Tsezos and Wang that the extent of desorption is significantly influenced by the sorption time (Tsezos and Wang, 1991). Longer sorption times, or exposure to a target compound results in a greater fraction of the target compound being irreversibly bound to the microbial biomass (Tsezos and Wang, 1991).

Sorptive partitioning of organic compounds is often incompletely reversible on time scales relative to degradation and transport processes. Slowly reversible non

equilibrium behavior has been observed in several types of compounds including Polynuclear Aromatic Hydrocarbons (PAHs), Polychlorinated Biphenyls (PCBs), chlorinated benzenes and halogenated aliphatic hydrocarbons (Pignatello, 1990). Sorption reversibility can change with time and other factors that are poorly understood, and as a result desorption times up to years have been observed for certain soil-sediment systems (Pignatello, 1990). In field samples containing PAHs, soil fumigants and herbicides, only a small fraction of the total analyte was found to be reversibly sorbed when suspended in water over a period of days (Pignatello, 1990). Available evidence suggests that molecular diffusion within the matrix is a major reason for retarded desorptive equilibria. Many nonpolar molecules lacking interactive functional groups that can form specific bonds with the matrix can form slowly reversible fractions, desorption being retarded by molecular diffusion of molecules from remote locations in the absorbent matrix. Even Halogenated Aliphatic Hydrocarbons (HHCs) that are weakly hydrophobic and have low K_d values can generate such fractions (Pignatello, 1990). In a study with halogenated aliphatic hydrocarbons, it was concluded that the sorption of HHCs to soils or sediments generates small amounts of relatively immobile fractions, which increase nonlinearly with sorption equilibration time and concentration of the chemical in the medium (Pignatello, 1990).

Desorption kinetics have been expressed most often as the reverse of sorption coefficients, and determined using Freundlich or Langmuir isotherms. Lindqvist and Enfield expressed the desorption coefficient as a rearrangement of the original equation, Equation (2.2.5), describing the distribution of a target compound in the aqueous and solid phase through Equation (2.3.1).

$$\frac{X_e}{X_T} = \frac{1}{\frac{m}{V} K_p + 1} \quad (2.3.1)$$

where

X_e = desorbed target compound, mg

X_T = total target compound, mg

m = mass of suspended solids (sorbent matrix), g

V = volume of sample, mL

K_p = desorption coefficient, mg/g

In this research study desorption data is analyzed and treated in the same manner as the sorption experiment using the Freundlich isotherm to determine the desorption coefficients for the halogenated aliphatic hydrocarbons evaluated. The data analysis and derivation of desorption coefficients are discussed in detail in later chapters.

2.4 Measurement of Sorption-Desorption in Wastewater Solids

Little information is available on the rate of biosorption processes and the influence of other factors like the nature of biomass solids, temperature, initial pollutant concentration and physical and chemical characteristics of the pollutant (Tsezos and Wang, 1991). A standard, universally applied protocol for determination of the partition coefficient or

sorption and desorption capacity of wastewater solids for toxic organic compounds is not available in the current literature (Dobbs *et al.* 1986, 1995, Scharp *et al.* 1994, Tsezos *et al.* 1986, 1989, Crittenden *et al.*, 1986, Moretti and Neufeld, 1989). Reported literature on studies conducted by different investigators present inconsistent experimental protocol and sometimes even conflicting reports on (i) the effect of solids-water ratio on the partition coefficient, (ii) rate of attainment of equilibrium, and (iii) use of viable/active solids (biomass) versus the use of non-viable/inactivated solids.

A review of the literature provides grossly different equilibration times for different studies indicating perhaps that equilibrium time is influenced by solute, solvent and experimental conditions (Dobbs *et al.* 1986, Shimizu *et al.* 1992, Wang, 1991, 1993). Because sorption isotherms are parameters determined at equilibrium, it is a necessary condition to ascertain that equilibrium has been attained before measurements are made to obtain a mass balance. Insufficient equilibration times can result in an under estimation of sorption capacities, and thereby adversely influence any conclusions that may be inferred about the process, or about other related processes (Wang, 1993, Wilczak, 1988, Lindqvist and Enfield, 1992, Brusseau *et al.*, 1991, Wilmanski, 1990). In a study conducted by Herbes, it was observed that equilibrium conditions between an aromatic hydrocarbon (^{14}C -anthracene) in a suspension of inactivated yeast cells was attained in a matter of minutes (Herbes, 1977). A 60 minute equilibration time was observed in the case of PAHs and certain pesticides with activated sludge (Morreti and Neufeld, 1989, Tsezos and Bell, 1991). Other equilibration times have been reported to range between a few hours to days or sometimes weeks for target compounds ranging from dyes to pesticides using a variety of microbial cultures (Michaels and Lewis, 1985, Lindqvist and

Enfield, 1992, Gschwend and Wu, 1985, Wang and Korte, 1982, Tsezos *et al.*, 1987, 1991, Karickhoff, 1985). While there is no confirmed theory as to why different equilibration times are observed, sometimes even for apparently similar matrices, there is evidence to prove that intraorganic matter diffusion is responsible for non-equilibrium (Brusseau *et al.*, 1991). It is a general consensus, however, that if “sufficient” time is provided, equilibrium is not a critical consideration (Wang, 1993). Biomass used in sorption-desorption experiments can retain their original physical, chemical and biological characteristics only for a short duration of time, after which death, decay and cell lysis can significantly affect the experimental validity and purpose. From the above discussion it is clear that there is really no common ground for establishing a right equilibration time for sorption-desorption experiments, and that it would be best if an appropriate equilibration time were developed for this experimental study.

The effect of the ratios of solids to the aqueous phase, and solids to the aqueous phase concentration of the target compound remains an unresolved issue. It has been reported by some researchers that the equilibrium partition coefficient, K_p , decreases with increasing solids to water ratios, while others have suggested that there is no significant solids effect for a wide range of solids to water ratio (Wang, 1993). There is some evidence to show that the observed decrease in unit sorption, as the mass of available adsorbent per unit volume increases, is due to factors other than those related to the solids to water ratios (Voice and Weber, 1985). It has been suggested that the sorbate that is apparently dissolved can actually exist in a free state (truly dissolved) or be complexed by material which derives from the solid phase but which remains in solution after phase separation due to the inefficiencies in the separation methods (Wang, 1993). In an

experiment used to measure the partition coefficient for 1,3,6,8-Tetrachlorodibenzo-*p*-dioxin sorbed on to suspended sediment at concentrations ranging over 4 orders of magnitude, it was found that the partition coefficient was inversely related to the log of the suspended sediment concentration, but that the slopes were dependent on the method of solid liquid separation (Servos and Muir, 1989). It was concluded that a third phase, Dissolved Organic Carbon (DOC) can explain many observations of decreasing partition coefficient versus increasing suspended sediment concentrations (Voice and Weber, 1985, Servos and Muir, 1989). DOC from natural water and sewage has been observed to influence sorption of hydrophobic organic compounds due to either the formation of soluble complexes between hydrophobic compounds and dissolved organic matter and/or due to competition between various species of organic matter for surface adsorption sites (Hassett and Anderson, 1982). DOC and/or non settling particulate material remaining in the aqueous solution after centrifugation tends to over estimate the concentration of the target compound in the aqueous phase, and hence under estimate the partition coefficient. Research conducted by other researchers have also indicated that in most cases when a solids concentration effect was claimed, it could be probably explained by other factors and can not be considered as a true solids concentration effect, at least in the solids concentration ranges that are experienced in municipal wastewater treatment (Dobbs *et al.*, 1986, McKinley and Jenne, 1991). Since no consensus exists about the right solids to aqueous phase ratio, it was decided to experimentally evaluate the effect of different activated sludge solids and target compound concentrations on the sorption coefficients for this research study.

Another important issue in the conduct of sorption-desorption experiments using microbial biomass is the difficulty in coming up with an accurate mass balance that can be attributed only to sorption process of the target compound in the soluble phase. To achieve an accurate mass balance it is important to have an experimental protocol that can accurately account for removal mechanisms other than sorption, such as biological degradation, adsorption to reaction vessel and volatilization that may occur during the course of the experiment. While the effects of adsorption to reaction vessel and volatilization may be minimized and accounted for by using suitable control(s), and the use of completely filled reactors with zero head space, the impact of biodegradation/biotransformation of the target compound during the sorption-desorption experiments is a more difficult problem, and there is no method currently that can accurately quantify this process accurately enough without undermining the physical integrity of the microbial biomass.

When bioutilization and sorption uptake are occurring simultaneously, mass balance calculations are extremely difficult as shown in a study on the bioconcentration of different insecticides by yeast capable of utilizing the insecticides (Kumar *et al.*, 1989). Various processes have been reported in the literature about using inactivated solids as a control. The processes that are commonly used to generate these inactivated control solids do not serve as very good controls as they change the physical texture of the solids and hence their "sorption response" (Bell, 1987, Tsezos, 1989, Selvakumar, 1989). Some of the more popular techniques include, drying and powdering of microbial cells, freeze drying, autoclaving, cyanide treatment, mercury addition, etc. (Tsezos and Wang, 1991, Dobbs *et al.*, 1986, 1989, 1995). Most sorption-desorption experiments conducted to

evaluate sorption response in activated sludge biomass is done using dead cells as a means of controlling bioutilization of a target compound based on the premise that biosorption is a purely physical process even though this has been proven not to be the case by every researcher who has explored the mechanistic aspects of biosorption (Wang *et al.*, 1993). It was found in a study conducted to study the sorption behavior of chloroethanes, the sorption coefficients appeared to correlate better with organic matter (principally lipids) leached from the microbial cells during contact with the chloroethanes (Tsezos and Seto, 1986). It was found in this study that the principal source of the organics leached into solution was from the lysis of living cells on contact with the target compound and rupture of cells caused during the course of the sorption experiments (Tsezos and Seto, 1986). This would indicate that sorption parameters would be influenced by the activity of the biomass as lipids and other cytoplasmic material would be denatured through most of the inactivation processes used for the preparation of cell material for sorption experiments.

There are conflicting reports on the effect of inactivation on the uptake of target compounds by microbial biomass. A study conducted using live and dead samples of algae, *Chlorella fusca*, concluded that the uptake of PCBs by algal cells was purely a physico-chemical process (Wang *et al.*, 1982). While in another study conducted by Dobbs *et al.* using Methylene Blue dye as the target compound on sludge samples inactivated using different techniques, it was found that the determination of sorption coefficients was strongly influenced by the inactivation process used to prepare the biomass matrix (Dobbs *et al.*, 1986, 1989, 1995). While some authors ventured to make broad categorizations stating that for molecules which are not readily biodegradable

(Tsezos and Bell, 1989), the overall uptake by live biomass appears to be less than that of the same dead biomass, and the opposite for more readily biodegradable compounds, the basic problem still exists that there is no concrete evidence to prove any of the opinions for certain. The rate of desorption in an experiment using lindane as the target compound with activated sludge biomass was also found to depend on the activity of the microbial cells (Tsezos and Wang, 1991). The rate of lindane desorption was also found to be much slower in the case of active *R. arrhizus* fungi cells as compared to the dead ones (Tsezos and Wang, 1991). Based on available evidence, there is little doubt that there is significant difference between sorption observed in dead cells to those that have been relatively inactivated through other means (Tsezos and Wang, 1991, Dobbs *et al.*, 1986, 1989, 1995). It has been suggested in the literature that adjusting the pH to about 3.0 may effectively inhibit biological activity without significantly affecting the partitioning process for neutral and acidic compounds (Dobbs *et al.*, 1986). This research study used a phosphate buffer at pH 3.0 and a temperature of 20°C as the method of choice for controlling bioactivity.

CHAPTER 3

QUANTITATIVE STRUCTURE ACTIVITY RELATIONSHIPS (QSAR)

Information on environmental fate and adverse effects of pollutants are basic needs in environmental planning. Fate processes such as adsorption to sediment or biomass, chemical or microbial degradation, evaporation, etc. determine the concentration of a chemical that is accessible for uptake by biota from a specific environment (bioavailability). When rates of these processes are known, environmental fate modeling can supply an estimate of the availability of a target compound to a specific transport mechanism in the environment. Attempts have been made to estimate fate as well as effects of pollutants and correlate these observations to develop a predictive relationship. One of these estimation techniques is based on Quantitative Structure Activity Relationships (QSAR).

QSARs may be defined as the categorization of atoms or molecules systematically according to common features, called structure, and to relate these assignments to the values of measured properties (Gupta, 1987). A property or activity of a molecule is a characteristic which can be determined or measured. By subjecting a target compound to a form of energy, numerical values can be obtained. Repeated subjection of a molecule to such an assault yields numerical measurements which are highly reproducible. By defining the physical events underway in such a process, we can define the observations as a property. A profile of properties thus measured is characteristic to that atom or molecule under study. Thus every compound has a boiling point, molar refraction,

partition coefficient, density, etc. Information about its form or structure is not self evident from physical property measurements. The structure is inferred from these measurements because it is known that properties are a consequence of structure. However, in contrast to measured physical properties, the information associated with structure permits the visualization of an image of the molecule which can be manipulated, rearranged or altered in any manner and to any extent limited only by the imagination of the researcher (Kier and Hall, 1986).

Although, QSAR has been almost exclusively and extensively used in drug design and pharmaceutical research, recent research has shown that they may be used as effectively in modeling environmental fate processes (Sabljic 1987, Nirmalakhandan and Speece 1988, 1989). This may perhaps be explained by the similarity of underlying processes that give drugs their beneficial effects and environmental pollutants their adverse effects. However, there are some important differences in characteristics and approaches between using QSAR in pharmaceutical and environmental research, some of which are summarized in Table 3.1.

QSAR analysis describes the dependence of activity on structure and typically include several physical-chemical parameters, such as electronic (σ , pK_a), hydrophobic (π , P_{OW} , K_{OW}), and steric (E_s , MR) (Moore *et al.* 1989). Since the properties of a molecule are dependent on the nature of the independent atoms and their chemical bonds, a fixed relationship exists between topological indexes conveying information on bond types and bond characteristics, and properties exhibited by a molecule. These topological or structural indexes may be defined as a count of selected topological features such as number of skeletal atoms or bonds, the number of bonds or atoms of a given type, number

of double bonds, number of rings and other structural parameters. Molecular topology provides a rationale for correlating interactions between a molecule and its environment through molecular connectivity indexes, which are based on the graphical depiction of molecular structure and may be described by a set of numerical values (Kier and Hall, 1986).

Table 3.1. Some characteristics of QSAR in drug design and environmental sciences.

QSAR in drug design research	QSAR in environmental sciences
OBJECTIVES	
Optimize biological activity of drugs	Estimate rates of fate processes
Find new active lead compounds	Analyze Processes
CHARACTERISTICS	
Response in isolated systems	Whole organism response
Effects are specific and well defined	Net effects (mortality, growth, etc.)
Specific mechanism of action	Specific & non-specific mechanisms
Receptor is known in most cases	Receptor unknown in most cases
TECHNIQUES	
Hansch Approach	Hansch Approach
Multivariate Analysis	Multivariate Analysis
Computerized molecular modeling	Molecular modeling not applied

3.1 Molecular Connectivity

At the molecular level, structure may be defined by a few characteristics: (i) the total number of atoms, (ii) the number of different kinds of atoms, and (iii) the linking pattern or bonding scheme of the atoms. These three elements of structural information depict a molecule as a graphic structural formula. There are two general approaches to structure

description. In the first, the identities of atoms and their connections form one set of information about molecular structure called the “topology” of the molecule. The second includes various three dimensional aspects called “molecular topography”. Characteristics such as size, shape, volume, surface area, etc. can be directly explained by three dimensional molecular topography.

Generally the properties of a molecule are dependent upon three dimensional topography of the molecule, the geometry of which in turn depends on molecular topology (nature of the individual atoms and the bonded connections between them). Because of the relationship between bond types and characteristics such as bond strength, length and polarity, there are relationships between topology and properties. Hence, it is most useful to express molecular structure in terms of its molecular topology (Kier and Hall, 1986). The starting point in representing molecular structure, is the molecular skeleton, which in chemical graph theory is defined as the hydrogen suppressed graph. Figure 3.1.1 shows several molecular structure representations as molecular skeletons. Hydrogen atoms are shown only on heteroatoms to identify the functional groups associated with a molecule.

The most basic element in the molecular structure is the existence of a connection or a chemical bond between a pair of adjacent atoms. The whole set of connections can be represented in a matrix form, called the connectivity matrix. Once all the information is written in the matrix form, relevant information can be extracted. The number of connected atoms to skeletal atom in a molecule, called the vertex degree or valence, is equal to the number of σ bonds involving that atom, after hydrogen bonds have been suppressed.

Structural Formula	Graph	Connection Matrix
$\text{CH}_3\text{CH}_2\text{CH}_2\text{CH}_2\text{CH}_3$		$\begin{bmatrix} 0 & 1 & 0 & 0 & 0 \\ 1 & 0 & 1 & 0 & 0 \\ 0 & 1 & 0 & 1 & 0 \\ 0 & 0 & 1 & 0 & 1 \\ 0 & 0 & 0 & 1 & 0 \end{bmatrix}$
$\text{CH}_3\text{CH}(\text{CH}_3)\text{CH}_2\text{OH}$	OH	$\begin{bmatrix} 0 & 1 & 1 & 1 & 0 \\ 1 & 0 & 0 & 0 & 0 \\ 1 & 0 & 0 & 0 & 0 \\ 1 & 0 & 0 & 0 & 1 \\ 0 & 0 & 0 & 1 & 0 \end{bmatrix}$
$\text{CH}_3\text{CH}(\text{CH}_3)\text{OCH}_3$	O	$\begin{bmatrix} 0 & 1 & 1 & 1 & 0 \\ 1 & 0 & 0 & 0 & 0 \\ 1 & 0 & 0 & 0 & 0 \\ 1 & 0 & 0 & 0 & 1 \\ 0 & 0 & 0 & 1 & 0 \end{bmatrix}$
$\text{ClCH}(\text{CH}_3)\text{CH}_2\text{NH}_2$	Cl NH ₂	$\begin{bmatrix} 0 & 1 & 1 & 1 & 0 \\ 1 & 0 & 0 & 0 & 0 \\ 1 & 0 & 0 & 0 & 0 \\ 1 & 0 & 0 & 0 & 1 \\ 0 & 0 & 0 & 1 & 0 \end{bmatrix}$
$\text{CH}_2\text{CH}_2\text{CH}_2\text{CH}_2\text{CH}_2$		$\begin{bmatrix} 0 & 1 & 0 & 0 & 1 \\ 1 & 0 & 1 & 0 & 0 \\ 0 & 1 & 0 & 1 & 0 \\ 0 & 0 & 1 & 0 & 1 \\ 1 & 0 & 0 & 1 & 0 \end{bmatrix}$

Figure 3.1.1. Structural formulae, graphs and connection matrices for different molecules.

The number δ_i , for atom i , is equal to the number of non-zero elements in the connectivity matrix (row or column i). For example in the connectivity matrix for n-pentane in Figure 3.1.1, there are two 1's in row 3, that is $\delta_3 = 2$. It can be shown that the number of non-zero entries in the connectivity matrix is twice the number of bonds or connections in the molecular skeleton. A similar approach can be used to develop a distance matrix for topological distances in a molecule. However, a distance matrix has limited usage as some information is lost when cyclic structures are encountered. To explain the differences between observed properties for different isomers of alkanes, the relative degree of branching among alkanes was studied (Randic, 1975). In the alkane skeletons the degree of branching at each carbon, or the number of adjacent carbons, is a cardinal number associated with the carbon. Each carbon-carbon bond is describable by a pair of numbers, which are a count of the number of adjacent atoms linked to each carbon forming the bond. The higher the number in the set, the greater the branching found at one or the other carbon atom, or both, forming the bond. These bond description sets can be converted to a real number by raising the product of the atom adjacency values to -0.5 power. The sum of these numbers over all bonds in the molecule yields an index associated with each molecule. The greater the degree of branching in a molecule of an isomeric series, the lower the numerical value of the index. If the isopentane skeleton is considered, each carbon is assigned a cardinal number which is a count of all adjacent or bonded atoms, as shown in Figure 3.1.2. The molecule can then be dissected into bonds described by the adjacency numbers of the two atoms forming the bond as : (1,3), (1,3), (3,2), (2,1).

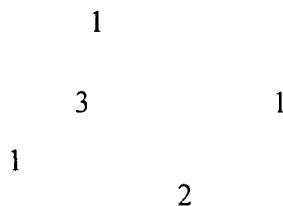


Figure 3.1.2. Isopentane skeleton showing the cardinal numbering scheme.

These bond descriptions are converted into a real number by taking the product within each parenthesis. The Randic index is derived by taking the reciprocal square root of this product (power of -0.5). The numbers are then summed up over all subsets to give a numerical value, a branching index (Randic Index) associated with this particular molecule.

$$\text{Randic Index} : -\frac{1}{\sqrt{(1.3) + (1.3) + (3.2) + (2.1)}} = 2.270$$

The Randic branching index correlates well with some properties in alkanes such as boiling points, Kovats constants and calculated surface areas (Kier and Hall, 1986). However, the Randic index does not describe adequately properties for chemical species with heteroatoms, double bonds, etc. A number of structure based studies have appeared since, incorporating and developing on the scheme originally proposed by Randic. Kier and Hall extended this method to consider unsaturation, heteroatoms, and extended bond analysis.

Kier and Hall developed a general method, “molecular connectivity”, leading to the calculation of indexes derived from molecular structure (Kier and Hall 1986). In the simplest form of the index, the structural formula is written down as a molecular skeleton in which all atoms are identical. Hydrogen atoms are suppressed and not included in the direct calculation of these indexes. The suppression of hydrogens does not result in the loss of any information as the number of hydrogens in the molecule attached to the skeletal carbons is related to the carbon valence minus the number of adjacent carbon

atoms. Each carbon atom is then designated by a cardinal number, as in the Randic scheme, called “ δ ”, the delta value. The molecular skeleton is then dissected into all constituent bonds, each designated by two carbons, i and j , forming the bond. Using the Randic algorithm, the index value can now be calculated as $(\delta_i \delta_j)^{-0.5}$. As shown in Equation (3.1.1), the molecular index, χ (chi), is then the simple sum of these bond values over the entire molecule; the prefix 1 indicates that the index is for a one bond dissection of the molecule.

$$^1\chi = \sum (\delta_i \delta_j)^{-0.5} \quad (3.1.1)$$

These indexes considered so far may be extended to heteroatom containing molecules by counting the heteroatoms just as adjacent carbon atoms. Hydrogens bonded to heteroatoms are suppressed. The delta value for an oxygen in an alcohol would be 1, in an ether it would be 2, and the connectivity index can be calculated as in the case of isopentane. In order to include more complex molecular structures, a scheme of extended indexes was proposed by Kier and Hall through the higher order dissection of the molecular skeleton (Kier and Hall, 1986). This scheme in its simplest form involves the dissection of the molecular skeleton into all “two contiguous bond” fragments. Figure 3.1.3 shows the two bond dissection of the isopentane molecular skeleton.

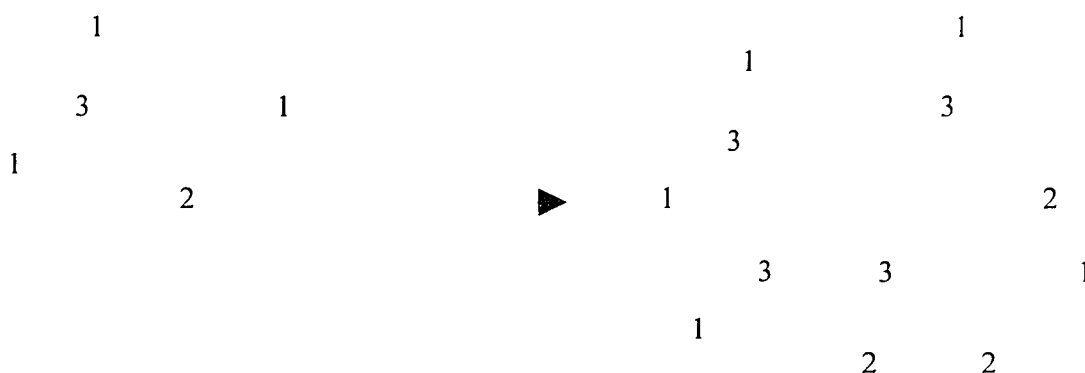


Figure 3.1.3. Two bond fragmentation of the isopentane molecular skeleton.

The index for the two bond dissection of the isopentane skeleton may be calculated using Equation (3.1.2). This index (${}^2\chi$) is called as the second order molecular connectivity index. The index is the sum of all four fragments : (1,3,1), (1,3,2), (1,3,2) and (3,2,1) as shown in Figure 3.1.3

$${}^2\chi = \sum (\delta_i \delta_j \delta_k)^{-0.5} \quad (3.1.2)$$

In the case of n-pentane, the molecule can be dissected into three two bond fragments, while the neopentane isomer can be dissected into six two bond fragments. It is evident here that a different pattern of structural information can be obtained with higher order indexes. Higher order molecular connectivity indexes are possible by the dissection of any molecule into all possible m-bond fragments to be calculated and summed to give an index, which may be represented as ${}^m\chi_p$, where p denotes a contiguous

path type of fragment. Potentially, as per graph theory, a molecule can be dissected into different commonly recurring structural features, as shown in Figure 3.1.4.

Path	Cluster	Path/Cluster	Chain
(2 nd order)	(3 rd order)	(4 th order)	(5 th order)

Figure 3.1.4. Dissection of a molecule into different path fragments.

The calculation of the index derived from each of these fragments in a molecule follows the same scheme as that adopted for the calculation of the other indexes (1st and 2nd order). For the isopentane molecule, the third order cluster index, ${}^3\chi_c$ can be calculated from the single fragment described by the delta values (1,3,1,2,1). The path/cluster index (4th order index), ${}^4\chi_{pc}$, calculated by considering the entire molecule as a single fragment with delta values of (1,3,1,2,1). When calculating indexes for molecules such as n-pentane which has neither the path/cluster nor the chain fragments, the respective indexes would equal zero. If a molecule is decomposed into fragments of atoms, the index calculated for such a molecule is called the zero order index, denoted by ${}^0\chi$ and defined as shown in Equation (3.1.3). This index, unlike the others relates to atoms and not bonds,

and describes the structure at the atomic level in terms of the number of adjacent atoms dictating the delta value.

$${}^0\chi = \Sigma(\delta)^{-0.5} \quad (3.1.3)$$

The primary limitation of the simple molecular connectivity index discussed so far is that the algorithm used to calculate the indexes are based on a count of the adjacent non-hydrogen atoms. As a result, the algorithm returns the same ${}^1\chi$ index values for both the saturated and unsaturated molecules as they have similar δ values. To get around this problem Kier and Hall proposed that the assignment of δ values be based on the explicit counting of each bond to an adjacent non-hydrogen atom (Kier and Hall, 1986). Hence, according to this theory a double bond would be counted twice when adding up adjacent atoms. As a comparison, Figure 3.1.5 shows the difference such a treatment of structure would make when butane and butadiene are considered as test examples.



Figure 3.1.5. Assignment of δ values based on count of adjacent bonds.

Such a procedure takes explicit account of the hybrid state of each carbon atom. This modified δ value is called valence delta, δ^v ; the calculation of index values based on valence deltas remains the same as in the other indexes. The indexes calculated based on

the valence delta are represented as, " χ_p^v " called valance chi of order n. The calculation of δ^v using such an approach would be through Equation (3.1.4).

$$\delta^v = Z^v - h \quad (3.1.4)$$

where

Z^v = number of valence electrons

h = number of hydrogen atoms suppressed

This theory was further enhanced by the development of an algorithm for the treatment of heteroatoms through the selection of specific delta values which reflect structural differences based upon an explicit count of the adjacent bonded atoms and a count of all pi and lone pair electrons. The valence delta values through such a treatment are expressions of the electronic structure of the skeletal atoms in a molecule. The simple delta is a count of the electrons in the sigma orbitals while the valence delta is a count of all valence electrons. When considering higher row atoms, specific account of the non-valence or core electrons needs to be taken as they strongly influence the atomic size and consequently influence other properties such as ionization potential and electron affinity. To take account of both valence and core electrons, the valence delta value can be written as Equation (3.1.5).

$$\delta^v = \frac{(Z^v - h)}{(Z - Z^v - 1)} \quad (3.1.5)$$

Table 3.1.1. Valence delta values for neutral third quantum level atoms and halogens.

Atom	$(Z^v - h)$	$(Z - Z^v - 1)$	$\delta^v = \frac{(Z^v - h)}{(Z - Z^v - 1)}$
P	3	9	0.33
	4	9	0.44
	5	9	0.56
S	5	9	0.56
	6	9	0.67
Cl	7	9	0.78
Br	7	27	0.26
I	7	47	0.16

It can be seen from the above equation that the valence delta value is a direct count of the valence electrons weighted by the core electrons, and is thus inversely related to the size of the atom. Valence delta values for a few neutral third quantum level atoms and halogens are shown in Table 3.1.1. From the discussion on molecular connectivity indexes, it is evident that specific molecular fragments are counted and encoded in the values calculated for the different indexes. Information about the presence and number of molecular fragments of a particular kind are contained in numerical value of a particular index. Indexes such as these can become the basis of relationships between molecular structure and physical, chemical or biological properties of a molecule. Molecular connectivity indexes have been shown to be rich in structural information related to topological, geometric and spatial attributes. The relative branching of a molecule is encoded in the ${}^1\chi$ index.

Standard statistical models are employed for QSAR analysis using molecular connectivity indexes. Simple linear as well as multiple linear models may be used (Kier and Hall, 1986). Simple non-linear cases may also be treated in the multiple linear

fashion (Kier and Hall, 1986). The molecular connectivity indexes provide the investigator with an array of quantitative descriptions of molecules, encoding information about molecular structure such as size, shape, branching, unsaturation and heteroatom content. Molecular connectivity indexes may be calculated for a variety of structural features. For molecules with a wide variety of structural features, the chi indexes afford great opportunity to find the best description of those structures and the mathematical correlation in the statistically determined QSAR model. Because of the wide variation of structural features encountered in biologically interesting molecules, many different chi indexes are possible. Simple indexes emphasize skeletal arrangement including branching and cyclization. The valence chi index encodes information about the specific nature of heteroatoms in a molecule. The choice of the chi indexes in the search for the best variables in a regression analysis is important. Chi indexes should not be included in a search when the numerical values are constant or zero for more than a few compounds. This criterion avoids the bias of chi indexes which are exclusively limited for a limited part of the compound list (Kier and Hall, 1986). A corollary to this rule is to select indexes which have a nonzero value for most of the compounds in the list. The valence indexes are included for study when heteroatoms are varied in a list of compounds. The same rule holds true if unsaturation or aromatic rings are predominant in a compound list (Kier and Hall, 1986). In the routine computation of chi indexes using a computer program such as GRAPHIII[®], a battery of indexes can be generated (Sabljić and Horvatic, 1993). Usually about 22 indexes are computed and stored in a computer file for subsequent analysis. These indexes include simple path, chain, path-chain and cluster as

well as their corresponding valence indexes. Depending on the structure of a molecule, certain higher order indexes may not be present.

Molecular connectivity description of a molecular structure gives rise to indexes of the general form ${}^m\chi_t$ or ${}^m\chi_t^v$, where m is the order of the molecular fragment, v indicates that the connectivity index takes into account the valence and t is the type. Molecular connectivity indexes are calculated from the non-hydrogen part of the molecule. Each hydrogen atom is described by its atomic delta value, which is equal to the number of adjacent non-hydrogen atoms. This index is described by the equation (Kier and Hall, 1986, Randic, 1975):

$${}^m\chi_t^v = \sum (\delta_i^v * \delta_j^v * \delta_k^v \dots \delta_{M+1}^v)^{-0.5} \quad (3.1.6)$$

Higher order indexes, such as, ${}^2\chi^v$, ${}^3\chi^v$ etc., are used to define the structural properties of the molecules through higher order dissection of the molecular skeleton into all possible bond fragments (m) to be calculated and summed to give an ${}^m\chi_p^v$ index, where the subscript "p" denotes a contiguous path type of fragment. Other types of fragmentation of the molecular structure include cluster ${}^m\chi_c^v$, path/cluster ${}^m\chi_{pc}^v$, and chain ${}^m\chi_{ch}^v$. Each of these indexes encode different information such as molecular volume and surface area, planar properties, 3-dimensional attributes such as conformation, structural analysis of substituted rings, degree of substitution, length and

heteroatom content, etc. The connectivity index is thus a method of encoding electronic, steric and branching information about a molecule in a simple reproducible combination of terms.

3.2 Applications of Molecular Connectivity Indexes in QSAR Analysis

Molecular structure and topological indexes aid in identifying structural features responsible for the fate and transport of toxic organic compounds at the molecular level, which has influenced their use in developing relationships that accurately predict a broad range of physico-chemical and biological responses, resulting in more consistent, statistically relevant and reliable models in recent years (Nirmalakhandan and Speece, 1988, Sabljic, 1987, 1992, 1995). The molecular connectivity indexes have been shown to be rich in structural information related to topological, geometric and spatial attributes (Kier and Hall, 1986). Information about different topological and geometric properties of a chemical structure are encoded in different molecular connectivity indexes. The relative degree of branching of a molecule is encoded in the $^1\chi$ index when compared to other structural isomers. This translates into encoding a molecular bulk or volume and surface area. The $^0\chi$ index encodes information about atoms or points, the $^2\chi$ index carries information about 3 atom fragments which are the minimum number necessary to describe a plane, while the $^3\chi_p$ index encodes information about three dimensional attributes such as conformation. The $^4\chi_{pc}$ index encodes information useful to the

structural analysis of substituted rings. Information such as degree of substitution, length and heteroatom content of these groups is contained in ${}^4\chi_{pc}$ and ${}^4\chi_{pc}^v$ indexes.

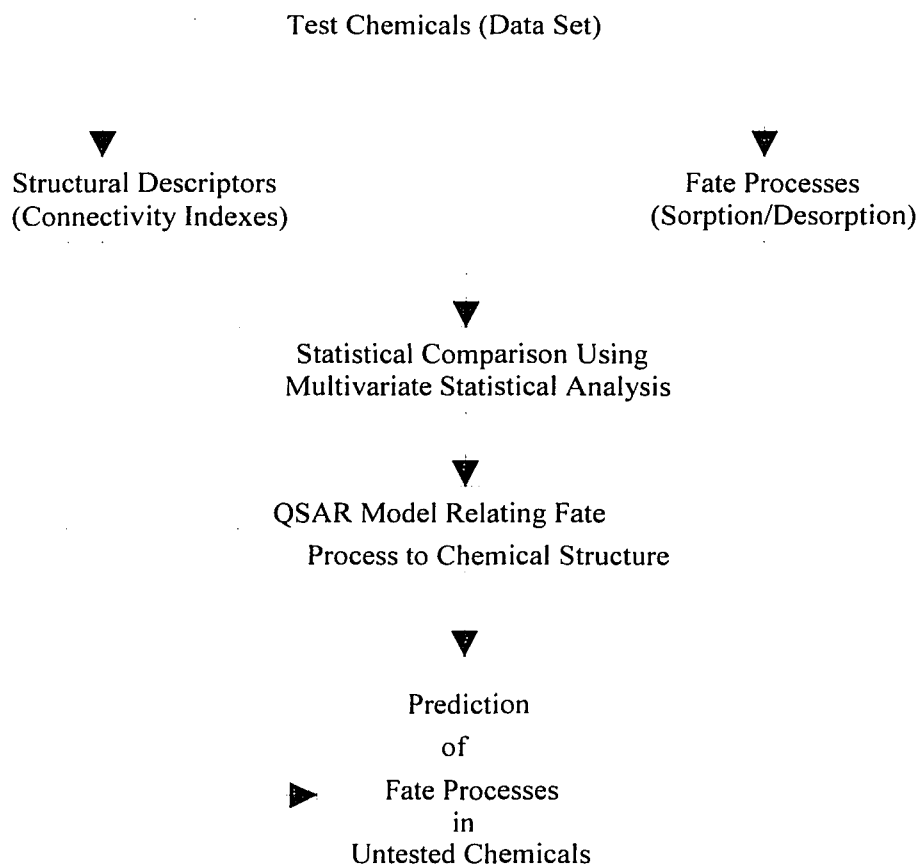


Figure 3.2.1. Principle of QSAR analysis.

As QSAR models use error-free descriptors (connectivity indexes) which are calculable purely from molecular structure, they have been used to successfully predict the properties of a number of compounds (Sabljic, 1987, Nirmalakhandan and Speece, 1988, 1989, Niemi *et al.*, 1992). QSAR models have been used to predict the aqueous

solubility, Henry's constant (Nirmalakhandan and Speece, 1988, Speece, 1992, Dunnivant and Eizerman, 1992), soil sorption coefficients of polycyclic aromatic hydrocarbons (PAHs), heterocyclic and substituted PAHs, polychlorinated biphenyls (PCBs), alkyl- and chlorobenzenes, halogenated alkanes and alkenes, and halogenated phenols (Sabljić, 1987), soil sorption coefficients, associated coefficients with dissolved humic substances, bioconcentration factors (BCFs) in aquatic organisms and vegetation, acute toxicities, applications in risk assessment, and biodegradation rates of phenols (Govers *et al.*, 1984, Boethling, 1986, Desai *et al.*, 1990, Mani *et al.*, 1991, Sabljic and Piver, 1992, Brusseau, 1993, Bintein and Devillers, 1994, Meylan and Howard, 1992, Reddy and Locke, 1995). Statistical validation of developed QSAR models demonstrate very good correlation between measured parameters ($r^2 > 0.9$) and very low standard deviations (0.2 to 0.3) for experiments conducted to evaluate soil sorption, ecotoxicological parameters used in risk assessment, biodegradation and other solute properties (Sabljić, 1987, Vaishnav *et al.*, 1987, Nirmalakhandan and Speece, 1988, 1989).

Molecular connectivity indexes have been extensively used in the recent years to predict soil sorption coefficients for a variety of organic substances (Meylan *et al.*, 1992, Sabljic *et al.*, 1995). The soil sorption coefficient ($\log K_{oc}$) provides an indication of the extent to which a chemical partitions between the solid and solution phases in soil, or between water and sediment in aquatic systems, and indicates whether a chemical is likely to leach through soil or be immobile. Compounds with higher $\log K_{oc}$ values will be less mobile than those with lower values. Although a large number of models have been used to predict soil sorption coefficients, Equation (3.2.1) is applicable to most classes of compounds and relates soil sorption coefficients $\log (K_{oc})$ to the first order

molecular connectivity index ($^1\chi$) and a fragment property contribution parameter ($\Sigma P_i N$), with $r^2 = 0.955$ and $SD = 0.21$ (Meylan *et al.*, 1992).

$$\log K_{oc} = 0.53 \ ^1\chi + 0.62 + \Sigma P_i N \quad (3.2.1)$$

Molecular connectivity indexes have been used to predict the aqueous solubility of a wide range of organic chemicals. Aqueous solubility is an important property of organic compounds that influences properties such as toxicity, biosorption, bioaccumulation, etc. (Nirmalakhandan and Speece, 1988, 1989, Speece, 1990). Solubility of a wide range of 470 chemical compounds has been successfully predicted using Equation (3.2.2) which relates solubility to a zero order simple molecular connectivity index ($^0\chi$) and a polarizability parameter (Φ), with a correlation $r^2 = 0.99$ and $SE = 0.33$ (Nirmalakhandan and Speece, 1989).

$$\log S = 1.543 + 1.638 \ ^0\chi + 1.003 \ \Phi \quad (3.2.2)$$

$$\Phi = 0.864 + 2.36 \ ^0\chi + 5.49 \ ^1\chi^v$$

Henry's constant of a wide range of compounds has also been predicted successfully using molecular connectivity indexes (Nirmalakhandan and Speece, 1988). The Henry's constant (H) of a compound dictates in which phase and how a chemical will tend to concentrate at equilibrium. Chemicals with a low H tends to accumulate in the aqueous phase, while those with a high H will partition more readily into the gaseous phase. The Henry's constant for a wide range of volatile compounds was estimated using

Equation (3.2.3), which relates H to the first order valence molecular connectivity index ($^1\chi^v$), polarizability parameter (Φ) and an indicator variable (I) (Nirmalakhandan and Speece, 1988).

$$\log H = 1.29 + 1.005 \Phi - 0.468 {}^1\chi^v - 1.258I \quad (3.2.3)$$

Biodegradation rates have also been successfully predicted using QSAR relationships. One such model is the AERobic Ultimate Degradation (AERUD) model which was developed by the U.S. EPA on the basis of collective judgment of 22 biodegradation experts as to the approximate time that might be required for complete aerobic biodegradation (Boethling and Sabljic, 1989). The AERUD model is described by Equation (3.2.4).

$$\text{AERUD} = 0.60 \ln {}^2\chi^v + 57.25 \frac{n \text{ Cl}}{M_w} + 17.56 \frac{{}^4\chi_{pc}}{M_w} + 1.45 \quad (3.2.4)$$

where

${}^2\chi^v$ = valence second order molecular connectivity index

${}^4\chi_{pc}$ = fourth order path-cluster molecular connectivity index

$n \text{ Cl}$ = number of covalently bound chlorine atoms

M_w = molecular weight of the compound

The AERUD model would calculate the ultimate aerobic biodegradation potential and assign a score to each chemicals as (i) days=1, (ii) weeks = 2, (iii) months = 3, and

(iv) longer = 4 (Boethling and Sabljic, 1989). A number of QSAR models have been developed successfully to predict the biodegradation rates and extent of a wide range of chemical compounds (Banerjee *et al.*, 1984, Moore *et al.*, 1989, Boethling, 1986, Sabljic and Piver, 1992, Brusseau, 1993, Bintein and Devillers, 1994, Meylan and Howard, 1992, Howard *et al.*, 1992, Reddy and Locke, 1995). Table 3.2.1 lists some of the QSAR biodegradation rate models that have been developed using molecular connectivity indexes (Moore *et al.*, 1989).

Table 3.2.1. QSAR models relating molecular connectivity indexes to biodegradation rates and extent of chemical compounds (Moore *et al.*, 1989).

Compound	QSAR Model	Correlation r^2
Phthalate Esters	$k_{\text{obs}} = 37.2 {}^2\chi + 547.5$	0.938
2,4-D Esters	$\log k_2 = 0.82 {}^2\chi^v - 11.93$	0.954
Carbamates	$\log \%D = 1.57 {}^4\chi_{\text{pc}} + 3.77$	0.971
Ethers	$\log \%ThOD = 0.52 {}^2\chi^v + 2.60$	0.974
Alcohols	$\% ThOD = -142 {}^4\chi_c - 32.2 {}^3\chi^v + 83.6$	0.904
Acids	$\% ThOD = -253 {}^4\chi_c - 22.0 {}^3\chi + 122$	0.961

Empirical models based on water solubility and n-octanol-water partition coefficients have been proposed as alternative accurate methods to estimate sorption coefficients (Sabljic, 1989, 1992). An analysis of these models show that the quality of these models suffer due to (i) low precision of water solubility and n-octanol/water partition coefficients and (ii) violations of statistical laws when these quantitative models were developed (Sabljic 1989). A non-empirical approach, as used in the development of QSAR models, provides a faster and less expensive means of determining empirical parameters, and offers the flexibility of being performed anywhere: office, laboratory, home or field. Lower production cost is a primary motive for trying to develop predictive

relationships between environmental behavior and structural data of xenobiotics. The other advantage is the higher accuracy of non-empirical parameters, which, by definition, have zero intrinsic error, making them ideally suitable within the rules of standard linear regression models. QSAR models represent the state of the art in modeling biological and chemical response to environmental perturbations. Through the integration and use of enormous computerized data bases that are available today on QSARs, the proposed research integrates well with an ever evolving and dynamic area of applied research, while carving a niche for itself in areas of fundamental research such as bioavailability and macromolecular transport.

CHAPTER 4

MODELING TECHNIQUES

The molecular shape of compounds influences biological activity, especially where enzymes and receptors are involved. Several research studies have been conducted to address the problem of finding a mathematical means to express differences in geometric features such as those evidenced in the measurement of both size (a bulk measure) and shape (vectorial quantity) of molecules. The first has been to find parameters suitable for use in the Hansch equation. Taft's E_s parameter or its variants derived from the acid and base hydrolysis rates of aliphatic esters has been most widely used (Topliss, 1983). Kier and Hall have adapted the molecular connectivity index χ for QSAR correlations, a number derived originally by Randic from graph theoretical principles to express the relative topology of variously branched hydrocarbon isomers (Kier and Hall 1986, Randic 1975). Many χ terms can be calculated for a given molecule, differing in the number of atoms taken together ($^n \chi$), and these may include or ignore the valence weighted indexes ($^n \chi_v$) for the specific atoms or bond types present. The various terms for the molecules of a series may be tested as parameters in the usual multiple regression correlation model (Kier and Hall 1986, Randic 1975).

Other approaches to expressing topological differences include treating the problem of directionality of steric effects by the direct expedient of modeling a substituent and calculating its extension in five orthogonal directions, the minimal steric difference method, etc. (Topliss, 1983). Other approaches that have been used to a limited

extent, include the use of quantum mechanical methods and molecular modeling techniques. A brief discussion about different modeling techniques used commonly is presented here. The various aspects of statistical analysis associated with multivariate data analysis for model development are also discussed briefly. A detailed methodology for some of the statistical methods employed is beyond the scope of this discussion, and hence details about some of the procedures have been referenced to their sources.

4.1 Free Energy Models

Among the first models proposed using QSAR methods is the one proposed by Hansch and co-workers (Topliss, 1983). It was the seminal contribution of this group to propose that the early observations of the importance of relative lipophilicity to biological potency into the useful formalism of Linear Free Energy Relationships (LFER) to provide a general model for QSAR in biological contexts. As a suitable measure of lipophilicity, the partition coefficient, $\log P$, between 1-octanol and water was proposed, and it was further demonstrated that this was roughly an additive and constitutive property and hence calculable in principal from molecular structure. Using a probabilistic model for transport across biological membranes, Hansch proposed the following equations (also called the Hansch Equation)

$$\log (1/C) = -k\pi^2 + k'\pi + \rho\sigma + k'' \quad (4.1.1)$$

$$\log (1/C) = -k(\log P)^2 + k'(\log P) + \rho\sigma + k'' \quad (4.1.2)$$

where

C = molar concentration (or dose) for a constant biological response (ED_{50} , LC_{50} , etc.)

π = substituent lipophilicity

$\log P$ = partition coefficient

σ = Hammett value for substituent electronic effect

k , k'' , ρ , and k''' = regression coefficients derived from statistical curve fitting

The reciprocal of the concentration reflects that higher potency is associated with lower dosage, and the negative sign for the π^2 or $(\log P)^2$ term reflects the expectation of an optimum lipophilicity. Multiple linear regression techniques may be used to determine these coefficients. A number of statistics are derived from such a calculation, which allow the statistical significance of the resulting correlation to be assessed. The most important of these are s , the standard error of the estimate (also called standard deviation), r^2 , the coefficient of determination or percentage of data variance accounted for by the model, F , a statistic for assessing the overall significance of the derived equation (statistical tables list critical values for the appropriate number of degrees of freedom and confidence level), and t values (also compared with statistical tables) and confidence intervals (usually 95%) for the individual regression coefficients in the equation. Also very important in multiparameter equations are the cross-correlation coefficients between the independent variables in the equation. These must be low to assure true “independence” or orthogonality of the variables, a necessary condition for meaningful results in multivariate linear regression models.

The applicability of Equation (4.1.1) to a broad range of biological structure activity relationships has been demonstrated convincingly by Hansch and associates and many others in the years since 1964 (Topliss, 1983). The success of this model led early to its generalization to include additional parameters. In attempts to minimize residual variance in such correlations, a wide variety of physicochemical parameters and properties, structural and topological features, molecular orbital indices, and for constant but for theoretically unaccountable features, indicator or “dummy” variables (1 or 0) have been employed. A wide spread use of Equation (4.1.1) has provided an important stimulus for the review and extension of established scales of substituent effects, and even for the development of new ones. It should be cautioned here however that the general validity or indeed the need for these latter scales has not been established.

Lipophilicity in particular, as reflected in partition coefficients between aqueous and non aqueous media, most commonly water (or aqueous buffer) and 1-octanol has received much attention. Log P for the octanol-water system has been shown to be approximately additive and constitutive and hence schemes for its *a priori* calculation from molecular structure have been devised using either substituent π values or substructural fragment constants (Topliss, 1983). The approximate nature of any partition coefficient has been frequently emphasized, and indeed, some of the structural features that cause unreliability have been identified and accommodated (Topliss, 1983). Other complications such as steric effects, conformational effects, and substitution at the active positions of hetero-aromatic rings have been observed but cannot as yet be accounted for completely and systematically (Topliss, 1983). Theoretical, statistical and topological methods to approach some of these problems have been reported (Topliss, 1983). The

observations of linear relationships among partition coefficients between water and various organic solvents have been extended and qualified to include other dose-response relationships.

The success of the Hansch model in demonstrating that free energy correlations can be successfully applied to biological processes has prompted many researchers to reexamine the derivation of the Hansch equation. Using the principles of theoretical pharmacology or pharmacokinetics, improved theoretical models have been sought to accommodate more complex relationships between biological activity and chemical structure or properties, or to broaden the scope of Equation (4.1.1) to include, for example, ionizable compounds. The free energy model of Hansch and its elaborations has been by far the most widely used. This has been due not only to its many successful applications, but also to its simplicity, its direct conceptual lineage to established physical organic chemical properties, and the ready availability of a database of substituent parameters.

4.2 Free Wilson Mathematical Model

The idea that substituents ought to contribute constant increments or decrements to biological response in a related series of compounds has been probably a long held intuition of medicinal chemists trained in organic chemistry (Topliss, 1983). However, only in the recent past can a few demonstrations of this can be found in the literature. The same time that the Hansch model was proposed, Free and Wilson demonstrated a general

mathematical method both for assessing the occurrence of additive substituent effects and quantitatively estimating their magnitude (Topliss, 1983). According to their method, the molecules of a drug series can be structurally decomposed into a common moiety or core that is variously substituted in multiple positions. In this approach, a series of linear equations of the form of Equation (4.2.1) are constructed :

$$BA_i = \sum_j a_j X_{ij} + \mu \quad (4.2.1)$$

where

BA = biological activity

$X_j = j^{\text{th}}$ substituent with a value of 1 if present and 0 if not

a_j = contribution of the j^{th} substituent to BA

μ = average overall activity

All contributions at each position of the substitution should sum to zero. The series of linear equations thus generated is solved by the method of least squares for terms a_j and μ . There must be several more equations than unknowns and each substituent should appear more than once at a position in different combinations with substituents at other positions. The attractiveness of this model, also referred to as the *de novo* method are : (i) any set of quantitative biological data may be employed as the dependent variable, (ii) no independently measured substituent constants are required, (iii) the molecules of a series may be structurally dissected in any convenient manner, and (iv) multiple sites of variable substitution are easily accommodated. There are also several

limitations: a substantial number of compounds with varying substituent combinations is required for a meaningful analysis; the derived substituent contributions give no reasonable basis for extrapolating predictions beyond the substituent matrix analyzed; and the model will break down if non-linear dependence on substituent properties is important or if there are interactions between the substituents.

4.3 Discriminant Analysis

In many cases of interest the biological measurements available are semiquantitative or qualitative in nature, and activity assessments must be evaluated. Such data may arise from measurements with inherent imprecision, subjective evaluation of behavioral or response observations, or a combination of several criteria of interest into a single index. Passing over the question of to what extent of this data type are suitable for correlation in free energy models, it is nevertheless interesting to try to obtain some insight into the operative properties or structural parameters responsible for the variations in such data. Discriminant analysis has been proposed to deal with this type of a problem. This method seeks a linear combination of parameters, called a linear discriminant function, that will successfully classify the observations into their observed or assigned categories. Parameters are added or deleted to improve discrimination, and the results are judged by the number of observations correctly classified.

4.4 Cluster Analysis

Cluster analysis is simply a method to group entities, for which a number of properties or parameters exist, by similarity. Various distance measurements are used, and the analysis is performed in a sequential manner, reducing the number of clusters at each step. Such a procedure has been described for use in drug design as a way to group substituents that have the most similarity when various combinations of the electronic, steric and statistically derived parameters are considered.

4.5 Principal Components and Factor Analysis

Principal Component Analysis (PCA) is probably the oldest and best known of the techniques of multivariate analysis (Jolliffe, 1986). Both PCA and factor analysis aim to reduce the dimensionality of a set of data, but the approaches to do so are different for the two techniques. Each technique gives a different insight into the data structure, with principal component analysis concentrating on explaining the diagonal elements of the covariance matrix, while factor analysis the off-diagonal elements (Jolliffe, 1986). An extensive review of PCA methods and theory is presented by Jolliffe (Jolliffe, 1986) and Manley (Manley, 1986).

Principal components are linear combinations of random or statistical variables which have special properties in terms of variances. The central idea of PCA is to reduce

the dimensionality of a data set which may consist of a large number of interrelated variables while retaining as much as possible of the variation present in the data set. This is achieved by transforming to a new set of variables, the Principal Components (PCs), which are uncorrelated, and which are ordered so that the first few retain most of the variation present in all of the original variables.

One of the statistical concerns in multiple regression analysis noted above is cross correlation between independent variables under consideration. This can simply be assessed by examination of the correlation matrix of the parameters responsible for variations of such data. Further manipulations can be performed on this matrix or on the variance-covariance matrix including the dependent variable. By methods of linear algebra such a matrix may be transformed by prescribed methods into one containing nonzero elements only on the diagonal. These are called eigen values of the matrix, and associated with each of these is an eigen vector that is a linear combination of the original set of variables. Eigen vectors, unlike the original set of variables, have the property of being exactly orthogonal, that is the correlation coefficient between any two of them is zero.

If a set of variables has substantial covariance, it will turn out that most of the total variance will be accounted for by a number of eigen vectors equal to a fraction of the original number of variables. A reduced set containing only the major eigen vectors or “principal components”, may then be examined or used in various ways. This method is often used as a preprocessing tool. If only the principal components are considered, new orthogonal variables can be constructed from the eigen vectors, and hence the dimensionality of the parameter space can be reduced while most of the information in

the original variable set is retained. This is particularly useful in the multidimensional methods that may be used as a preliminary step in series design, in multiple regression analysis of the Hansch variety and pattern recognition.

Factor analysis involves other manipulations of the eigen vectors and is aimed at gaining insight into the structure of a multidimensional data set. Weiner and Weiner first proposed the use of this technique in biological SAR and illustrated this with an analysis of the activities of 21 diphenylaminopropanol derivatives in 11 biological test (Topliss, 1983). This method has been more commonly used to determine the “intrinsic dimensionality” of certain experimentally determined chemical properties, that is the number of fundamental factors required to account for the variance. In this research study factor analysis has been used in conjunction with principal component analysis, and is discussed in greater detail later.

4.6 Pattern Recognition

Pattern recognition is an ensemble of techniques that utilize Artificial Intelligence to predict biological response. As they have been applied to QSAR, these methods comprise yet another approach to examining structural features and/or chemical properties for underlying patterns that are associated with different biological effects. Accurate classification of untested chemicals is again the primary goal. This is carried out in two stages. First, a set of compounds, designated the training set, is chosen for which the correct classification is known. A set of molecular or property descriptors is generated for

each compound. A suitable classification algorithm is then applied to find some combination and weight of the descriptors that allows perfect classification. Many different statistical and geometric techniques for this purpose have been used and compared (Topliss, 1983). The derived classification is then applied in the second step to compounds not included in the training set to test predictability. In published work these have been other compounds of known classification as well. Performance is judged by the percentage of correct predictions. Stability of the classifications is usually tested by repeating the training procedure several times with slightly altered, but randomly varied training sets.

The two pattern recognition systems that were used earliest in QSAR work were that of Kirschner and Kowalski, called ARTHUR (Kirschner and Kowalski, 1979), and that of Stuper and Jurs, named ADAPT (Topliss, 1983). The generally abstract structural descriptors used by these programs make the interpretation of a successful training vector difficult to impossible in terms useful to a drug designer. One is the SIMCA system as proposed by Wold *et al.* (Wold *et al.*, 1976, 1978, 1978, 1980). This method makes use of principal component analysis to provide structure and limits to the classification groups so that not only can group membership be determined, but also the level of activity within each group. The published applications of this method have tended to use physico-chemical parameters as molecular descriptors in preference to the structural features relied upon by other methods (Topliss, 1983).

4.7 Combined Multivariate Statistical Analysis

Multivariate statistical analysis is concerned with data that consist of sets of measurements on a number of individuals or objects (Anderson, 1984). In this application, some or all of the above described methods may be used to analyze a given set of biological data. Because many of the methods are complimentary, it seems likely that their combined use will be a major trend in future QSAR work (Topliss, 1983). A study of the QSAR of quinazoline inhibitors of tetrahydrofolate dehydrogenase (dihydrofolate reductase) thymidylate synthase used cluster analysis, factor analysis, discriminant analysis, and finally, multiple regression analysis to examine data from various view points (Topliss, 1983). In another research study conducted by Lewi, a technique called spectral mapping was outlined, in which the biological profile and potencies of closely related compounds may be analyzed by a combination of cluster and principal components analysis (Lewi, 1976, 1980).

Mager put together among the most impressively integrated multivariate statistical model, MASCA system, in which a whole battery of biometric statistical methods has been combined into a total system for the analysis of biological assay results, pharmacokinetic information, and series design, as well as structure activity relationships (Mager, 1980). A similar approach has been used in this research study where PCA, Factor analysis and multiple linear regression are all used for model development. PCA has been used to reduce the number of descriptor variables for the class of halogenated aliphatic hydrocarbons. The principal components derived from the PCA analysis serve as design points for the factor analysis which is used to select the training set of compounds.

Finally multiple linear regression techniques have been used to correlate the sorption-desorption parameters of the training set of compounds to their molecular connectivity indexes.

4.8 Selection of Training Set of Compounds

The predictive ability of a QSAR depends strongly on the composition of the training set selected. Most often, and unfortunately, the “standard way” of selecting this training set is either to take all available data in a database, or to start with a “lead compound” and generate the training set by changing one substituent at a time (Eriksson *et al.*, 1988). Usually these approaches lead to training sets with low information content and thereby to QSARs with low predictive power (Eriksson *et al.* 1988, Tosato *et al.*, 1990). Because of the complex mechanism of biological activity, the models used for QSAR must necessarily be statistical in nature. Furthermore, due to the variation in biological mechanisms, it is necessary to have separate models for different classes of compounds. (Jonsson *et al.* 1988, Eriksson *et al.*, 1988).

For the selection of an appropriate training set of compounds for a QSAR analysis, statistical designs such as factorial or fractional factorial design are essential. These designs have been used previously for QSAR development in a variety of applications . (Jonsson *et al.*, 1988, Eriksson *et al.*, 1988, Tosato *et al.*, 1990). A statistical design produces a well balanced training set by distributing the compounds over the entire class domain. This is because it generates a set of compounds by varying

all design factors simultaneously in contrast to the traditional approach of varying any one substructure or substituent at a time. To develop an empirical or semi-empirical model between structure (X) and biological response (Y), a training set of compounds needs to be selected for which both X and Y are defined. To make X and Y mathematically homogeneous, which is a prerequisite for model development, the compounds must be structurally similar and act according to the same biological mechanism with respect to the biological response of interest. Also, assuming that the variation in the biological response, Y, is related to a number of structural factors in the compounds, such as the size of a certain substituent group, total lipophilicity, ionization potential, van der Waals volume, etc., the training set of compounds must span the space of these factors. Thus the conditions that must be fulfilled for the training set of compounds that constitute the matrix formed by X, are: (i) structural similarity, (ii) similarity in biological mechanism, and (iii) together span the structural factor space. Provided that the structural variation over a fairly large set of compounds (larger than the training set) is described sufficiently by many relevant X variables, a Principal Components Analysis (PCA) of the X matrix will result in a few dominant factors that are linear combinations of the original X variables. These dominant factors, called principal components, can then be used as design variables for the training set of compounds. Theoretically, PCA corresponds to a mathematical decomposition of the descriptor matrix, X, into means (\bar{x}_k), scores (t_{ia}), loadings (p_{ak}) and residuals (e_{ik}), which can be expressed as

$$x_{ik} = \bar{x}_k + \sum_{a=1}^A t_{ia} p_{ak} + e_{ik} \quad (4.8.1)$$

where

x_{ik} = data elements used to describe the structural variation within the class of compounds

t_{ia} = location of the i^{th} compound along the a^{th} principal component (PC)

p_{ak} = loadings describe how much, and in what way the k^{th} chemical descriptor contributes to a certain PC

A detailed review of PCA methods can be found in the literature (Manly, 1986, Eriksson, *et al.*, 1990, Tosato *et al.*, 1990). Once these design variables have been calculated, they are used in a fractional factorial design. Compounds are selected from the list of possible candidates which have principal component values closest to the points specified by the design. This gives a training set that spans the space of dominant structural factors, resulting in QSAR models that have optimal predictive properties with the chosen descriptors and the biological response data. Similarly the biological response matrix, Y, should contain all relevant “effects”, appropriately quantified and kept multivariate. Provided that the X and Y data are multivariate, a projection of X and Y by partial least squares projection to latent structure (PLS) or a PCA gives indications of the structural and biological similarity. Such a methodology (fractional factorial design) has been used successfully by Eriksson *et al.* to generate a training set of 10 halogenated aliphatics from a X matrix composed of 58 selected halogenated aliphatics with 13 descriptor variables, to predict acute oral toxicity and the highest non-lethal dosage to mice (Eriksson *et al.*, 1990). The strategy used by these authors to develop a training set

of compounds for the class of halogenated aliphatic hydrocarbons is discussed in further detail in the following discussion.

The first step of the strategy is to divide the compounds of interest into classes on the basis of their chemical structure. The resulting classes may be overlapping, but they must be so narrow that one is rather certain that the mechanism of biological action is the same for all compounds in the class. The subsequent data analysis may give information about deviations from class similarity for some compounds, provided that the majority of compounds are chemically and biologically similar within a class. A multivariate data analysis will give information about such similarities among the compounds in a class provided that the structure and biological features of the compounds are appropriately parametrized.

The second step in the strategy is to develop appropriate ways to describe the structural variation in each class of compounds. The structural description has two objectives, which demand partly different descriptor variables. One objective is to have a few design variables as the basis for the statistically based selection of a small set of compounds for the “training” of the QSAR. These design variables may be derived from the multivariate analysis of measured physical and chemical properties of these compounds in various model systems. Such properties may be molecular weight, volume, other size descriptors, measures of lipophilicity, ionization potentials, spectroscopic methods such as NMR, IR, optical rotation, etc. Alternatively the design variables may be taken as independent “principal variables” such as lipophilicity, size, and oxidation-reduction potentials.

The other objective of the structural description is to give as rich and complete description as possible of the structural variation in the subsequently developed QSAR. The design variables used for the selection of the training set are usually not sufficient for the QSAR structural description since they are rather sparse. They must be supplemented with pertinent variables so that together they describe all factors that are related to the biological activity variation in the class. For this, properties such as molecular weight, Van der Waals volume (general size descriptors), lipophilicity, electronic properties of substituents and quantum mechanically calculated electron distributions, may be used in different combinations depending on the application. The use of multivariate analysis affords the freedom to choose between different descriptors, and not be locked into any one particular descriptor. This set can be expanded to include any kind of descriptors that have been proven useful in other studies. It is desirable that variables used for the structural description can either be derived theoretically or that they be tabulated.

The predictive success of statistical modeling in any application is strongly dependent on the data used to calibrate the model. A good predictive model over the whole range of compounds under examination is important. This can be accomplished only by careful selection of a training set of compounds, so that the selected set is well balanced and distributed over the entire class of compounds being evaluated. For the modeling process to be relevant, high quality experimental data has to be available - what this means is that the model is only as good as the quality of data that it is modeled with. Selection of the training set of compounds must not use the COST (Change One Structural factor at a Time) design approach. Although the COST approach has been used in the past, this design approach has been proven to give very little useful information for

model development (Jonsson *et al.*, 1988). A statistical design which generates a set of compounds by varying all design variables simultaneously is preferred (Jonsson *et al.*, 1988). The design variables have to be chosen based on a multivariate analysis of measurements made on a number of compounds from a particular class, yielding the “principal properties” of the class. In simple cases, variables known to significantly influence the activity or property under consideration can be used as design variables.

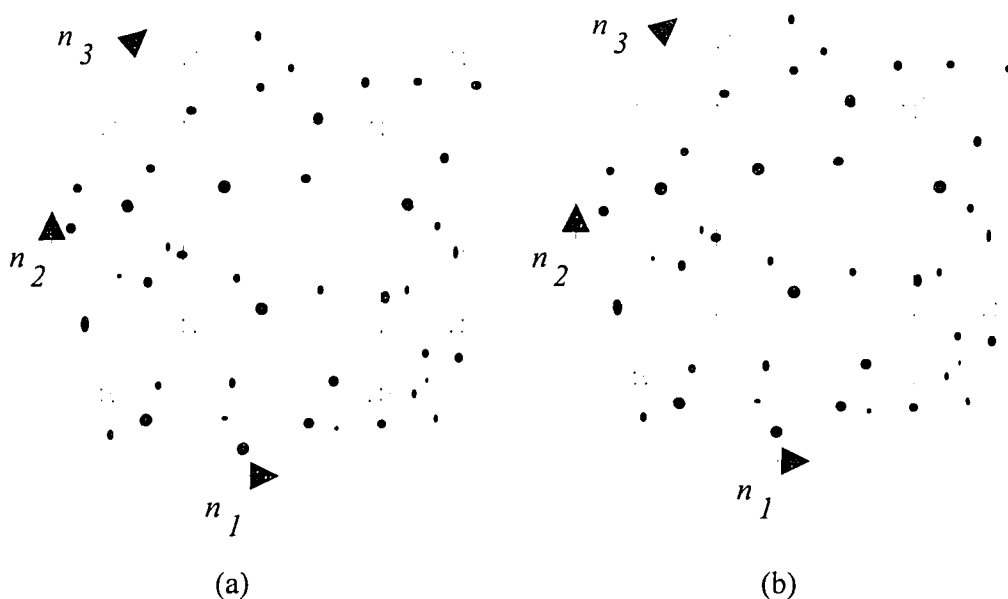


Figure 4.8.1. (a) Full factorial Design (FD) in three variables, 2^3 factorial design. (b) Fractional Factorial Design (FFD) in three variables, 2^{3-1} fractional factorial design. Open circles at the corners of the cube denotes design points, solid points denote compounds with structural variation (Jonsson *et al.*, 1988).

The design variables are not necessarily the same for different classes of compounds, since the chemical and biological factors responsible for the mode of action of the property under examination will differ between classes. Insight into the mode of action is often helpful to select certain design variables. After the design variables have

been selected, a simple statistical design, such as a factorial or fractional factorial design with center points is developed as shown in Figure 4.8.1. Such a treatment of the data potentially yields a set of compounds that are well balanced and well representative of a class (Jonsson *et al.*, 1988). Compounds are seldom located exactly at design points because of the discrete nature of the structural variation among compounds (Jonsson *et al.*, 1988). For practical purposes, such as easy availability for testing purposes, it is sufficient to select compounds that are close to the design points.

The compounds of the training set are subjected to measurements of biological end points of interest, sorption - desorption coefficients of chlorinated aliphatic hydrocarbons being the end points of interest in this research study. The observed biological responses constitute the Y matrix and are related through statistical modeling techniques to the X parameters. In this study the sorption and desorption coefficient will be related using multiple linear regression techniques to the molecular connectivity indexes generated using the algorithm developed by Kier and Hall (Kier and Hall, 1986).

Table 4.8.1. Distribution of environmental organic chemicals into four major classes (Tosato *et al.*, 1990).

Chemical Classes	High Volume		High Toxicity		Priority Pollutants	
	Number	%	Number	%	Number	%
Monofunctional Aliphatics	225	49	209	44	33	30
Monofunctional Aromatics	116	25	67	14	21	19
Difunctional Aliphatics	25	5	15	3	8	7
Difunctional Aromatics	9	2	21	4	20	18
Total	346	82	312	65	82	74

Tosato *et al.*, developed the training set of compounds for the class of halogenated aliphatics from a list of high production volume chemicals which was identified from the

first 1000 entries in the U.S. EPA TSCA inventory, a list of highly toxic chemicals from ANNEX 1 of the EEC directive on dangerous substances that lists about 900 chemicals, and a list of 200 chemicals from the International Program on Chemical Safety (IPCS) (Tosato *et al.*, 1990). About 250 inorganic chemicals, mixtures and pesticides were excluded from the compiled list of chemicals, the organic compounds in the lists were : 458 in the U.S. EPA list, 479 in the EEC ANNEX 1 list and 110 in the IPCS list. This selection of compounds represent those that have high exposure, or are hazardous, or are already recognized to be high risk (Tosato *et al.*, 1990). Each of the chemicals was assigned to the respective class on the basis of similarities in structural backbone and functional groups. The wide majority of the compounds belonged to 32 classes of mono or difunctional aliphatics or aromatics as shown in Table 4.8.1 (Tosato *et al.*, 1990).

The selection of the training set of compounds for this research study is described in detail in the following discussion and has been adapted from work conducted by various authors (Eriksson *et al.*, 1989, 1990, Jonsson *et al.*, 1988, Tosato *et al.*, 1990). This research study was conducted using a similar set of compounds, as selected by Eriksson *et al.*, to develop predictive QSAR models to estimate the sorption-desorption behavior of halogenated aliphatics in activated sludge solids. The development of the training set of compounds, as conducted by the authors referenced in this discussion, is elucidated in detail in the following discussion. The class of halogenated aliphatics (AX class) chosen for investigation of sorption-desorption processes consisted of both saturated and unsaturated compounds with one to four carbon atoms forming the backbone.

A set of 58 halogenated aliphatic hydrocarbons was chosen in this class for the proposed study primarily because this class of compounds consists of a number of compounds that are widely spread in the environment, and secondly this class can be characterized by a multitude of well established QSAR descriptors, which is advantageous for the stability and quality of the QSARs to be developed (Eriksson *et al.*, 1990). Thirteen variables which included boiling point at 760 mmHg, melting point, refractive index, density, van der Waals volume, lipophilicity, ionization potential and the number of carbons and other halogens in the compound were used as the descriptor variables. Table 4.8.2 summarizes the raw data for the AX class of compounds selected for this research study. The variables were autoscaled according to their standard deviation to obtain unit variance. This was done by multiplying each element of a variable by the inverse standard deviation of that variable. To prevent the indicator variables from having too strong an influence in the PCA, they were scaled down by a factor of $\frac{1}{\sqrt{5}}$. The X matrix of the AX class of 58 compounds was subject to Principal Components Analysis (PCA), as per the methodology outlined earlier. The PCA resulted in four significant principal components (t_1 , t_2 , t_3 and t_4) that together described 87% of the total variation. Principal component t_1 accounted for 54%, t_2 accounted for 14%, t_3 accounted for 12% and t_4 accounted for 7% of the total variation. Figures 4.8.2 through 4.8.7 show the scores and loading plots for the AX class of compounds. A detailed interpretation of these plots can be found elsewhere (Jonsson *et al.*, 1988). An inspection of the relationship between loading vector 1 and vector 2 shows that the first principal component mainly describes the size/bulk of the compounds.

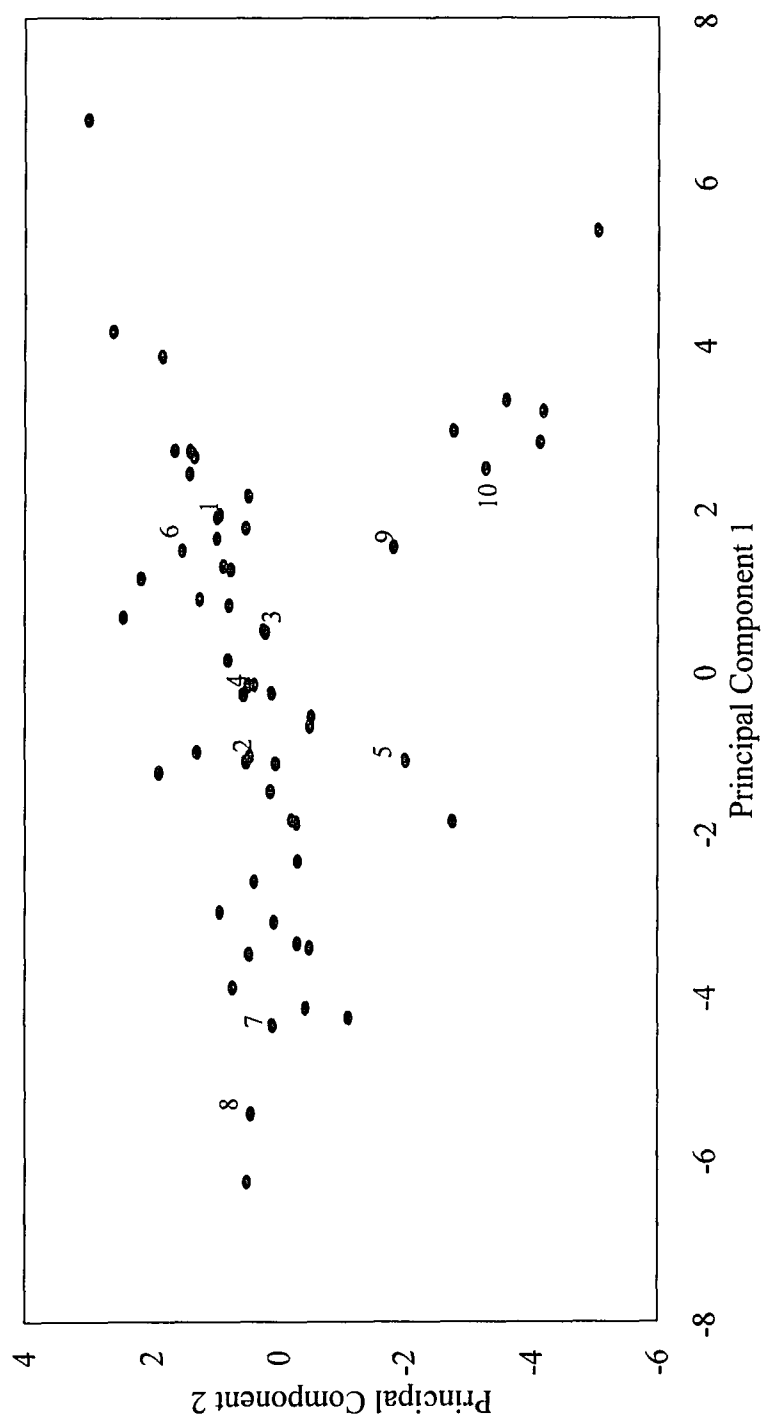


Figure 4.8.2. Score plot of principal component 1 (t_1) against principal component 2 (t_2). Circles represent compounds used to establish principal component models as shown in Table 4.8.2. Numbers indicate training set of compounds from Table 4.8.3.

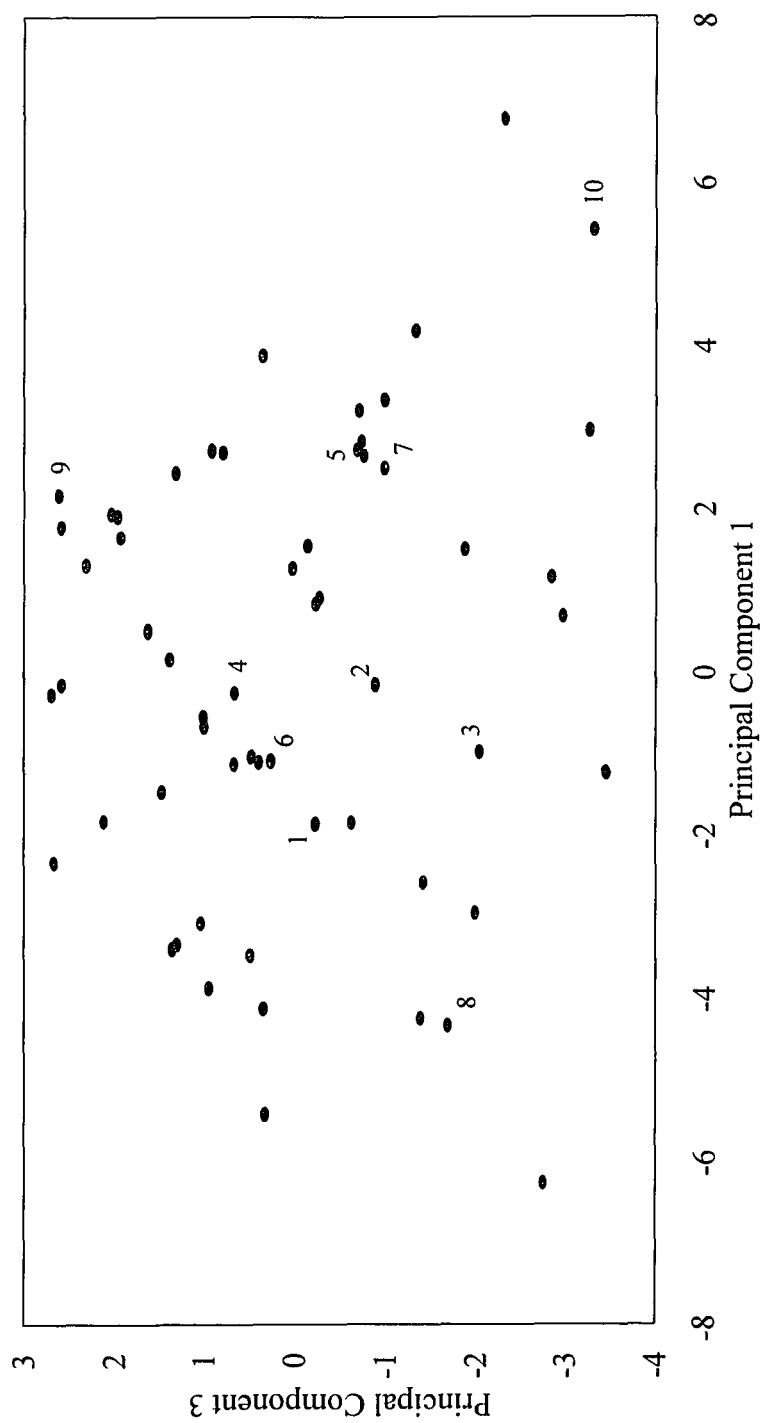


Figure 4.8.3. Score plot of principal component 1 (t_1) against principal component 3 (t_3). Circles represent compounds used to establish principal component models as shown in Table 4.8.2. Numbers indicate training set of compounds from Table 4.8.3.

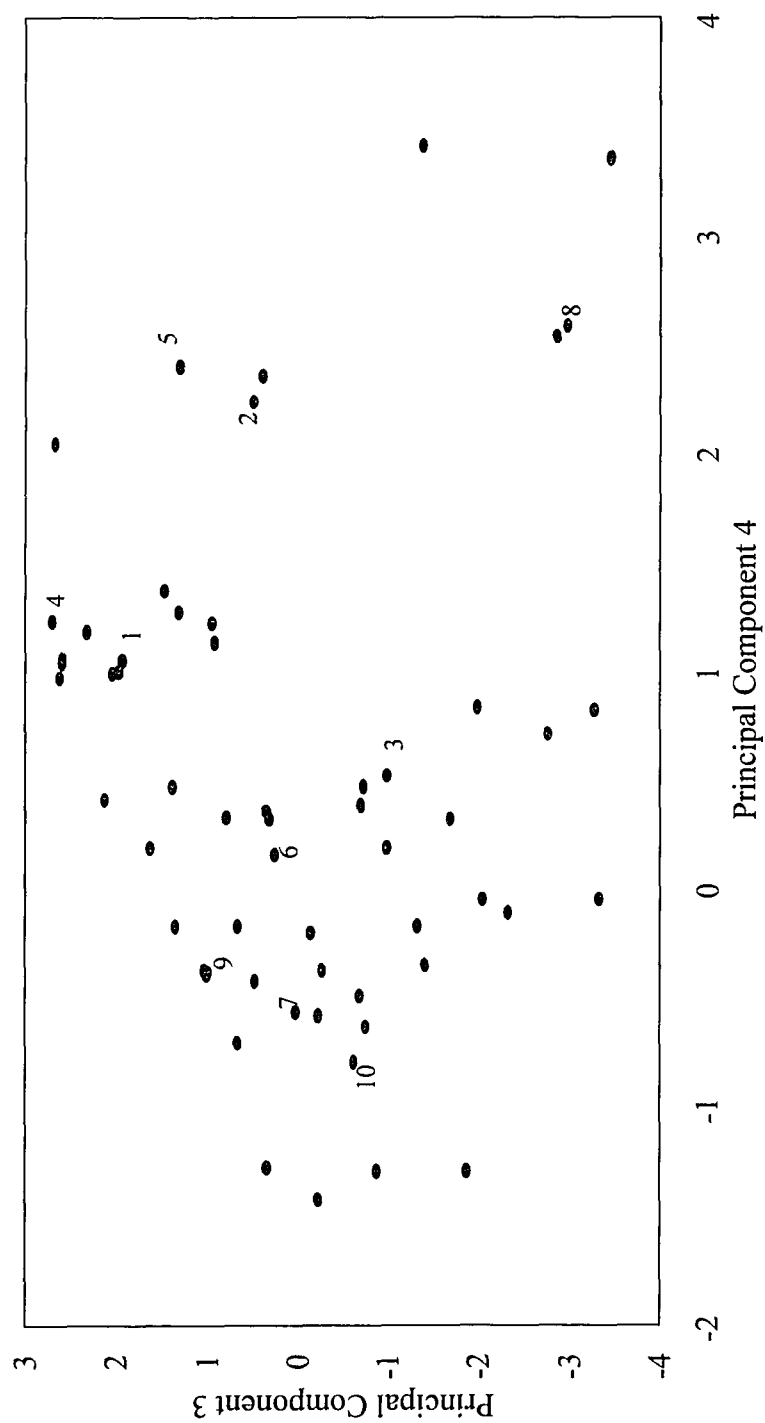


Figure 4.8.4. Score plot of principal component 1 (t_1) against principal component 3 (t_3). Circles represent compounds used to establish principal component models as shown in Table 4.8.2. Numbers indicate training set of compounds from Table 4.8.3.

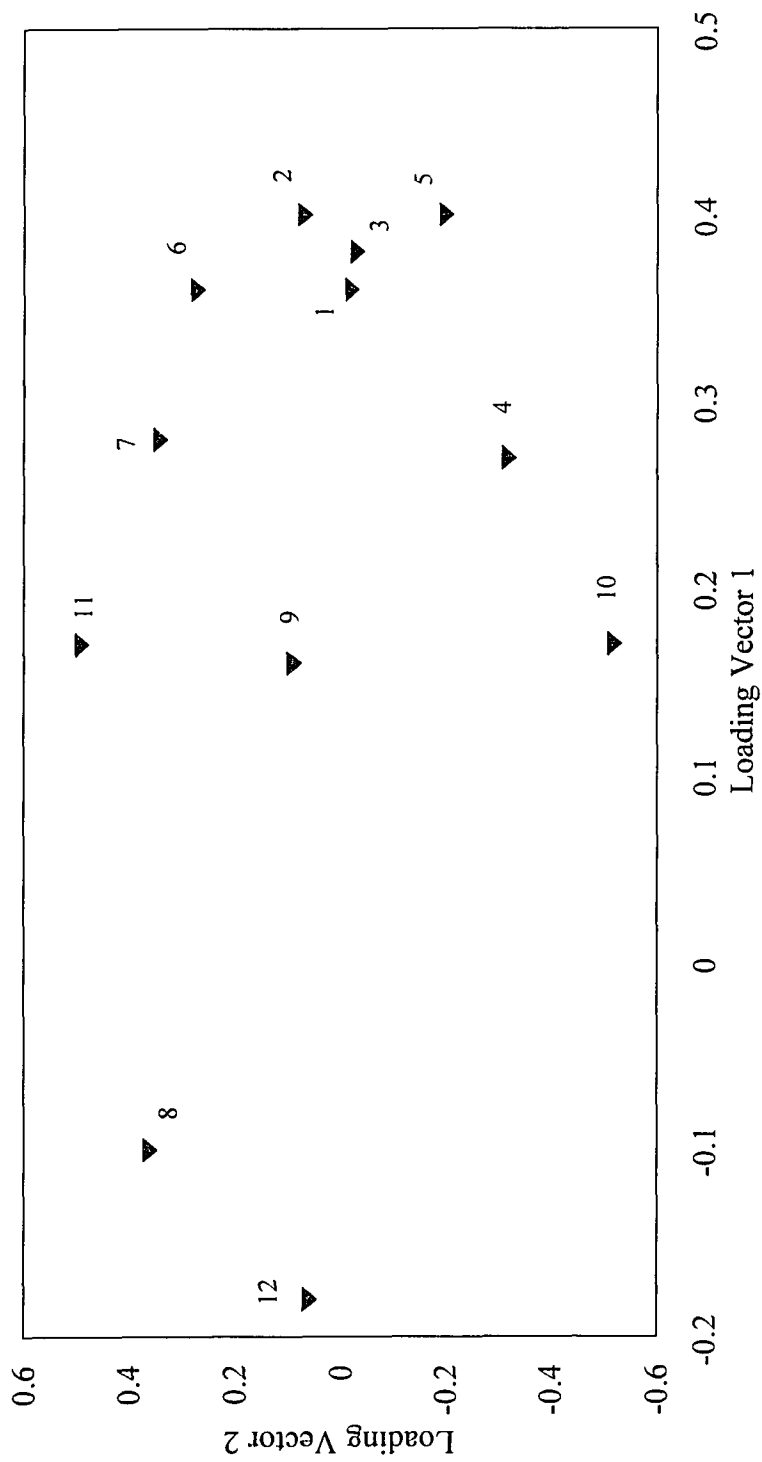


Figure 4.8.5. Loading plot of loading vector 1 (p_1) against loading vector 2 (p_2). The numbers correspond to variables listed in Table 4.8.2.

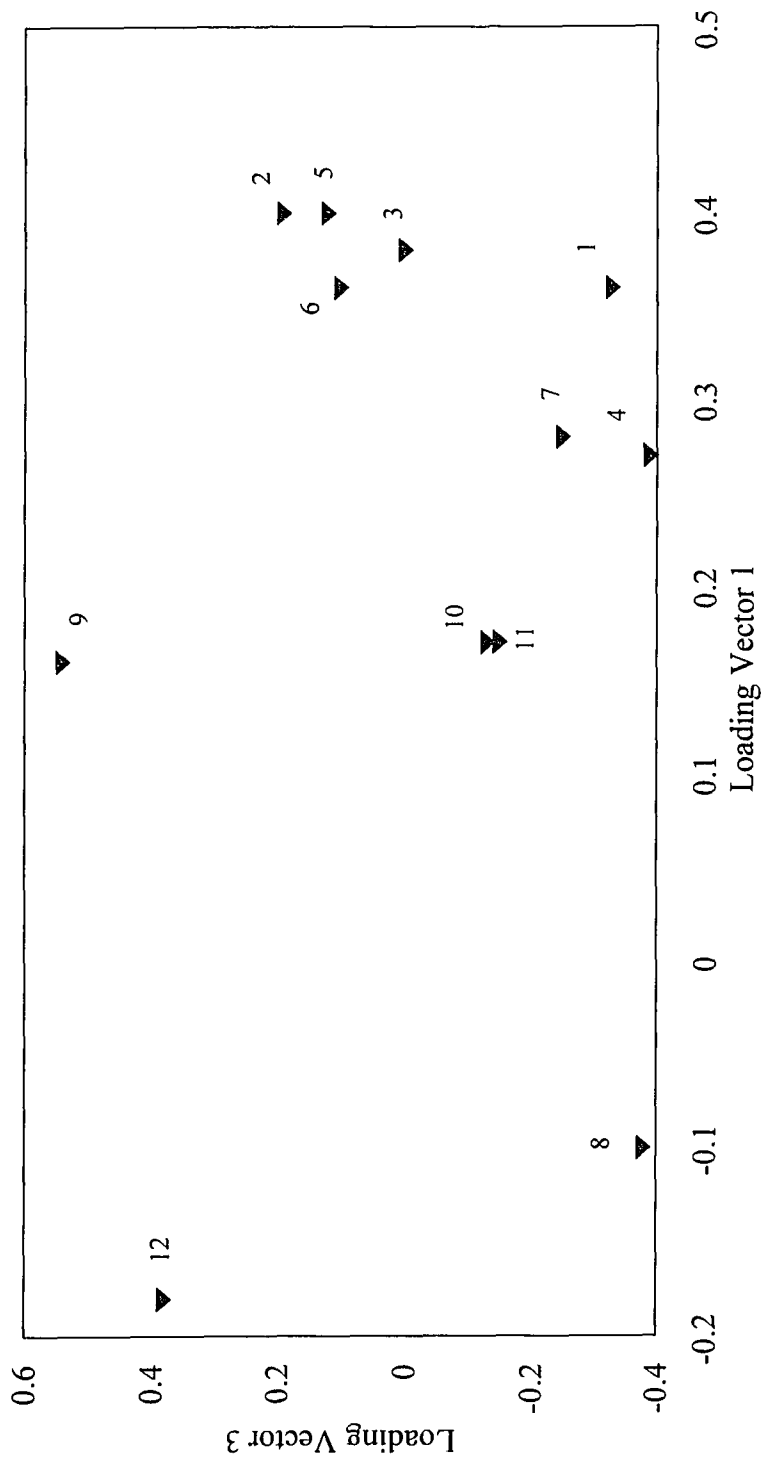


Figure 4.8.6. Loading plot of loading vector 1 (p_1) against loading vector 3 (p_3). The numbers correspond to variables listed in Table 4.8.2.

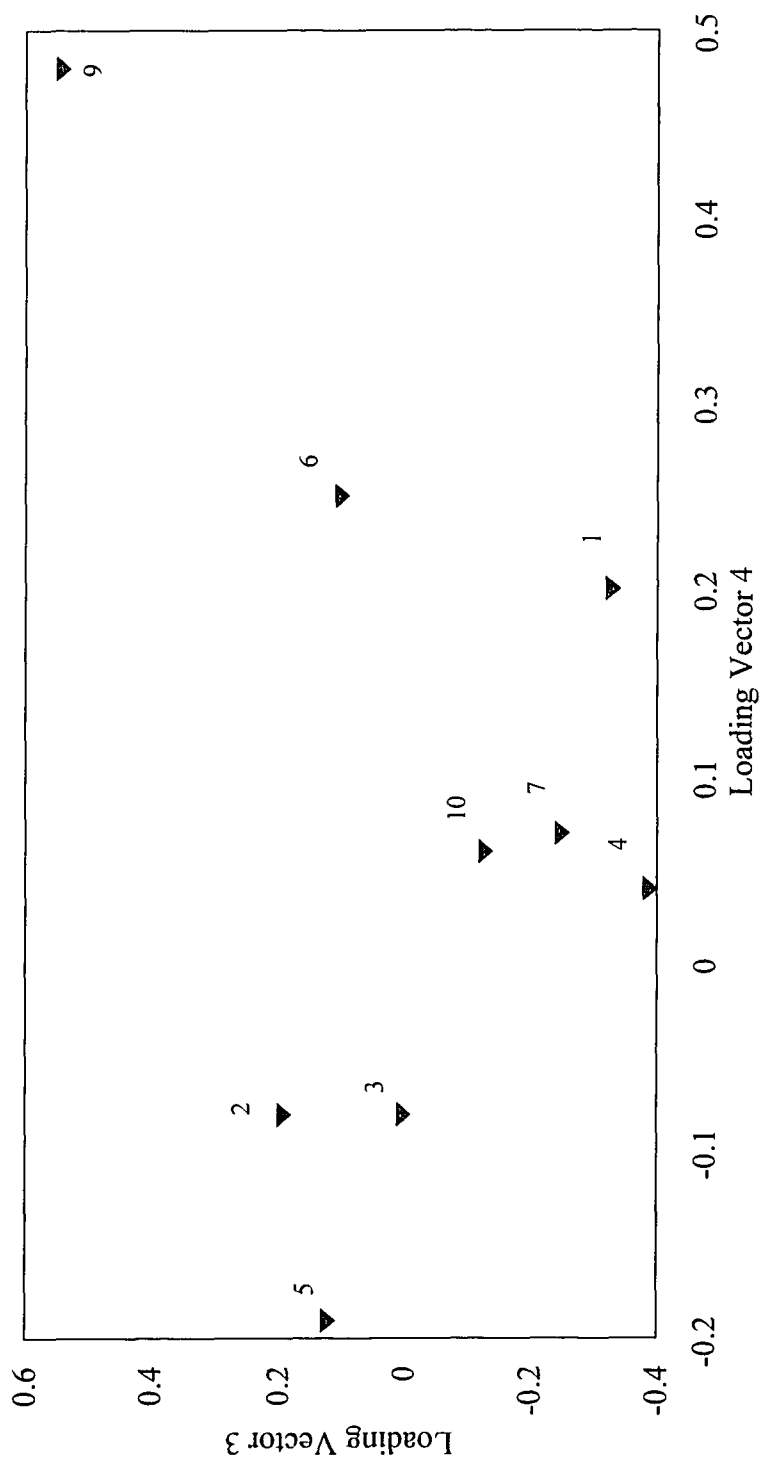


Figure 4.8.7. Loading plot of loading vector 4 (p_4) against loading vector 3 (p_3). The numbers correspond to variables listed in Table 4.8.2.

Table 4.8.2. Descriptor variables for a selected set of aliphatic hydrocarbons (AX Class).

No. of Atoms													
Compound name	MW ¹	BP ²	MP ³	D ⁴	η _p ⁵	vdW ⁶	log P ⁷	Ip ⁸	C	Br	Cl	F	I
CH ₃ Cl	50.49	-24.20	-97.10	0.92	1.34	25.29	0.91	11.28	1	0	1	0	0
CH ₂ Cl ₂	84.93	40.00	-95.10	1.33	1.42	33.47	1.25	11.32	1	0	2	0	0
CHCl ₃	119.38	61.70	-63.50	1.48	1.45	41.64	1.94	11.37	1	0	3	0	0
CHCl ₂ F	102.92	9.00	-135.00	1.41	1.37	35.74	1.55	12.00	1	0	2	1	0
CHClF ₂	86.47	-40.80	-146.00	-	-	29.84	1.08	12.60	1	0	1	2	0
CCl ₄	153.82	76.50	-23.00	1.59	1.46	49.91	2.83	-	1	0	4	0	0
CCl ₃ F	137.37	23.70	-111.00	1.49	1.38	43.91	2.53	11.77	1	0	3	1	0
CCl ₂ F ₂	120.91	-29.80	-158.00	1.18	-	38.01	2.16	11.75	1	0	2	2	0
CH ₃ Br	94.94	3.60	-93.60	1.68	1.42	28.07	1.19	10.54	1	1	0	0	0
CH ₃ -CH ₂ Cl	64.52	12.30	-136.40	0.90	1.37	35.52	1.43	11.01	2	0	1	0	0
CHCl-CH ₂ Cl	98.96	83.50	-35.30	1.24	1.44	43.70	1.48	11.05	2	0	2	0	0
CH ₂ Br-CH ₂ Cl	143.42	107.00	-16.70	1.74	1.49	46.49	1.62	10.55	2	1	1	0	0
CH ₂ Cl-CHCl ₂	133.41	113.80	-36.50	1.44	1.47	51.87	1.89	-	2	0	3	0	0
CH ₃ -CCl ₃	133.41	74.10	-30.40	1.34	1.44	51.97	2.49	11.25	2	0	3	0	0
CHCl ₂ -CHCl ₂	167.85	146.20	-36.00	1.60	1.49	60.04	2.39	11.45	0	0	4	0	0
CHCl ₂ -CCl ₃	202.30	162.00	-29.00	1.68	1.50	68.21	3.64	11.28	2	0	5	0	0
CCl ₃ -CCl ₃	236.74	180.00	-	2.09	-	76.38	4.00	11.22	2	0	6	0	0
CCl ₃ F-CClF ₂	187.39	47.70	-36.40	1.56	1.36	58.69	3.30	12.05	2	0	3	3	0
CH ₂ Br-CH ₂ Br	187.87	131.30	9.80	2.18	1.54	49.26	0.01	10.37	2	2	0	0	0
CH ₃ -CHCl ₂	98.96	57.30	-97.00	1.18	1.42	43.69	1.79	11.06	2	0	2	0	0
CClF ₂ -CClF ₂	170.92	-	-	-	-	52.78	2.82	12.47	2	0	2	4	0
CH ₃ -CHCl-CH ₂ Cl	112.99	96.40	-100.40	1.16	1.44	53.92	2.07	-	3	0	2	0	0
CH ₂ Cl-CHCl-CH ₂ Cl	147.43	156.80	-14.70	1.39	1.49	62.10	2.57	-	3	0	3	0	0
CH ₃ -CH ₂ -CH ₂ F	62.09	2.50	-159.00	0.80	1.31	39.85	1.59	11.96	3	0	0	1	0
CH ₃ F-CH ₂ -CH ₂ F	80.08	41.60	-	1.01	1.32	42.13	0.86	-	3	0	0	2	0
CH ₃ -CF ₂ -CH ₃	90.09	-0.40	-104.80	0.92	1.29	42.11	1.46	11.42	3	0	0	2	0
CH ₂ Cl-CHCl-CHCl ₂	181.89	180.00	-	1.51	1.50	70.27	2.60	-	3	0	4	0	0
CH ₃ F-CF ₂ -CH ₂ Cl	96.53	70.00	-	-	1.39	48.03	1.30	-	3	0	1	1	0

¹ Molecular weight, ² Boiling Point, ³ Melting Point, ⁴ Density, ⁵ Refractive Index, ⁶ van der Waals volume, ⁷ octanol-water partition coefficient,⁸ Ionization Potential, ^C Carbon, ^{Br} Bromine, ^{Cl} Chlorine, ^F Fluorine, ^I Iodine.

Table 4.8.2. Descriptor variables for a selected set of aliphatic hydrocarbons (AX Class) (Continued).

Compound name	MW ¹	BP ²	MP ³	D ⁴	n _D ⁵	vdW ⁶	log P ⁷	Ip ⁸	No. of Atoms				
									C	Br	Cl	F	I
CH ₃ -CF ₂ -CH ₂ Cl	114.52	55.00	-56.20	1.20	1.35	50.29	1.73	-	3	0	1	2	0
CH ₃ -CH ₂ Br	108.97	38.40	-118.60	1.46	1.42	38.30	1.61	10.28	2	1	0	0	0
CHBr ₃	252.75	149.50	8.30	2.89	1.60	49.98	2.38	10.48	1	3	0	0	0
CH ₃ -CH ₂ F	40.06	-37.70	-143.20	0.72	1.27	29.62	1.05	12.43	2	0	0	1	0
CH ₃ -CHBr ₂	187.87	108.00	-63.00	2.06	1.51	49.25	2.08	10.17	2	2	0	0	0
CBr ₂ ClF	226.27	80.30	-	2.32	1.48	49.47	2.60	-	1	2	1	1	0
CH ₂ Br ₂	173.85	97.00	-52.50	2.50	1.54	39.03	1.54	10.52	1	2	0	0	0
CH ₂ I	141.94	42.40	-66.40	2.28	1.54	32.85	1.51	9.63	1	0	0	0	1
CH ₂ BrCl	129.39	68.10	-86.50	1.93	1.48	36.25	1.40	-	1	1	1	0	0
CBrF ₃	148.91	-59.00	-	1.59	-	35.73	1.86	12.07	1	1	0	3	0
CBr ₃ F	270.72	107.00	-73.60	2.77	1.52	52.25	2.94	10.67	1	3	0	1	0
CH ₂ Br-CH ₂ F	126.96	71.50	-	1.04	1.42	40.58	1.18	10.57	2	1	0	1	0
CH ₃ -CHF ₂	66.05	-24.70	-117.00	0.95	-	31.89	0.75	12.80	2	0	0	2	0
CH ₃ -CH ₂ I	155.97	72.30	-108.00	1.94	1.51	43.08	2.00	9.35	2	0	0	0	1
CH ₂ Br-CH ₂ -CH ₂ Br	201.89	167.30	-34.20	1.98	1.52	59.49	2.02	10.26	3	2	0	0	0
CH ₂ Br-CH ₂ -CH ₂ F	140.98	101.40	-	1.54	1.43	50.81	1.44	10.38	3	1	0	1	0
CH ₃ -CH ₂ -CH ₂ Br	122.99	71.00	-110.00	1.35	1.43	48.53	2.10	10.19	3	1	0	0	0
CH ₃ -CHBr-CH ₃	122.99	59.40	-89.00	1.31	1.43	48.53	2.17	10.23	3	1	0	0	0
CH ₃ -CH ₂ -CH ₂ Cl	78.54	46.60	-122.80	0.89	1.39	45.75	2.04	10.85	3	0	1	0	0
CH ₃ -CHCl-CH ₃	78.54	35.70	-117.20	0.86	1.38	45.75	1.90	10.89	3	0	1	0	0
CH ₃ -CH ₂ -CH ₂ I	169.99	102.40	-101.00	1.75	1.51	53.31	2.56	9.26	3	0	0	0	1
CH ₃ -CHI-CH ₃	169.99	89.40	-90.10	1.70	1.50	53.31	2.56	9.18	3	0	0	0	1
CH ₂ Br-CH ₂ -CH ₂ -CH ₂ Br	215.92	197.00	-16.50	1.79	1.52	79.28	2.56	10.27	4	2	0	0	0
CH ₃ -CH ₂ -CH ₂ -CH ₂ Br	137.02	101.60	-112.40	1.28	1.44	63.54	2.71	10.15	4	1	0	0	0
[CH ₃] ₃ -CBr	137.02	73.20	-16.20	1.22	1.43	63.54	2.71	10.05	4	1	0	0	0
CH ₂ -CH ₂ -CH ₂ -CH ₂ Cl	92.57	78.40	-123.10	0.89	1.40	55.98	2.64	10.84	4	0	1	0	0
[CH ₃] ₃ -CCI	92.57	51.00	-25.40	0.84	1.39	55.98	2.57	10.76	4	0	1	0	0
CH ₃ -CH ₂ -CH ₂ -CH ₂ I	184.02	130.50	-103.00	1.62	1.50	71.10	3.10	9.26	4	0	0	0	1
[CH ₃] ₃ -CI	184.02	100.00	-34.2	1.54	1.49	71.10	3.10	9.18	4	0	0	0	1
CH ₂ -CH ₂ -CHI-CH ₃	184.02	110.00	-104.20	1.59	1.50	71.10	3.10	9.40	4	0	0	0	1

¹ Molecular weight, ² Boiling Point, ³ Melting Point, ⁴ Density, ⁵ Refractive Index, ⁶ van der Waals volume, ⁷ octanol-water partition coefficient,⁸ Ionization Potential, ^C Carbon, ^{Br} Bromine, ^{Cl} Chlorine, ^F Fluorine, ^I Iodine.

Table 4.8.3. Descriptor variables for selected halogenated aliphatic compounds (Eriksson *et al.*, 1990).

Compound	MW ¹	BP ²	MP ³	D ⁴	n _D ⁵	vdW ⁶	log P ⁷	Ip ⁸	No. of Atoms				
									C	Br	Cl	F	I
CH ₂ Cl ₂	84.93	40.0	-95.1	1.33	1.42	33.47	1.25	11.32	1	0	2	0	0
CHCl ₃	119.38	61.7	-63.5	1.48	1.45	41.64	1.94	11.37	1	0	3	0	0
CCl ₃ F	137.37	23.7	-111.0	1.49	1.38	43.91	2.53	11.77	1	0	3	1	0
CH ₂ Cl-CH ₂ Cl	98.96	83.5	-35.3	1.24	1.45	43.70	1.48	11.05	2	0	2	0	0
CHCl ₂ -CHCl ₂	167.85	146.2	-36.0	1.60	1.49	60.04	2.39	11.45	2	0	4	0	0
CH ₃ -CH ₂ Br	108.97	38.4	-118.6	1.46	1.42	38.30	1.61	10.28	2	1	0	0	0
CH ₃ -CHBr ₂	187.87	108.0	-63.0	2.06	1.51	49.25	2.08	10.17	2	2	0	0	0
CB ₃ F	270.72	107.0	-73.6	2.77	1.52	52.25	2.94	10.67	1	3	0	1	0
CH ₃ -CHCl-CH ₃	78.54	35.7	-117.2	0.87	1.38	45.75	1.90	10.89	3	0	1	0	0
CH ₃ -CH ₂ -CH ₂ -CH ₂ Br	137.02	101.6	-112.4	1.28	1.44	63.54	2.71	10.15	4	1	0	0	0

¹ Molecular weight, ² Boiling Point, ³ Melting Point, ⁴ Density, ⁵ Refractive Index, ⁶ van der Waals volume, ⁷ octanol-water partition coefficient, ⁸ Ionization Potential,

^C Carbon, ^{Br} Bromine, ^{Cl} Chlorine, ^F Fluorine, ^I Iodine.

Descriptor variables like molecular weight (1), boiling point (2), density (4) and van der Waals volume (6) are important for the first dimension. The second principal component is dominated by log P (7), van der Waals volume and density, and can be interpreted to reflect a combination of size and lipophilicity. The third and fourth principal components do not seem to convey any definite distribution, and hence information. The four principal components derived were then used as the design variables for the AX class of compounds. A 2^{4-1} fractional factorial design, as shown in Figure 4.8.1, was constructed for the four design variables. This corresponds to the representation of the compounds as points in a space with four dimensions. The fractional factorial design was used to select eight compounds with values of their design variables corresponding to the design points as closely as possible. Geometrically, the selected compounds form the corners of a hypercube in a space defined by the design variables. To preclude chemicals with extreme properties, compounds located at about two thirds of the maximum or minimum values of the design variables were selected. Since compounds corresponding exactly to the design points could not be found, emphasis was made to select compounds with t_1 and t_2 scores matching the design points because the first two principal components account for a greater part of the variance. To get information about curvature and variability, two center compounds were selected with near zero values in the design variables. Thus a training set of 10 aliphatic halogenated hydrocarbons was generated. Table 4.8.3 lists the selected training set of compounds. From Tables 4.8.2 and 4.8.3, it can be seen that the class of compounds selected for this study is relevant to present day problems of sequestering of priority pollutants (especially VOCs) in municipal and industrial wastewater sludges.

CHAPTER 5

MATERIALS AND METHODS

5.1 Sources of Activated Sludge Solids

The experimental study was conducted in two phases : (i) In the first phase the use of different experimental conditions for quantifying the sorption-desorption processes was validated, and (ii) in the second phase the actual sorption-desorption experiments were carried out. All analytical procedures in this research study were conducted as per Standard Methods for the Examination of Water and Wastewater (APHA, 1989), or U.S. EPA SW - 846 where appropriate (U.S. EPA, 1982). All chemicals used in this research study were of reagent grade. Activated sludge solids collected from three different unit processes were used as the sorbent matrix to test sorption capacities of halogenated aliphatic hydrocarbons. These unit processes are :

1. Laboratory scale activated sludge process with sludge recycle
2. Laboratory scale Aerobic Sequencing Batch Reactor (ASBR)
3. Pure oxygen activated sludge process (Passaic Valley Sewerage Commissioners)

The objective of using activated sludge solids from these distinctly different sources was to provide a strong basis for model building that would have the potential of

predicting sorption and desorption behavior observed in activated sludge biological treatment plant residuals across process boundaries. The process conditions are an important factor in measuring sorption-desorption coefficients since different activated sludge unit processes are known to generate biosolids of different chemical, physical and microbiological characteristics (Tchobanoglous, 1985, 1991). For example, floc size, strength and texture would vary according to the mixing conditions in the biological unit process, chemical composition would vary according to the feed substrate, and lipid concentration would vary according to the sludge age (mean cell residence time, θ_c). Each of these process are discussed in detail to elucidate the difference in environmental and operational conditions under which the activated sludge biomass was cultivated and collected. QSAR models to predict the biosorption and desorption of aliphatic hydrocarbons from activated sludge solids was based on data obtained from testing biomass from the laboratory scale activated sludge reactor and the ASBR. The model was then verified using data obtained from using activated sludge solids from a pure oxygen treatment process (PVSC) as the test matrix.

5.1.1 Laboratory Scale Activated Sludge Reactor with Recycle

An activated sludge reactor was constructed with methyl acrylate at the Civil and Environmental Engineering workshop. The dimensions of the reactor were 365mm (H) x 300 mm (D) with a total volume of 25.8 L and an active volume of 20.5 L. The reactor

was equipped with three sampling ports on its side at heights of 75mm, 150mm, and 360 mm from the top. To effect better mixing conditions, the reactor was equipped with 4 baffles measuring 360 mm x 25 mm. The head plate was also made of methyl acrylate and had ports for the introduction of influent substrate, an air sparging tube, a condenser, a temperature controller (Fisher Isotemp Model 70), a pH probe, a variable speed mixer with a marine impeller (T-Line Laboratory Stirrer Model 102, Talboys Engineering Corp., PA, USA) and four other inlet ports for pH control, nutrient addition, and auxiliaries. Air was introduced into the reactor using a diaphragm air pump (Model No.475-3010, Barnant Co., IL, USA) equipped with an air flow controller. Air was diffused into the liquid volume of the reactor in the form of coarse bubbles through a sparger plate also made with methyl acrylate.

Substrate, nutrients and buffer solutions were pumped into the reactor from a refrigerated feed tank maintained at 10°C. pH control was achieved using a pH controller (Cole-Parmer, Model 5656) connected to a computer operating on an Intel 80286 processor and a 287 Math coprocessor. ANALOG CONNECTION[®] software from Strawberry Tree, Inc., CA, USA, was used for data acquisition and control. Pumps were controlled using the ANALOG CONNECTION[®] software through a hardware interface board (ACPC 12-12, Strawberry Tree, Inc., CA, USA) connected to an electrical interface breadboard on which switching relays were located. The sampling port located 75 mm below the top of the reactor was used as the effluent discharge pipe and was connected to a clarifier located 150 mm below the effluent discharge pipe. As the clarifier was gravity fed through the overflow effluent pipe, the liquid volume in the reactor was constantly

maintained at the height of the effluent pipe, i.e. at 20 L. The activated sludge reactor setup is shown schematically in Figure 5.1.1.1.

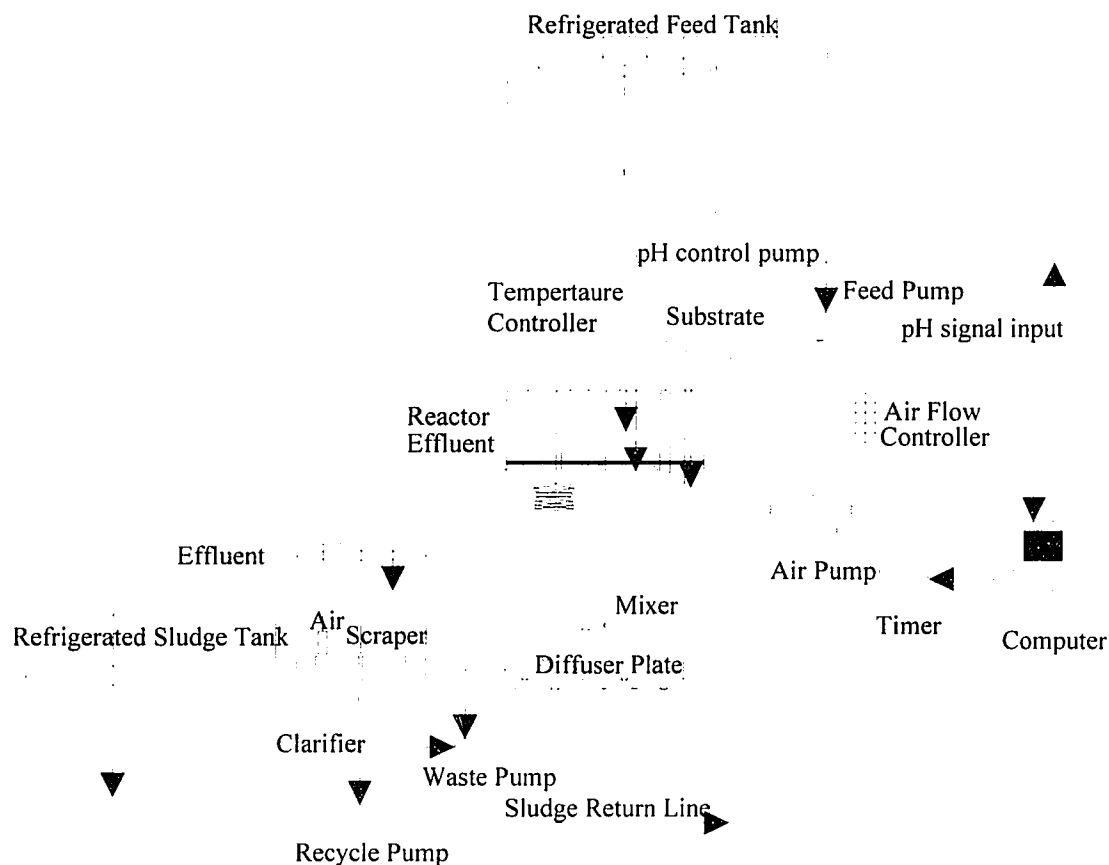


Figure 5.1.1.1. Schematic of 20 L activated sludge reactor with recycle.

The clarifier was a funnel shaped glass vessel with diameter 18 cm and an active liquid volume of 6 L. As shown in Figure 5.1.1.1, the clarifier was equipped with a scraper and an air sparger, both of which were connected to a computer controlled timer. The air sparger was provided to ensure that anoxic conditions did not prevail in the sludge zone of the clarifier. It was found from practical experience that maintaining a

residual concentration of dissolved oxygen in the clarifier resulted in better settling sludge, and hence improved process efficiency. The liquid volume in the clarifier was aerated for 5 minutes every hour to maintain dissolved oxygen concentrations at about 0.5 to 1 ppm.

The bottom of the clarifier was plugged with a silicon coated butyl rubber stopper which had three outlet pipes. One outlet was connected to a sludge recirculation pump, another was connected to a waste sludge pump and the third was used as a contingency outlet. The recycle sludge pump pumped sludge back to the reactor for 15 minutes once every two hours to maintain an overall recirculation ratio of 0.7. The scraper was operated in tandem with the sludge pump, to direct the sludge into the sludge recycle line. The effluent from the clarifier was discharged through an overflow pipe located at a 6 L liquid volume level from the bottom of the clarifier. Substrate, nutrients, pH buffer solutions, recirculation sludge and waste sludge biomass were pumped using computer interfaced peristaltic pumps (Model Nos. 7553-20 and 7543-06, Cole-Parmer, IL, USA). Excess sludge was pumped from the clarifier daily into a refrigerated container at 4°C. All connections between different units in the activated sludge reactor setup was made using TYGON® tubing (Fisher Scientific, NJ, USA), while PharMed® (Fisher Scientific, NJ, USA) tubing was used in all pump heads. Pump head tubing was changed periodically as per manufacturers recommendations, while all connecting tubing was either replaced or autoclaved to prevent biological back growth in the transfer lines.

Careful attention was paid to the composition of the feed substrate to simulate an actual domestic wastewater, with a particle size distribution ranging from soluble to supra-colloidal (Levine *et al.* 1985, 1991). Wastewater constituents exhibit a particle size

distribution ranging from 0.001 to over 100 μm (Levine et al., 1985). Sedimentation which is usually the first stage of removal of suspended matter in wastewater is effective in removing constituents that are greater than 50 μm in size (Levine et al., 1985). As a result wastewater fed into an activated sludge process has majority of the particle in the size range below 50 μm . These particles can be broadly categorized to be in the soluble ($<0.08 \mu\text{m}$), colloidal (0.08 to 1.0 μm) and supra-colloidal (1 to 100 μm) range. These different size fractions exhibit different chemical properties and therefore can influence the activated sludge process significantly. Hence, to setup a bench scale activated process and retain its real world relevance, it was necessary that the synthetic substrate fed into the reactor be as close as possible to a real wastewater. The composition of the feed substrate is summarized in Table 5.1.1.1. The substrate was designed to have a COD : N ratio of about 10 : 1.

Table 5.1.1.1. Composition of feed substrate used for the activated sludge process.

Constituent	Concentration, mg/L
Glucose, as COD (expressed as oxygen)	200
Ethanol, as COD (expressed as oxygen)	75
Acetic acid, as COD (expressed as oxygen)	75
Peptone, as COD (expressed as oxygen)	75
Hard boiled eggs, as COD (expressed as oxygen)	75
Ammonium Chloride, NH_4Cl	94
Magnesium Sulfate, $\text{MgSO}_4 \cdot 7 \text{H}_2\text{O}$	100
Ferric Chloride, $\text{FeCl}_3 \cdot 6 \text{H}_2\text{O}$	5
Calcium Chloride, $\text{CaCl}_2 \cdot 2 \text{H}_2\text{O}$	10
Potassium Chloride, KCl	7
Potassium Phosphate, Monobasic, KH_2PO_4	50
Potassium Phosphate, Dibasic, K_2HPO_4	50
Tap water	To volume

Table 5.1.1.2. Operational details of 20 L activated sludge reactor with recycle at equilibrium.

Description	Value
Volume of reactor (Liters)	20
Influent COD (mg/L as oxygen)	500
Effluent COD (mg/L as oxygen)	20
Mean cell residence time (MCRT) (days)	10
Hydraulic detention time (HRT) (days)	0.83
MLVSS in reactor (mg/L)	2250
MLSS in reactor (mg/L)	2800
Ratio of MLVSS to MLSS :	0.8
Food to Microorganism ratio (F/M)	0.27
Air flow @8% transfer efficiency, SF = 2 (LPM)	5
Surface area of clarifier (sq. cm)	255
Volume of clarifier (Liters)	6
Hydraulic detention time in clarifier (hours)	6

Previous research has shown that the soluble fraction of the wastewater may be simulated by a mixture of glucose, ethanol and acetic acid, while the particulate fraction with a mixture of peptone and a suspension prepared from hard boiled eggs (Wanner and Novak, 1990). The peptone used simulates the high molecular weight substrate which has to be solubilized prior to utilization by bacterial cells. The suspension of hard boiled eggs simulates the slowly biodegradable particulate matter in wastewater. The suspension of hard boiled eggs was prepared by homogenizing a boiled egg in a commercial blender at 15000 rpm for 1 minute (Waring Commercial Blender, Model 31 BL 91, Waring Products Division, CT, USA). The size distribution of the egg suspension was found to span the entire size distribution of interest. Although an alternative source of particulate matter may be used, the reasons for using hard boiled eggs were, (i) a wholesome nutritive food which has been well researched for its nutritional effects (ii) has been used in a previous study successfully, (iii) provides a carbon source in a particle size

distribution ranging from soluble to supra-colloidal, and (iv) relatively low operational cost.

The operational parameters of the activated sludge reactor are summarized in Table 5.1.1.2. It was operated as a continuous flow CSTR with recycle sludge flow. This reactor set up was run at steady state conditions (equilibrium) for a period of 11 months from July 1992 through May 1993. Steady state conditions in Table 5.1.1.2 reflect an average value over the experimental period during which sorption-desorption experiments were conducted. The activated sludge reactor was operated at a constant temperature of 30°C. The contents of the reactor and the clarifier had to be occasionally treated with Sodium Hypochlorite (Chlorox[™], Chlorox Professional Products Company, California) in a contact chamber for control of filamentous organisms. The contact chamber was a glass vessel similar to the clarifier used for solids separation. It was equipped with a high speed mixer and used occasionally to chlorinate the reactor contents when control of filamentous organisms became necessary. After a 5 minute contact time, the biomass from the contact chamber was returned directly to the activated sludge reactor. The dissolved oxygen concentration in the reactor and the clarifier was measured periodically. pH, Oxygen Uptake Rate (OUR), total and volatile suspended solids concentration in the reactor, effluent COD concentration and suspended solids in the effluent were measured daily. The Sludge Volume Index (SVI) of the activated sludge solids was also determined occasionally to test the settling properties of the flocculant biomass.

5.1.2 Aerobic Sequencing Batch Reactor (ASBR)

An Aerobic Sequencing Batch Reactor (ASBR) is in principal a batch reactor which is operated as a fill and draw system (Irvine *et al.*, 1979, Lewandowski and Baltziz, 1992). There are five discrete operational periods during one cycle in a sequencing batch treatment system. These are called fill, react, settle, draw, and idle periods. During the fill period the ASBR containing an active and sizable microbial population is filled with the influent substrate (wastewater). As a result, a significant fraction of the influent substrate may be utilized prior to the end of the fill period, unless measures are taken to minimize this effect, such as stopping the aeration of the reactor. During the react period, the reactor operates as a batch system with no inflow. The reactor contents are mixed and aerated till the organic matter in the influent substrate has been stabilized to the desired extent. During the settle period, all mixing and aeration are stopped, and the organisms (sludge biomass) are allowed to settle, leaving a clear supernatant above. After sufficient solids separation has been attained, the supernatant or clarified wastewater is pumped out as effluent. The activated sludge in the reactor is allowed to idle for a short period before the next cycle is started. A measured quantity of sludge was removed periodically from the reactor and stored at 4oC. The quantity of sludge removed was dictated by the MLSS concentration in the reactor to maintain a MCRT of 6 days.

In this research study, the ASBR was operated using the same reactor as the activated sludge reactor described earlier. However, the ASBR was operated with a

maximum fill volume of 7.0 L. The ASBR setup is shown schematically in Figure 5.1.2.1. As can be seen from the Figure 5.1.2.1, the main difference between the activated sludge reactor with recycle and the ASBR, is that the ASBR was operated without a sedimentation clarifier and without any sludge recycle. Air flow to the reactor was controlled through a flow meter and an electronic solenoid air valve controlled by a computer.

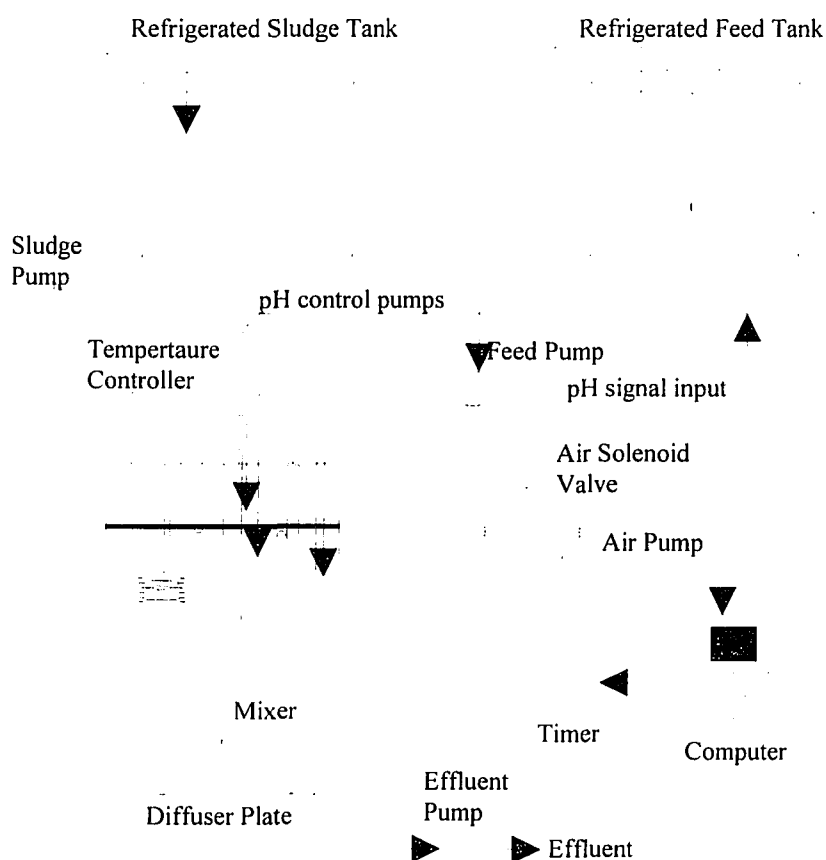


Figure 5.1.2.1. Schematic showing the Aerobic Sequencing Batch Reactor (ASBR) setup.

As in the case of the operation of the 20 L activated sludge reactor, all operations were controlled by a computer operating on an Intel 80286 processor and a 287 math

coprocessor. ANALOG CONNECTION[®] software from Strawberry Tree, Inc., CA, USA was used for data acquisition and control. The same equipment as described in the activated sludge reactor set up was used for the ASBR operation.

The operational characteristics of the ASBR are summarized in Table 5.1.2.1. The ASBR was operated on three cycles a day with five operational periods of fill, react, settle, draw and idle, as mentioned earlier in the discussion. The influent feed concentration was maintained at a COD value of 500 mg/L, expressed as oxygen. The feed composition to the reactor was also kept the same as described for the activated sludge reactor with recycle. The only exception was that pH control was achieved through buffering capacity provided in the feed substrate itself, instead of an active pH control system. Buffering capacity was added to the substrate by adding sodium bicarbonate to the feed mix. The ASBR was operated at room temperature which was about $20 \pm 5^{\circ}\text{C}$. Solids were wasted daily from the ASBR to maintain a total suspended solids concentration in the reactor at about 2500 mg/L. Air was pumped into the reactor during the react phase at a rate of 10 L/min. No air was pumped into the reactor during other phases of the cycle as it was found from experience that control of filamentous organisms was best achieved when an anoxic condition was provided during the fill phase of the cycle. This can be explained by the higher affinity to soluble substrate of flocculant microorganisms in near anoxic conditions as compared to filamentous organisms which have higher half saturation constants (K_s) for soluble substrates.

The ASBR was operated on a continuous basis from September 1993 through March 1994, and then again from October 1994 through March 1995. Daily analysis consisted of measuring the dissolved oxygen concentration during the react phase, pH,

Oxygen Uptake Rate (OUR), total and volatile suspended solids concentration in the reactor, effluent COD concentration and suspended solids in the effluent. The Sludge Volume Index (SVI) of the activated sludge solids was also determined occasionally to test the settling properties of the flocculant biomass. Excess sludge was pumped from the reactor daily into a refrigerated container at 4°C, and stored for subsequent characterization and sorption-desorption studies.

Table 5.1.2.1. Operational characteristics of the Aerobic Sequencing Batch Reactor (ASBR.).

Description	Value
Volume of reactor (Liters)	7
Influent COD (mg/L)	500
Effluent COD (mg/L)	16
Number of cycles per day	3
Fill time (hours)	2
React time (hours)	4
Settle time (hours)	0.75
Draw time (hours)	0.75
Idle time (hours)	0.5
Mean cell residence time (MCRT) (days)	6
MLSS in reactor (mg/L)	2500
MLVSS in reactor (mg/L)	2100
Ratio of MLVSS to MLSS :	0.84
Food to Microorganism ratio (F/M)	0.3
Air flow (LPM)	10

5.1.3 Pure Oxygen Process Activated Sludge

For the sorption-desorption study, activated sludge solids was also collected from an activated sludge treatment plant operated by the Passaic Valley Sewerage Commissioners

(PVSC), Newark, NJ, USA. PVSC uses a pure oxygen activated sludge treatment for secondary treatment of municipal and industrial wastewaters. The plant's influent is about 15% industrial by volume, and about 50% by strength. The dominant industries that discharge into PVSC include electroplating, pharmaceutical and organic chemical manufacturers, hospitals, etc.

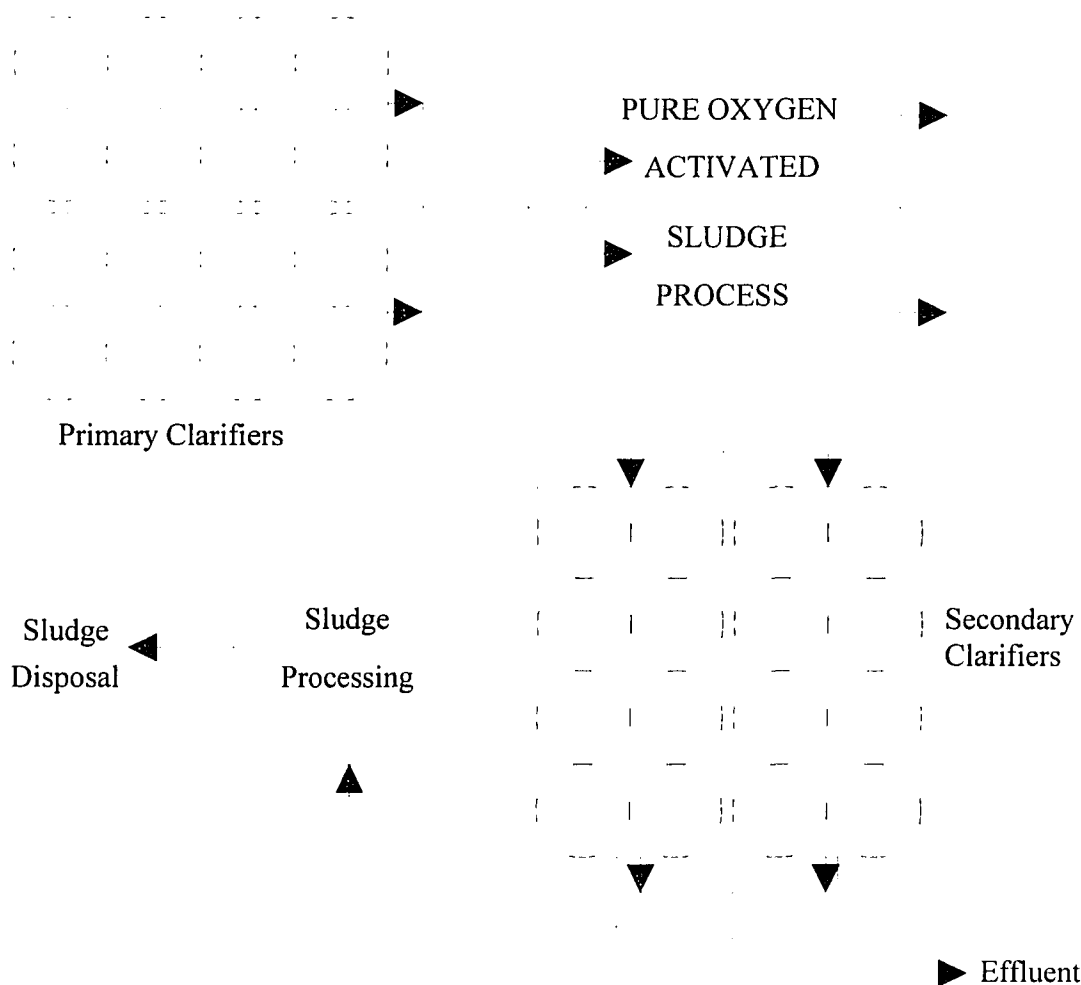


Figure 5.1.3.1. Schematic of the pure oxygen activated sludge treatment facility operated by the Passaic Valley Sewerage Commissioners (PVSC).

Operationally the treatment plant handles influent wastewater whose pollutant strength is double of that of the usual domestic sewage with industrial shock loads of 50 to 100% above the average. The plant is designed to handle an average of 330 MGD of wastewater with peak dry weather flows of 400 MGD, and peak wet weather flows of 550 MGD. Influent wastewater is pumped into twelve primary clarifiers using screw pumps. The effluent from the primary clarifiers are fed into twelve, four compartment biological oxidation tanks, each 58 ft by 235 ft by 30 ft deep, with mixer type rotating oxygen spargers utilizing pure oxygen for biological stabilization of the sewage. These activated sludge basins are located underground to ensure efficient utilization of pumped pure oxygen which is generated at the rate of 1000 tons per day.

The effluent from the activated sludge plant flows into twelve, three compartment final clarifiers. The overall layout of the treatment plant is shown in Figure 5.1.3.1. Activated sludge solids were collected from the aeration basins and transported in an ice box to the environmental engineering laboratory at NJIT for the experimental study. A microbiological analysis of sludge biomass from this treatment plant indicated an undesirably high concentration of filamentous organisms. The physical and chemical characteristics of sludge collected from this treatment facility are presented in Table 5.3.1 and 5.3.2.

5.2 Centrifugal Fractionation of Activated Sludge Solids

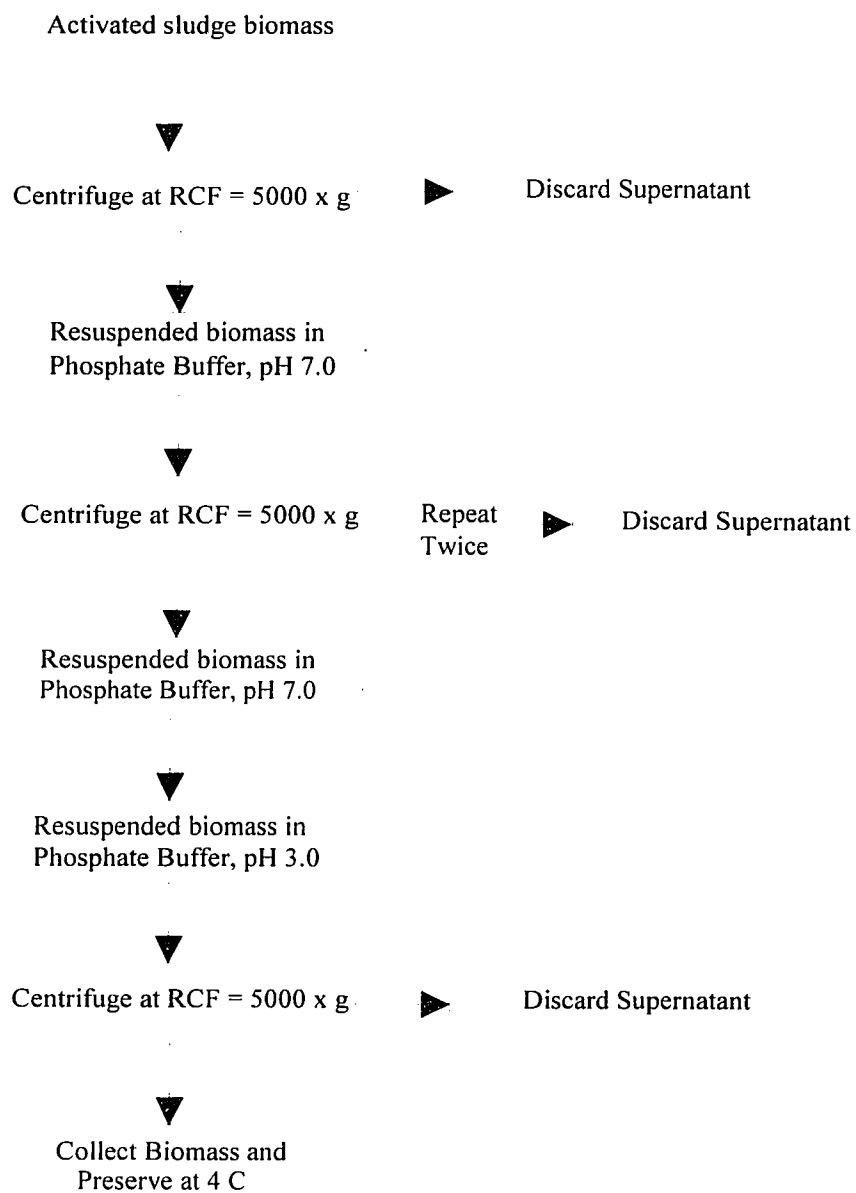


Figure 5.2.1. Experimental protocol used for the centrifugal fractionation of biosolids from waste activated sludge.

Activated sludge solids were collected from the different unit processes under evaluation and stored at 4°C in a refrigerator. The activated sludge solids were centrifuged at a Relative Centrifugal Force (RCF) of 5000 x g for 15 minutes. Centrifugal separations were conducted in an IEC centrifuge with a maximum attainable RCF of 5000 x g (International Equipment Company, MA, USA) using inert polypropylene copolymer centrifuge tubes.

After centrifugation, the supernatant was decanted from the centrifuge tubes, and the biomass was resuspended in a phosphate buffer at pH 7.0. This suspension was centrifuged once again at 5000 x g for 15 minutes. Biosolids were resuspended each time by scooping out the settled material with a thin spatula into a beaker of phosphate buffer solution at 4°C. The suspension of biosolids in phosphate buffer was then stirred gently using a magnetic stirrer bar until any large clumps that had settled in the beaker were resuspended in solution. The “washing” process was repeated twice with phosphate buffer at pH 7.0, and once with phosphate buffer at pH 3.0. Even though an acetate buffer would be the best suited for maintaining a pH of 3.0, phosphate buffer was used because it would not supply any additional carbon into the system that could be available for microbial utilization, or stimulate microbial activity. After the centrifugal fractionation, the “washed” biomass was stored in the concentrated form at 4°C in a glass PYREX[™] bottle for subsequent characterization and sorption-desorption experiments.

The centrifugal fractionation process was adapted from a procedure used earlier by Mukherjee and Levine for the separation of particulate organics from wastewater, and also by Ho and Tan for the fractionation of particulate material in palm oil effluent (Mukherjee, 1992, Mukherjee and Levine, 1992, Ho and Tan, 1983). The centrifugal

separation process is shown schematically in Figure 5.2.1. The characterization study included determination of Total and soluble organic carbon, Total and soluble COD, TSS, TVSS, TKN, etc. The characterization study is described in further detail in the following discussion.

5.3 Characterization of Activated Sludge Solids

Activated sludge solids collected from different activated sludge processes were characterized as received from these processes as well as after centrifugal fractionation of the biomass solids in a phosphate buffer solution, and the findings are summarized in Tables 5.3.1 and 5.3.2. Background concentrations of the target compounds (from the training set) in the biosolids were measured only on the “washed” and fractionated biosolids using hexane as the extraction solvent. All analytical determinations were conducted as specified by the Standard Methods for the Examination of Water and Wastewater, and the U.S. EPA’s Test Methods for Evaluating Solid Wastes, where applicable (APHA, 1989, U.S. EPA, 1982). Microbiological tests were conducted as per methods described by U.S. EPA (U.S. EPA, 1978). Microscopic examination of the activated sludge solids from the different sources was conducted periodically using a Zeiss microscope (Carl Zeiss, Germany). Particle size distribution determination was conducted on activated sludge solids as received from the different unit processes, and also on biomass prepared for sorption -desorption experiments using filtration techniques.

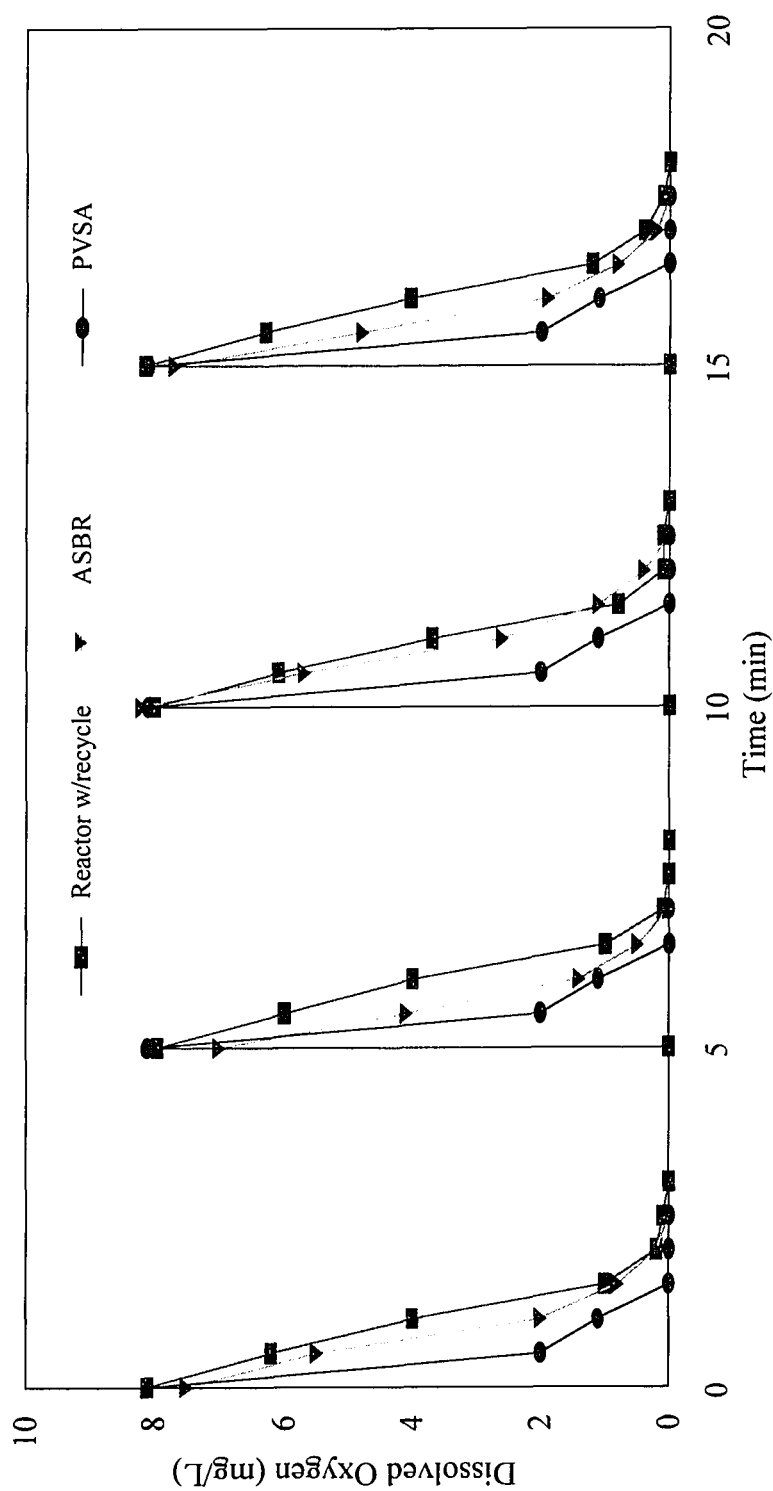


Figure 5.3.1. Dissolved oxygen uptake rates measured for activated sludge solids as received from the different activated sludge processes at 20°C.

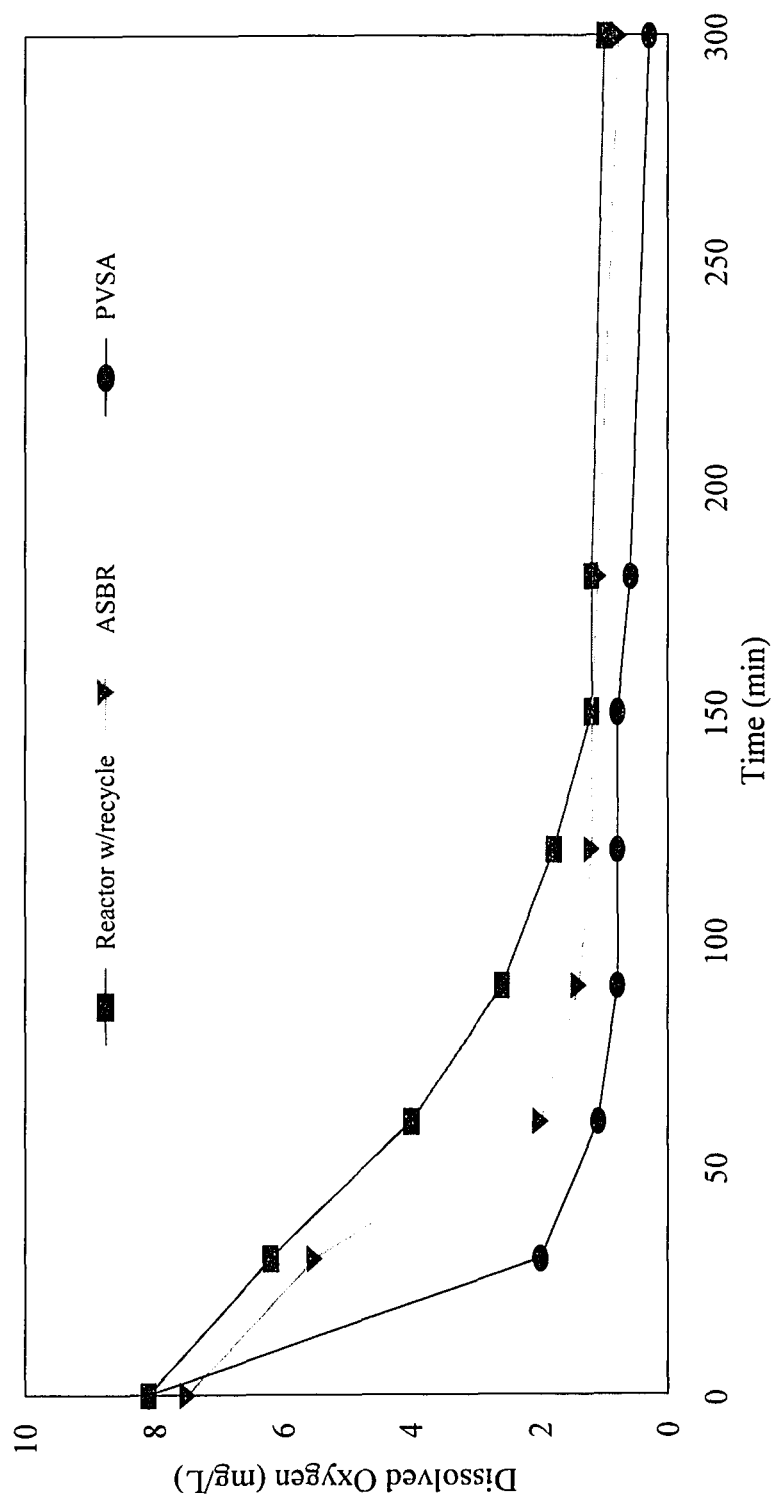


Figure 5.3.2. Dissolved oxygen uptake rates measured for activated sludge solids from the different activated sludge processes at pH 3.0 and temperature 20°C.

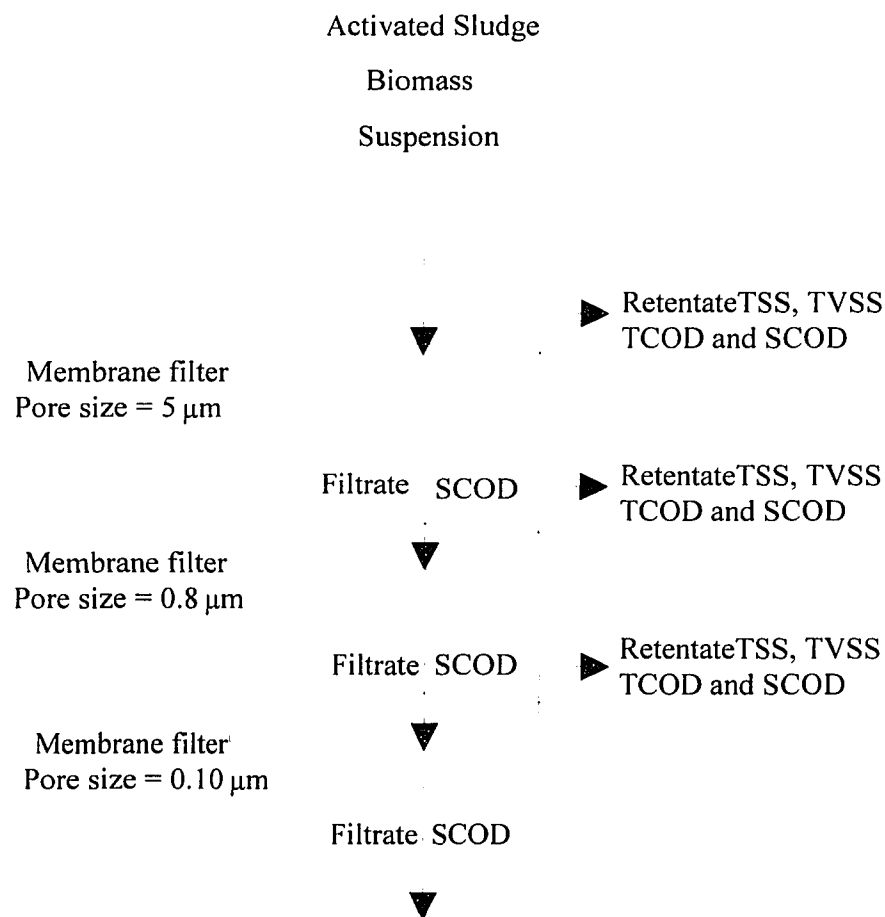


Figure 5.3.3. Experimental protocol used for quantification of particle size distribution in WAS using filtration techniques.

Mixed cellulose ester membrane filters obtained from Gelman with pore openings of 5 μm, 0.8 μm and 0.1 μm were used for this study (Gelman Sciences Inc., MI). The size distribution was determined by passing a suspension of activated sludge solids sequentially through a series of filters with pore openings of varying sizes. Figure 5.3.2 shows schematically the procedure adopted for measuring the particle size distribution of the activated sludge solids.

Table 5.3.1. Characterization of activated sludge solids before centrifugal fractionation of biosolids from different processes.

Parameter	Pure Oxygen	Reactor w/Recycle	ASBR
Total Solids, mg/L	2635	3050	3200
Total Suspended Solids, mg/L	1700	2800	2500
Total Volatile Suspended Solids, mg/L	1360	2250	2100
Total Organic Carbon	1088	1750	1820
Total Kjeldahl Nitrogen	151	225	241
pH	6.6	7.2	6.85
Oxygen Uptake Rate, OUR, mg O ₂ /g MLSS. h	33	21	11
Sludge Volume Index, SVI, ml/g ¹	203	157	109

¹Measured after a 30 min. settling time, vol. in mL occupied by 1 g of sludge

Table 5.3.2. Characterization of activated sludge solids prepared for sorption-desorption experiments.

Parameter	Pure Oxygen Process	Reactor w/Recycle	ASBR
Total Solids, mg/L	704	673	655
Total Suspended Solids, mg/L	672	644	624
Total Volatile Suspended Solids, mg/L	540	517	522
Total Organic Carbon, mg/L as carbon	500	500	500
Total COD, mg/L as oxygen	991	1045	1165
Soluble COD, mg/L as oxygen	15	42	61
pH	3.1	3.05	3.02

The particle size distribution of the different activated sludge solids was calculated on a mass basis. As shown in Figure 5.3.2, the different fractions of the activated sludge solids was analyzed for total and soluble COD as well as total suspended solids (TSS) and total volatile suspended solids (TVSS). The characteristics of the different particle sizes are summarized in Table 5.3.3. It was found that, on an average, 88% of the TVSS was greater than 5 μm in effective diameter, 8 % of the TVSS was between the size range of 5 to 0.8 μm . and retentate on the 0.1 mm filter accounted for the remaining. In this experiment, TSS is described as the total suspended solids content of the retentate, and TVSS is described by the volatile content of the retentate on the

respective filters. It should be noted here that these definitions for the measured solids parameters does not refer to the solids described by the Standard Methods (APHA, 1989).

The analysis on the different fractions of the activated sludge solids from the three unit processes was conducted on the same biomass stock whose gross characteristics are presented in Tables 5.3.1 and 5.3.2. The results from this characterization study were found to be in good agreement with those available in the literature (Droste and Sanchez, 1983, Hoepker and Schroeder, 1979, Dammel and Schroeder, 1991, Knocke, 1992, Pujol, 1992, Jacobsen *et al.*, 1993).

Table 5.3.3. Characteristics of organic material fractionated using filtration techniques.

Parameter	Pure Oxygen			Reactor w/Recycle			ASBR		
	a	b	c	a	b	c	a	b	c
TSS, mg/L	1420	150	130	2000	150	350	2200	200	100
TVSS, mg/L	1200	120	40	1825	145	280	1850	168	82
TCOD, mg/L (as O ₂)	2184	235	12	3400	310	23	3500	965	15
SCOD, mg/L (as O ₂)	78	17	11	150	25	3	105	30	5

a = > 5 μm

b = < 5 μm but > 0.8 μm

c = < 0.8 μm but > 0.1 μm

5.4 Sorption-Desorption Experiments

From the discussion presented earlier on the effects of experimental conditions on the measurement of sorption-desorption coefficients, it was evident that the first step in this research study would have to be to resolve the uncertainties and develop an experimental protocol ideally suited for the objectives of this research study, the biomass matrix and the resources available at this research facility. The aspects of experimental methodology that would have to be developed and verified as being appropriate to our study included investigation of (i) the concentration of biosolids used as the sorbent matrix, (ii) the range

of concentrations for the target compound, (iii) the equilibration time, and (iv) the protocol for fractionation/separation of the solid phase from the aqueous phase.

An experimental protocol to evaluate the above mentioned parameters was developed on the basis of the best available study on the effects of experimental conditions on sorption-desorption experiments (Dobbs *et al.*, 1986). In their experimental work, activated sludge was collected from numerous wastewater treatment plants in and around Cincinnati, Ohio, USA. The collected sludge was centrifuged in a bowl centrifuge at $2000 \times g$, and then stored at 4°C for subsequent sorption experiments. It was found that centrifugation of Waste Activated Sludge (WAS) at $2000 \times g$ resulted in a solids capture of $> 99\%$ of the biosolids present in WAS. However, no mention was made of the efficiency of Total Organic Carbon (TOC) recovery, even though the authors have based some of their linear regression models on the concentration of organic carbon (Dobbs *et al.*, 1986). The presence of Dissolved Organic Carbon (DOC) along with organic material that is difficult to settle has been acknowledged as being an important factor in sorption studies as they can act as a sorbent medium with high sorption capacities (Wang, 1993, Wang *et al.*, 1993). Based on this information, the calculation of Stokes' diameter of particles settling in a force field, and the availability of an appropriate centrifuge, it was decided to conduct this experimental study at a RCF of $5000 \times g$, the maximum attainable with equipment available in the laboratory. The apparent Stokes' diameter for particulates in a force field is shown in Figure 5.4.1. The Stokes' diameter of the particulates in wastewater was calculated using Equation (5.4.1).

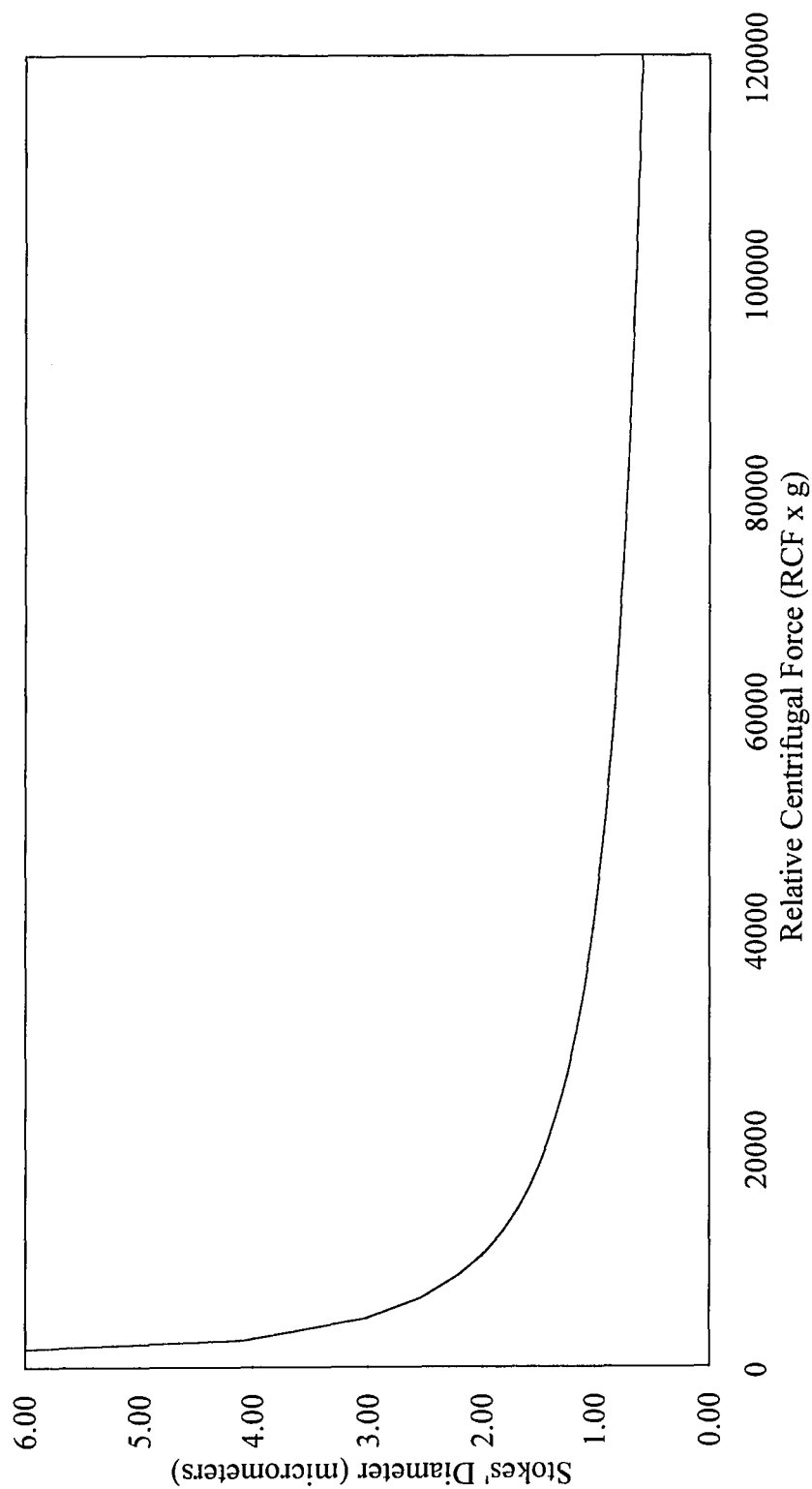


Figure 5.4.1. Centrifugal separation of activated sludge solids at different RCFs at 20°C, water density = 998.2 kg/m³, density of biomass = 1050kg/m³, dynamic viscosity = 0.001002 N.s/m², and settling velocity = 0.0012 m/s.

$$d_s = \sqrt{\frac{18 \mu_s v_s}{(\rho_s - \rho_w) g}} \quad (5.4.1)$$

where

d_s = Calculated Stokes' diameter, m

μ_s = dynamic viscosity, N.s/m²

v_s = settling velocity, m/s

ρ_s = density of particle, kg/m³

ρ_w = density of water, kg/m³

g = acceleration due to gravity, m/s²

Suspensions of biosolids for the measurement of sorption-desorption parameters was prepared to the desired TOC concentration range by resuspending previously fractionated and preserved activated sludge solids in phosphate buffer. The amount of biomass added to the phosphate buffer was dictated by a final target TOC concentration for the biomass suspension. The TOC was measured on an O-I Analytical automatic TOC analyzer using the persulfate oxidation technique (O-I Analytical, CA, USA). Methodology for the determination of TOC was adapted to the measurement of biosolids as per the O-I Analytical instruments guidelines. TOC determinations were only made when a fresh batch of biosolids was fractionated from the original activated sludge. The ratio of TOC to TVSS was used for all other estimates as a surrogate measure.

Preserved biomass with a known TOC value was added to a beaker of phosphate buffer (pH 3.0, 20°C) and stirred gently with a magnetic stirrer bar till all clumps that had

settled to the bottom of the beaker were resuspended, and the overall solution temperature was 20°C. This protocol was followed for all the sorption experiments using activated sludge solids from different unit processes. All sorption-desorption experiments were conducted in 50 mL disposable centrifuge tubes equipped with TEFLON[®] lined screw caps, in a phosphate buffer medium at pH 3.0, temperature of 20°C and shaken on a gyratory shaker (Junior Orbit Shaker, Lab-Line Instruments, Inc., IL, USA) at 300 RPM.

The first step in the preliminary study was to evaluate the effect of the concentration of biosolids on the determination of sorption coefficients. Since this protocol was based on the experimental work by Dobbs *et al.*, this part of the study was conducted using methylene blue dye as the target compound (Dobbs *et al.*, 1986). In their experiment methylene blue dye was chosen as the target compound since this compound is known to be non-volatile and non biodegradable, making design of preliminary experiments and analysis relatively easy. In this research study varied concentrations of activated sludge solids collected from the 20 L activated sludge reactor with recycle was used as the test sorbent matrix, while the concentration of methylene dye was kept constant. The range of biosolids used was 0, 0.05, 0.1, 0.5 and 1 g/L as TOC, and the methylene blue dye concentration was kept constant at 10 mg/L. Biomass suspensions prepared as a batch were dispensed into centrifuge tubes and methylene blue dye was added to each tube. Two set of controls were run with each experiment, (i) phosphate buffer and dye with no biomass, and (ii) phosphate buffer and biomass with no dye. The centrifuge tubes were placed in a gyratory shaker and shaken for a period of six hours at 20°C. Tubes were removed for analysis and centrifuged at 5000 x g, and the supernatant was analyzed at 665 nm on a spectrophotometer (Spectronic 501, Milton Roy, USA).

It was observed that no color from the dye was visible after a half hour to forty five minutes of the experiment. Neither the data collected by Dobbs *et al.* or his research paper discussed this phenomenon, and so it was assumed that an error was being made in the experimental protocol somewhere. However, after many months of observations, no reasonable data could be collected. On searching the literature for clues, it was found that methylene blue dye is converted to a colorless form (leucomethylene blue) in a reduced environment (Jorgensen, 1984). During the sorption process, the biomass is not totally inactive and hence exhibit a small oxygen uptake, thereby reducing the oxidation potential of the biomass suspension. Since the oxidation reduction potential (ORP) in the biomass suspension was reduced during the course of the experiment causing decoloration of the methylene blue dye, no observations could be made using this compound. It is evident from this that methylene blue dye cannot be used as a tracer compound even in slightly bioactive systems. Hence, azo dye 151 (also called acid red 151, $C_{22}H_{15}N_4O_4SNa$), obtained from Sigma (Sigma Chemical Co. USA), was used as the target compound, and the same experiment was repeated. The concentration of the azo dye was measured in the supernatant at a wavelength of 512 nm using a spectrophotometer. The results from this study are shown in Figure 5.4.2. The collected experimental data was found to be best described by the Freundlich isotherm, and a computer software (Quattro Pro[®], Novell, Inc., USA) was used to perform a linear regression and curve fit the data. The raw data collected from the experiment are presented in the Appendix. Equation (5.4.2) is the Freundlich isotherm calculate to describe the results of this sorption study.

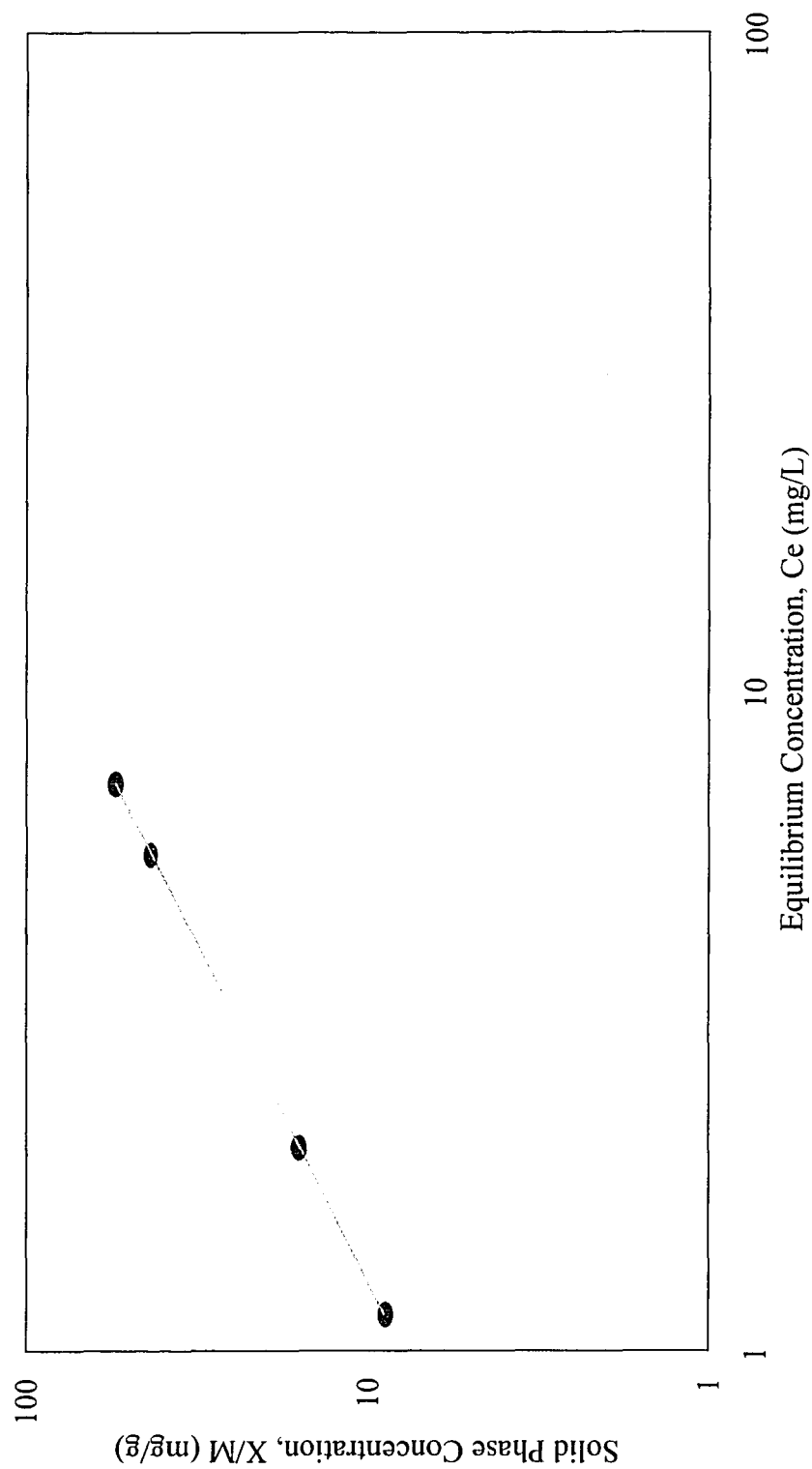


Figure 5.4.2. Freundlich isotherm developed for varying concentrations of substrate biosolids, azo dye concentration remaining constant.

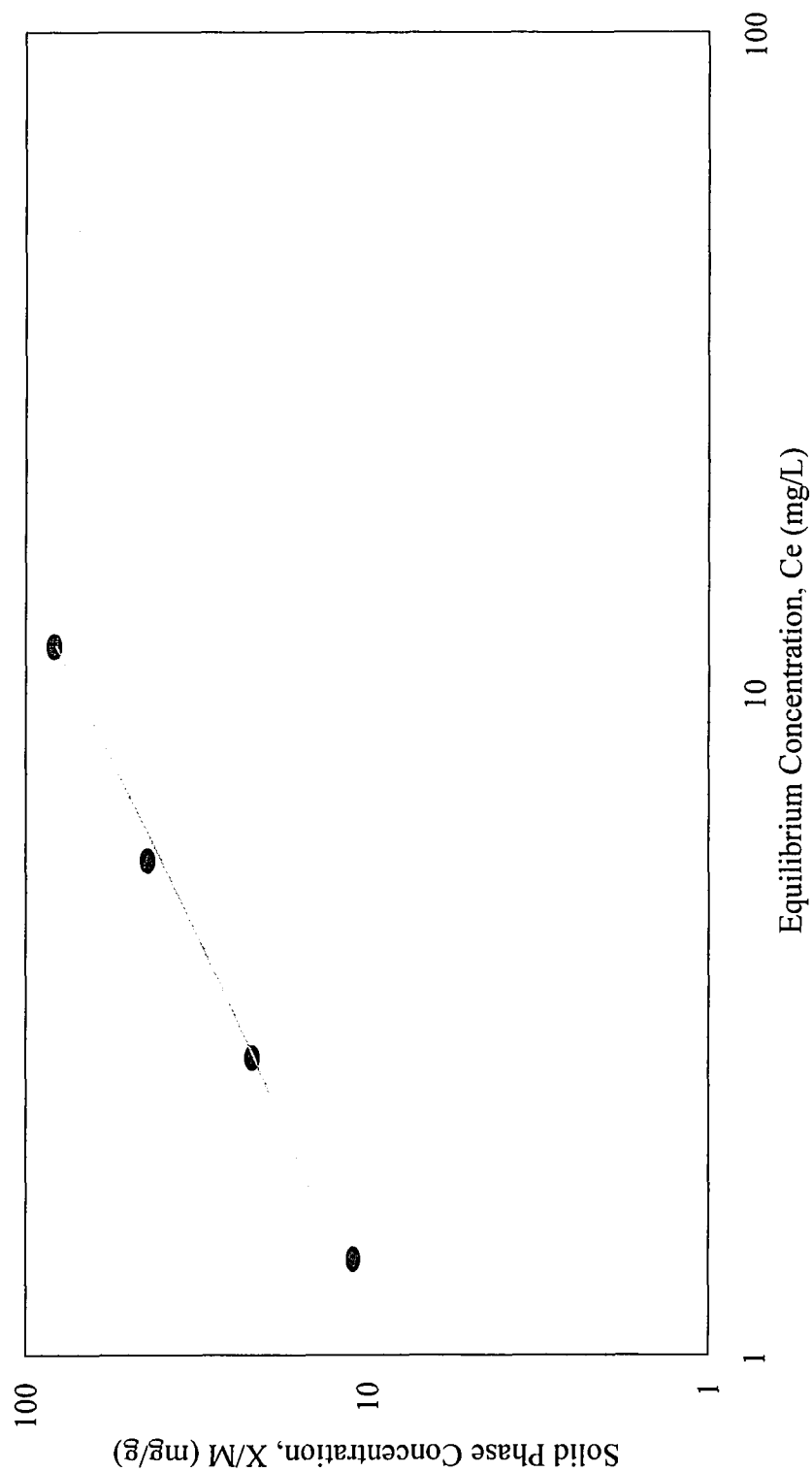


Figure 5.4.3. Freundlich isotherm developed for varying concentrations of azo dye 151, substrate biosolids concentration remaining constant.

$$\log \left(\frac{x}{m} \right) = \log (7.89) + 0.98 \log (C_e) \quad (5.4.2)$$

In the next phase of the preliminary study, the effect of the concentration of the target compound on sorption parameters was evaluated. In this study the concentration of the biosolids in suspension was maintained constant at a TOC of 0.5 g/L, while the concentration of azo dye 151 was varied over a range of 0, 2.5, 5, 10 and 20 mg/L. The same experimental procedure was followed as described earlier for the determination of sorption coefficients using varied solids concentrations. The results from this study is shown in Figure 5.4.3. As in the previous case, the collected experimental data was found to be best described by the Freundlich isotherm, and a linear regression was used to curve fit the data. The raw data collected from the experiment are presented in the Appendix. Equation (5.4.3) is the Freundlich isotherm describing this experiment.

$$\log \left(\frac{x}{m} \right) = \log (7.86) + 0.99 \log (C_e) \quad (5.4.3)$$

It can be seen from the evaluation of the Freundlich parameters in equations (5.4.2) and (5.4.3) for the sorption of azo dye 151 on activated sludge solids for varied concentrations of dyes and biosolids that there is no significant “solids-effect” observable over the range of solids and target compounds examined. The concentrations chosen gave a ten fold variation in the solids to liquid ratio which are typical of the conditions used to measure partition coefficients in wastewater (Dobbs *et al.* 1986).

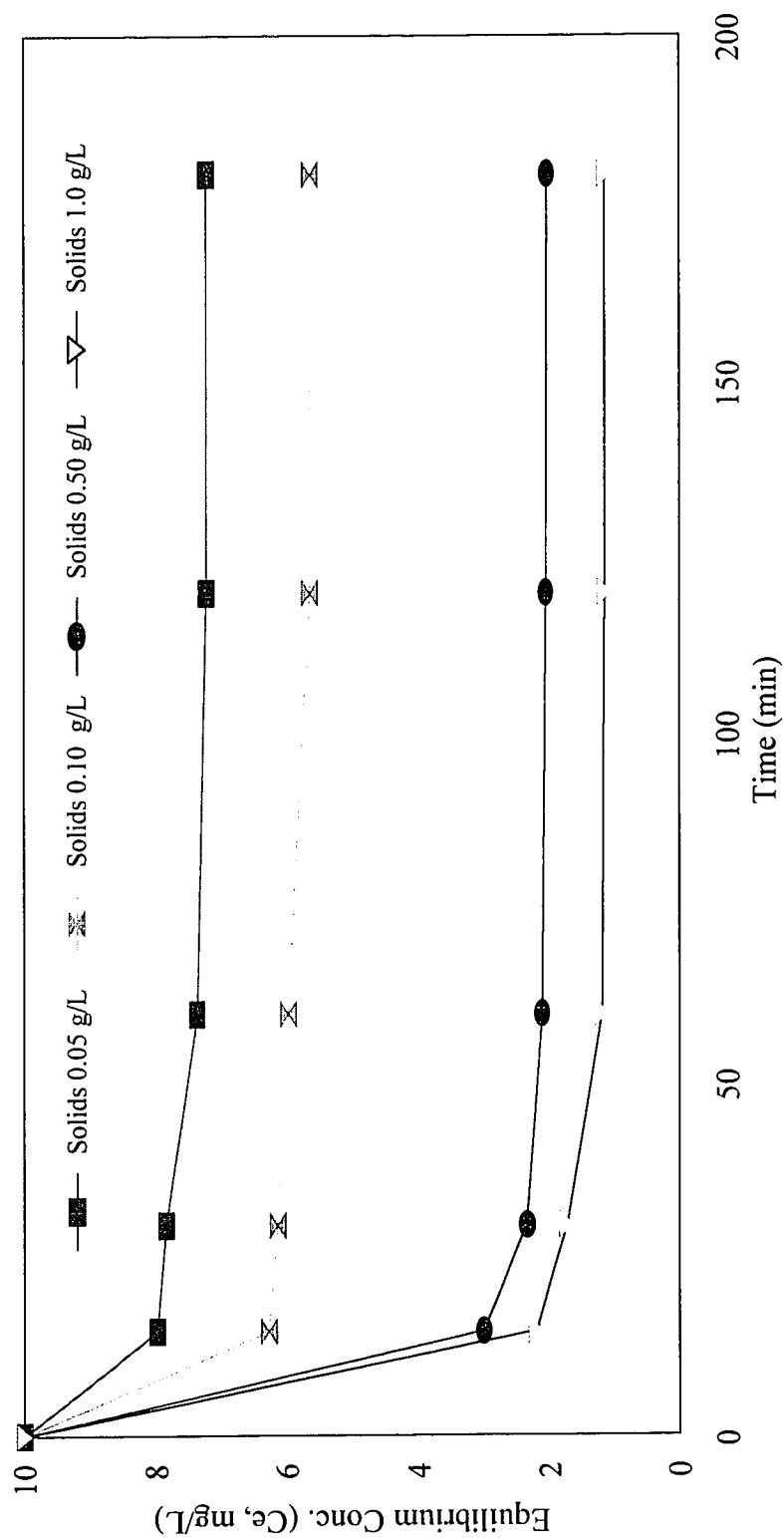


Figure 5.4.4. Kinetics of sorption of azo dye 151 on activated sludge solids. Concentration of azo dye is constant, biomass solids concentration varied.

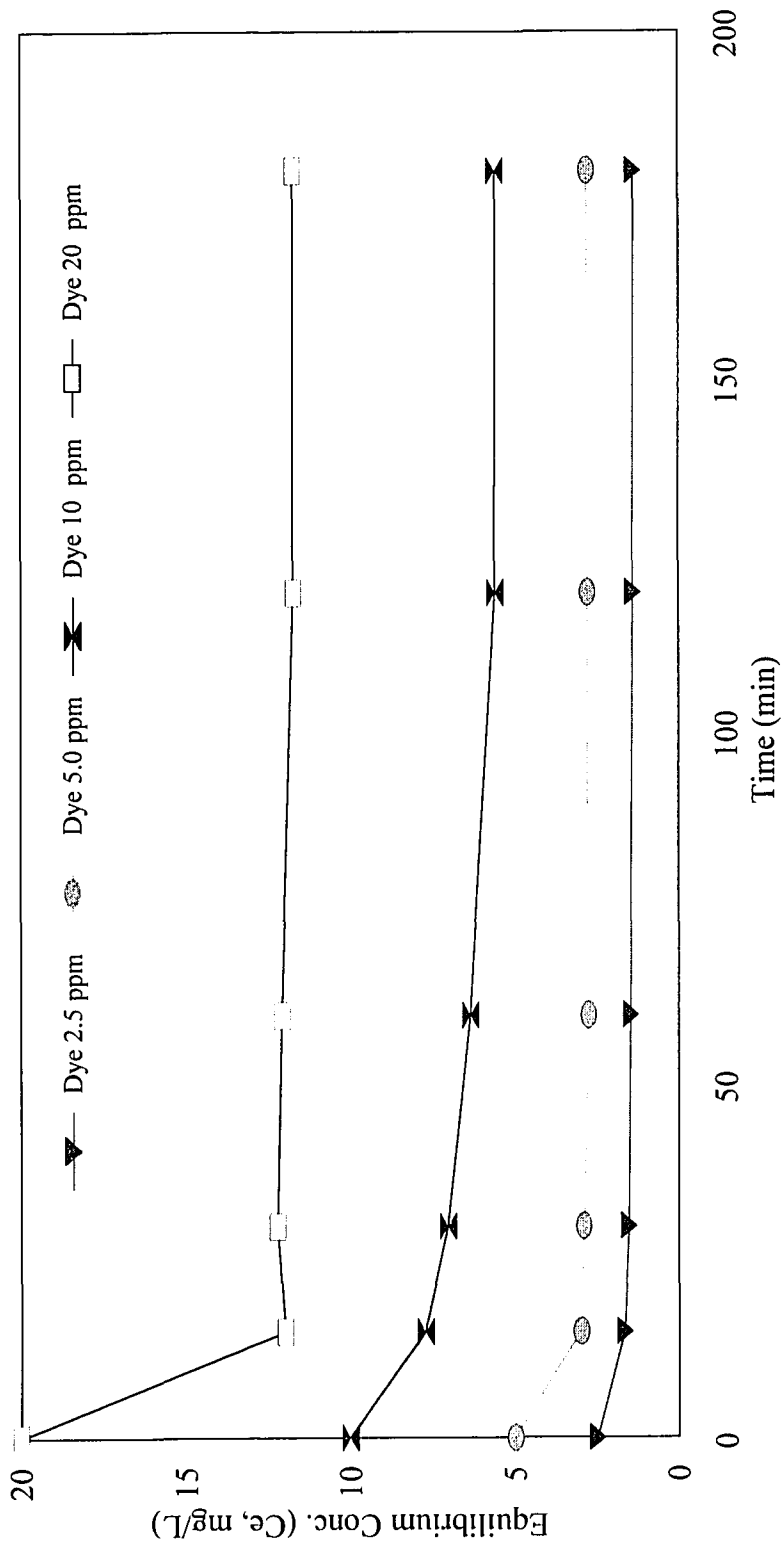


Figure 5.4.5. Kinetics of sorption of azo dye 151 on activated sludge solids. Concentration of biomass solids is constant, azo dye concentration varied.

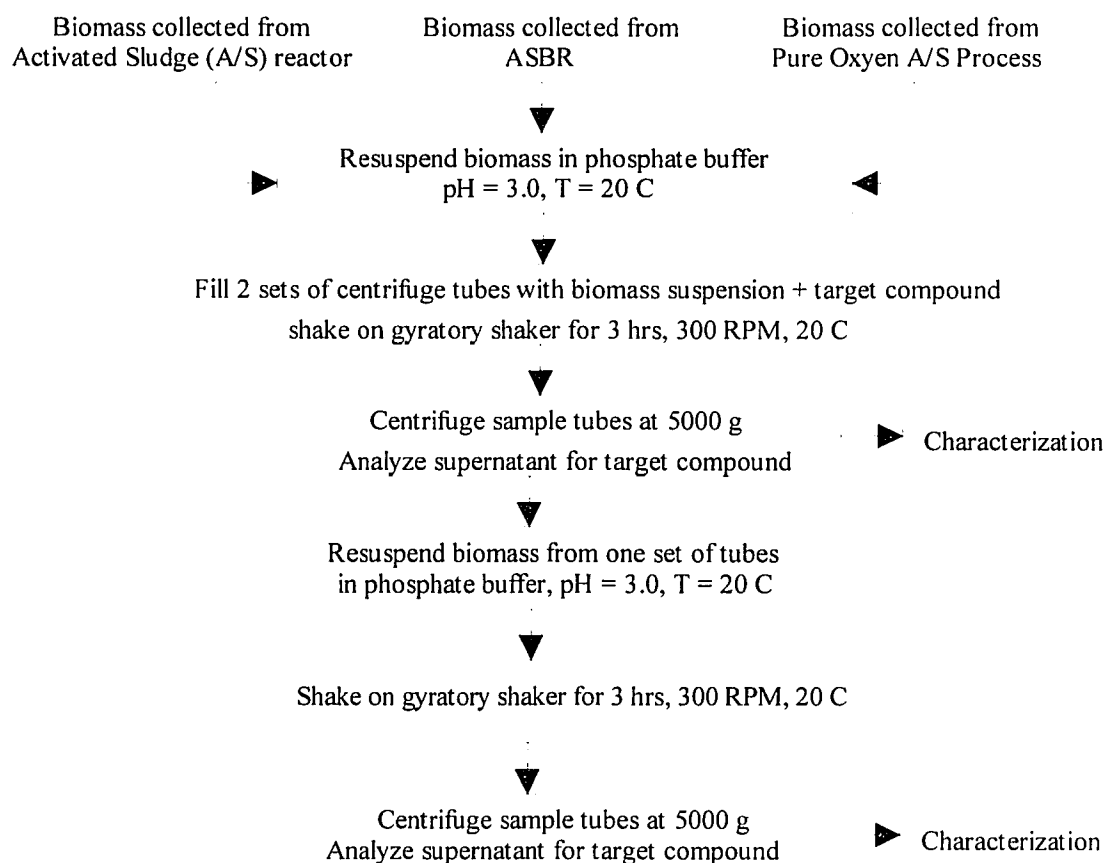


Figure 5.4.6. Experimental protocol used for quantifying sorption-desorption processes in activated sludge solids.

Since it was shown that solids to aqueous phase ratio is not an issue of concern, it was decided that all sorption-desorption experiments would be conducted at a biosolids concentration of 500 mg/L as TOC, and the concentration of the target compound would be varied across its solubility range. The biosolids concentration of 500 mg/L was chosen as an experimental constant as this corresponds to about 1500 mg/L as TSS, which is the TSS concentration at which many activated sludge plants operate. Secondly, a constant solids concentration as opposed to a constant target compound concentration was chosen as it is easier to correct analytical values of the equilibrium concentrations in the samples

by a constant amount, if the natural background of the target compound is found to be high or varied (Dobbs *et al.*, 1986). Studies conducted in this research study, using azo dye 151 have shown that maximum sorption was observed during the first 30 minutes of contact. There was no observable change in the liquid and solid phase concentrations after 3 hours, indicating that a condition of “near-equilibrium” had been attained.

An exposure time of about 3 hours would reduce the probability of biodegradation being a likely pathway for the removal of the target compound from the soluble phase as well. It was also observed from experimental experience with subsequent desorption studies that a longer sorption time seriously affected the characteristics of the biosolids. It was found that after a six hour exposure during the sorption experiment, and half way into the desorption experiment, efficient separation of phases could not be made with the RCFs used for this experimental study due to the physical deterioration of the biosolids. Also, since most activated sludge treatment operations have a hydraulic detention time of 3 to 4 hours (intimate contact between solid phase and bulk liquid), the equilibrium time chosen for this study would be appropriate. Figures 5.4.4 and 5.4.5 show the equilibrium concentration of the azo dye in the aqueous phase relative to time, from experiments conducted to evaluate the effect of equilibration time on sorption experiments.

Based on the results from the preliminary experiments, the following experimental protocol was developed for the conduct of all sorption-desorption experiments. For each set of sorption-desorption experiments, a biomass suspension of 500 mg/L TOC was prepared as a batch in a phosphate buffer at pH 3.0 and temperature 20°C. Measured aliquots of this biomass suspension were dispensed into disposable 50 mL centrifuge tubes with TEFLON[®] lined screw caps, using a Brinkmann Dispensette[®]

(Brinkmann, Germany). Care was taken to ensure that the centrifuge tubes were filled to the top to ensure zero head space conditions. Pure target compound was then introduced into each centrifuge tube, at the bottom using a Micro-Mate[®] interchangeable glass syringe equipped with a Luer lock hypodermic needle (Popper & Sons, Inc., NY, USA). Each centrifuge tube was capped immediately after introduction of the target compound. Two sets of five centrifuge tubes each, were identically prepared for every sorption-desorption study. Two sets of controls were also prepared for each experiment: (i) phosphate buffer and target compound with no biomass, and (ii) phosphate buffer and biomass with no target compound. The centrifuge tubes were then shaken on a gyratory shaker at 300 RPM for 3 hours in a controlled temperature environment at 20° C. Both sets of tubes and controls were centrifuged at the end of 3 hours at 5000 x g for 15 minutes. The supernatant from both sets of tubes were analyzed for the target compound using a gas chromatograph.

While activated sludge solids from one set of tubes was subject to a characterization study, activated sludge solids from the other set of tubes was resuspended in phosphate buffer at pH 3.0, and temperature 20° C. The centrifuge tubes were filled with phosphate buffer ensuring zero head space conditions. The desorption experiment was conducted using the same experimental protocol as the sorption experiment. At the end of 3 hours, the sample tubes and controls were centrifuged at 5000 x g, and the supernatant was analyzed for the target compound using a gas chromatograph. The biomass from these tubes were subject to a characterization study as well. The experimental protocol used for the sorption-desorption study is shown schematically in Figure 5.4.6.

Gas chromatographic analysis was performed using either a Perkin Elmer GC 8500 (Perkin Elmer, Norwalk, CT, USA) or a HP 5890 (Hewlett Packard, USA). The chromatographic conditions used for the analysis are presented in Table 5.4.2. The analytical procedure adopted for the analysis conformed to those specified by U.S. EPA Method 624 for the examination of volatile compounds in soil and water matrices. Direct aqueous injections were made for the determination of the analytes. 2 μ L samples were injected into a stainless steel SUPELCOPORT 8' x 1/8", 60/80 Carboxen B/1% SP-1000 packed column. Helium (purity 99.999%) was used as carrier gas, while air and hydrogen were used for the Flame Ionization Detector (FID). Determinations of the concentration of the target compound in the aqueous phase was made easy by the presence of a single target analyte at any given time in each aqueous injection.

Table 5.4.1. Frequency and methodology for different analytical determinations during the sorption and desorption studies.

Measurement	Frequency	Method
Halogenated Aliphatic	0, 180, 360 min	GC, FID
Total Organic Carbon	Initial	TOC Analyzer
Soluble Organic Carbon	Initial	TOC Analyzer
Total COD	Initial, Final	Closed Reflux, Titrimetric
Soluble COD	Initial, Final	Closed Reflux, Titrimetric
Total Suspended Solids (TSS)	Initial, Final	Gravimetric
Total Volatile Suspended Solids (TVSS)	Initial, Final	Gravimetric
Particle Size Distribution	Initial, Final	Filtration Techniques
Microbiological Characterization	Periodical	Microscopic Observations

Mass balance calculations based on the initial concentration of the target compound in the aqueous phase and at the end of sorption experiments showed that the accuracy of the experimental and analytical protocol was about $\pm 5\%$. However, the accuracy of the mass balance dropped to $\pm 17\%$ at the end of the desorption experiments.

It was observed that scatter in data was the most for the highly volatile organic compounds like trichlorofluoromethane and methylene chloride, and relatively better for compounds with higher boiling points.

Table 5.4.2. Gas chromatographic conditions used for determination of target compounds.

Description/Parameter	
Detector	FID
Oven temperature program	35°C (3 min) to 225°C at 10°C/min, hold 5 min
Injector temperature	145°C
Detector temperature	250°C
Column (Supelco, Inc., PA, USA)	8' x 1/8" OD stainless steel 60/80 Carbopack B/1% SP-1000
Carrier gas, Flow rate	Helium, 30 mL/min
Hydrogen flow rate	30 mL/min
Air flow rate	300 mL/min
Carrier gas flow rate	30 mL/min
Sample injection volume	2 µl

5.5 Phase Separation at Higher RCFs

To evaluate the effect of RCF in the separation efficiency of centrifugal techniques to separate suspended organic matter from the aqueous phase, activated sludge from the PVSC was centrifuged using a sequential technique that has been used successfully in the past to fractionate particulate organics from wastewater (Mukherjee, 1992, Mukherjee and Levine, 1992). Centrifugation of activated sludge solids from the three different activated sludge solids was conducted using a Sorvall® RC-28 S supraspeed high capacity refrigerated centrifuge equipped with a F 16/250 rotor capable of generated a RCF of up to 40000 x g (Du Pont Company, Delaware, USA). The activated sludge solids

suspension was prepared using preserved samples of biomass from different activated sludge unit processes. The suspensions were prepared using the same experimental protocol as discussed earlier. The activated sludge solids fractionated at different RCFs were characterized for their Soluble COD (SCOD) and Total COD (TCOD) to quantify the efficacy of organic materials capture at corresponding RCFs.

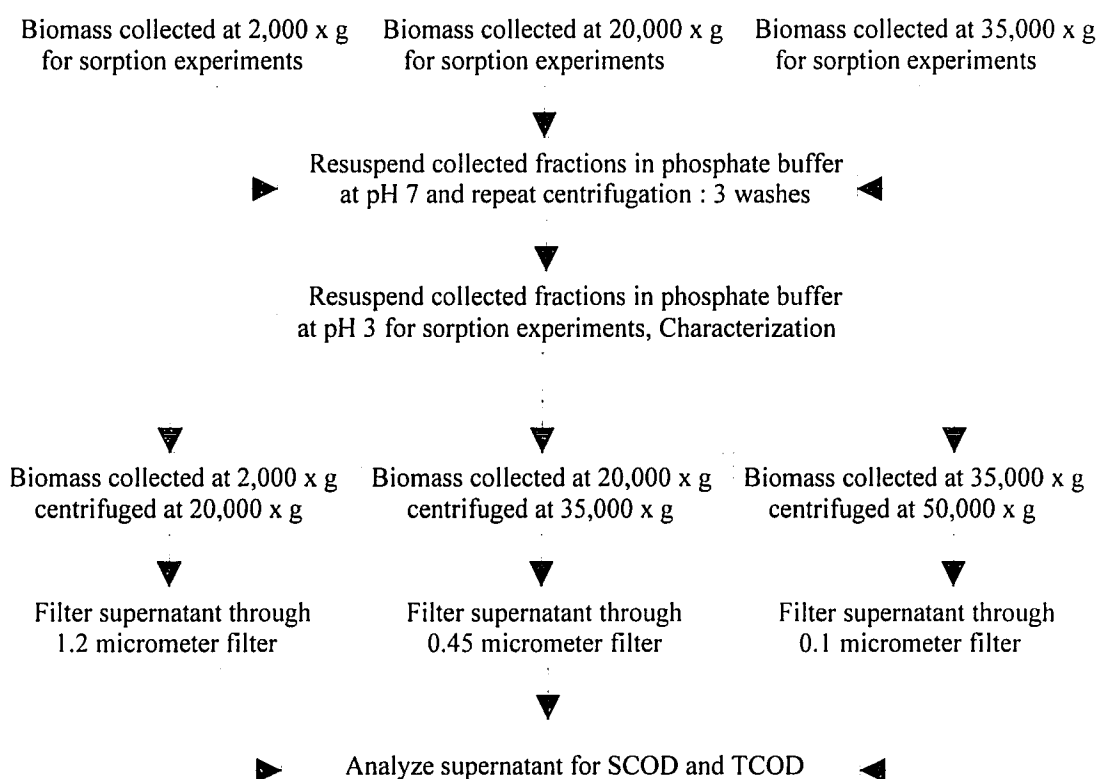


Figure 5.5.1. Experimental protocol used to evaluate the effect of using higher RCFs for phase separation on the determination of sorption-desorption parameters.

Sorption experiments were conducted using activated sludge solids collected from the pure oxygen activated sludge process (PVSC). Experiments were conducted using azo dye 151 with solids fractionated at phase separation RCFs of 2,000 x g, 20,000 x g and

35,000 x g. The experimental protocol adopted for this study was the same as that used in the previously discussed sorption experiments. As shown in Figure 5.5.1, the only difference was that higher RCFs were used for phase separation at the end of the sorption experiments. A higher RCF was used at the end of the equilibration time to make sure that organic material released from the sorbent matrix during the sorption experiment was captured as the solid phase, hence making mass balance calculations more relevant.

5.6 Calculation of Molecular Connectivity Indexes using GRAPHIII[®]

Molecular connectivity indexes were calculated using GRPAHIII[®] software developed by Dr. Alexander Sabljic (Sabljic, 1989). The software was provided free of charge for use in this research study by Dr. Robert Boethling, U.S. EPA, Office of Risk Evaluation, Washington D.C., USA. Molecular connectivity indexes in this research study were either calculated by creating an input file in GRAPHIII[®] or by inputting data in the SMILES format into a subroutine that could indirectly calculate the molecular connectivity indexes. The GRAPHIII[®] program can calculate up to the sixth order simple and/or valence molecular connectivity chi index. The GRAPHIII[®] program essentially uses the same algorithms as those developed by Kier and Hall discussed earlier in the section on molecular connectivity indexes. The calculated simple and valence χ indexes for the AX class of compounds is presented in the Appendix.

CHAPTER 6

RESULTS AND DISCUSSION

6.1 Effect of RCF on Phase Separation Efficiency

As reported in the literature review, there is evidence that quantification of sorption-desorption processes are strongly influenced by phase separations techniques employed to separate the aqueous phase from the particulate phase to which contaminants sorb on to. It is still unclear as to which fraction of the sorbent matrix is favored most during the sorption process, and why. Although it was beyond the initially stated scope of this research study, it was felt that an attempt should be made to quantify the efficacy of using different RCFs for the centrifugal fractionation of particulate organics in activated sludge solids. Activated sludge solids from the three different unit processes were sequentially centrifuged, and a mass balance was made on the basis of COD. The mass balances were calculated using Equation (6.1.1), which assumes that the total organic content, as measured by COD, of the system remains constant, while a fraction of the particulate organics in the activated sludge solids may undergo decay and lysis, resulting in increased “solubilized” fractions in the aqueous phase during sorption-desorption experiments (Mukherjee, 1992, Mukherjee and Levine, 1992).

$$\begin{aligned}\text{Organic}_{\text{Total}} &= \text{Organic}_{\text{Particulate}} + \text{Organic}_{\text{Soluble}} = \text{Constant} \\ \Delta \text{Organic}_{\text{Soluble}} &= -\Delta \text{Organic}_{\text{Particulate}}\end{aligned}\tag{6.1.1}$$

COD was measured as a surrogate parameter to organic carbon concentration in the activated sludge solids. The use of COD as a basis for quantifying the soluble and the particulate phases in wastewater has been shown to be effective earlier (Mukherjee, 1992). Also, COD to TOC ratios were found to be very consistent for the range of activated sludge solids used in this research study. Similarly, Soluble COD (SCOD) was measured as a surrogate parameter to the measurement of Dissolved Organic Carbon (DOC). Soluble, in this phase of the study is defined as that fraction which passes through a membrane filter with pore openings of 1.2, 0.45 and 0.1 μm , as shown in Figure 5.5.1. The extent of soluble COD recovered at different RCFs is indicative of the efficiency of phase separation technique employed, and is expressed as a ratio of the soluble to the total COD. The best possible fractionation is at the RCF where the SCOD/TCOD ratio is the lowest.

The separations possible at different RCFs as related to the Stokes' diameter of the suspended particles at 20°C is shown in Figure 5.4.1. Since a major fraction of the activated sludge solids occurs around the size range of 1 to 100 μm , it can be seen from this figure that optimum removal efficiencies can be attained from 20000 x g to about 40000 x g. This hypothesis was evaluated by measuring the SCOD/TCOD ratio in the supernatant at different RCFs. During this experimental study it was found that complete separation of SCOD from the aqueous phase could not be achieved even at a RCFs of up to 40000 x g. This may be explained by the presence of Dissolved Organic Carbon (DOC) and colloidal species in the aqueous phase of the activated sludge which require significantly higher RCFs and longer durations of centrifugation (Brock and Madigan,

1991). The results from this experimental study are presented in Figures 6.1.1, 6.1.2 and 6.1.3.

In a typical procaryotic cell fractionation, in which a cell is mechanically ruptured through sonication or high pressure, the cell material suspension is first centrifuged at $10000 \times g$ for 10 minutes. The material at the bottom of the centrifuge tube (pellet) contains membrane fragments, ribosomes and cytoplasmic cell constituents (Brock and Madigan, 1991). An ultracentrifugation of the supernatant at RCFs of up to $100000 \times g$ can yield other cell constituents in the pellet. In this research study a RCF of $5000 \times g$ was used for the fractionation of biosolids from the activated sludge solids suspensions. The loss of organic material in the aqueous phase supernatant with every wash become even more evident when the SCOD/TCOD ratios are considered. The loss of organic material with every wash indicates a potential loss of sorption capacity, particularly for material in the lower particle size ranges.

It is evident from Figures 6.1.1, 6.1.2 and 6.1.3., relating RCF to the SCOD/TCOD ratios of the different activated sludge solids suspensions that the need for effective phase separation becomes pronounced with increasing lengths of the equilibration time. It can be seen that almost twice as much organic material is present in the aqueous phase after three hours of equilibration and fractionation at $2000 \times g$ as compared to fractionation at $35000 \times g$ for all biomass samples evaluated. After 6 hours of equilibration time, this difference is significant enough to seriously affect the validity of analytical measurements made with relatively low phase separation RCFs.

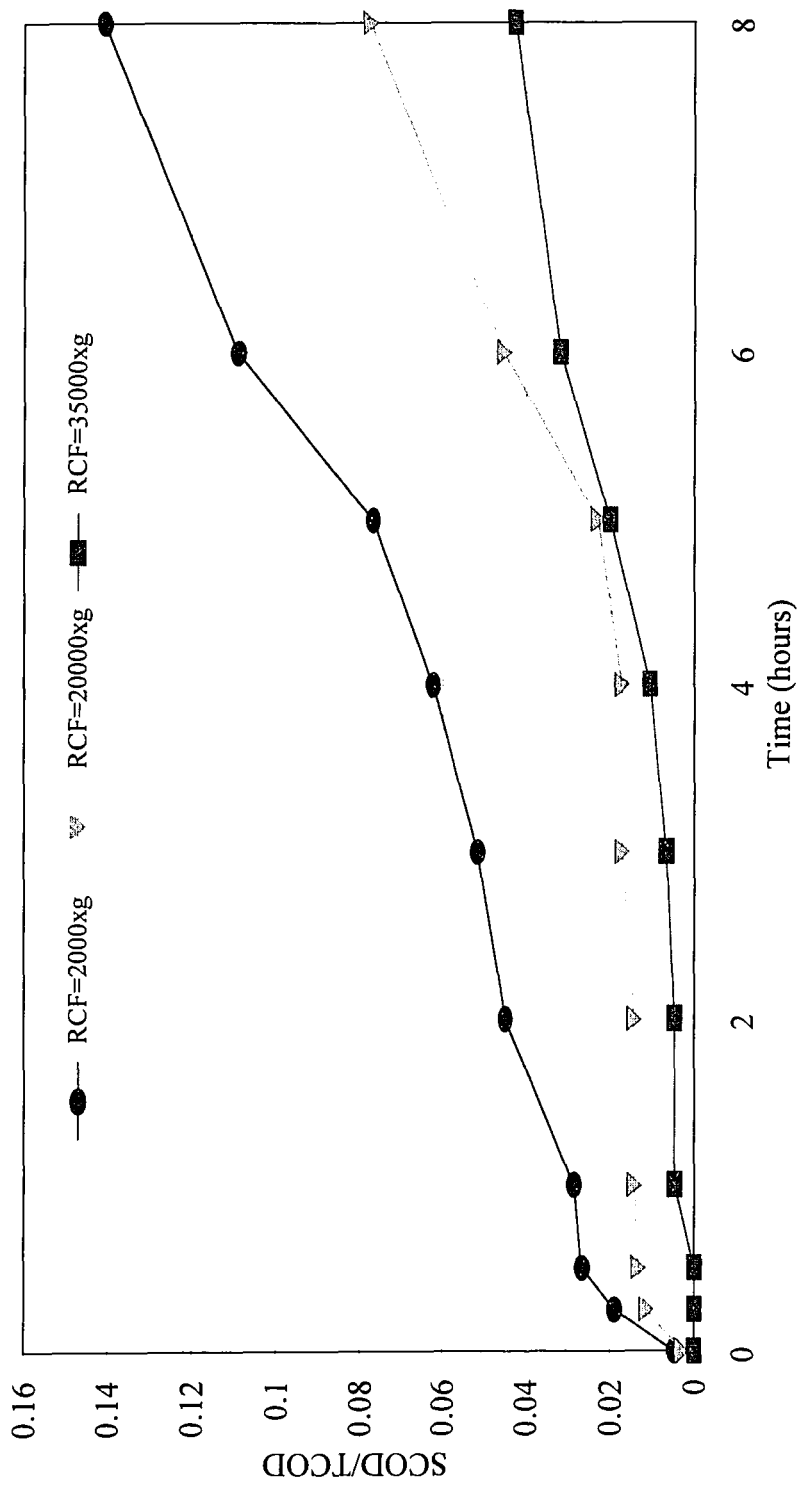


Figure 6.1.1. Effect of varying RCFs on the phase separation efficiency of a biosolids suspension at 20°C from a laboratory scale activated sludge reactor with recycle.

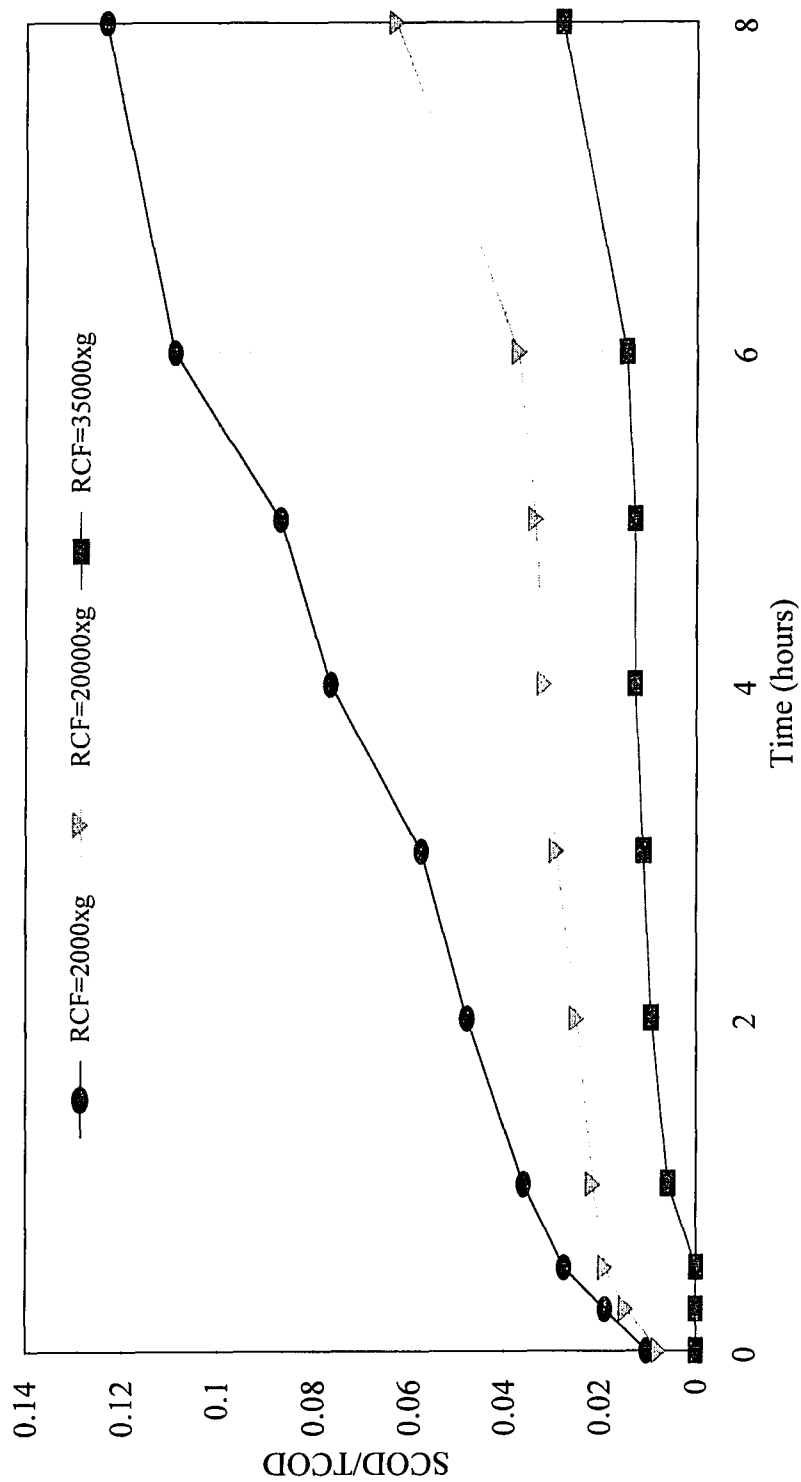


Figure 6.1.2. Effect of varying RCFs on the phase separation efficiency of a biosolids suspension at 20°C from an ASBR.

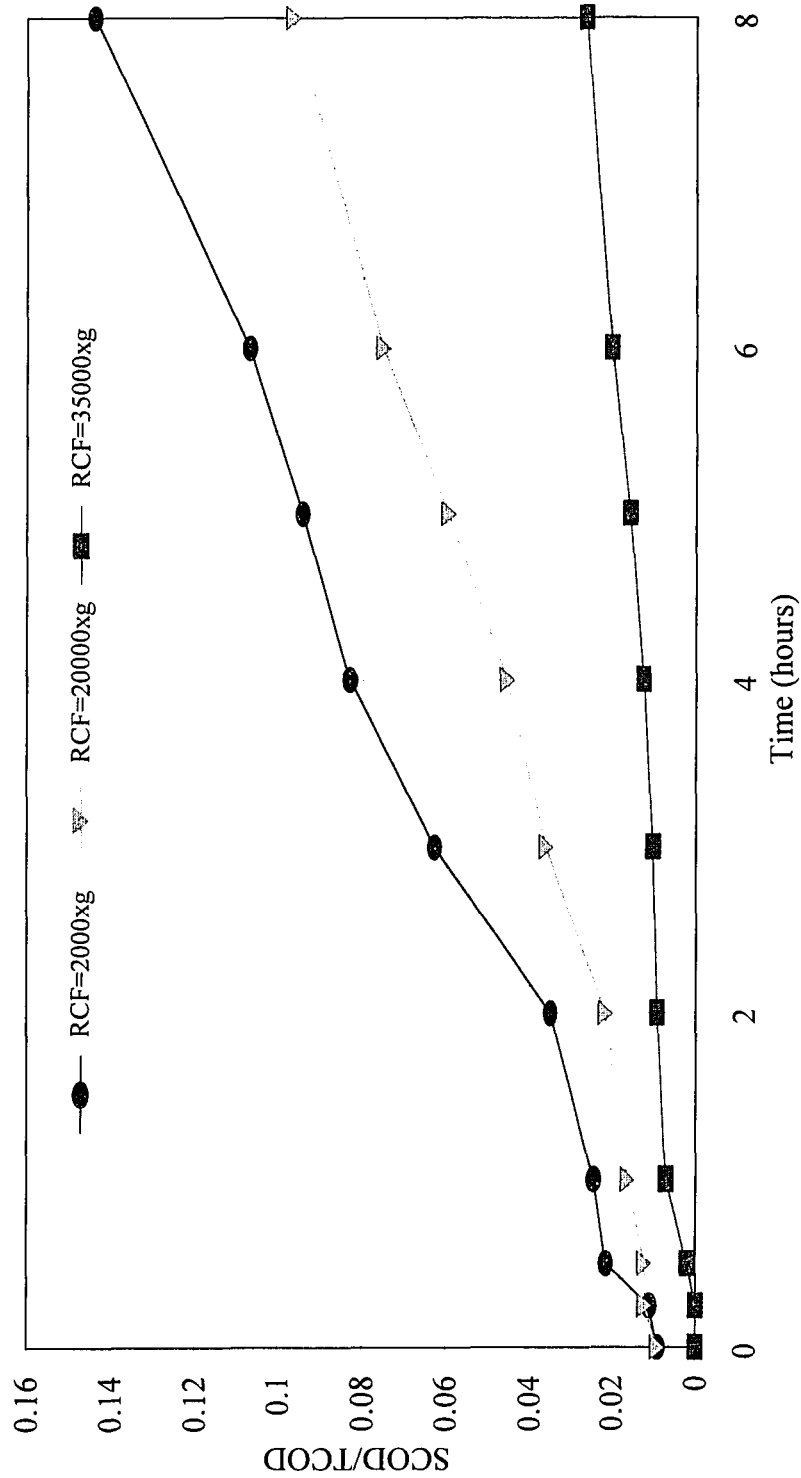


Figure 6.1.3. Effect of varying RCFs on the phase separation efficiency of a biosolids suspension at 20°C from a pure oxygen activated sludge process.

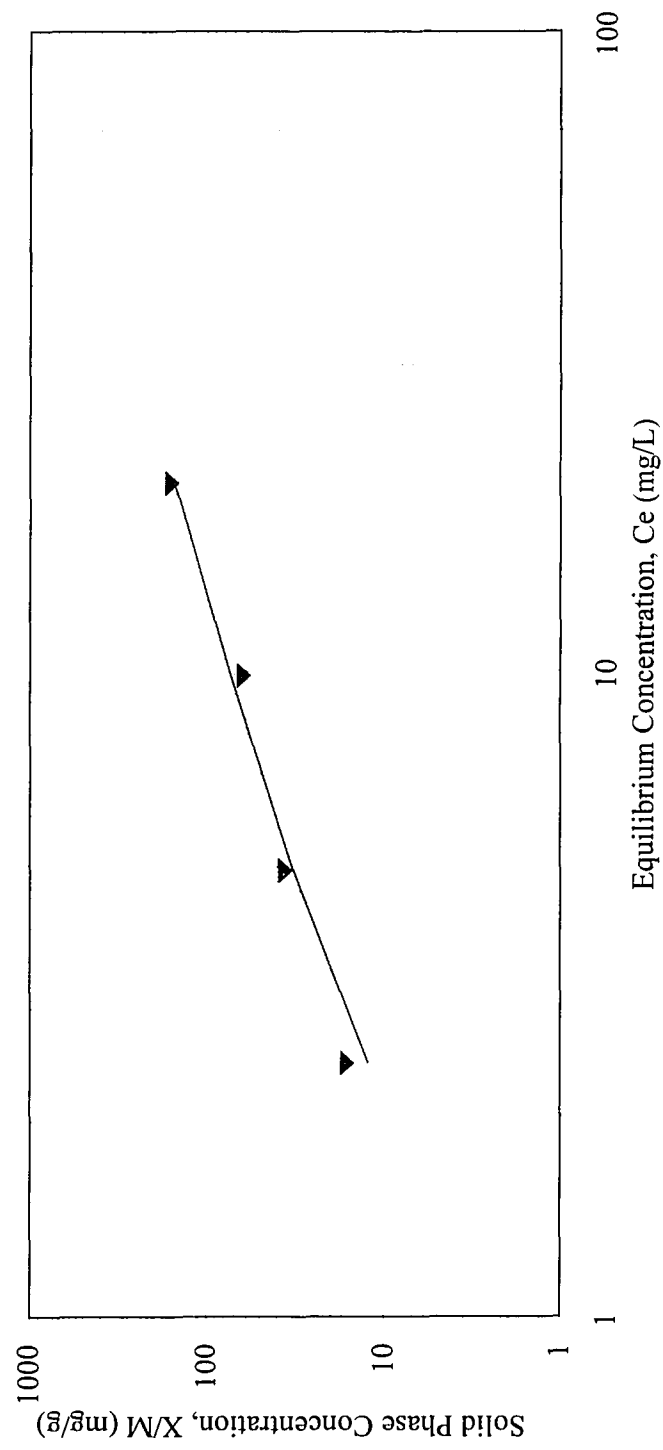


Figure 6.1.4. Sorption of azo dye 151 onto activated sludge solids (PVSC) fractionated at 2000 x g. Biomass was collected from a pure oxygen activated sludge treatment system.

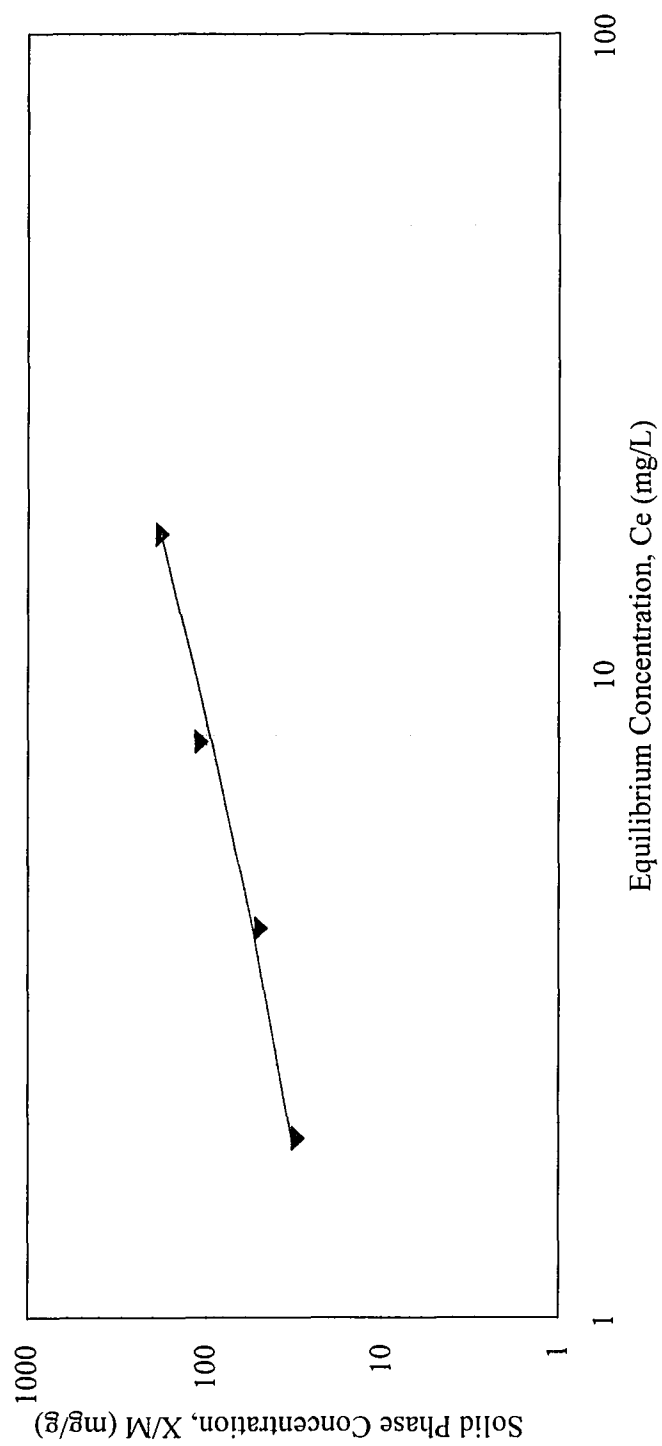


Figure 6.1.5. Sorption of azo dye 151 onto activated sludge solids (PVSC) fractionated at 20000 x g. Biomass was collected from a pure oxygen activated sludge treatment system.

Although the data collected from this study is not extensive enough to suggest the best or the most appropriate RCF to be used for optimum separations, RCFs between 20000 to 40000 x g would result in more accurate quantification of analytes associated with the aqueous phase in sorption-desorption experiments. However, the effects of higher RCFs on the physical texture of activated sludge solids has not been quantified. Additional research needs to be conducted to suggest an optimum balance between high RCFs and potential denaturing of biosolids.

If longer equilibration times are to be investigated, the RCF used for phase separation becomes a critical issue for activated sludge solids. It was clear from this study that by using a phase separation RCF of 5000 x g for biosolids washing and fractionation, sorption-desorption effects were quantified for only those solids captured or retained corresponding to a particular range of Stokes' diameters. The sorption experiments were carried out using the same methodology as that used for the other sorption-desorption experiments. The concentration of the azo dye in the aqueous phase was measured at 512 nm using a spectrophotometer.

The results from this study are summarized in Figures 6.1.4 and 6.1.5. It was not possible to derive reliable information from biosolids fractionated at 35000 x g because the concentration of azo dye 151 could not be measured accurately enough above the background measurements with spectrophotometric methods - a limitation of optical methods when measuring colloidal suspensions. However, experiments conducted with biomass fractionated at 2000 x g and 20000 x g were successfully quantified for sorption parameters. It can be seen from Figures 6.1.4 and 6.1.5 that biomass fractionated at different RCFs showed markedly different sorption responses. Biomass fractionated at

20000 x g showed a much higher sorption capacity ($K = 16.5$ mg/g) than the biomass separated at a RCF of 2000 x g ($K = 6.05$ mg/g). The sorption data was modeled as Freundlich isotherms described by equations 6.1.2 for biomass fractionated at 2000 x g, and by equation 6.1.3 for biomass fractionated at 20000 x g. The raw data from the experimental study is included in the Appendix.

$$\log \left(\frac{x}{m} \right) = \log (6.05) + 1.07 \log (C_e) \quad (6.1.2)$$

$$\log \left(\frac{x}{m} \right) = \log (16.50) + 0.86 \log (C_e) \quad (6.1.3)$$

The greater sorption capacity of the smaller size fractions could potentially be due to a combination of factors such as greater available surface area per unit mass of sorbent, different physical and/or chemical composition of the biomass matrix, etc. Since the experimental data are modeled best by a Freundlich isotherm which models sorption as a surface phenomenon, the primary mechanism in biosorption could be dominated by the available surface area of the sorbent matrix. If this hypothesis is true, biosolids with a smaller particle size distribution would exhibit higher sorption capacities per unit mass of organic carbon. Also, it is known that smaller fragments of the cell which can be fractionated only at very high RCFs, have a different chemical composition as compared to either a whole unfragmented cell or cell walls (Brock and Madigan, 1991). It has been shown through the characterization of different fractions of the activated sludge solids used in this research study that the composition of the cell material in different size

ranges vary markedly. Since activated sludge solids is composed of a complex mixture of material ranging from colloidal to supracolloidal in particle size, and made up of live and dead cells, cytoplasmic material, macromolecular compounds etc., properties exhibited by such a suspension would be strongly influenced by the presence or exclusion of certain fractions of the components that constitute activated sludge. A detailed analysis of the different fractionation products could potentially yield information about the mechanisms of sorption, kinetics, transport and sequestering of chemical compounds in biological sludges. Information from such a characterization analysis would be useful in designing engineered treatments systems that target specific particle size distributions for their operations.

Results from the particle size distribution of particulate organics in wastewater using filtration techniques points to the presence of organic material at size ranges below 0.1 μm . In this research study, it was found that 77% of the biosolids in the activated sludge solids had a particle size distribution greater than 5 μm , 17 % was in the size range between 5 and 0.8 μm , and the remaining 6% below 0.1 μm . Although not in exact agreement with results reported by other researchers, the results are close to those reported elsewhere for secondary activated sludge solids (Balmat, 1957, Karr and Keinath, 1978, Levine *et al.*, 1991).

As indicated in this research study the smaller size fractions fractionated at 20000 x g show significantly higher sorption capacities. Hence, considering that about 20% of the TOC in wastewater activated sludge lies in the size range below 5 μm , phase separation techniques that can attain such removals should be used. Very little information is available about the physical chemical or biochemical composition of the

various size fractions in activated sludge solids. Research focused towards the complete characterization of these subfractions in wastewater will help gain better insight of interactions of the actual mechanistic aspects of biosorption and desorption processes.

It was seen during this study that the fractionation RCFs used resulted in different SCOD removals for the three activated sludge solids samples. The soluble fraction which is probably an indicator of cell lysis through decay, is different for biomass from different unit operations. It was observed in all cases during the sorption-desorption experiments that biomass from the pure oxygen activated sludge process “deteriorated” faster than biomass from the other two processes tested. The results from this study quite clearly demonstrates that results reported by authors over many years only succeed in quantifying sorption-desorption parameters for solids fractionated at a defined RCF. All calculations based on such data should be evaluated and used judiciously on the basis of this information.

6.2 Sorption Experiments

Sorption experiments were conducted using eight of the ten compounds in the training set chosen to represent the class of halogenated aliphatic hydrocarbons. Two compounds were selected randomly and removed from the data set. The compounds excluded from the initial phase of the sorption-desorption study were dichloroethane ($\text{CH}_2\text{Cl}-\text{CH}_2\text{Cl}$) and tribromofluoromethane (CBr_3F). Sorption capacities were determined for the compounds shown in Table 6.2.1, and this data was used to develop a predictive model to estimate

sorption capacities of aliphatic hydrocarbons to activated sludge solids. Dichloroethane and tribromofluoromethane were later used to validate of the developed model.

Sorption experiments were conducted as per experimental protocols discussed in Chapter 5. Data collected from the sorption experiments were evaluated for different sorption isotherms, which included Freundlich, Langmuir and BET isotherms. It was observed that data collected from the sorption experiments were found to be best described by Freundlich isotherms. Experimental data collected from the samples were corrected for losses of the analyte from the aqueous phase in centrifuge tubes and during analytical procedures due to factors other than sorption. It was found that volatilization of the analyte made mass balance calculations most difficult, particularly for the low boiling point compounds such as CCl_3F and CH_2Cl_2 . Since, five centrifuge tubes were used for each determination of the target compound in the aqueous phase, equilibrium concentrations were averaged using the group of three closest determinations, and the outliers were rejected. The average value for the concentration of the target compound in the analyte was then used to determine the Freundlich isotherm parameters for that particular sorbent matrix (biomass from the different unit processes).

The results from this analysis summarizing the Freundlich isotherm parameters are presented in Table 6.2.1. It can be seen from the different sorption isotherms that the parameters are fairly consistent for each compound for biomass from different unit process operations. Also, the $1/n$ exponent in all the Freundlich isotherms are close to 1, which makes calculation of sorption capacities based solely on K easier, and is also typical for low concentrations of target compounds usually seen in wastewater treatment systems.

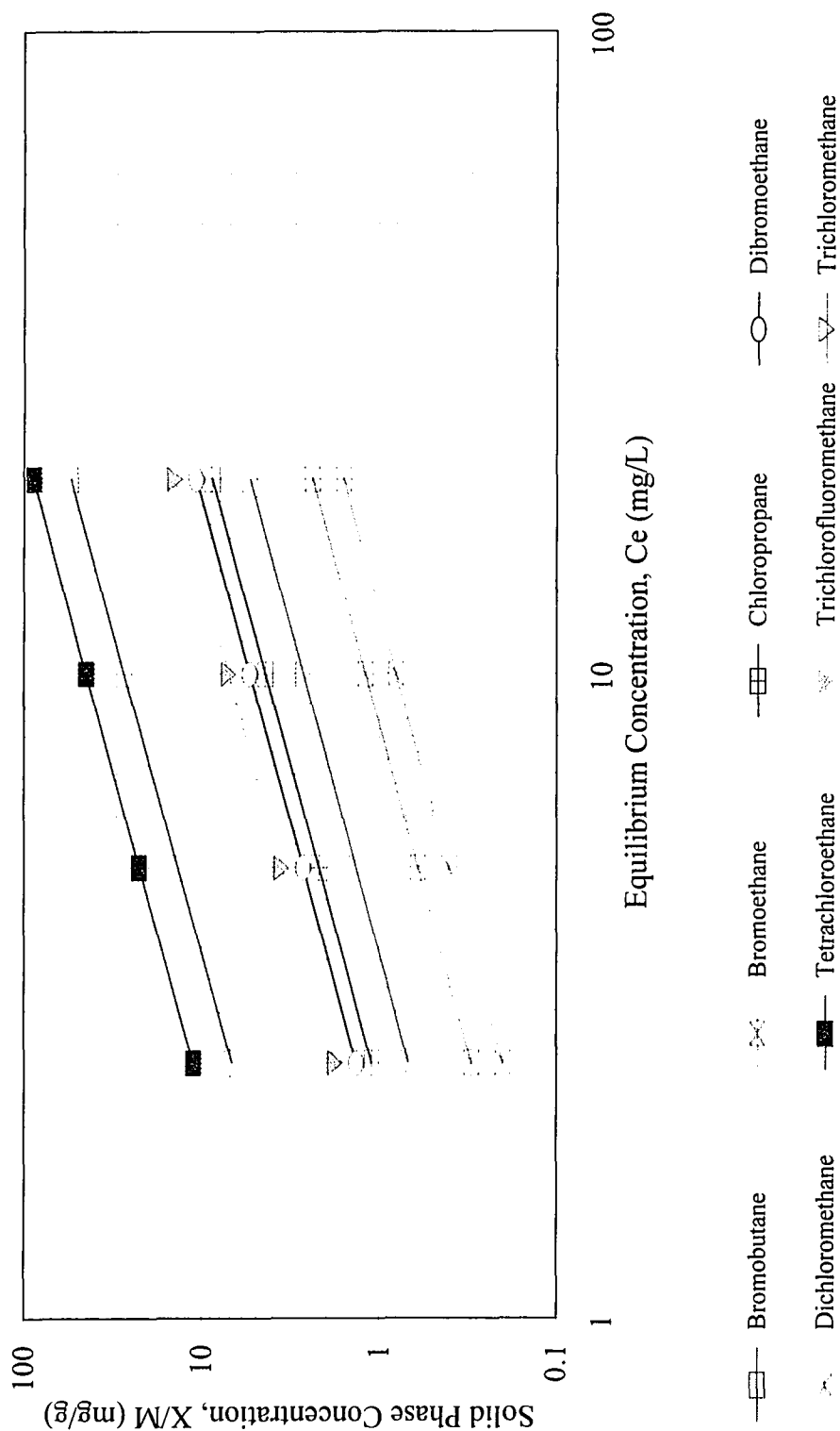


Figure 6.2.1. Comparison of estimated sorption isotherms for the compounds in the training set using sorption capacities in Table 6.2.2 estimated at aqueous phase equilibrium concentrations of 2.5, 5, 10 and 20 mg/L, slope $n = 1$.

Table 6.2.1. Freundlich isotherms showing sorption behavior of compounds in the training set using biomass from two different unit operations.

Compound	Reactor w/recycle	ASBR
Bromobutane	$\log \left(\frac{x}{m} \right) = \log (2.77) + 0.98 \log (C_e)$	$\log \left(\frac{x}{m} \right) = \log (2.64) + 1.02 \log (C_e)$
Bromoethane	$\log \left(\frac{x}{m} \right) = \log (0.11) + 1.06 \log (C_e)$	$\log \left(\frac{x}{m} \right) = \log (0.13) + 0.94 \log (C_e)$
Chloropropane	$\log \left(\frac{x}{m} \right) = \log (0.50) + 0.97 \log (C_e)$	$\log \left(\frac{x}{m} \right) = \log (0.38) + 1.04 \log (C_e)$
Dibromoethane	$\log \left(\frac{x}{m} \right) = \log (0.51) + 1.01 \log (C_e)$	$\log \left(\frac{x}{m} \right) = \log (0.56) + 0.94 \log (C_e)$
Methylene Chloride	$\log \left(\frac{x}{m} \right) = \log (0.08) + 1.08 \log (C_e)$	$\log \left(\frac{x}{m} \right) = \log (0.09) + 0.98 \log (C_e)$
Tetrachloroethane	$\log \left(\frac{x}{m} \right) = \log (4.40) + 1.00 \log (C_e)$	$\log \left(\frac{x}{m} \right) = \log (4.49) + 1.00 \log (C_e)$
Trichlorofluoromethane	$\log \left(\frac{x}{m} \right) = \log (0.68) + 0.96 \log (C_e)$	$\log \left(\frac{x}{m} \right) = \log (0.73) + 0.91 \log (C_e)$
Trichloromethane	$\log \left(\frac{x}{m} \right) = \log (0.26) + 1.01 \log (C_e)$	$\log \left(\frac{x}{m} \right) = \log (0.28) + 0.93 \log (C_e)$

The sorption capacities determined for the training set of compounds is summarized in Table 6.2.2. Sorption capacities shown in Table 6.2.2 were determined by averaging the sorption capacities at an equilibrium aqueous phase concentration of $C_e = 1$ mg/L. The mean sorption capacity for each compound was calculated by the mean of the sorption capacities determined for the two different biomass. All sorption and desorption capacities expressed in this research study are based on a unit mass of TOC, i.e., the sorption coefficients calculated in this research study are a measure of the sorbing capacity of activated sludge solids, mg compound/g TOC of solids. Statistical analysis of the sorption capacities for Freundlich parameters shows that the calculated isotherms for all the compounds have a correlation coefficient of > 0.9 indicating a very good linear fit. The raw data from the experimental study is presented in the Appendix. The sorption isotherm from each sorption experiment is also presented in the Appendix.

Table 6.2.2. Sorption capacities calculated using data from Freundlich isotherms for each compound in the training set of compounds.

Compound	Sorption Capacity (K), mg/g ¹		
	Reactor w/recycle ± SD ²	ASBR ± SD ²	Mean
Bromobutane	2.77 ± 0.10	2.64 ± 0.08	2.71
Bromoethane	0.11 ± 0.06	0.13 ± 0.03	0.12
Chloropropane	0.50 ± 0.05	0.38 ± 0.08	0.44
Dibromoethane	0.51 ± 0.05	0.56 ± 0.03	0.54
Methylene Chloride	0.08 ± 0.08	0.09 ± 0.01	0.08
Tetrachloroethane	4.40 ± 0.02	4.49 ± 0.07	4.45
Trichlorofluoromethane	0.68 ± 0.03	0.73 ± 0.03	0.71
Trichloromethane	0.26 ± 0.09	0.28 ± 0.02	0.27

¹ K = sorption coefficient = $\left(\frac{x}{m}\right)$ at $C_e = 1.0$ mg/L

²Standard deviation of all samples from the mean

Freundlich isotherms were plotted using the equations presented in Table 6.2.1. The solid phase concentration of the target compounds was estimated using these equations for aqueous phase equilibrium concentrations of the target compound at 2.5, 5.0, 10.0 and 20.0 mg/L. It should be noted here that the exponential coefficient (1/n) was approximated to be 1. It can be seen from the equations presented in Table 6.2.1 and the data presented in the Appendix, that this is a valid assumption since the (1/n) values are very close to unity for all the sorption experiments conducted in this research study. Similar results for the exponent of the aqueous phase equilibrium concentration (C_e) have been observed by other researchers for sorption of toxic organic compounds on to activated sludge solids. The comparison of the different sorption isotherms are shown in Figure 6.2.1.

6.3 Desorption Experiments

The equilibrium concentration in the aqueous phase after three hours of equilibration was used to calculate the desorption potential of halogenated aliphatic hydrocarbons from activated sludge solids. The concentration of the target compound in the aqueous phase at the beginning of the desorption experiment was assumed to be zero. This assumption is valid in this research study since the supernatant aqueous phase after centrifugation was decanted from the centrifuge tubes and a fresh solution of phosphate buffer was added to the tubes. The final concentration of the target compound in the aqueous phase was used to determine the desorption capacity of the activated sludge solids. Equation (6.3.1) shows the mass balance relationship used to calculate the residual concentration in the biosolids at the beginning of the desorption experiments.

$$C_{o \text{ (biosolids)}} = C_o - (C_e + \sum C_l) \quad (6.3.1)$$

where

$C_{o \text{ (biosolids)}}$ = initial concentration of target compound in the biosolids (desorption), mg/L

C_o = initial concentration of target compound in the aqueous phase (sorption), mg/L

C_e = equilibrium concentration of target compound in aqueous phase (desorption), mg/L

C_l = losses due to experimental factors (desorption), mg/L

Desorption isotherms from activated sludge solids were plotted using the calculated $C_{o \text{ (biosolids)}}$ as the initial concentration of the target compound in the biomass. The final concentration of the target compound concentration in the biomass after 3 hours

of desorption experiment was estimated from the aqueous phase concentration of the target compound. No reliable desorption isotherms could be plotted for two highly volatile compounds in the training set of compounds. Trichlorofluoromethane and methylene chloride could not be detected in the aqueous phase at the lower concentration ranges. Although for higher initial sorbed concentration ranges these compounds could be detected, their presence above controls could not be statistically verified as being different. Extraction of the biosolids with hexane to test for the presence of trichlorofluoromethane and methylene chloride also failed to detect residual concentration of the target compound above method detection limits. As can be seen from the list of properties of the training set of compounds, trichlorofluoromethane has a boiling point of 23.7°C and methylene chloride of 40°C. However, it can also be observed from this list that bromobutane which has a boiling point of 38.4°C, was detected consistently for all concentration ranges, indicating that there might have been other mechanisms in addition to volatilization that this research study could not account for accurately during the desorption experiments. However, it was generally observed in this research study that the recovery of the target compound was significantly affected by the volatility of the compound. Mass balance calculations of the target compound after desorption experiment showed a variation of about $\pm 17\%$.

The results of the desorption study are presented in Table 6.3.1. As in the case of the sorption experiments, equilibrium concentrations were averaged using the three closest grouped determinations, and the outliers were rejected. The average value for the concentration of the target compound in the analyte was then used to determine the Freundlich isotherm parameters for that target compound, for that particular sorbent

matrix (biomass from the different unit processes). The raw data and isotherms for each experiment in the sorption study are presented in the Appendix.

Table 6.3.1. Ratio of target compound initially present in the biomass to the aqueous phase concentration at the end of the experiment.

Compound	Fraction desorbed from activated sludge solids ¹		
	Reactor w/recycle \pm SD	ASBR \pm SD	Mean
Bromobutane	0.96 ± 0.07	0.98 ± 0.03	0.97
Bromoethane	0.99 ± 0.01	1.00 ± 0.03	1.00
Chloropropane	0.95 ± 0.03	0.97 ± 0.01	0.96
Dibromoethane	0.98 ± 0.12	0.99 ± 0.04	0.99
Dichloromethane ²	-	-	-
Tetrachloroethane	1.00 ± 0.06	1.00 ± 0.09	1.00
Trichlorofluoromethane ²	-	-	-
Trichloromethane	0.96 ± 0.06	0.95 ± 0.08	0.95

¹ratio of $C_o(\text{biosolids}) / C_e$ in Equation (6.3.1)

²equilibrium concentrations in the aqueous phase could not be determined

An analysis of the experimental data reveals that the amount of compound sorbed onto the biomass matrix calculated as per Equation (6.3.1) was released back totally into the aqueous phase during the desorption experiment. This indicates that biosorption of halogenated aliphatics from activated sludge solids is a reversible process. This cannot be inferred directly for the two compounds, trichlorofluoromethane and methylene chloride as their concentrations could not be evaluated in either the aqueous phase or the biomass matrix. Since neither trichlorofluoromethane nor methylene chloride are susceptible to biodegradation by an unacclimated aerobic culture in a 6 hour period, their relative low boiling points suggest that volatilization could be the only likely pathway for the removal of these compounds from the aqueous phase. It is also important to note from this experience that while determining the fate and transport of toxic organic compounds, the

effect of other fate processes such as volatilization, solubility and biodegradation should be taken into account to realistically design an engineered treatment and disposal system.

Since sorption of halogenated aliphatic hydrocarbons to activated sludge biosolids is a totally reversible process, the desorption capacity of the biosolids is equal in magnitude to the sorption capacity. Hence, the concentration of the target compound available in the aqueous phase through desorption can be estimated using the same equations as those developed to estimate the sorption parameters. Hence model development and validation was conducted using data obtained from the sorption experiments.

6.4 Model Development and Validation

The next step in the data analysis was to develop a model that could adequately quantify the sorption capacity of the biosolids using molecular connectivity indexes. Molecular connectivity indexes were calculated for all the compounds in the AX Class (58 compounds) using the GRAPHIII[®] computer program. The use of this program and the calculation methods have already been discussed in Chapter 3. Simple and valence chi indexes of up to sixth order (${}^0\chi$ to ${}^6\chi$, and ${}^0\chi^v$ to ${}^6\chi^v$) were calculated and stored in a computer data file. The output files from statistical analysis and ANOVA tables have been summarized in Table 6.4.1. The raw experimental data has been included in the Appendix.

Table 6.4.1. Statistical analysis of sorption data using multiple linear regression techniques.

Input data:

Compound name	Molecular connectivity indexes (Chi values)								Mean K
	χ^0	χ^1	χ^2	χ^3	χ^0_v	χ^1_v	χ^2_v	χ^3_v	
Bromobutane	4.121	2.414	1.354	0.707	5.082	3.094	1.834	1.047	2.71
Bromoethane	2.707	1.414	0.707	0.000	3.668	2.094	1.387	0.000	0.12
Chloropropane	3.414	1.914	1.000	0.500	3.546	2.008	1.066	0.566	0.44
Dibromoethane	3.414	1.914	1.000	0.500	5.207	2.927	1.601	1.570	0.54
Methylene Chloride	2.707	1.414	0.707	0.000	2.972	1.601	0.907	0.000	0.08
Tetrachloroethane	5.207	2.561	2.914	1.061	5.606	2.641	3.231	1.110	4.45
Trichlorofluoromethane	4.500	2.000	3.000	0.000	4.275	1.887	2.565	0.000	0.71
Trichloromethane	3.577	1.732	1.732	0.000	3.974	1.961	2.221	0.000	0.27

Output file:

Regression Statistics

Multiple R	0.89
R Square	0.79
Adjusted R Square	0.76
Standard Error	0.77
Observations	8.00

Analysis of Variance

	<i>df</i>	<i>Sum of Squares</i>	<i>Mean Square</i>	<i>F</i>	<i>Significance F</i>
Regression	1.00	13.75	13.75	23.13	0.00
Residual	6.00	3.57	0.59		
Total	7.00	17.32			
	<i>Coefficients</i>	<i>Standard Error</i>	<i>t Statistic</i>	<i>P-value</i>	
Intercept	-5.31	1.37	-3.87	0.01	
χ^1	3.37	0.70	4.81	0.00	

Data collected on the sorption capacities of the different activated sludge solids was then subject to a multiple linear regression analysis to develop a quantitative model relating them to molecular connectivity indexes. Multiple linear regression techniques used for such an analysis have already been discussed earlier. In this analysis, the sorption capacity (K) was used as the Y parameter, and the molecular connectivity indexes were used as the X parameters. Advanced linear regression was performed using a macro program written for use with Quattro Pro[®] on an IBM PC running on an Intel[®] Pentium

133 MHz processor. All data processing, modeling and statistical analysis was conducted on this personal computer.

As can be seen from Table 6.4.1, six of the higher order chi indexes (${}^4\chi$ to ${}^6\chi$, and ${}^4\chi^v$ to ${}^6\chi^v$) were removed from the correlation matrix, as for most compounds in the training set, these higher order indexes returned zero values. As per standard methodology used in QSAR analysis and multiple correlational analysis, when most values of a parameter are zero, that parameter cannot be used for model development.

The values for all chi indexes calculated are reported in the Appendix. Multiple correlation analysis was performed using standard multiple linear regression methods of analyzing the whole data set at the same time, and then sequentially reducing the number of parameters in the regression analysis. After this initial treatment of the data by multiple linear regression, it was found that among the eight molecular connectivity indexes evaluated, the ${}^1\chi$ index was the strongest indicator of sorption capacity in biological sludges. However, as shown in Table 6.4.1, correlation of sorption capacity with this index yielded a relatively poor correlational coefficient of about 0.76, and a relatively high Standard Error (SE). The correlation between ${}^1\chi$ and K dramatically improved however, when the biomass partition coefficient was calculated using methods used earlier by other researchers (Dobbs *et al.*, 1986, 1989). The biomass partition coefficient can be calculated by dividing the sorption capacity as determined by the Freundlich isotherm, K_f , by 1000 and linearizing the data over the experimental range, using equation (6.4.1).

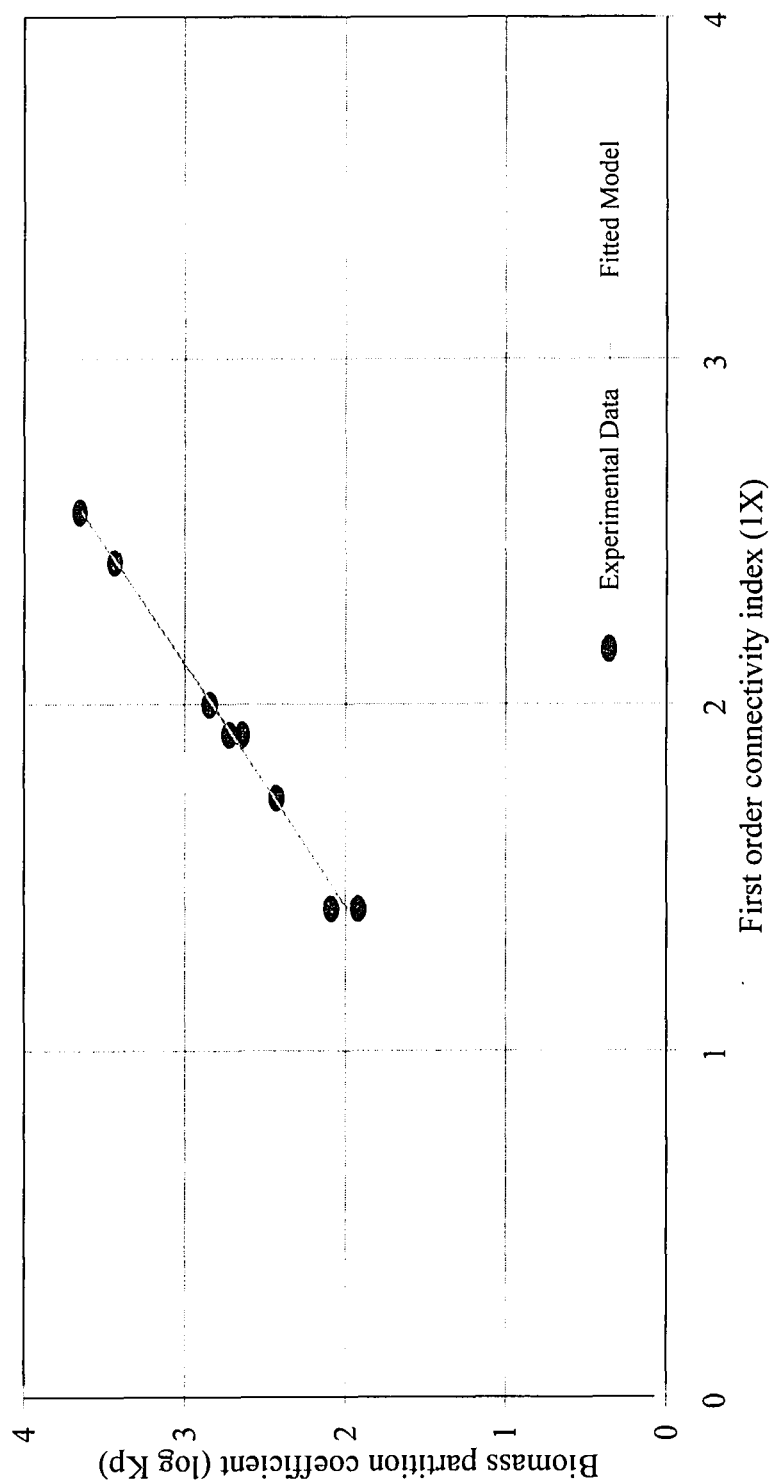


Figure 6.4.1. Correlation between first order molecular connectivity index ($^1\chi$) and biomass partition coefficient ($\log K_p$).

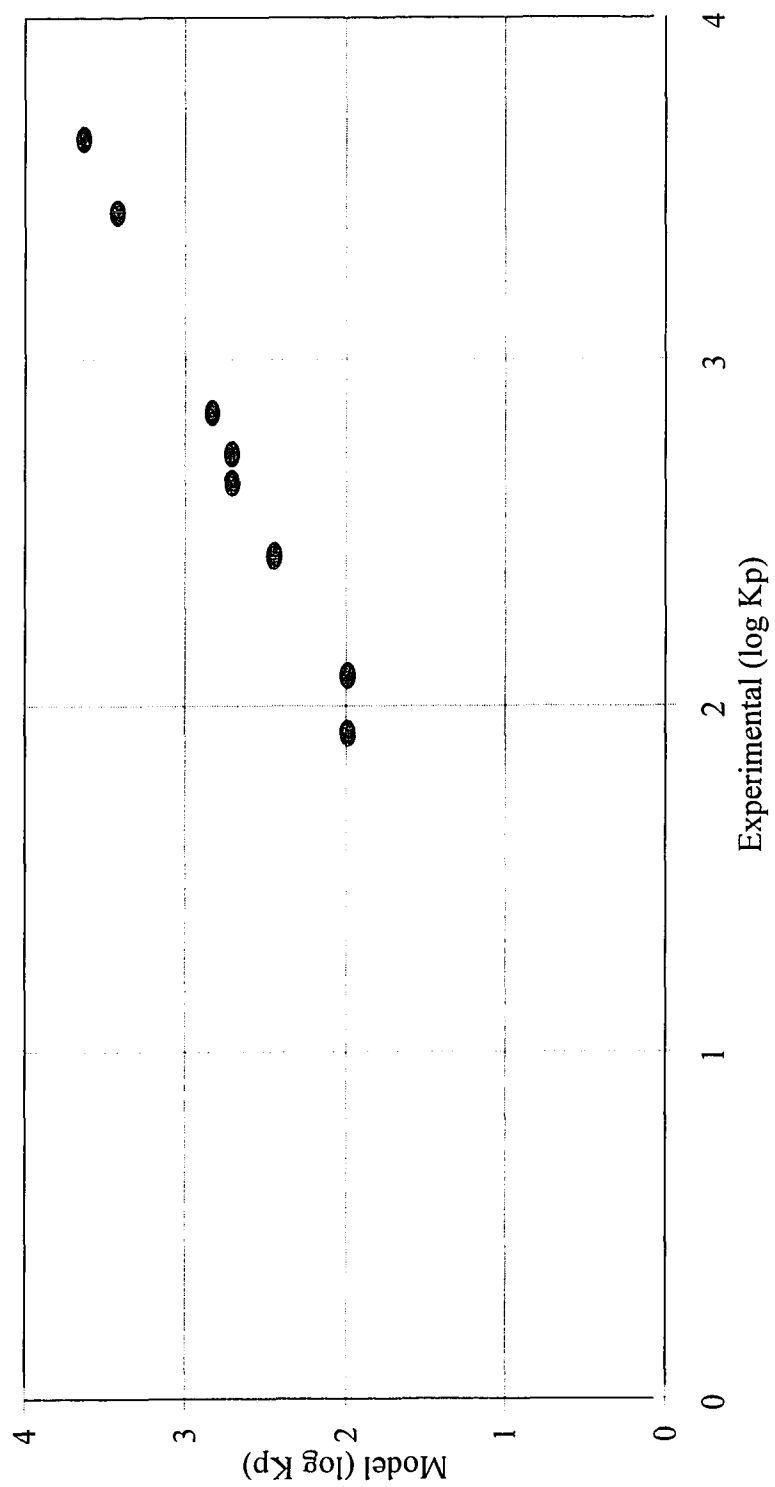


Figure 6.4.2. Comparison between experimentally determined values and predicted value for the biomass partition coefficient.

Table 6.4.2. Multiple linear regression analysis using molecular connectivity indexes and the partition coefficient, log K_p.

Input Data :

Compound name	Molecular connectivity indexes (Chi values)								Log K _p
	⁰ χ	¹ χ	² χ	³ χ	⁰ χ ^v	¹ χ ^v	² χ ^v	³ χ ^v	
Bromobutane	4.121	2.414	1.354	0.707	5.082	3.094	1.834	1.047	3.43
Bromoethane	2.707	1.414	0.707	0.000	3.668	2.094	1.387	0.000	2.09
Chloropropane	3.414	1.914	1.000	0.500	3.546	2.008	1.066	0.566	2.64
Dibromoethane	3.414	1.914	1.000	0.500	5.207	2.927	1.601	1.570	2.73
Methylene Chloride	2.707	1.414	0.707	0.000	2.972	1.601	0.907	0.000	1.92
Tetrachloroethane	5.207	2.561	2.914	1.061	5.606	2.641	3.231	1.110	3.65
Trichlorofluoromethane	4.500	2.000	3.000	0.000	4.275	1.887	2.565	0.000	2.85
Trichloromethane	3.577	1.732	1.732	0.000	3.974	1.961	2.221	0.000	2.43

Output file:

Regression Statistics

Multiple R	0.996
R Square	0.992
Adjusted R Square	0.991
Standard Error	0.057
Observations	8.000

Analysis of Variance

	<i>df</i>	<i>Sum of Squares</i>	<i>Mean Square</i>	<i>F</i>	<i>Significance F</i>
Regression	1.00	2.48	2.48	764.40	0.00
Residual	6.00	0.02	0.00		
Total	7.00	2.50			
	<i>Coefficients</i>	<i>Standard Error</i>	<i>t Statistic</i>	<i>P-value</i>	
Intercept	-0.03	0.10	-0.33	0.75	
^X1	1.43	0.05	27.65	0.00	

$$\log K_p = \log \left(\frac{K_f}{1000} \right) \quad (6.4.1)$$

As in the previous case, the six chi indexes were used as the X variables, and log K_p was used as the Y parameter. The results from the multiple linear regression shown in Table 6.4.2 indicate that ¹χ continued to be the most significant of all the X parameters. Further analysis by the sequential removal of single parameters, confirmed that the best possible correlation could be obtained by relating the biomass partition coefficient to the first order molecular connectivity index ¹χ. As can be seen from the statistical analysis

presented in Table 6.4.2 for this correlation, the r^2 value of 0.992 and a SE of 0.057 indicates an excellent fit for the data collected from the experimental study. Figure 6.4.1 shows the relationship between the first order molecular connectivity index and the biomass partition coefficient. The biomass partition coefficient can now be related to the first order molecular connectivity index using Equation (6.4.2). The biomass partition coefficients were estimated using Equation (6.4.2) and compared to actual experimental data collected. The comparison is summarized in Table 6.4.3 and elucidated in Figure 6.4.1 and 6.4.2.

$$\log K_p = 1.43 {}^1\chi - 0.03 \quad (6.4.2)$$

Table 6.4.3. Comparison of experimental biomass partition coefficients to estimated values.

Compound name	Experimental log (K_p)	Model log (K_p)
Bromobutane	3.43	3.42
Bromoethane	2.09	1.99
Chloropropane	2.64	2.71
Dibromoethane	2.73	2.71
Methylene Chloride	1.92	1.99
Tetrachloroethane	3.65	3.63
Trichlorofluoromethane	2.85	2.83
Trichloromethane	2.43	2.45

As can be seen from Figure 6.4.2 and Table 6.4.3, the values predicted by the model are very close to those observed experimentally. However, to further validate the robustness of the proposed correlational parameters, two of the compounds which had been deleted from the original training set of target compounds were tested. The compounds which had been excluded from the correlation matrix were dichloroethane

and tribromofluoromethane. The sorption and desorption capacities for these two compounds was evaluated using the same experimental protocol as was used for the other eight compounds in the training set. The results from the experimental study and that obtained from the model proposed through Equation (6.4.2) are shown in Table 6.4.4. Freundlich isotherms were used to model the data for these two compounds. The Freundlich isotherms are shown in Table 6.4.5. Sorption and desorption isotherms and data from this study are presented in the Appendix. A student t-test on the observed experimental data and those predicted by the model shows that there is no significant difference between the model and the experimental data, indicating a good fit. Inclusion of the data obtained from this part of the experimental study in the data set used for the development of the model described by Equation (6.4.2) resulted in a very similar equation. Since there was no statistically significant difference between the two, Equation (6.4.2) was used as the model of choice.

Table 6.4.4. Model validation by comparing predicted sorption capacities for dichloroethane and tribromofluoromethane to experimental values.

Compound	Biomass Partition Coefficient ($\log K_p$), mg/g	
	Experimental Value	Predicted from Model
Dichloroethane	2.66	2.71
Tribromofluoromethane	2.85	2.83

Table 6.4.5. Freundlich isotherms showing sorption behavior of compounds in the training set using biomass from different unit operations.

Compound	Reactor w/recycle	ASBR
Dichloroethane	$\log \left(\frac{x}{m} \right) = \log (0.47) + 0.99 \log (C_e)$	$\log \left(\frac{x}{m} \right) = \log (0.46) + 0.98 \log (C_e)$
Tribromofluoromethane	$\log \left(\frac{x}{m} \right) = \log (0.71) + 0.97 \log (C_e)$	$\log \left(\frac{x}{m} \right) = \log (0.69) + 0.96 \log (C_e)$

As discussed earlier in Chapter 2, each molecular connectivity index encodes structural information that can potentially indicate the mechanism of action for a particular phenomenon under study. Although the objective of this discussion is not to speculate about the exact mechanism of action for the biosorption of halogenated aliphatics on activated sludge solids, the relationship between the first order molecular connectivity index and the biomass partition coefficient indicates that the mechanism of action is probably a simple adsorption phenomenon for the period of time (equilibrium time of 3 hours) for which this research study was conducted. It can be seen from the sorption data collected on the sorption of azo dye 151 that more than 90% of the sorption occurred during the first hour of the experimental study, with limited uptake over the next two hours. This rapid sorption process in the initial stages would weight the outcome of any analysis to suggest that at least during the initial phase of rapid sorption of target compounds, the phenomenon is primarily governed by the mechanisms of surface adsorption driven by a chemical concentration gradient and favorable thermodynamic interactions. It is possible that there is active transport of the target compound through the bacterial cell wall during the initial phase of the experiment as well, but its evidence is overshadowed by the significantly higher uptake due to surface adsorption.

6.5 Comparison with Other Models and Studies

As discussed earlier, the sorption model developed in this research study was based on data collected from a laboratory scale activated sludge reactor with recycle and a laboratory scale ASBR. This model described by Equation (6.4.2) was validated using

experimental data collected on activated sludge solids from a pure oxygen treatment process (PVSC) using the entire training set of compounds (10). It was necessary to conduct a comparative study in the laboratory as no reliable data is available in the literature to check for the validity of this model. Biomass collected from the PVSC was used for the sorption desorption experiments to evaluate the sorption-desorption parameters. The experimental conditions, protocol for the fractionation and preparation of biosolids, and other experimental and analytical procedures were the same as those discussed earlier for the sorption of halogenated aliphatics on to activated sludge solids from the activated sludge reactor with recycle and the ASBR.

Table 6.5.1. Comparison of experimental and predicted biomass partition coefficient using biomass from a pure oxygen activated sludge treatment system.

Compound	Biomass Partition Coefficient ($\log K_p$), mg/g	
	Experimental	Predicted from Model
Bromobutane	3.43	3.42
Bromoethane	2.08	1.99
Chloropropane	2.67	2.71
Dibromoethane	2.72	2.71
Dichloroethane	2.65	2.71
Methylene Chloride	1.98	1.99
Tetrachloroethane	3.64	3.63
Tribromofluoromethane	2.85	2.83
Trichlorofluoromethane	2.80	2.83
Trichloromethane	2.39	2.45

t-Test Two Sample Assuming Equal Variance

t	-0.0256	
P(T<=t) one-tail	0.4899	
t Critical one-tail	1.7341	
P(T<=t) two-tail	0.9798	
t Critical two-tail	2.1009	

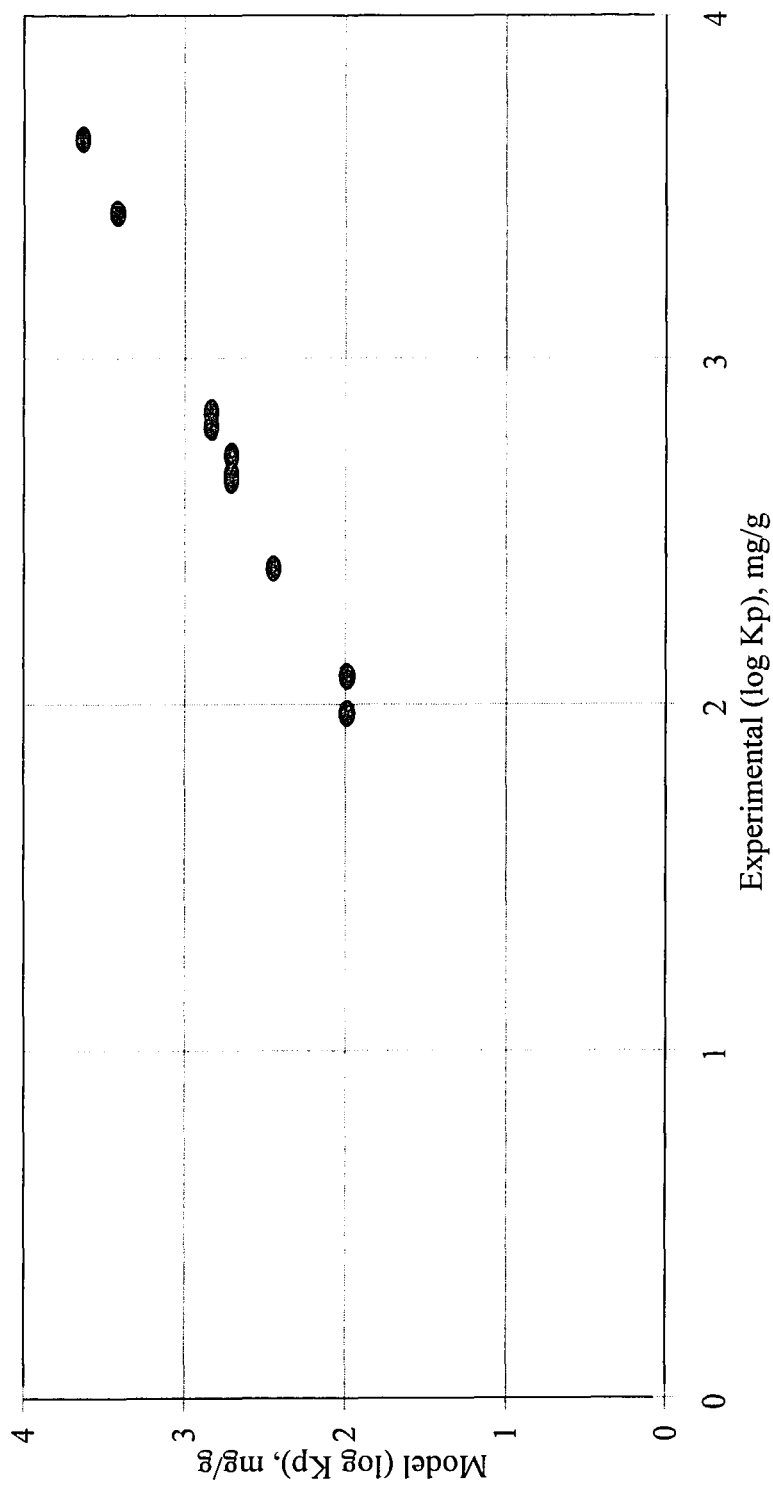


Figure 6.5.1 Comparison between experimental and predicted biomass partition coefficient using biomass from a pure oxygen activated sludge treatment system (PVSC).

Sorption coefficients were calculated from Freundlich isotherms plotted for the training set of compounds. The Freundlich isotherms for the training set using activated sludge solids from PVSC are shown in Table 6.5.2. Biomass partition coefficients calculated from data collected from this study and the predicted values using Equation (6.4.2) are compared in Table 6.5.1. A statistical analysis to compare the two values using the t-test is also shown in Table 6.5.1. No significant difference was observed at a significance level of 5% for biomass partition coefficients evaluate for experimental data for the PVSC biomass from the predicted values. This indicates that the model developed is capable of predicting biomass partition coefficients for activated sludge solids from different unit operations using first order molecular connectivity indexes.

Table 6.5.2. Freundlich isotherms showing sorption behavior of compounds in the training set using biomass from a pure oxygen treatment process.

Compound	Freundlich Isotherm
Bromobutane	$\log \left(\frac{x}{m} \right) = \log (2.66) + 1.00 \log (C_e)$
Bromoethane	$\log \left(\frac{x}{m} \right) = \log (0.12) + 0.97 \log (C_e)$
Chloropropane	$\log \left(\frac{x}{m} \right) = \log (0.47) + 0.99 \log (C_e)$
Dibromoethane	$\log \left(\frac{x}{m} \right) = \log (0.53) + 1.03 \log (C_e)$
Dichloroethane	$\log \left(\frac{x}{m} \right) = \log (0.45) + 1.01 \log (C_e)$
Methylene Chloride	$\log \left(\frac{x}{m} \right) = \log (0.1) + 1.01 \log (C_e)$
Tetrachloroethane	$\log \left(\frac{x}{m} \right) = \log (4.37) + 1.00 \log (C_e)$
Tribromofluoromethane	$\log \left(\frac{x}{m} \right) = \log (0.71) + 0.96 \log (C_e)$
Trichlorofluoromethane	$\log \left(\frac{x}{m} \right) = \log (0.64) + 0.95 \log (C_e)$
Trichloromethane	$\log \left(\frac{x}{m} \right) = \log (0.25) + 1.00 \log (C_e)$

It is difficult to compare either experimentally determined sorption coefficients or those calculated using the model described by Equation (6.2.2) with other research studies as the basis of calculation of sorption coefficients is not always the same. Comparisons between published literature values is extremely difficult due to the variations in the way the results are reported and the different experimental conditions used.

An attempt has been made here to express some of the data available in the literature on the basis of organic carbon through the use of estimated solids to TOC ratios discussed in Chapter 3. The data used for comparison have been collected from two studies conducted for a few of the compounds discussed in this research study (Dobbs *et al.*, 1986, Tsezos and Seto, 1986). Although data is available for only a few of the compounds, the values are within 10% to 15% agreement of these measurements. The comparison made is on the basis of the assumption that 60 to 80% of TSS is volatile, and that the volatile suspended solids constitutes the TOC of the sorbent matrix. The comparison of the different sorption coefficients are presented in Table 6.5.3.

Table 6.5.3. Comparison of estimated sorption coefficients for some halogenated aliphatics on activated sludge solids.

Compound	Sorption Coefficients, mg/g		
	Model	Dobbs <i>et al.</i> , 1986	Tsezos and Seto, 1986
Dichloromethane	1.99	1.85	-
Trichloromethane	2.45	2.07	-
Tetrachloromethane	2.83	2.80	-
Trichloroethane	2.83	-	2.85 ¹
Tetrachloroethane	3.63	-	3.95 ¹

¹estimated by assuming constant TOC/VSS ratio, at unit equilibrium concentrations.

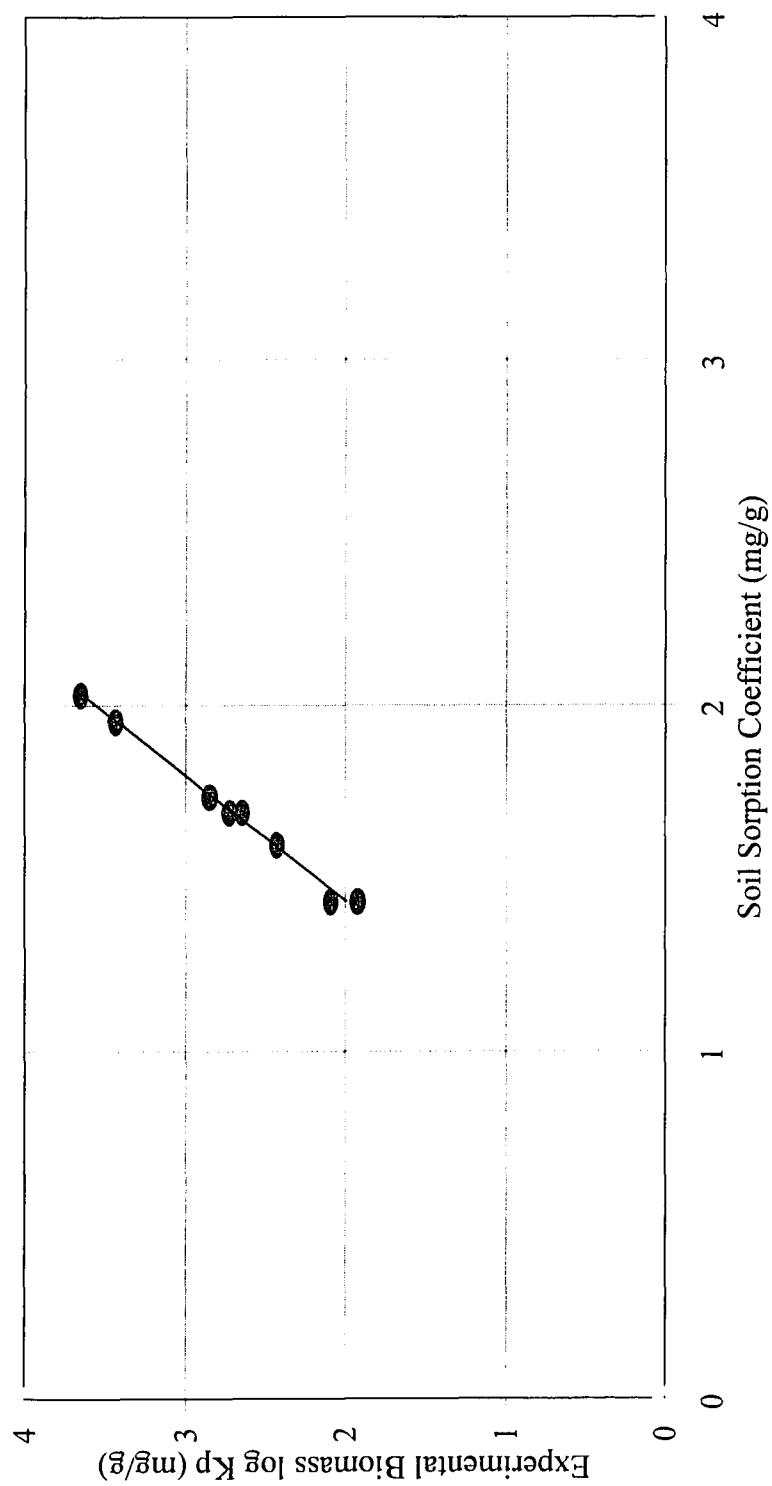


Figure 6.5.2. Correlation of experimentally determined biomass partition coefficient with soil sorption coefficient estimated from the Sabljic model.

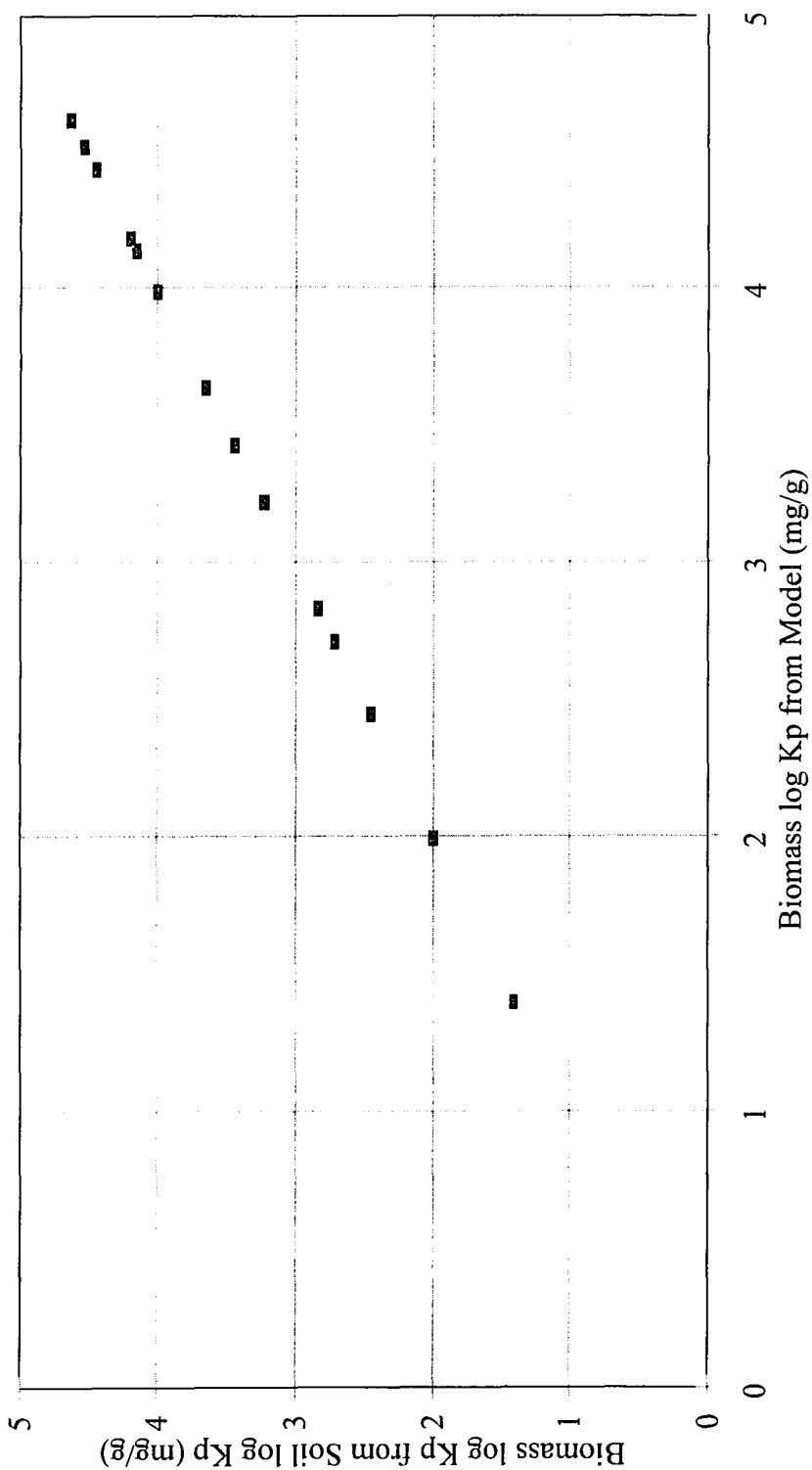


Figure 6.5.3. Correlation of predicted biomass partition coefficient with biomass coefficient estimated from soil sorption coefficients for the AX class of halogenated aliphatic hydrocarbons.

Biomass partition coefficients calculated from the model were compared to soil sorption coefficients calculated from a model suggested by Sabljic *et al.* described by Equation (6.5.1) (Sabljic *et al.*, 1995). This equation was developed for predicting soil sorption coefficients for predominantly hydrophobic chemical compounds based on organic carbon content of the soil matrix.

$$\log K_{oc} = 0.52 \, {}^1\chi + 0.70 \quad (6.5.1)$$

The correlation between the soil sorption coefficient determined by using Equation (6.5.1) and experimental biomass partition coefficient is shown in Figure 6.5.2. The correlation between the sorption capacity of halogenated aliphatic hydrocarbons to soil sorption coefficient is shown by Equation (6.5.2), with a r^2 value of 0.99 and a SE of 0.06.

$$\log K_p = 2.76 \log K_{oc} - 1.96 \quad (6.5.2)$$

From Figure 6.5.2 and 6.5.3, it can be seen that there is a good correlation between experimentally determined biomass partition coefficients and soil sorption data for halogenated aliphatic hydrocarbons. Both the biomass partition coefficient for halogenated aliphatic hydrocarbons and the soil sorption coefficient are related linearly to the first order molecular connectivity index.

As discussed earlier, it is known that the relative branching of a molecule is encoded in the ${}^1\chi$ indexes in structural isomers. Experimentally determined evidence has

shown that the first order molecular connectivity index shows a good correlation with molecular surface area and volume. Since molecular connectivity indexes are known to be indicative of mechanisms of action, it is possible that soil sorption and biomass partitioning of aliphatic hydrocarbons follow similar mechanisms. In conclusion, it can be said that the sorption-desorption capacity of halogenated aliphatic hydrocarbons has been successfully modeled using the first order molecular connectivity index ($^1\chi$) from activated sludge solids. The sorption-desorption behavior reported in this research study is based on the organic carbon content of the sorbent matrix fractionated from activated sludge solids at a RCF of 5000 x g. The sorption and desorption capacities may vary significantly in actual treatment processes if other competing fate processes such as volatilization and biodegradation are the dominant mechanisms of action. Hence, design of sludge treatment or disposal systems should take into account other fate processes before the application of the model developed in this research study.

6.6 Application of QSAR Model to a Secondary Wastewater Treatment Process

A number of QSAR models based on molecular connectivity indexes and other theoretically derived parameter have been developed to predict the fate and transport of volatile organics in the environment (Nirmalakhandan and Speece, 1988, 1989, Moore *et al.*, 1989, Sabljic *et al.*, 1995). A typical secondary wastewater treatment scheme is shown in Figure 6.6.1, which consists of a grit chamber, a primary clarifier, a secondary activated sludge treatment system, a secondary clarifier and a sludge disposal system for

waste activated sludge (WAS). A mass balance of the contaminant concentration in the treatment process can be calculated using Equation (6.6.1).

$$C_i = C_{v1} + \frac{C_{ps}}{X_{ps}} + C_{v2} + C_{bio} + \frac{C_s}{X_s} + C_e \quad (6.6.2)$$

where

C_i = influent concentration of contaminant into wastewater treatment facility, mg/L

C_{v1} = contaminant lost through volatilization from primary clarifier, mg/L

C_{ps} = sorbed concentration of contaminant to primary sludge solids, mg/g

X_{ps} = TOC concentration of primary solids, g/L

C_{v2} = contaminant lost through volatilization from activated sludge process, mg/L

C_{bio} = contaminant transformed from original structure due to biotransformation, mg/g

C_s = concentration of contaminant in activated sludge solids, mg/g

X_s = TOC concentration of activated sludge solids, g/L

C_e = effluent concentration of the contaminant, mg/L

Most of the material removed in the grit chamber consists of large debris which are usually removed using bar and rack screens. In the primary clarifier, a longer detention time is used where settleable solids are removed through sedimentation processes. It can be assumed that a majority of the suspended material settled out in the primary clarifiers is in the form of clays, soils, naturally occurring organic matter (NOM) such as leaves, sticks, etc. and other relatively small debris. The effluent from the primary clarifier flows into the activated sludge basin where the organic matter in the wastewater is stabilized.

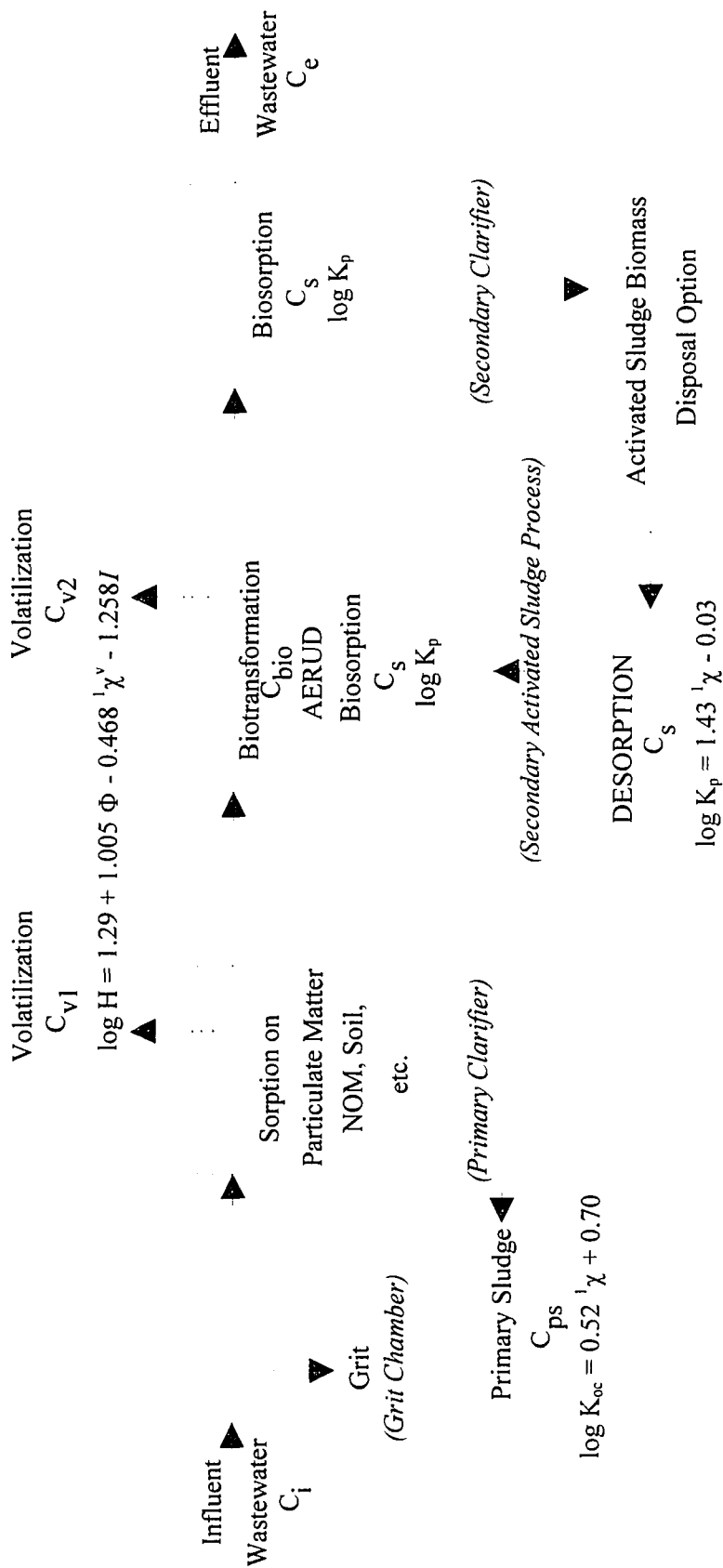


Figure 6.6.1. Schematic showing potential use of QSAR models based on molecular connectivity indexes to predict the fate of halogenated aliphatic hydrocarbon compounds in a wastewater treatment plant.

The effluent from the activated sludge process is then allowed a long detention time in a secondary clarifier where the activated sludge solids is settled out and the effluent is discharged after disinfection. A fraction of the activated sludge solids may be returned to the activated sludge reactor, while the rest of the sludge has to be disposed. As can be seen from Equation (6.6.1) and Figure (6.6.1), a contaminant entering a wastewater treatment process is subject to a variety of fate processes such as volatilization, biodegradation and biotransformation, and sorption and desorption processes. Which fate process dominates would depend on a range of factors including the operational characteristics of the wastewater treatment plant, unit operation, composition of wastewater, etc.

As can be seen from Figure 6.6.1, each of the fate processes can be described by a QSAR model based on molecular connectivity indexes. The models shown in Figure 6.6.1 have been discussed earlier. The partition coefficient ($\log K_{oc}$) can be estimated from Equation (3.2.1), the solubility ($\log S$) from Equation (3.2.2), the volatilization ($\log H$) from Equation (3.2.3), the biodegradation (AERUD) from Equation (3.2.4), and the sorption and desorption ($\log K_p$) to biomass from Equation (6.4.2).

Volatilization of the target compound from the aqueous phase during primary sedimentation and secondary activated sludge treatment will reduce the concentration of the target compound in the aqueous phase and hence affect the sorption process. Since partitioning into the gas phase is driven by faster mass transfer kinetics, for highly volatile organic chemicals, it becomes important to account for the effects of volatilization. The concentration of the target compound in the aqueous phase, after volatilization can be expressed by Equation (6.6.3) (Sawyer *et al.*, 1994).

$$C_v = \frac{C_o}{\left[1 + \frac{\left(\frac{V_a}{V_w}\right) H}{RT}\right]} \quad (6.6.3)$$

where

C_v = equilibrium concentration of target compound in the aqueous phase, mg/L

C_o = initial concentration of target compound in the aqueous phase, mg/L

V_a = volume of air in the system, L

V_w = volume of water in the system, L

H = Henry's constant, atm-L/mol

R = universal gas constant, L-atm/mol K

T = absolute temperature, °K

Analysis of the data using the different QSAR models shows that for a three hour contact period, the fate of the halogenated aliphatic hydrocarbons contaminants considered in this study are volatilization and partitioning phenomena. As can be seen from Equation (6.6.3), the volume of air passed through the system, as in the case of activated sludge treatment, determines the residual concentration of the target compound in the aqueous phase. The concentration of the target compound in the aqueous phase after sorption to primary sludge solids can also be similarly estimated using Equation (6.6.4).

$$C_{ps'} = \frac{C_o}{1 + m K_{oc}} \quad (6.6.4)$$

where

$C_{ps'}$ = equilibrium concentration of the target compound in the aqueous phase after sorption to primary sludge solids, mg/L

C_o = initial concentration of the target compound in the aqueous phase after volatilization from the primary clarifier, mg/L

K_{oc} = sorption coefficient for primary sludge solids based on TOC concentration, mg/g

m = mass of primary sludge solids available for sorption, g

The concentration of aliphatic hydrocarbons accumulating in the activated sludge solids after secondary treatment can be estimated from the concentration of the target compound available for sorption after volatilization. The amount of target compound volatilized can be estimated from Equation (6.6.3). The concentration of the target compound sorbed onto activated sludge solids after secondary treatment can be estimated from Equation (6.6.5). As discussed earlier, since sorption of halogenated aliphatic hydrocarbons to activated sludge solids is a wholly reversible process, Equation (6.6.5) also estimates the desorption capacity of these compounds from activated sludge solids.

$$C_s = C_o \left(\frac{m K_p}{1 + m K_p} \right) \quad (6.6.5)$$

where

C_s = concentration of the target compound in the activated sludge solids, mg/L

C_o = initial concentration of target compound in the aqueous phase during secondary activated sludge treatment, after volatilization from system, mg/L

m = mass of activated sludge solids available for sorption, g

K_p = sorption coefficient estimated from Equation (6.4.2), mg/g

The concentration of a halogenated aliphatic hydrocarbon entering a wastewater treatment plant can thus be estimated fairly accurately in the different phases if the fate processes are correctly identified and the appropriate models applied. Since all models discussed here are based on molecular connectivity indexes, a data file with these indexes for different contaminants is all that is required to estimate the concentration of the contaminant in the activated sludge solids, and hence its desorption potential.

CHAPTER 7

CONCLUSIONS AND RECOMMENDATIONS

This research study was conducted with the primary objective of developing a predictive equation capable of estimating the desorption potential of halogenated aliphatic hydrocarbons from activated sludge solids. During the design and conduct of the experimental study, it was realized that for a number of critical issues related to the measurement of sorption and desorption experiments, there was either no consensus between various researchers, or sometimes no information was available at all. Some of these issues were addressed in this research study in addition to developing a QSAR model to predict the desorption capacity. The principal conclusions from this research study are:

1. The Relative Centrifugal Force (RCF) used in the separation of the sorbent matrix from the aqueous phase plays a critical role in the accurate determination of concentration of the target compound in the aqueous phase. A phase separation RCF between 10000 x g to 20000 x g is recommended for initial separations of activated sludge solids from a unit process, and a higher phase separation RCF during the course of sorption and desorption experiments.
2. It was found that sorption and desorption parameters are not influenced by either the sorbent concentrations or the concentrations of the target compound in the aqueous

phase for solids and target compound concentration ranges commonly encountered in wastewater treatment systems. It was also observed for the set of compounds evaluated that equilibrium was attained rapidly during the sorption and desorption experiments. Shorter equilibration times can potentially reduce variations induced into the sorbent matrix due to cell lysis or death.

3. Effective control of bioactivity for an equilibration time of 180 minutes was achieved by conducting sorption experiments at a pH of 3.0. The bioactivity was determined from measurement of the Oxygen Uptake Rate (OUR) of the activated sludge solids. Microscopic examination of the bacteria revealed that there was no significant damage to the cell structure of bacteria in the activated sludge solids at a pH of 3.0.
4. The sorption and desorption processes of halogenated aliphatic hydrocarbons in activated sludge solids can be modeled using the Freundlich isotherm. Target compounds sorbed onto activated sludge solids was released back entirely into the aqueous phase during the desorption experiments, indicating that sorption of halogenated aliphatic hydrocarbons onto activated sludge solids is a totally reversible process.
5. A QSAR model to quantify the desorption capacity of halogenated aliphatic hydrocarbons was modeled using a first order molecular connectivity index, shown by the equation below. The model was developed using activated sludge solids from a laboratory scale activated sludge reactor with recycle and an ASBR, and was

validated using activated sludge solids from a pure oxygen activated sludge treatment process: $\log K_p = 1.43 \chi - 0.03$, with correlation coefficient $r^2 = 0.99$, and $SE = 0.05$.

6. The experimentally determined sorption parameters ($\log K_p$) for the halogenated aliphatic hydrocarbons were found to be linearly related to soil sorption coefficients ($\log K_{oc}$) through the equation : $\log K_p = 2.76 \log K_{oc} - 1.96$, with correlation coefficient $r^2 = 0.99$, and $SE = 0.06$.
7. The fate and transport of halogenated aliphatic hydrocarbon compounds may be modeled in a wastewater treatment plant using a simple data base of molecular connectivity indexes and appropriate QSAR models. Such a system can effectively predict the concentration of halogenated aliphatic hydrocarbons in different unit operations in a treatment plant if the influent concentration of the toxic organic compound is known.

A standard experimental protocol needs to be developed to measure sorption and desorption parameters from various sorbent matrices of environmental interest. The lack of standardized techniques for the measurement of these parameters results in each researcher having to develop his own methodology through a series of preliminary experimental tests which costs both time and money without significant contribution to the knowledge pool. A common protocol would help understand and compare measured phenomena in its right perspective and make cross correlations meaningful.

This research study has shown that sorption and desorption parameters can be accurately modeled using QSAR models based on molecular connectivity indexes. The advantages of using theoretically derived parameters such as molecular connectivity indexes is obvious, and hence models for other classes of compounds such as phthalate esters, pesticides, PAHs, etc., which are commonly found to concentrate in wastewater treatment plant sludges need to be developed.

APPENDIX A

SORPTION AND DESORPTION ISOTHERMS

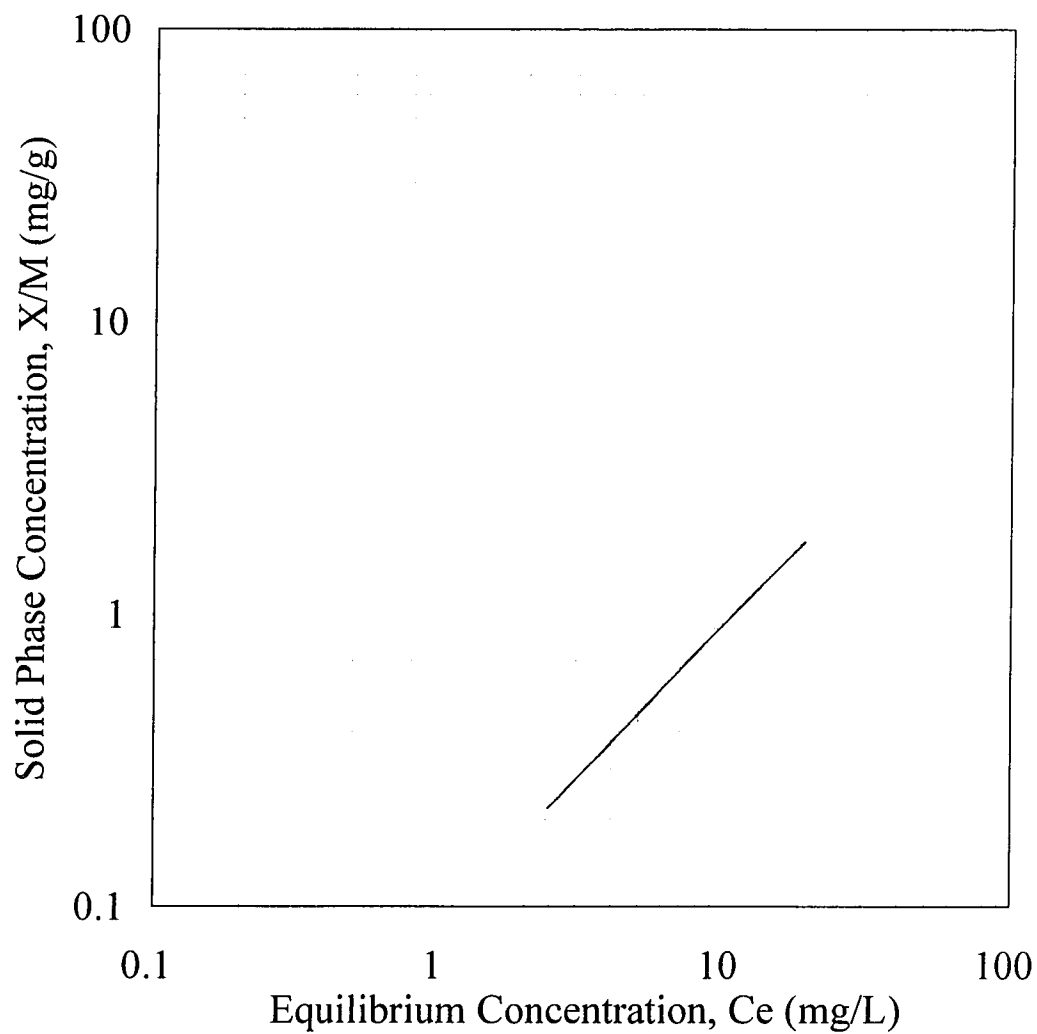


Figure A.1. Sorption isotherm for Methylene Chloride with biomass from activated sludge reactor with recycle. Desorbed concentrations of methylene chloride could not be determined.

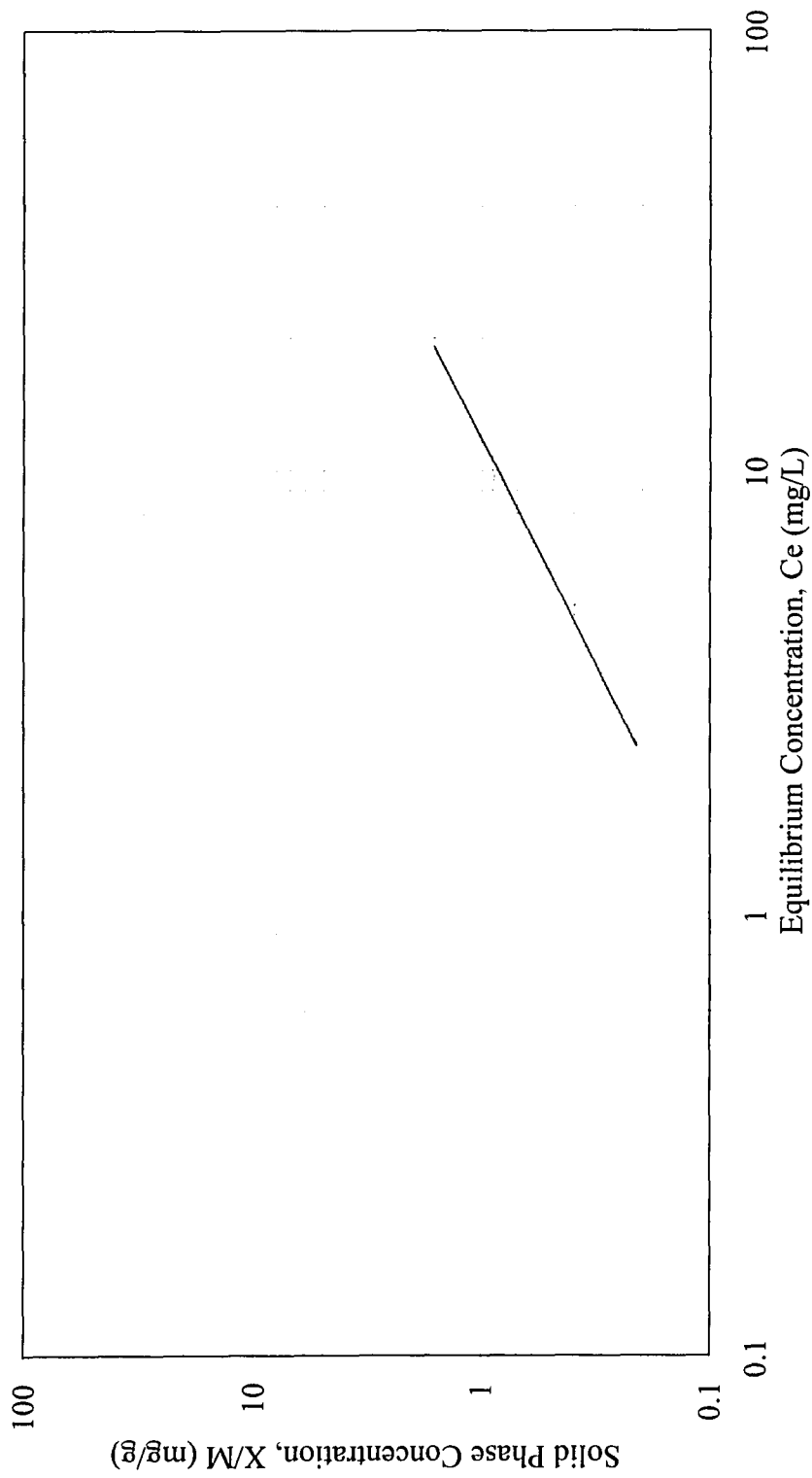


Figure A.2. Sorption isotherm for Methylene Chloride with biomass from ASBR. Desorbed concentrations of methylene chloride could not be determined.

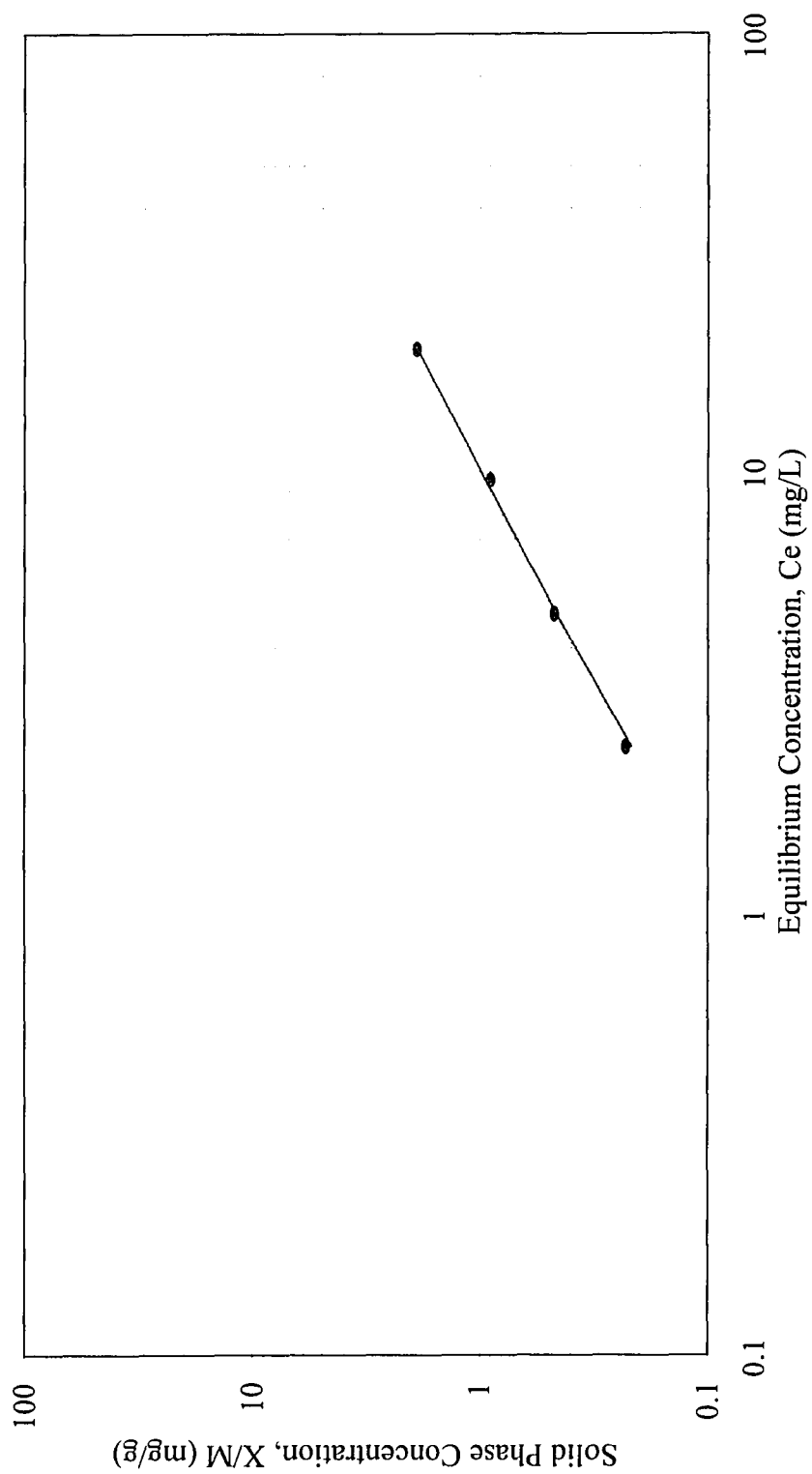


Figure A.3. Sorption isotherm for Methylene Chloride with biomass from pure oxygen activated sludge process. Desorbed concentrations of methylene chloride could not be determined.

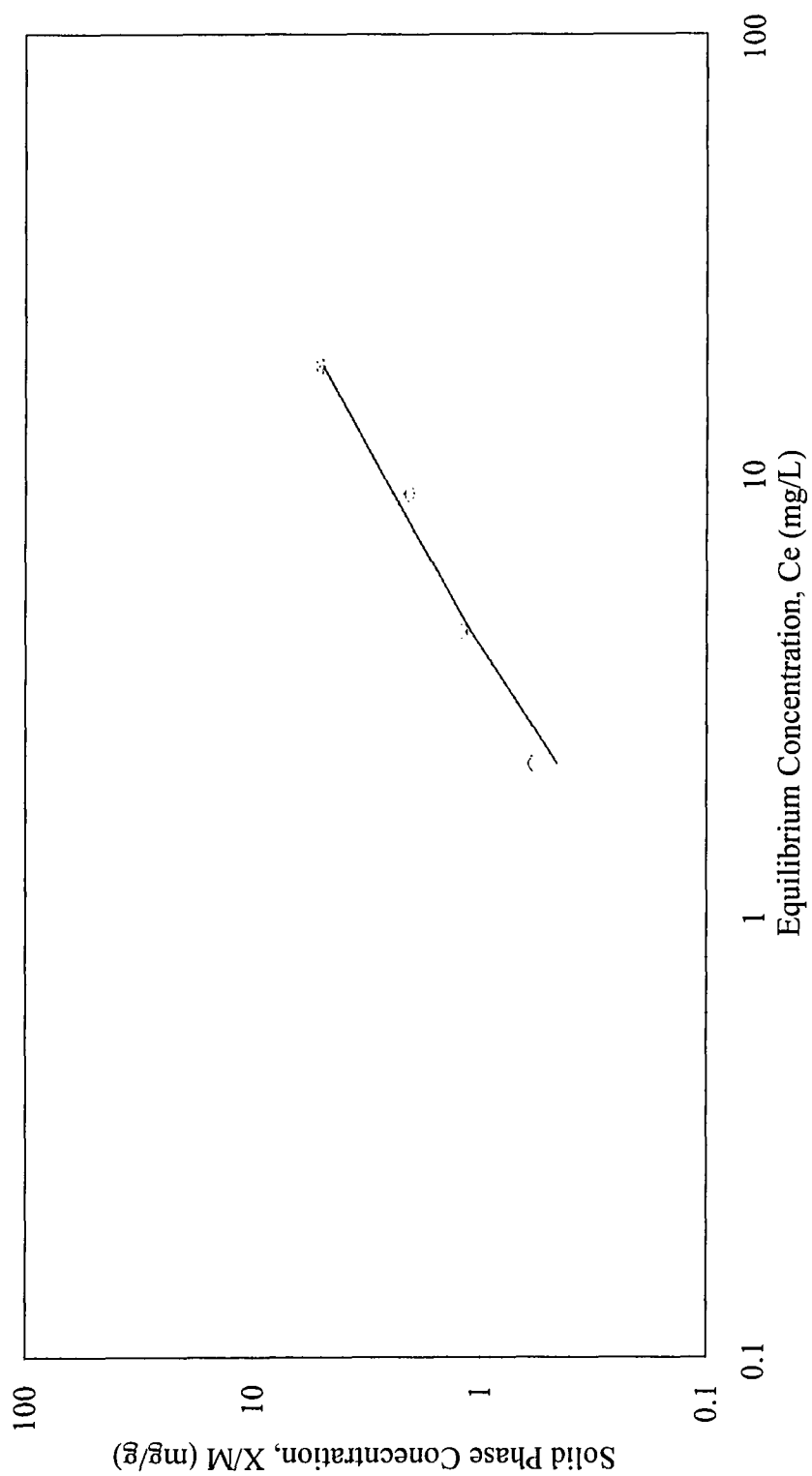


Figure A.4. Sorption and desorption isotherms for Trichloromethane with biomass from activated sludge reactor with recycle. Circles represent sorbed concentrations and crosses represent desorbed concentrations.

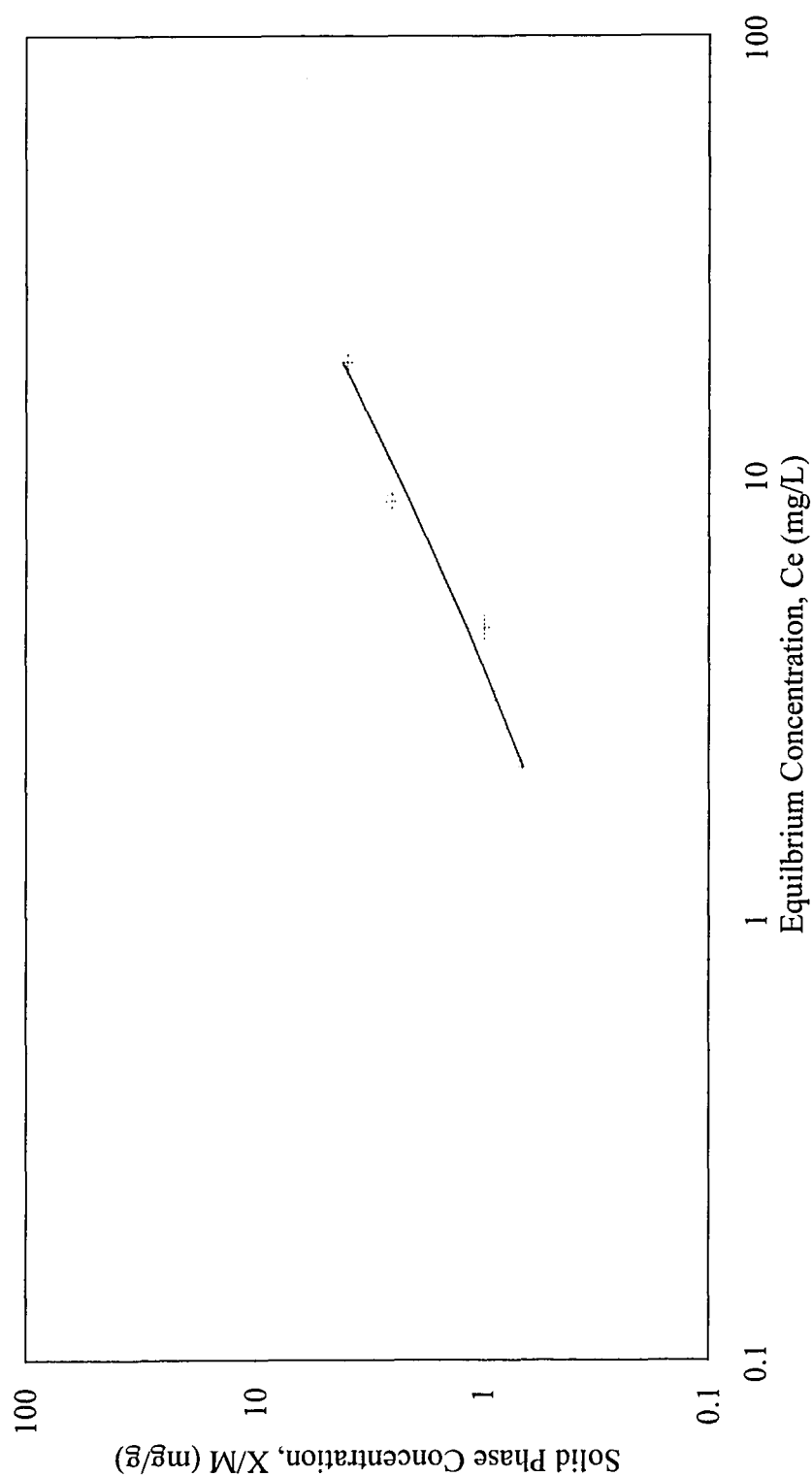


Figure A.5. Sorption and desorption isotherms for Trichloromethane with biomass from ASBR. Circles represent sorbed concentrations and crosses represent desorbed concentrations.

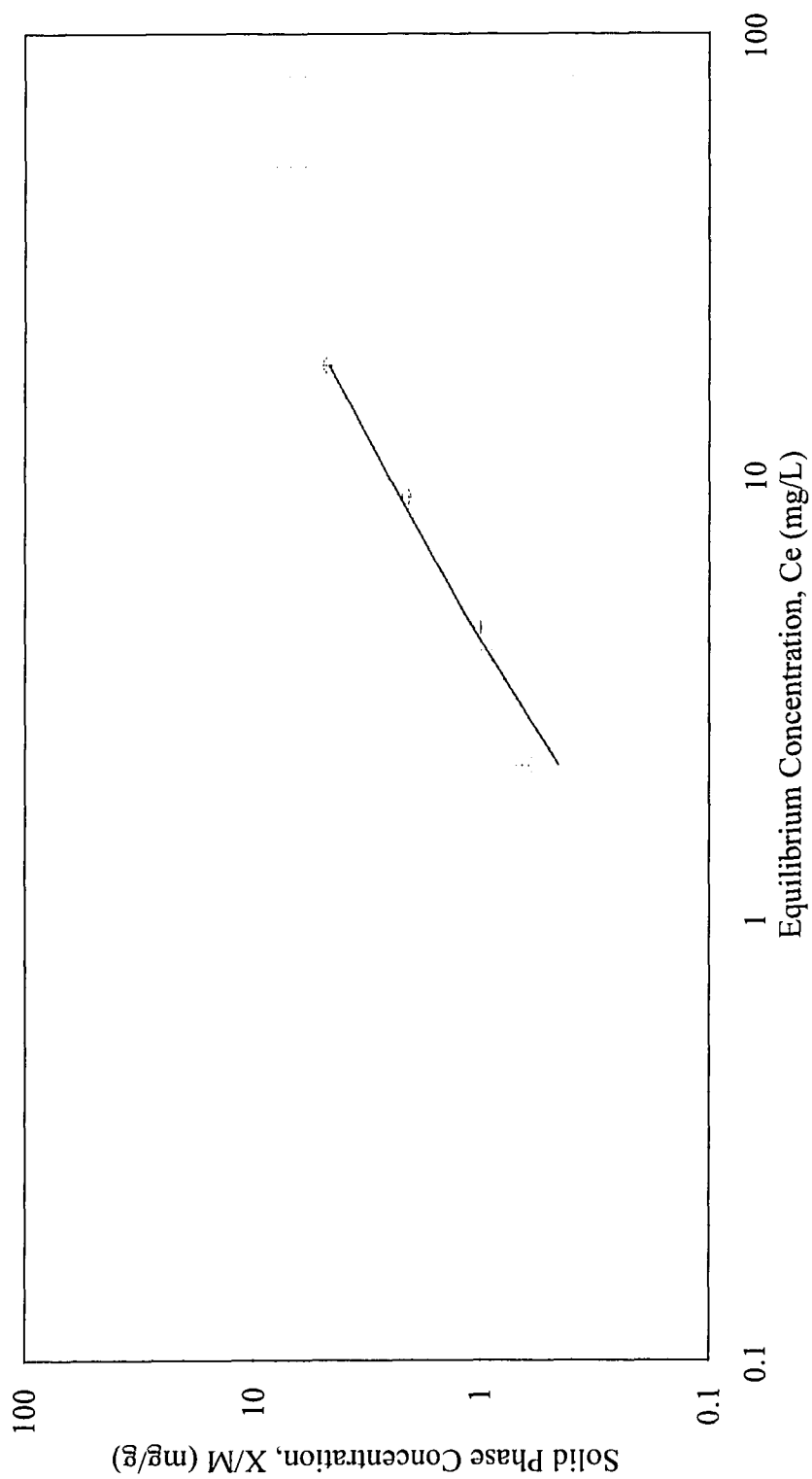


Figure A.6. Sorption and desorption isotherms for Trichloromethane with biomass from pure oxygen activated sludge process (PVSC). Circles represent sorbed concentrations and crosses represent desorbed concentrations.

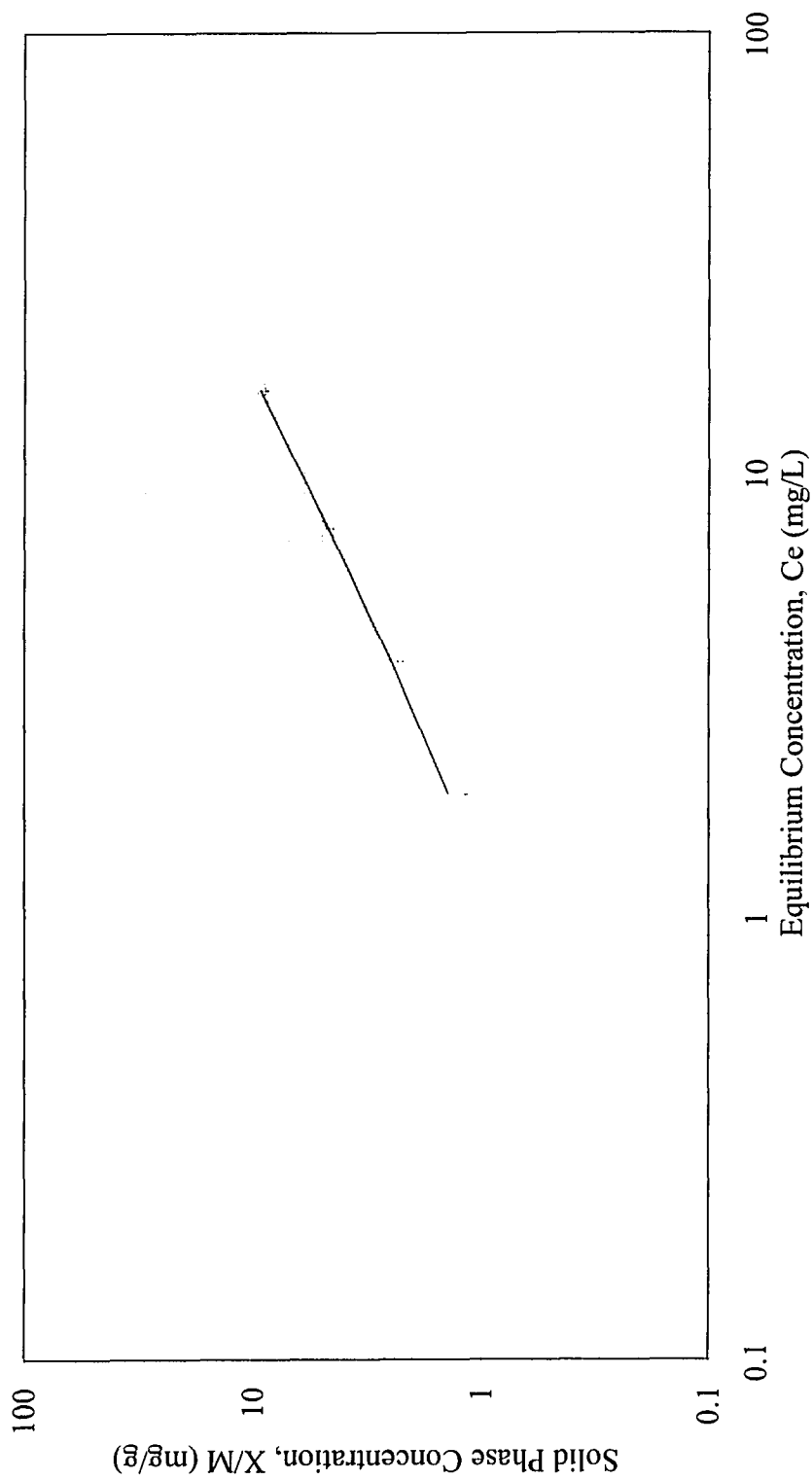


Figure A.7. Sorption and desorption isotherms for Trichlorofluoromethane with biomass from activated sludge reactor with recycle. Circles represent sorbed concentrations and crosses represent desorbed concentrations.

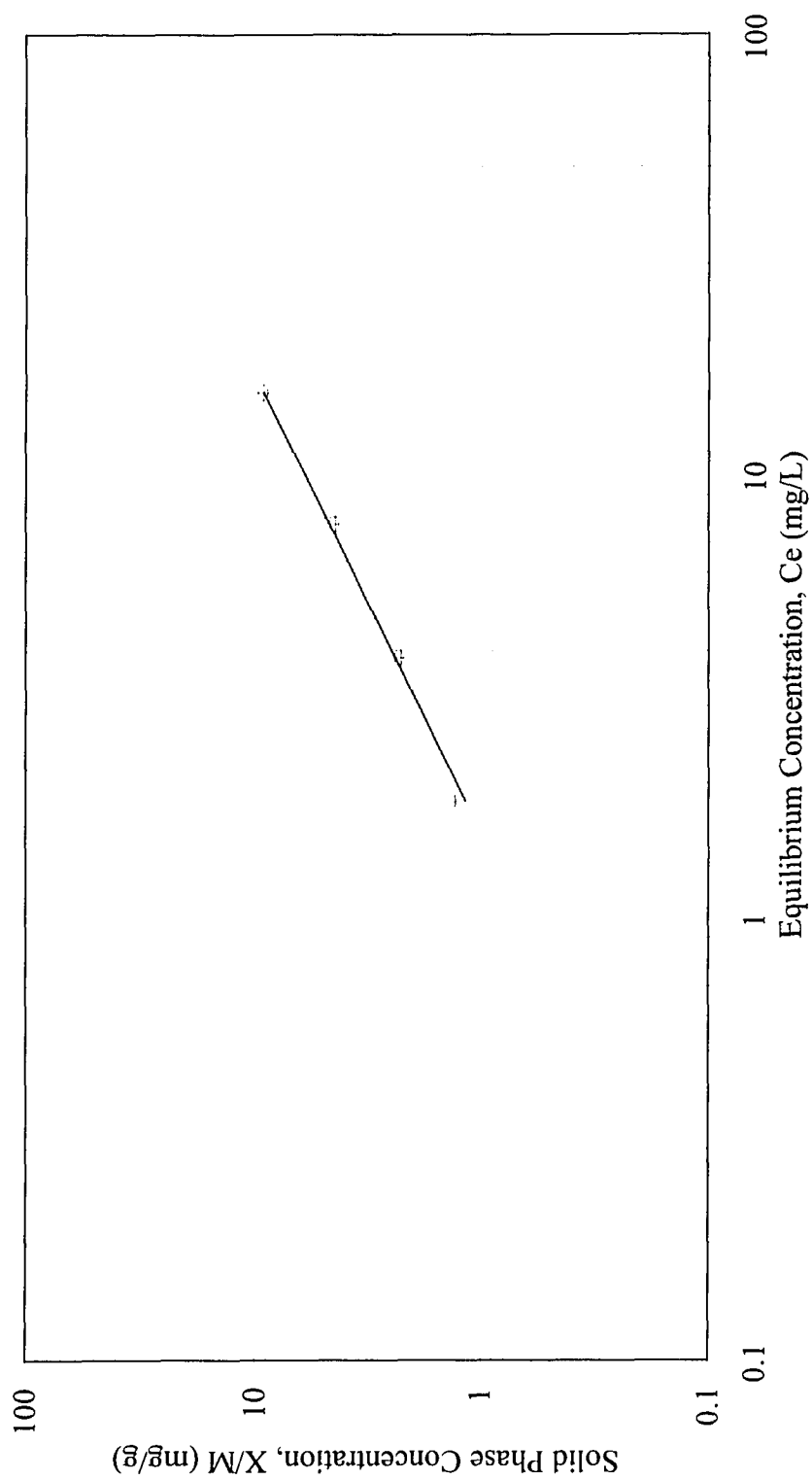


Figure A.8. Sorption and desorption isotherms for Trichlorofluoromethane with biomass from ASBR. Circles represent sorbed concentrations and crosses represent desorbed concentrations.

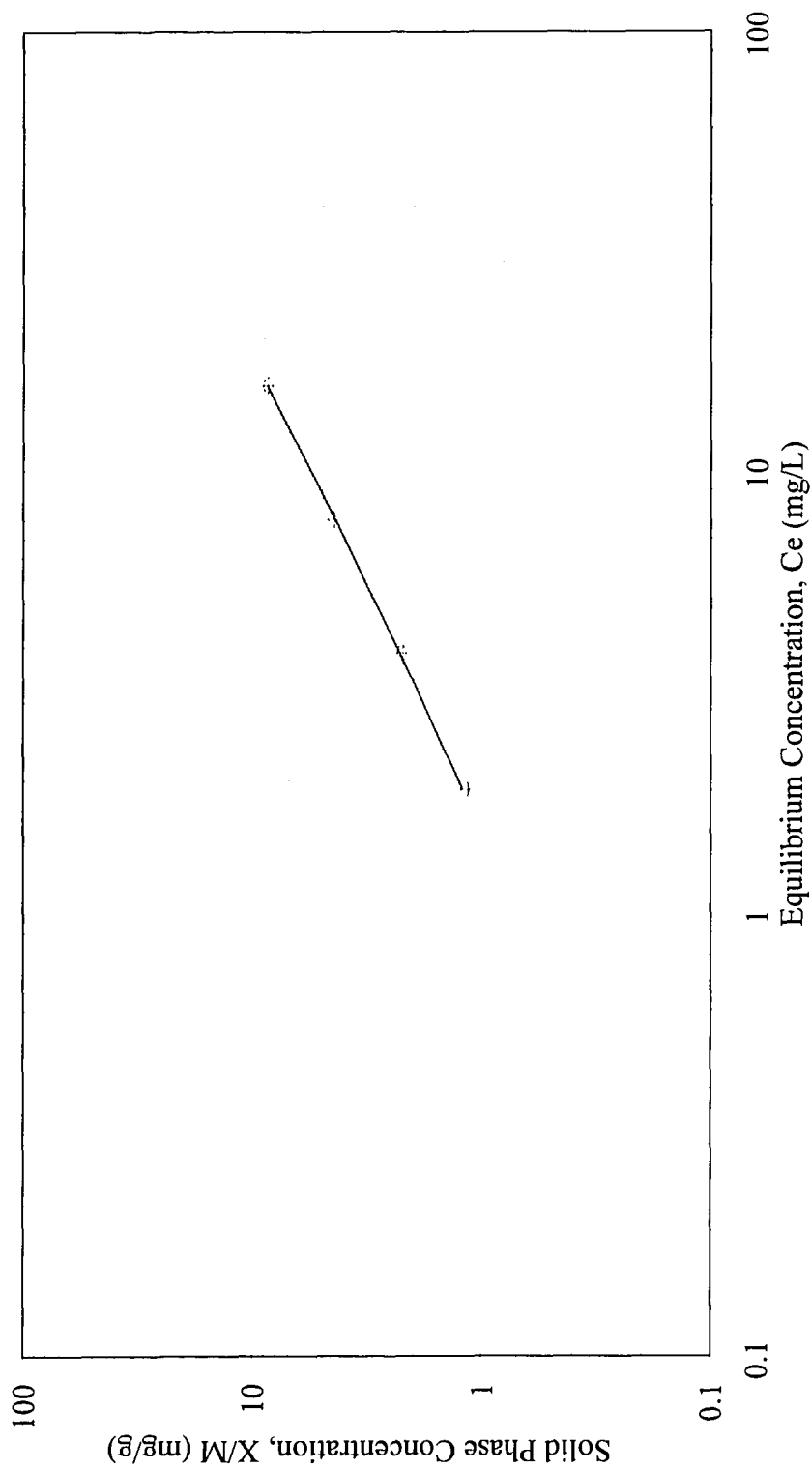


Figure A.9. Sorption and desorption isotherms for Trichlorofluoromethane with biomass from pure oxygen activated sludge process (PVSC). Circles represent sorbed concentrations and crosses represent desorbed concentrations.

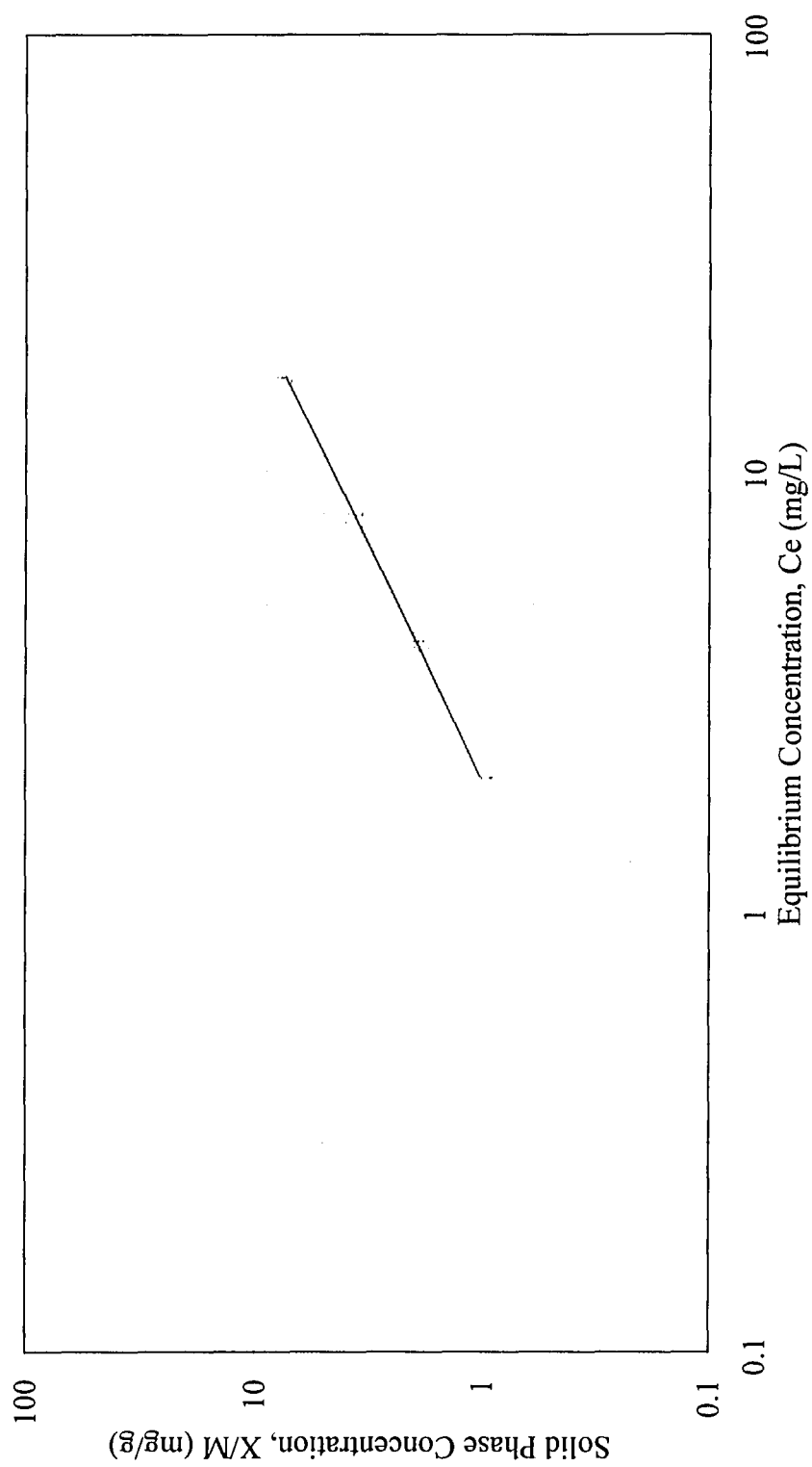


Figure A.10. Sorption and desorption isotherms for Dichloroethane with biomass from activated sludge reactor with recycle. Circles represent sorbed concentrations and crosses represent desorbed concentrations.

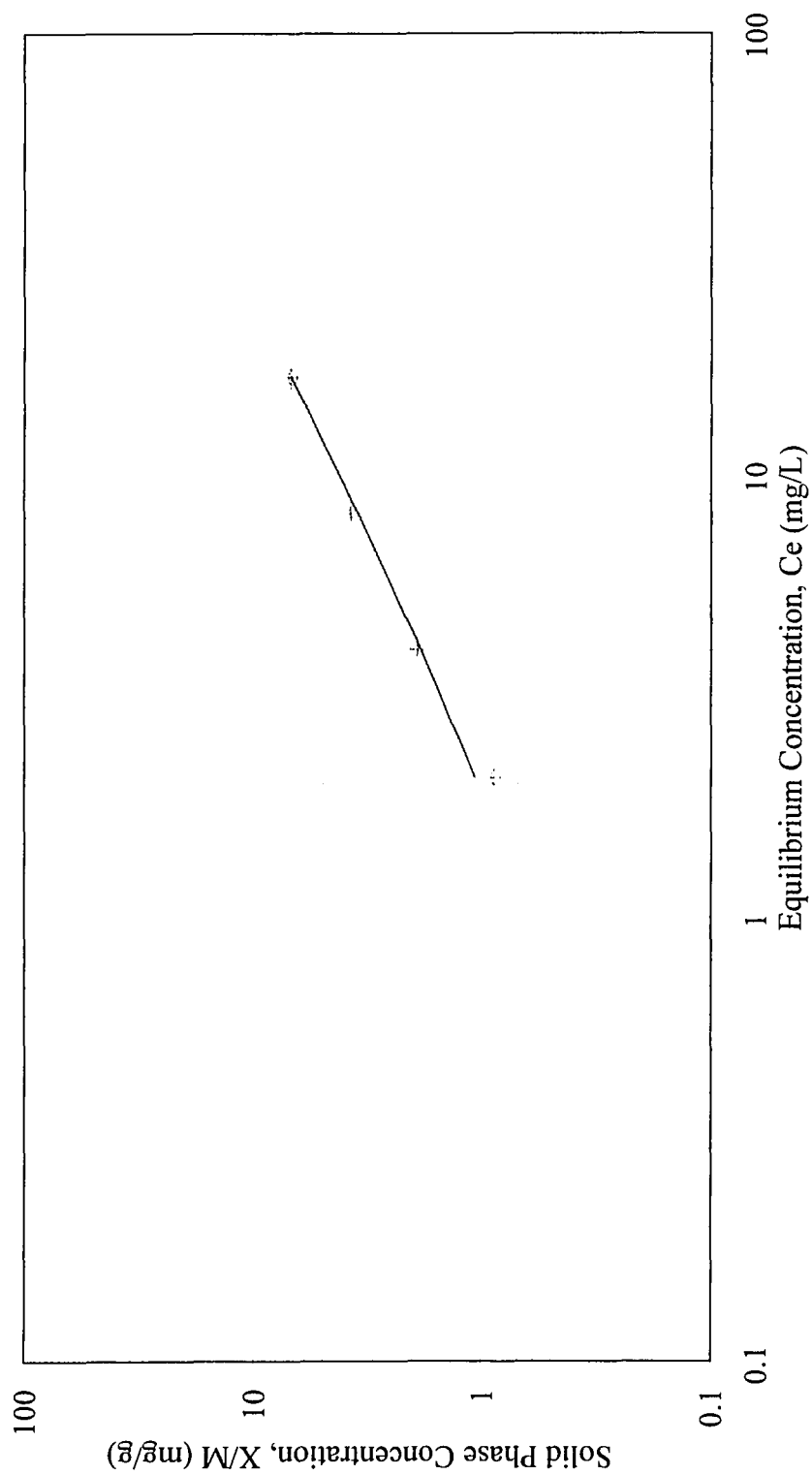


Figure A.11. Sorption and desorption isotherms for Dichloroethane with biomass from ASBR. Circles represent sorbed concentrations and crosses represent desorbed concentrations.

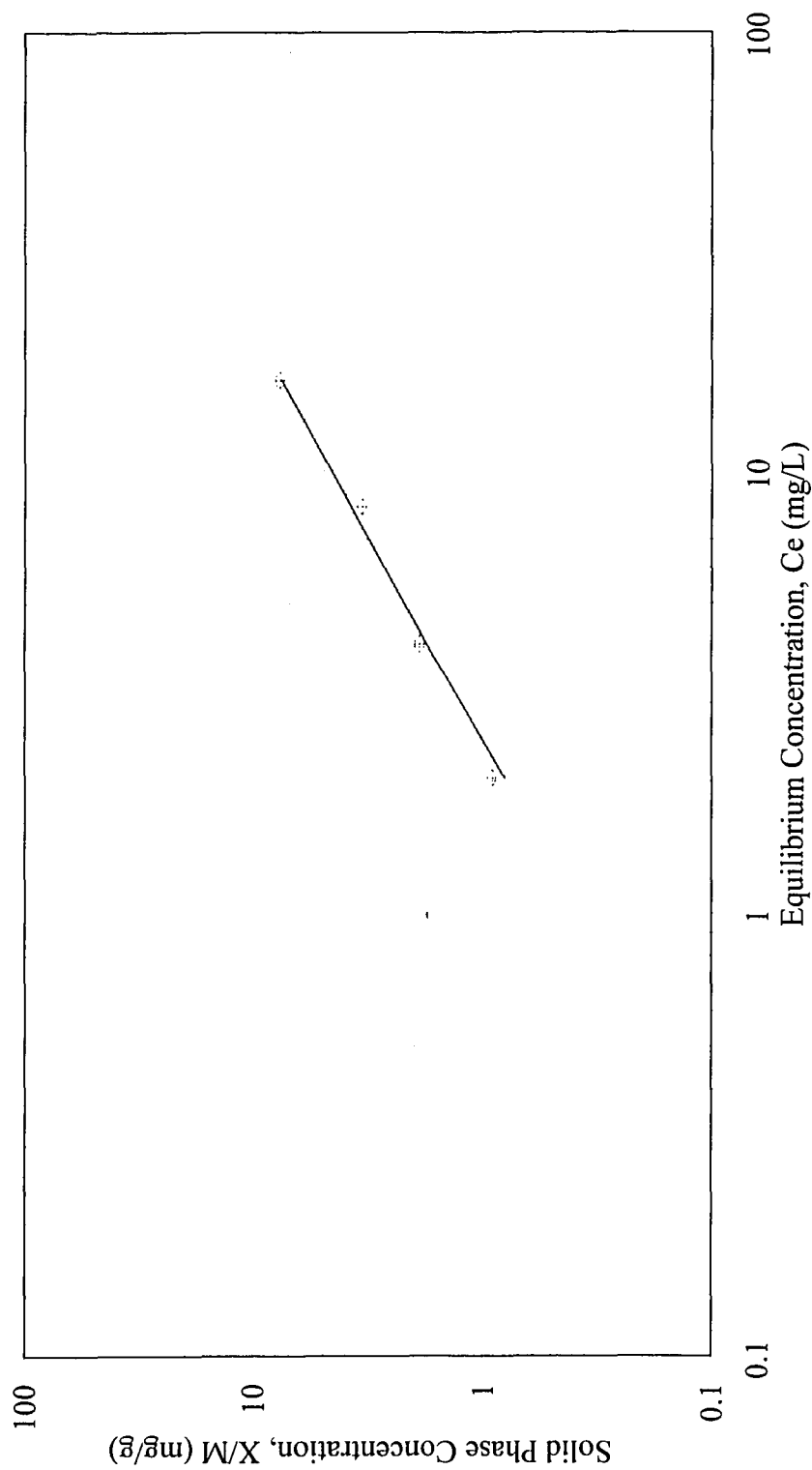


Figure A.12. Sorption and desorption isotherms for Dichloroethane with biomass from pure oxygen activated sludge process (PVSC). Circles represent sorbed concentrations and crosses represent desorbed concentrations.

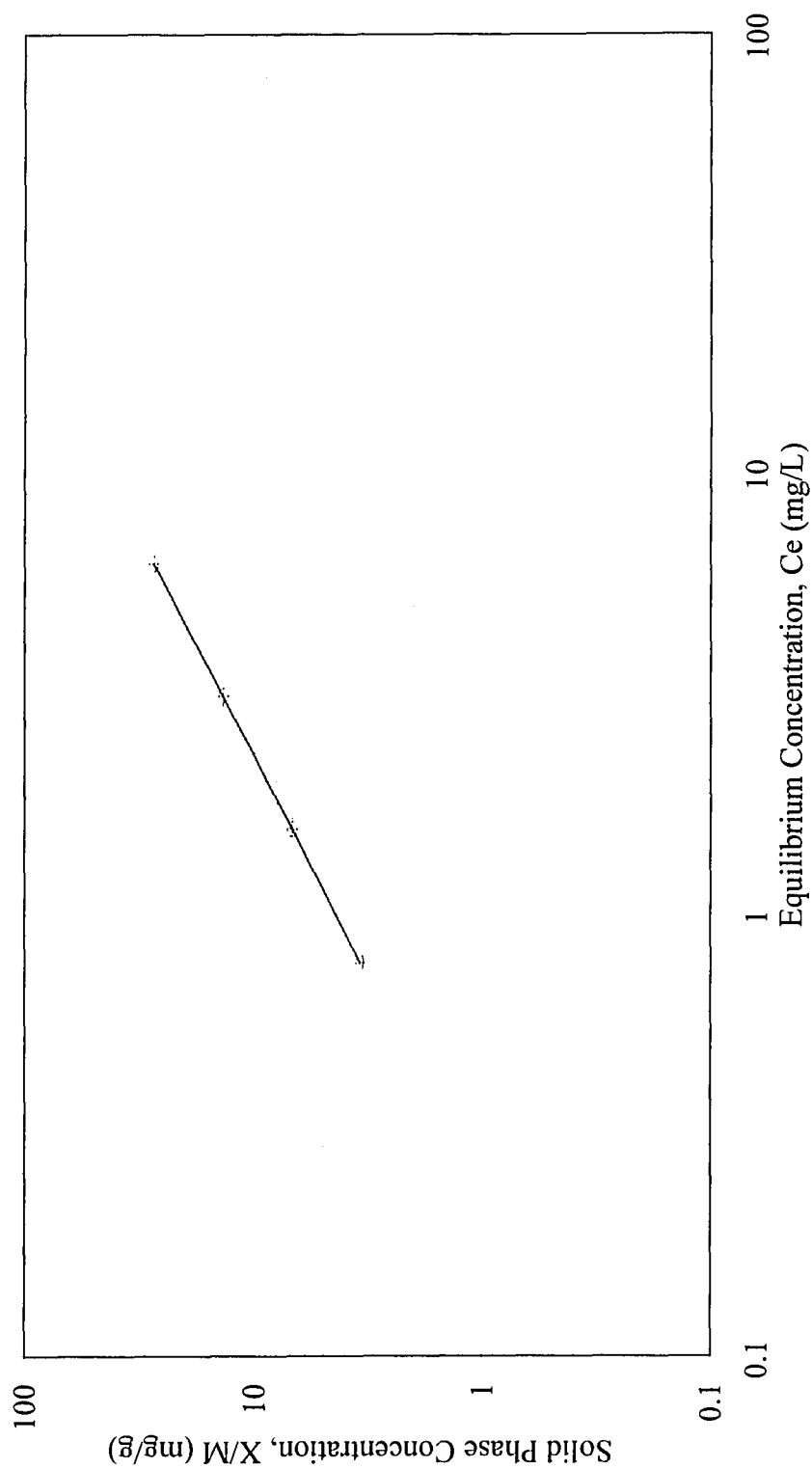


Figure A.13. Sorption and desorption isotherms for Tetrachloroethane with biomass from activated sludge reactor with recycle. Circles represent sorbed concentrations and crosses represent desorbed concentrations.

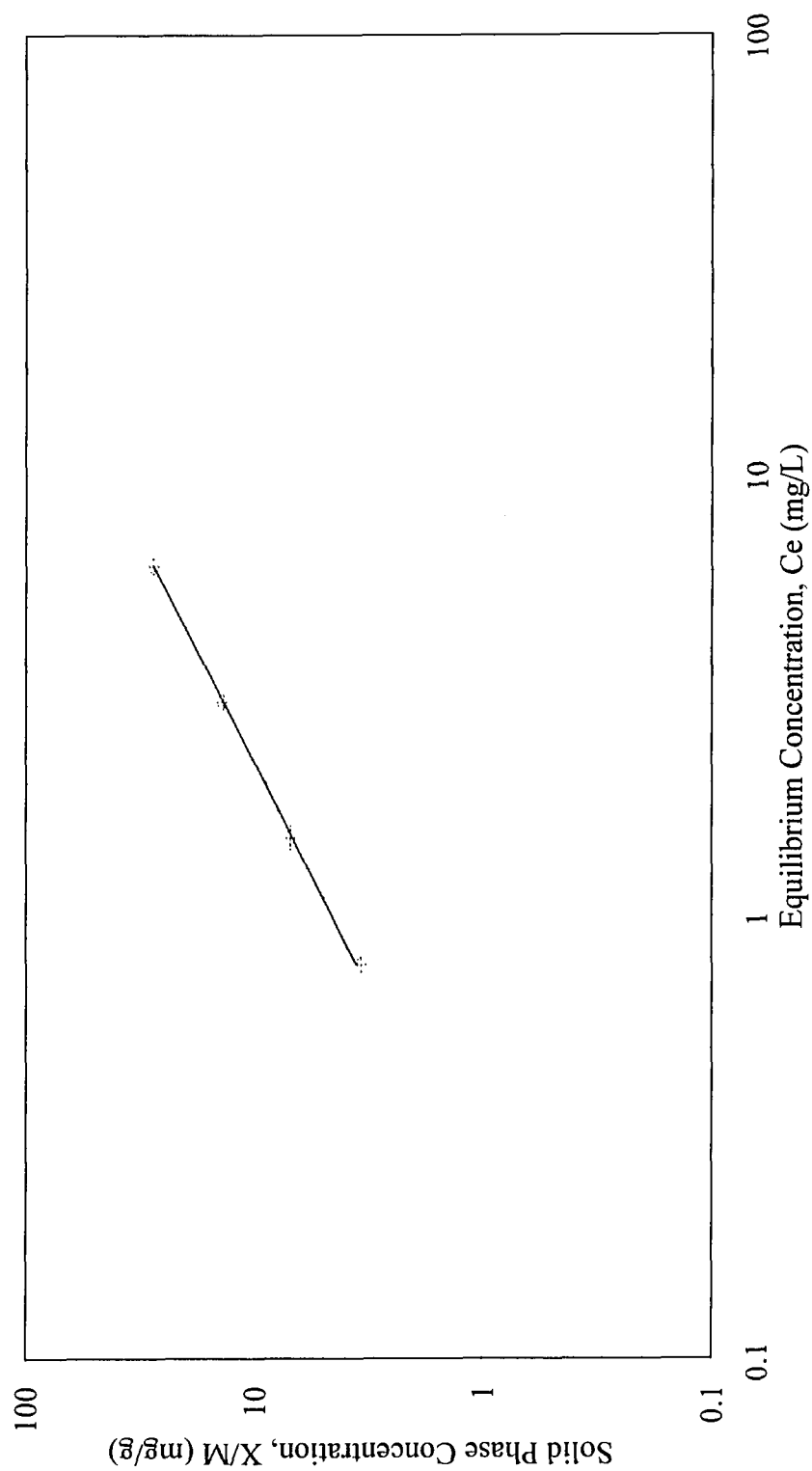


Figure A.14. Sorption and desorption isotherms for Tetrachloroethane with biomass from ASBR. Circles represent sorbed concentrations and crosses represent desorbed concentrations.

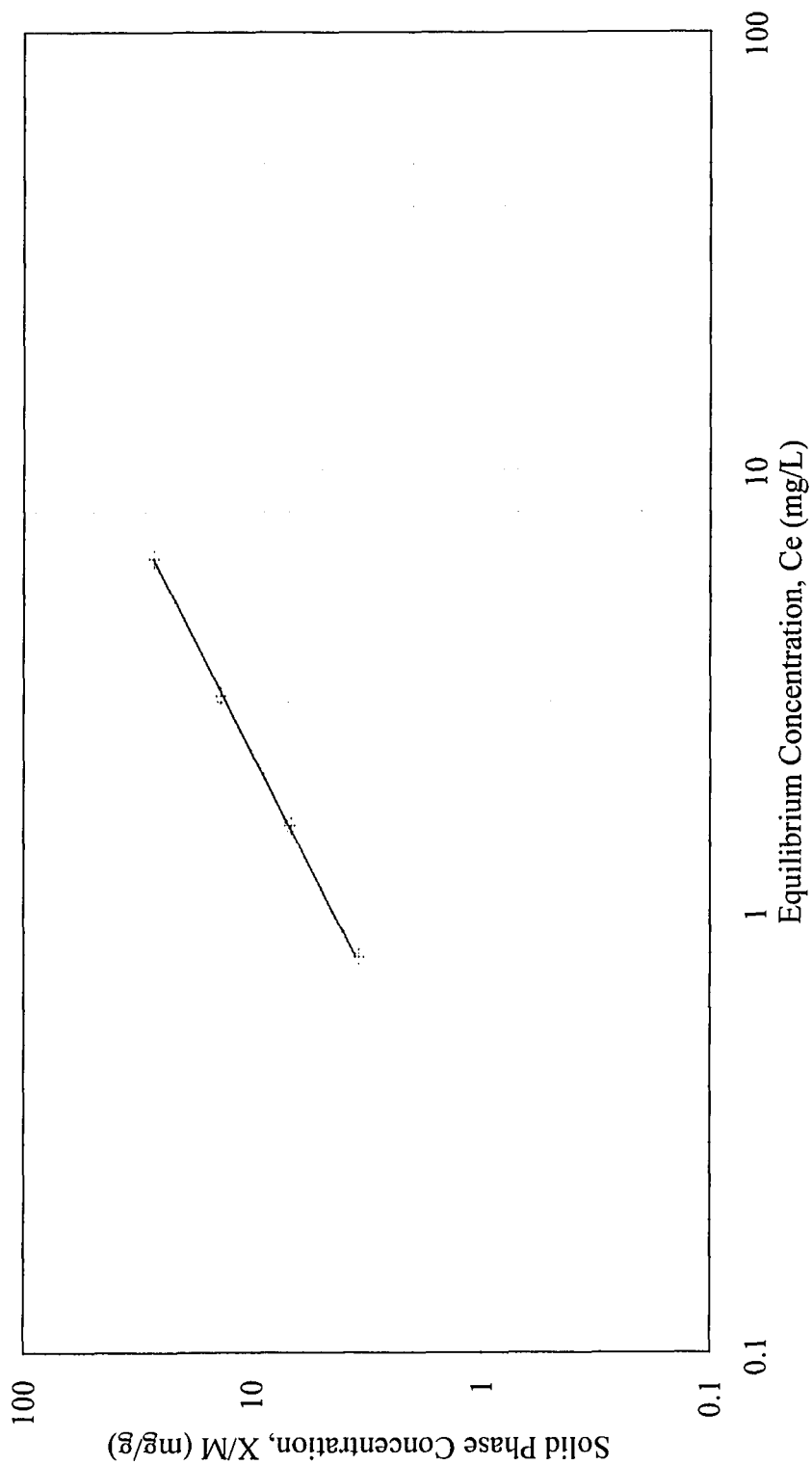


Figure A.15. Sorption and desorption isotherms for Tetrachloroethane with biomass from pure oxygen activated sludge process (PVSC). Circles represent sorbed concentrations and crosses represent desorbed concentrations.

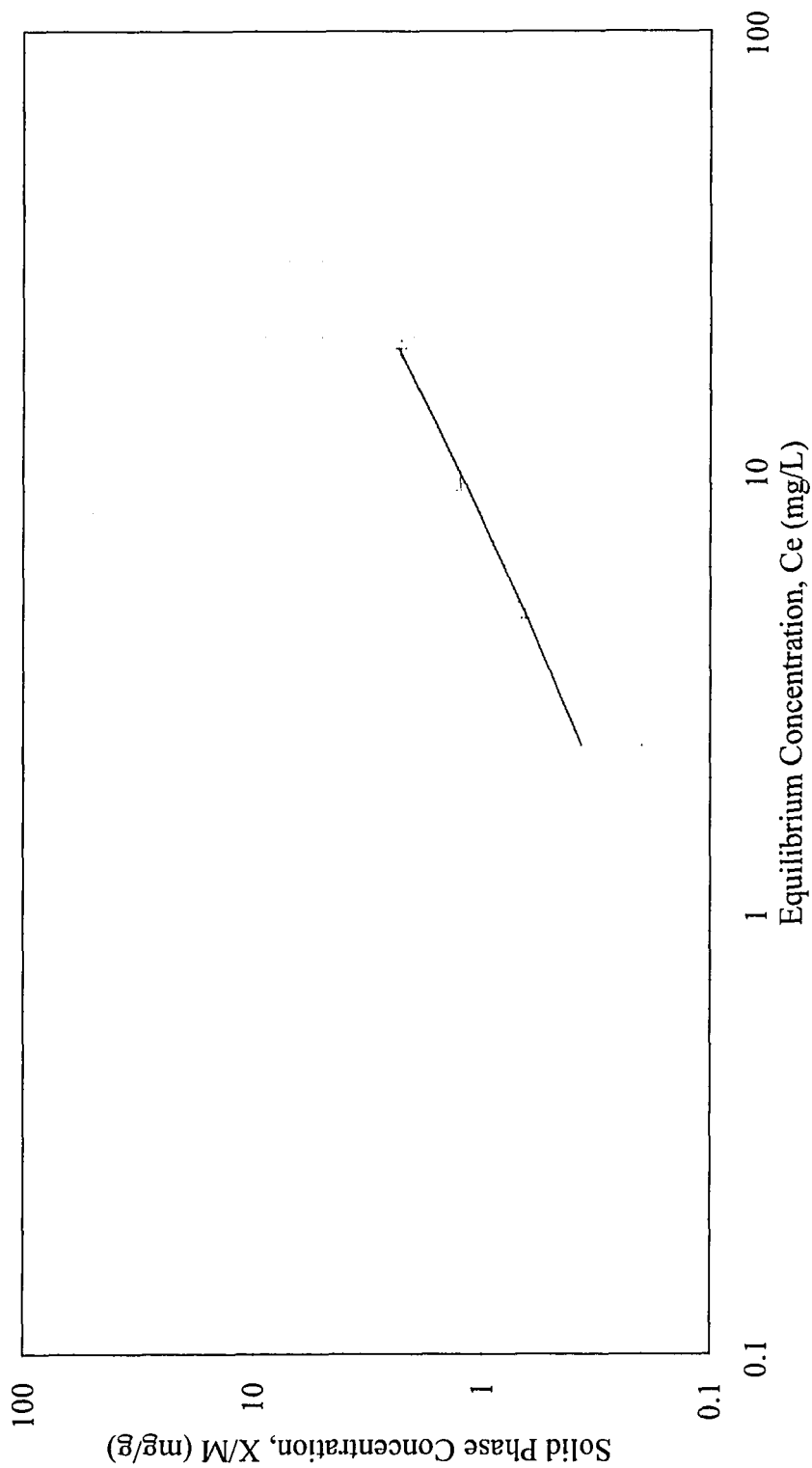


Figure A.16. Sorption and desorption isotherms for Bromoethane with biomass from activated sludge reactor with recycle. Circles represent sorbed concentrations and crosses represent desorbed concentrations.

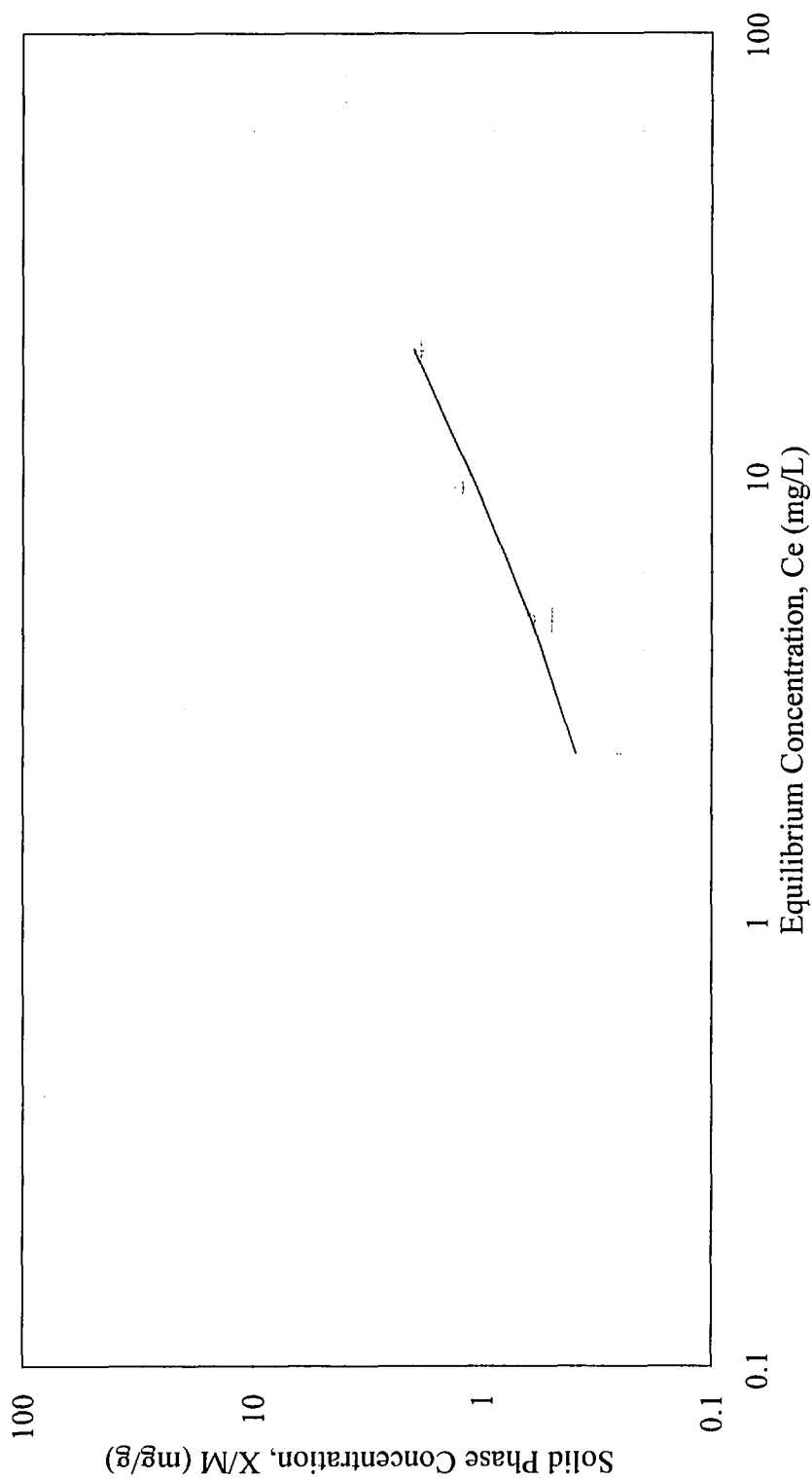


Figure A.17. Sorption and desorption isotherms for Bromoethane with biomass from ASBR. Circles represent sorbed concentrations and crosses represent desorbed concentrations.

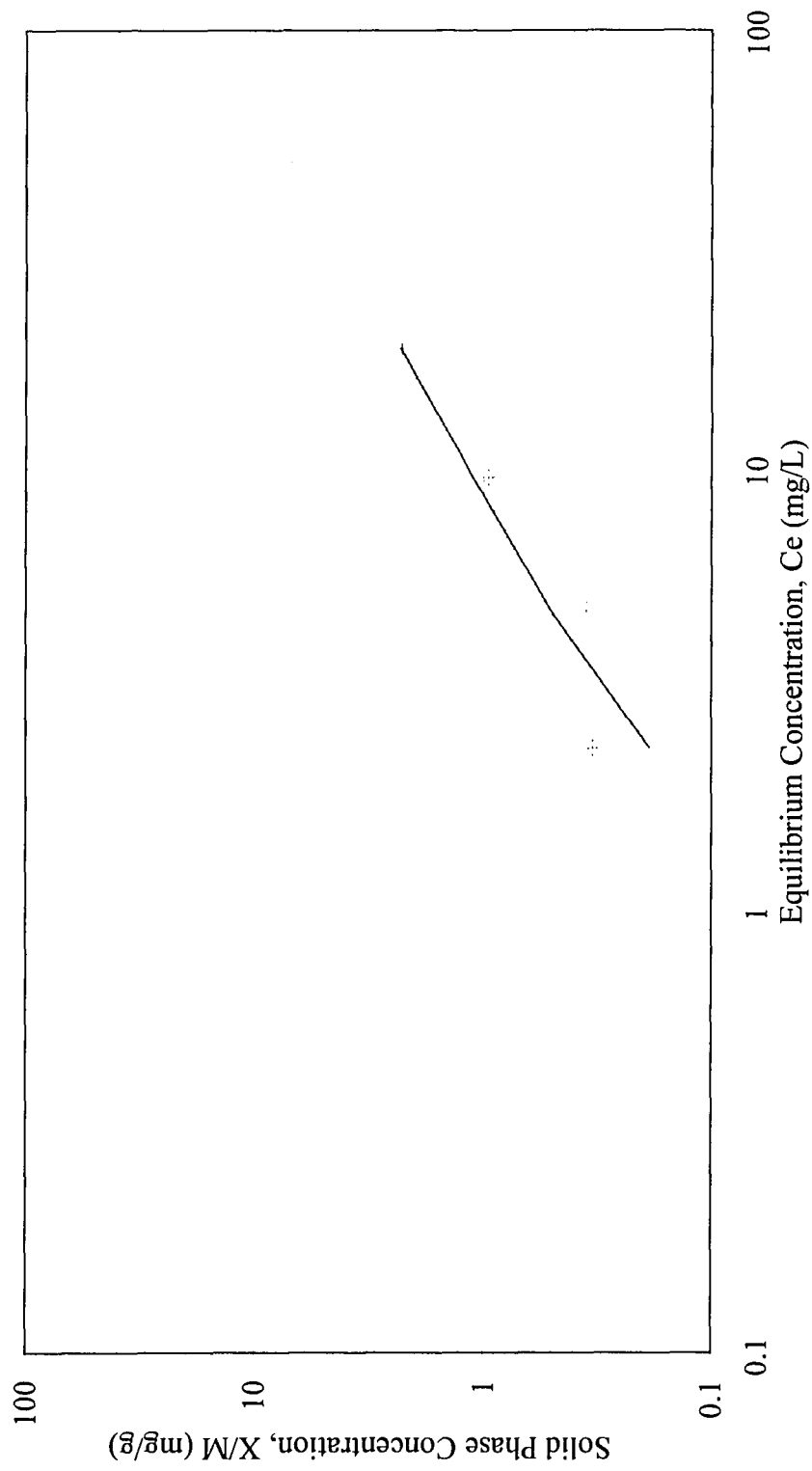


Figure A.18. Sorption and desorption isotherms for Bromoethane with biomass from pure oxygen activated sludge process (PVSC). Circles represent sorbed concentrations and crosses represent desorbed concentrations.

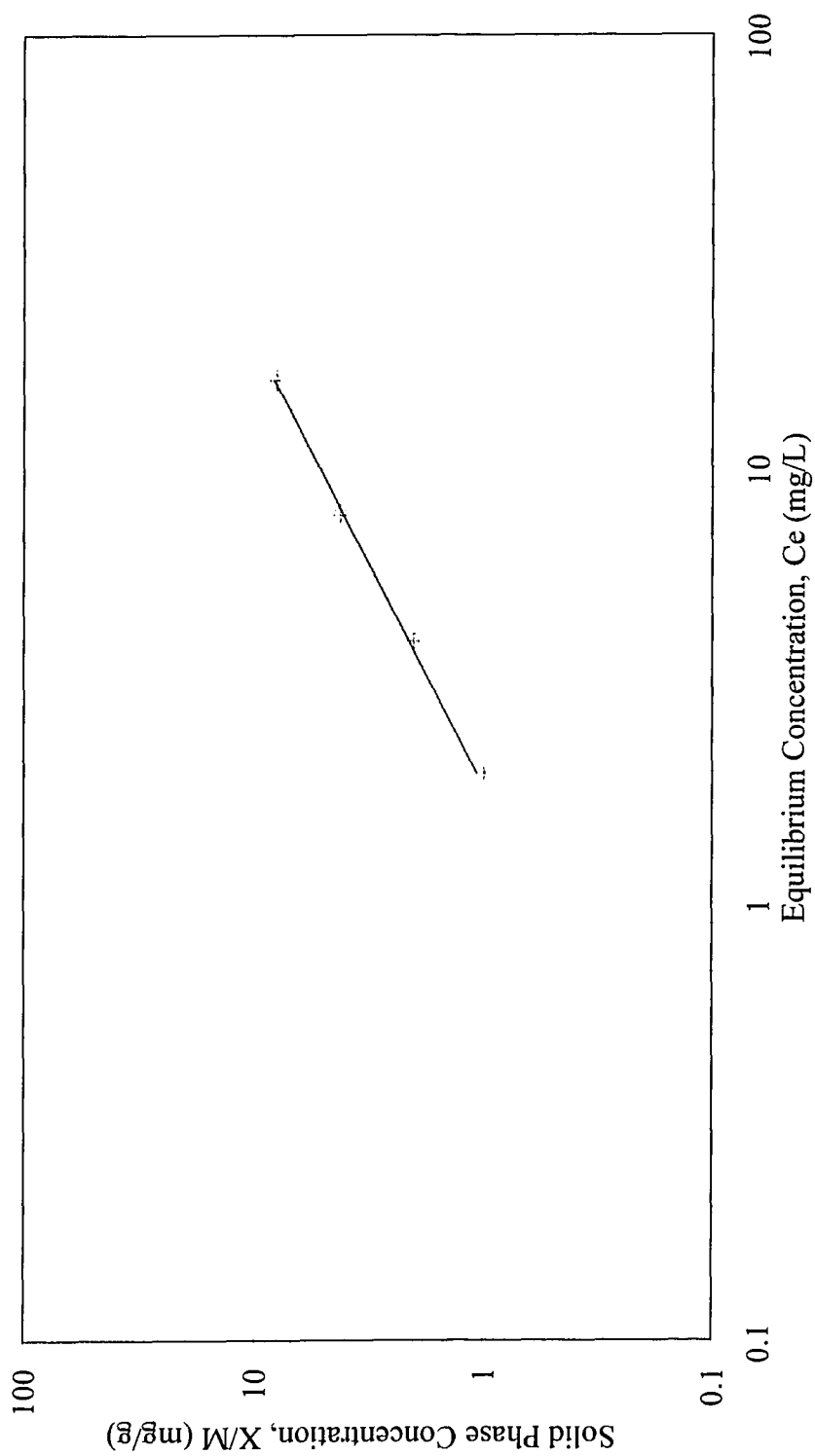


Figure A.19. Sorption and desorption isotherms for Dibromoethane with biomass from activated sludge reactor with recycle. Circles represent sorbed concentrations and crosses represent desorbed concentrations.

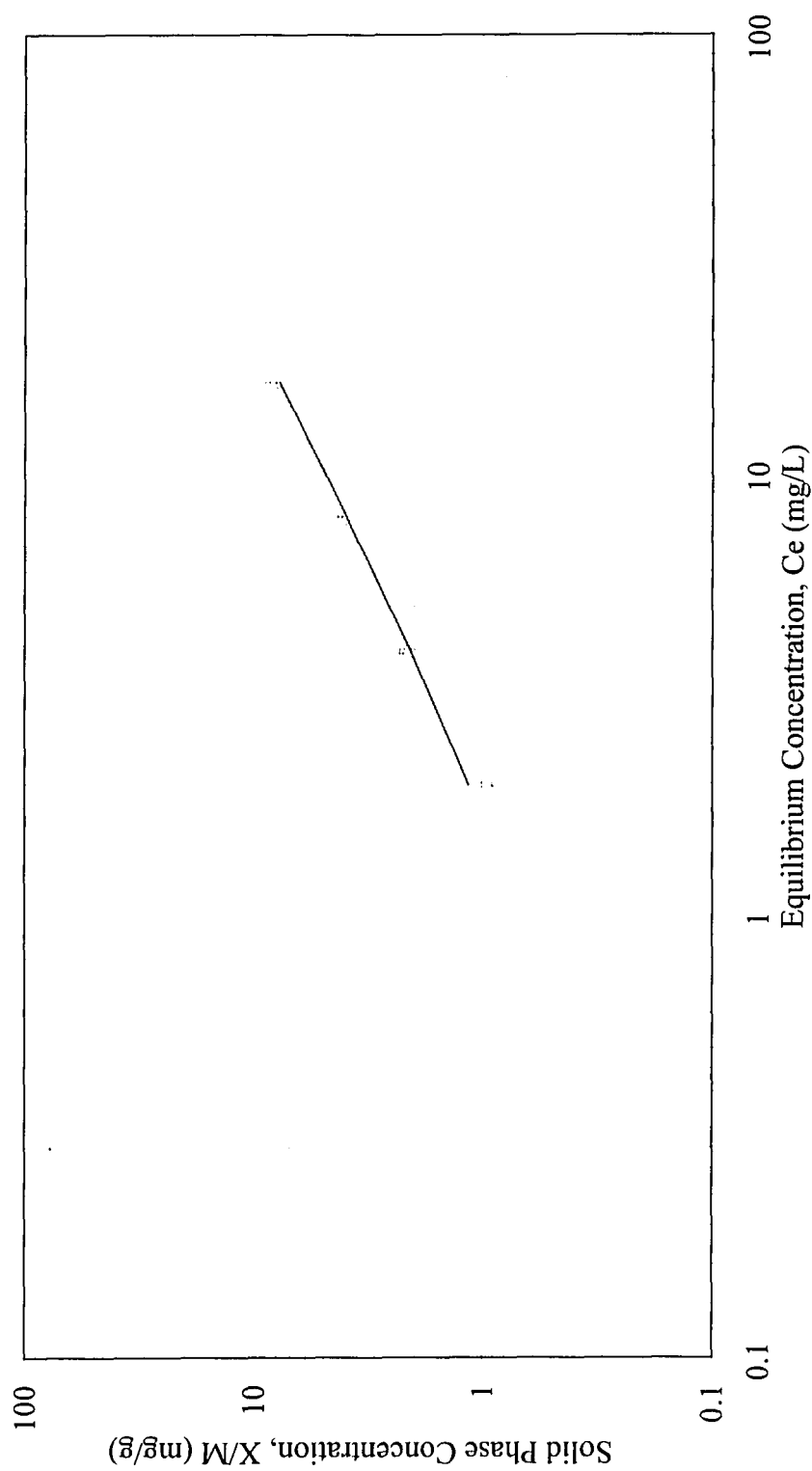


Figure A.20. Sorption and desorption isotherms for Dibromoethane with biomass from ASBR. Circles represent sorbed concentrations and crosses represent desorbed concentrations.

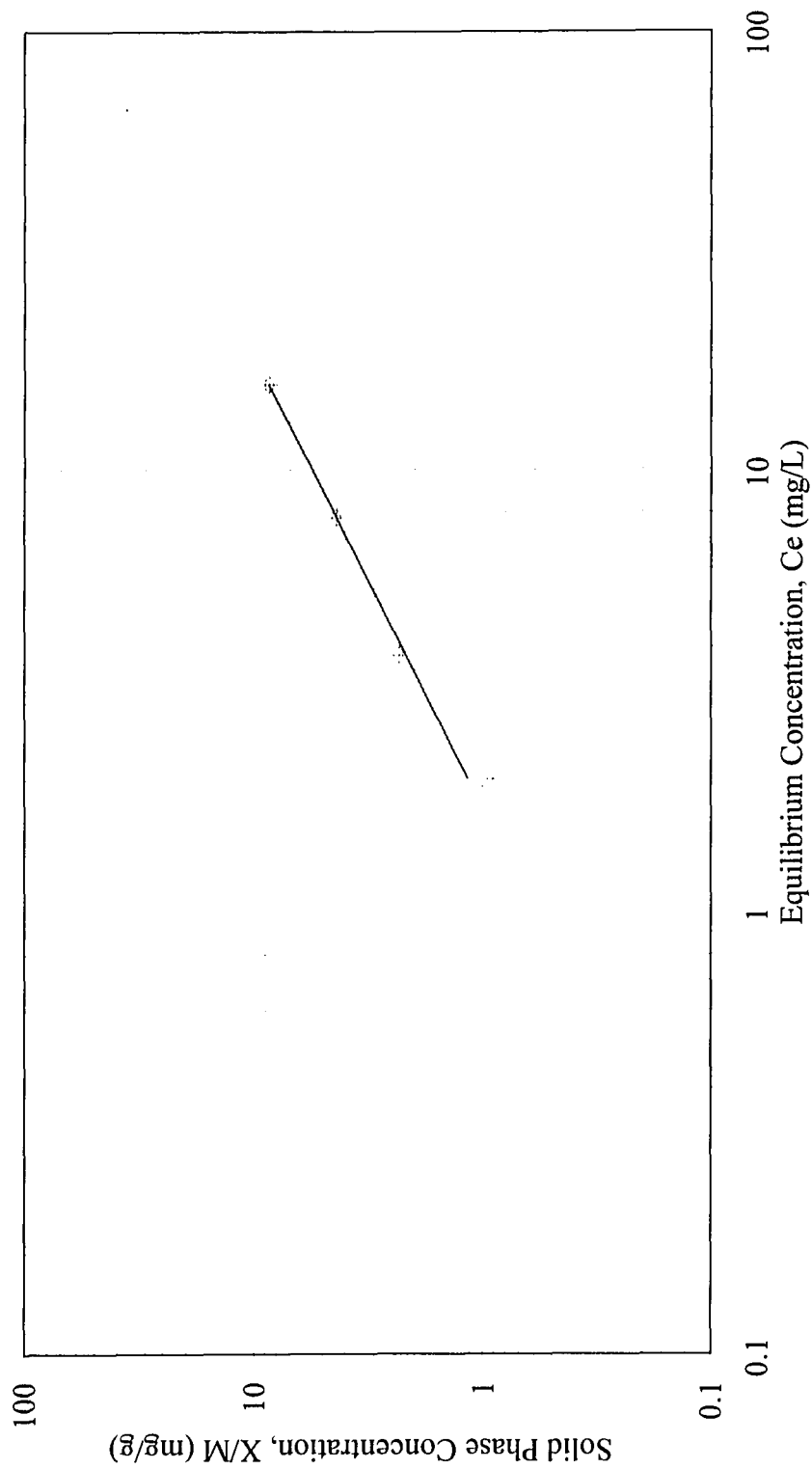


Figure A.21. Sorption and desorption isotherms for Dibromoethane with biomass from pure oxygen activated sludge process (PVSC). Circles represent sorbed concentrations and crosses represent desorbed concentrations.

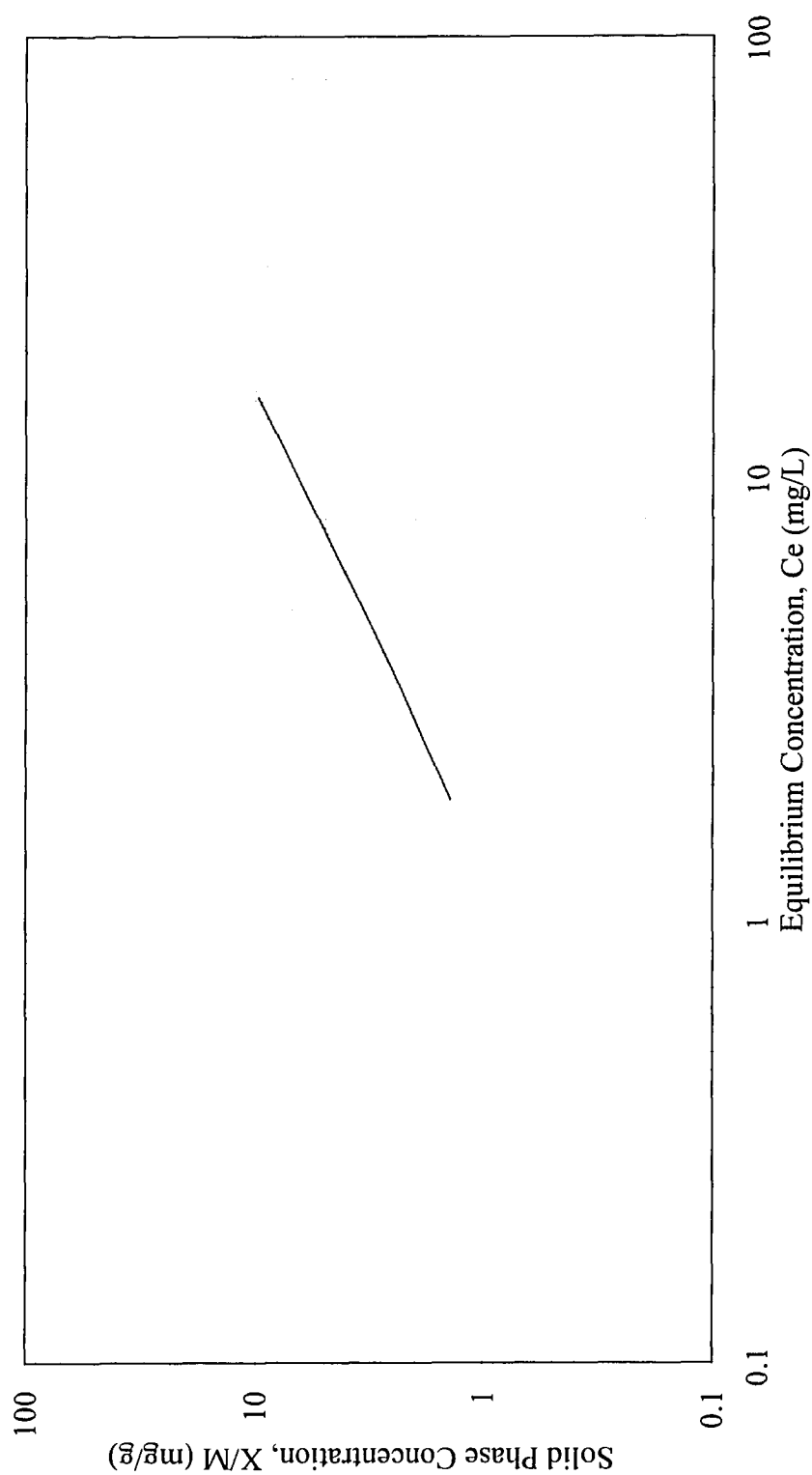


Figure A.22. Sorption isotherm for Tribromofluoromethane with biomass from activated sludge reactor with recycle. Desorption concentrations could not be measured..

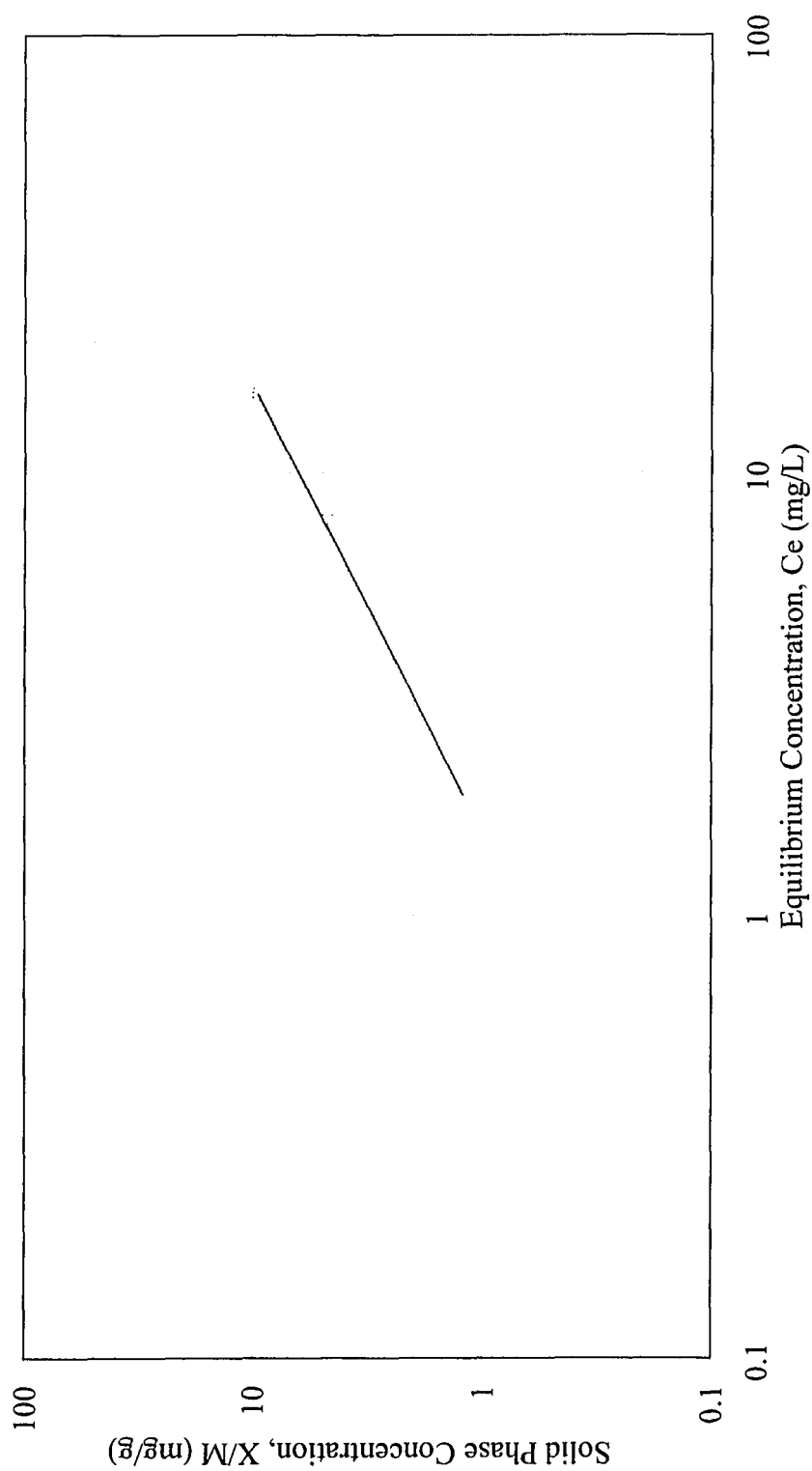


Figure A.23. Sorption isotherm for Tribromofluoromethane with biomass from ASBR. Desorption concentrations could not be measured.

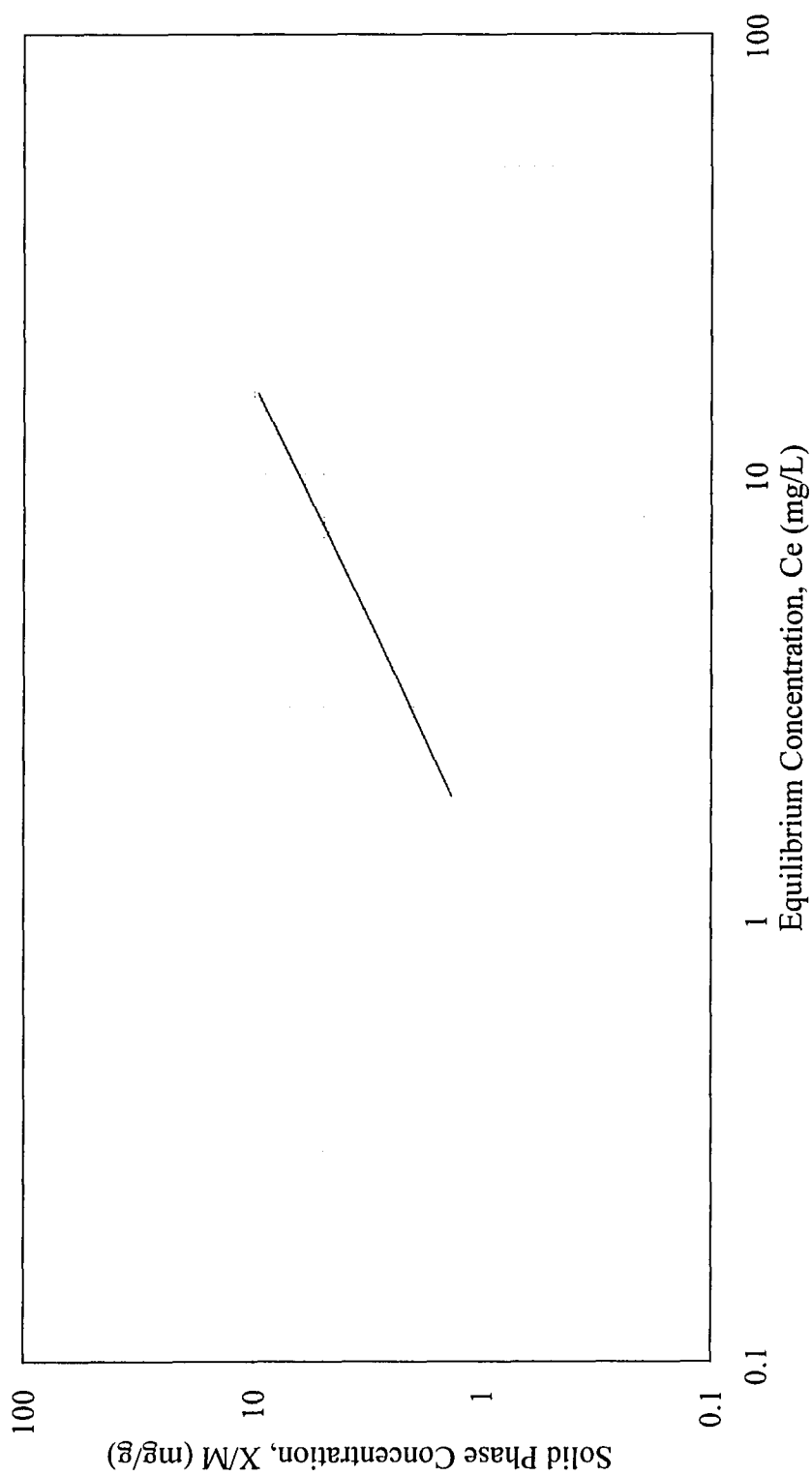


Figure A.24. Sorption isotherm for Tribromofluoromethane with biomass from pure oxygen activated sludge process (PVSC). Desorption concentrations could not be measured.

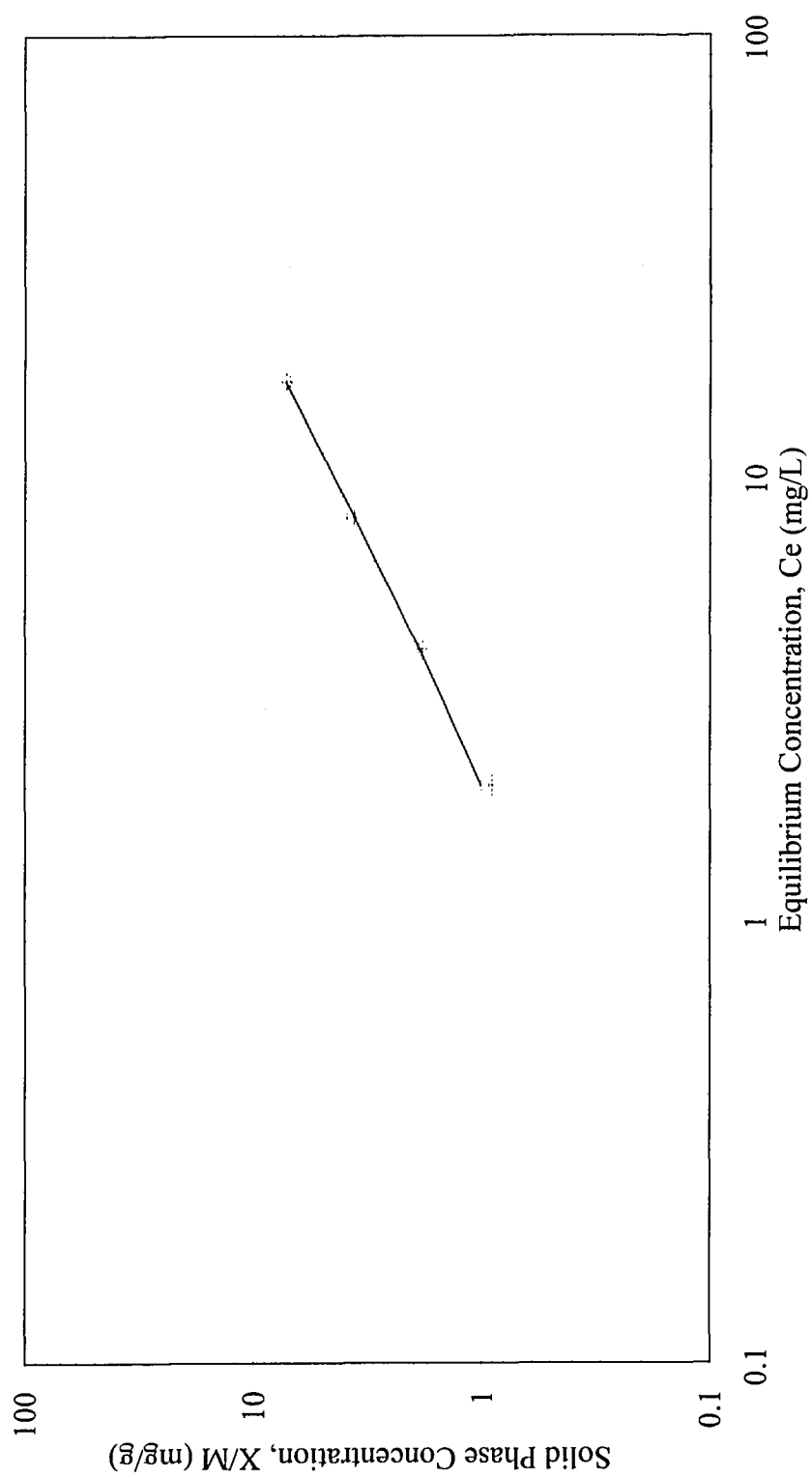


Figure A.25. Sorption and desorption isotherms for Chloropropane with biomass from activated sludge reactor with recycle. Circles represent sorbed concentrations and crosses represent desorbed concentrations.

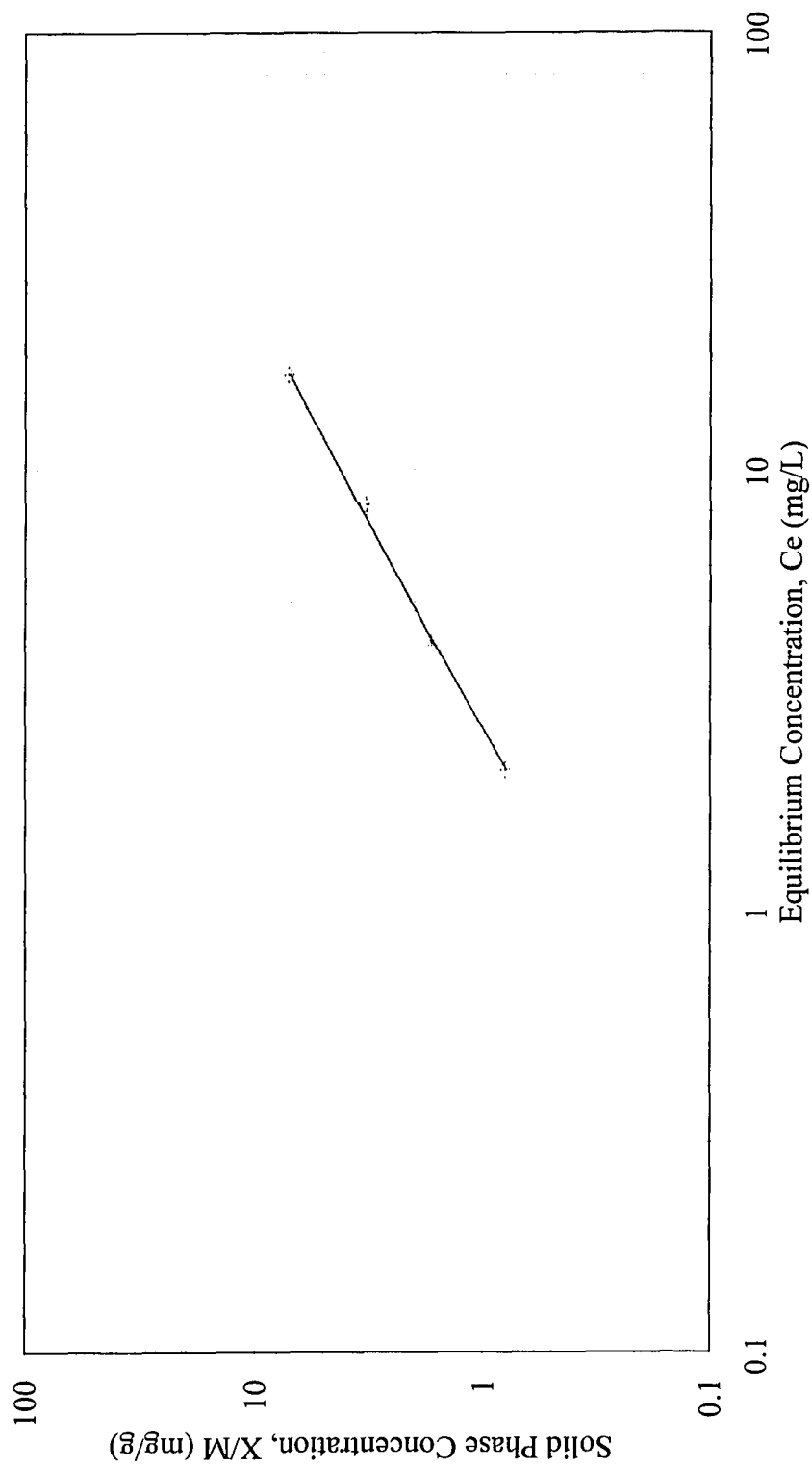


Figure A.26. Sorption and desorption isotherms for Chloropropane with biomass from ASBR. Circles represent sorbed concentrations and crosses represent desorbed concentrations.

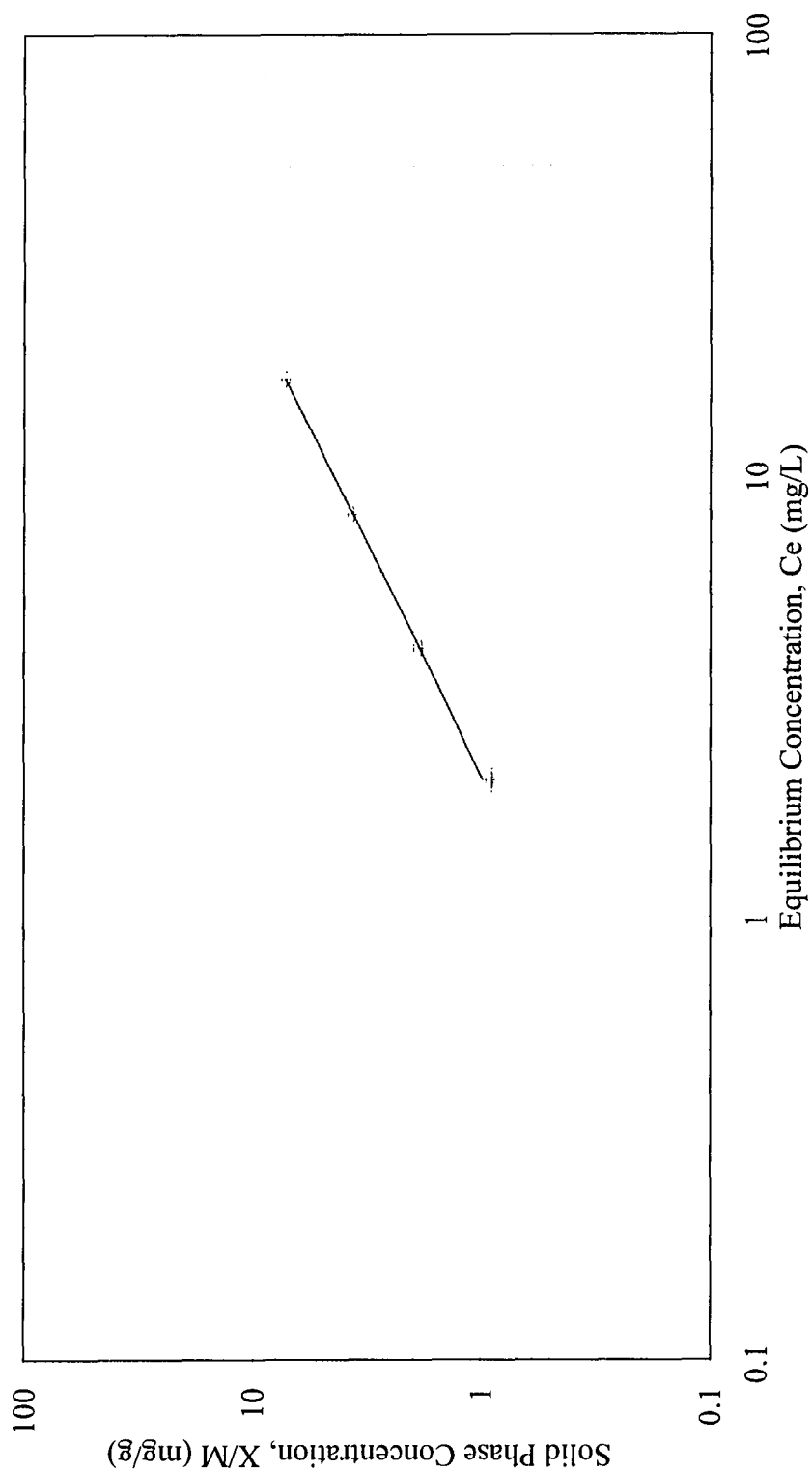


Figure A.27. Sorption and desorption isotherms for Chloropropane with biomass from pure oxygen activated sludge process (PVSC). Circles represent sorbed concentrations and crosses represent desorbed concentrations.

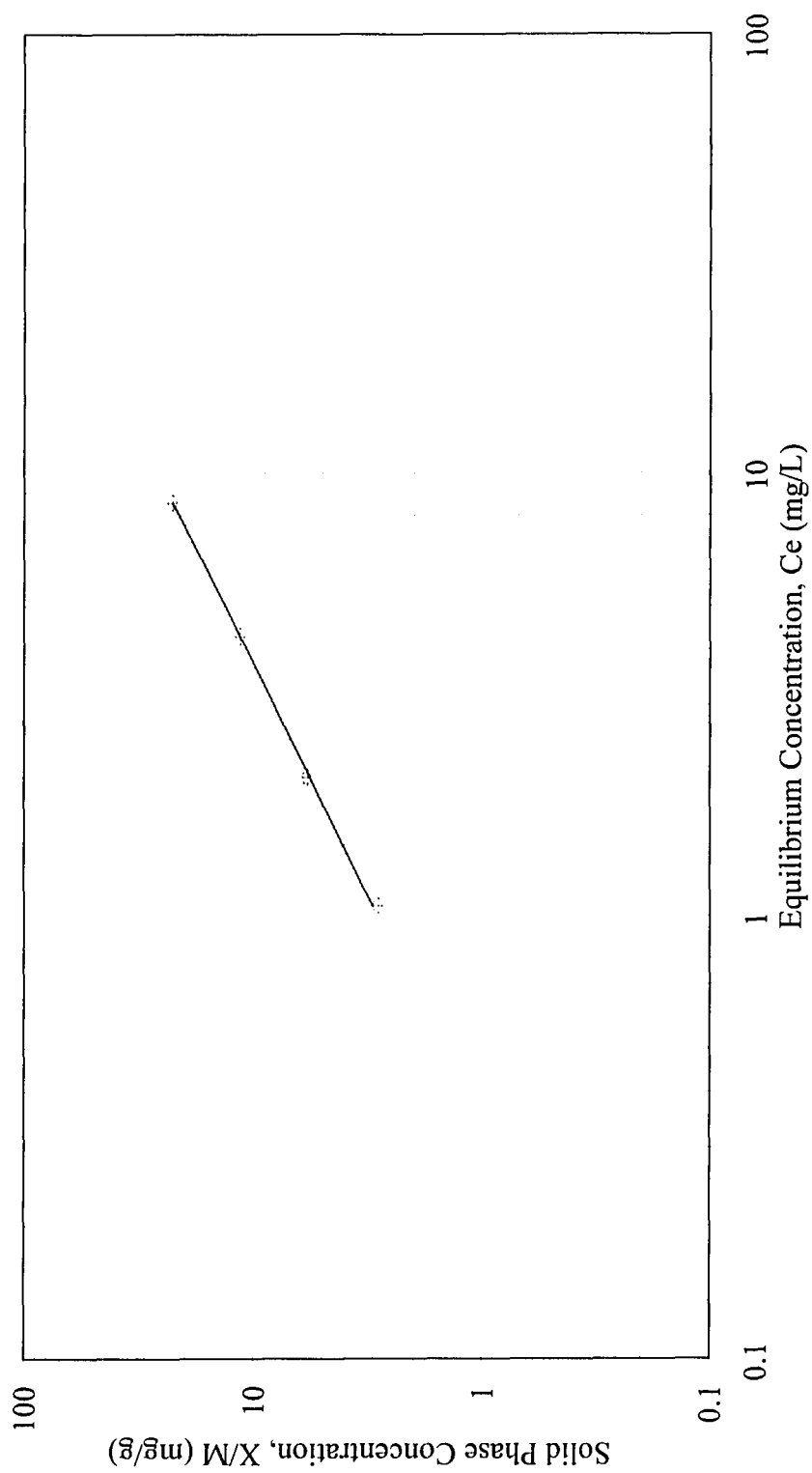


Figure A.28. Sorption and desorption isotherms for Bromobutane with biomass from activated sludge reactor with recycle. Circles represent sorbed concentrations and crosses represent desorbed concentrations.

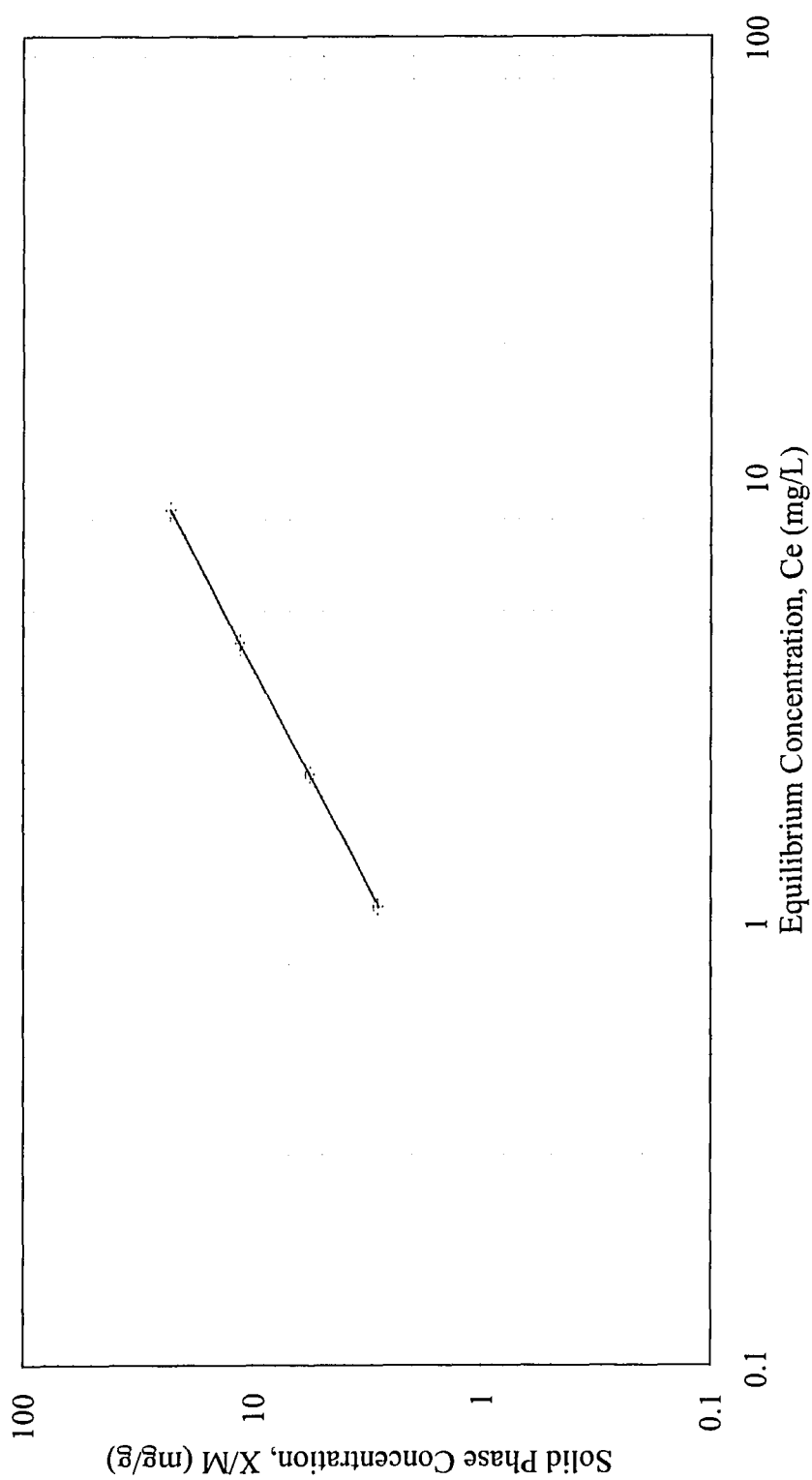


Figure A.29. Sorption and desorption isotherms for Bromobutane with biomass from ASBR. Circles represent sorbed concentrations and crosses represent desorbed concentrations.

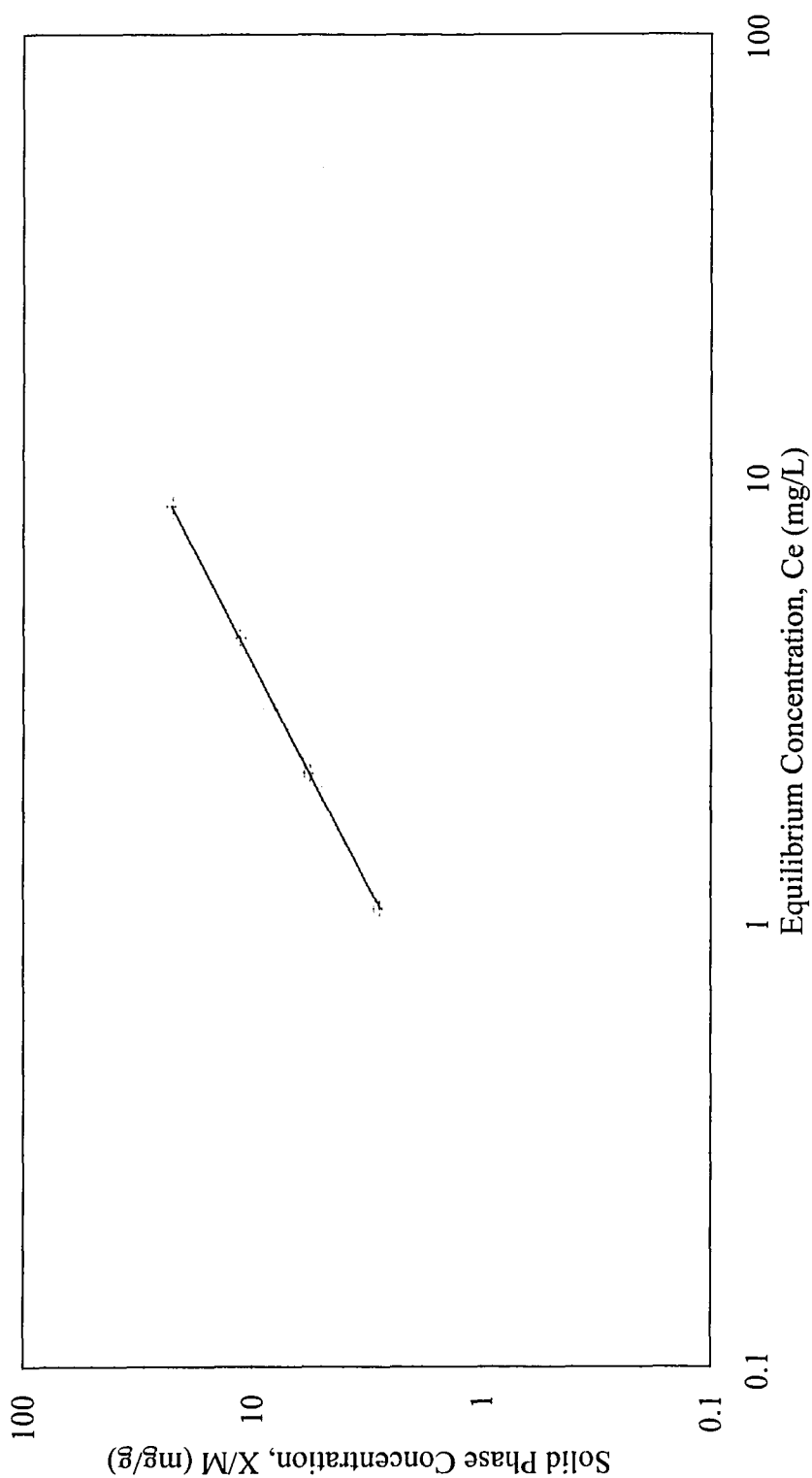


Figure A.30. Sorption and desorption isotherms for Bromobutane with biomass from pure oxygen activated sludge process (PVSC). Circles represent sorbed concentrations and crosses represent desorbed concentrations.

APPENDIX B

SORPTION AND DESORPTION EXPERIMENTAL DATA

Table B.1. Sorption and desorption data for methylene chloride with biomass from activated sludge reactor with recycle.

Solids concentration 0.5 g/L TOC

Case 1. Methylene Chloride Conc. = 2.5 mg/L

Time (Mins)	Co (mg/L)	Ce (mg/L)	X (Co - Ce) mg/L	M (g/L)	X/M (mg/g)	log (X/M)	log (Ce)
0.00	2.50	2.50	0.00	0.50	0.00		0.40
180.00	2.50	2.41	0.09	0.50	0.19	-0.72	0.38

Case 2. Methylene Chloride Conc. = 5 mg/L

Time (Mins)	Co (mg/L)	Ce (mg/L)	X (Co - Ce) mg/L	M (g/L)	X/M (mg/g)	log (X/M)	log (Ce)
0.00	5.00	5.00	0.00	0.50	0.00		0.70
180.00	5.00	4.78	0.22	0.50	0.44	-0.35	0.68

Case 3. Methylene Chloride Conc. = 10 mg/L

Time (Mins)	Co (mg/L)	Ce (mg/L)	X (Co - Ce) mg/L	M (g/L)	X/M (mg/g)	log (X/M)	log (Ce)
0.00	10.00	10.00	0.00	0.50	0.00		1.00
180.00	10.00	9.54	0.46	0.50	0.93	-0.03	0.98

Case 4. Methylene Chloride Conc. = 20 mg/L

Time (Mins)	Co (mg/L)	Ce (mg/L)	X (Co - Ce) mg/L	M (g/L)	X/M (mg/g)	log (X/M)	log (Ce)
0.00	20.00	20.00	0.00	0.50	0.00		1.30
180.00	20.00	19.12	0.88	0.50	1.76	0.25	1.28

Freundlich Isotherm Parameters for Linear Regression

X/M	Ce	fit	log Ce	log X/M	Ce Desorb
0.19	2.41	0.22	0.38	-0.72	-
0.44	4.78	0.44	0.68	-0.36	-
0.93	9.54	0.88	0.98	-0.03	-
1.76	19.12	1.78	1.28	0.25	-

Table B.2. Sorption and desorption data for methylene chloride with biomass from ASBR.

Solids concentration 0.5 g/L TOC

Case 1. Methylene Chloride = 0 mg/L

Time (Mins)	Co (mg/L)	Ce (mg/L)	X (Co - Ce) mg/L	M (g/L)	X/M (mg/g)	log (X/M)	log (Ce)
0.00	0.00	0.00	0.00	0.50	0.00		
180.00	0.00	0.00	0.00	0.50	0.00		

Case 2. Methylene Chloride Conc. = 2.5 mg/L

Time (Mins)	Co (mg/L)	Ce (mg/L)	X (Co - Ce) mg/L	M (g/L)	X/M (mg/g)	log (X/M)	log (Ce)
0.00	2.50	2.50	0.00	0.50	0.00		0.40
180.00	2.50	2.39	0.11	0.50	0.22	-0.66	0.38

Case 3. Methylene Chloride Conc. = 5 mg/L

Time (Mins)	Co (mg/L)	Ce (mg/L)	X (Co - Ce) mg/L	M (g/L)	X/M (mg/g)	log (X/M)	log (Ce)
0.00	5.00	5.00	0.00	0.50	0.00		0.70
180.00	5.00	4.81	0.19	0.50	0.38	-0.43	0.68

Case 4. Methylene Chloride Conc. = 10 mg/L

Time (Mins)	Co (mg/L)	Ce (mg/L)	X (Co - Ce) mg/L	M (g/L)	X/M (mg/g)	log (X/M)	log (Ce)
0.00	10.00	10.00	0.00	0.50	0.00		1.00
180.00	10.00	9.57	0.43	0.50	0.85	-0.07	0.98

Case 5. Methylene Chloride Conc. = 20 mg/L

Time (Mins)	Co (mg/L)	Ce (mg/L)	X (Co - Ce) mg/L	M (g/L)	X/M (mg/g)	log (X/M)	log (Ce)
0.00	20.00	20.00	0.00	0.50	0.00		1.30
180.00	20.00	19.20	0.80	0.50	1.61	0.21	1.28

Freundlich Isotherm Parameters for Linear Regression

X/M	Ce	fit	log Ce	log X/M	Ce Desorb
0.22	2.39	0.21	0.38	-0.66	-
0.38	4.81	0.41	0.68	-0.42	-
0.85	9.57	0.81	0.98	-0.07	-
1.61	19.20	1.62	1.28	0.21	-

Table B.3. Sorption and desorption data for methylene chloride with biomass from pure oxygen activated sludge process.

Solids concentration 0.5 g/L TOC

Case 1. Methylene Chloride = 0 mg/L

Time (Mins)	Co (mg/L)	Ce (mg/L)	X (Co - Ce) mg/L	M (g/L)	X/M (mg/g)	log (X/M)	log (Ce)
0.00	0.00	0.00	0.00	0.50	0.00		
180.00	0.00	0.00	0.00	0.50	0.00		

Case 2. Methylene Chloride Conc. = 2.5 mg/L

Time (Mins)	Co (mg/L)	Ce (mg/L)	X (Co - Ce) mg/L	M (g/L)	X/M (mg/g)	log (X/M)	log (Ce)
0.00	2.50	2.50	0.00	0.50	0.00		0.40
180.00	2.50	2.38	0.12	0.50	0.23	-0.63	0.38

Case 3. Methylene Chloride Conc. = 5 mg/L

Time (Mins)	Co (mg/L)	Ce (mg/L)	X (Co - Ce) mg/L	M (g/L)	X/M (mg/g)	log (X/M)	log (Ce)
0.00	5.00	5.00	0.00	0.50	0.00		0.70
180.00	5.00	4.76	0.24	0.50	0.47	-0.33	0.68

Case 4. Methylene Chloride Conc. = 10 mg/L

Time (Mins)	Co (mg/L)	Ce (mg/L)	X (Co - Ce) mg/L	M (g/L)	X/M (mg/g)	log (X/M)	log (Ce)
0.00	10.00	10.00	0.00	0.50	0.00		1.00
180.00	10.00	9.55	0.45	0.50	0.90	-0.05	0.98

Case 5. Methylene Chloride Conc. = 20 mg/L

Time (Mins)	Co (mg/L)	Ce (mg/L)	X (Co - Ce) mg/L	M (g/L)	X/M (mg/g)	log (X/M)	log (Ce)
0.00	20.00	20.00	0.00	0.50	0.00		1.30
180.00	20.00	19.04	0.96	0.50	1.92	0.28	1.28

Freundlich Isotherm Parameters for Linear Regression

X/M	Ce	fit	log Ce	log X/M	Ce Desorb
0.23	2.38	0.22	0.38	-0.64	-
0.47	4.76	0.46	0.68	-0.33	-
0.90	9.55	0.94	0.98	-0.05	-
1.92	19.04	1.90	1.28	0.28	-

Table B.4. Sorption and desorption data for trichloromethane with biomass from activated sludge reactor with recycle.

Solids concentration 0.5 g/L TOC

Case 1. Trichloromethane = 0 mg/L

Time (Mins)	Co (mg/L)	Ce (mg/L)	X (Co - Ce) mg/L	M (g/L)	X/M (mg/g)	log (X/M)	log (Ce)
0.00	0.00	0.00	0.00	0.50	0.00		
180.00	0.00	0.00	0.00	0.50	0.00		

Case 2. Trichloromethane Conc. = 2.5 mg/L

Time (Mins)	Co (mg/L)	Ce (mg/L)	X (Co - Ce) mg/L	M (g/L)	X/M (mg/g)	log (X/M)	log (Ce)
0.00	2.50	2.50	0.00	0.50	0.00		0.40
180.00	2.50	2.20	0.30	0.50	0.59	-0.23	0.34

Case 3. Trichloromethane Conc. = 5 mg/L

Time (Mins)	Co (mg/L)	Ce (mg/L)	X (Co - Ce) mg/L	M (g/L)	X/M (mg/g)	log (X/M)	log (Ce)
0.00	5.00	5.00	0.00	0.50	0.00		0.70
180.00	5.00	4.40	0.60	0.50	1.19	0.08	0.64

Case 4. Trichloromethane Conc. = 10 mg/L

Time (Mins)	Co (mg/L)	Ce (mg/L)	X (Co - Ce) mg/L	M (g/L)	X/M (mg/g)	log (X/M)	log (Ce)
0.00	10.00	10.00	0.00	0.50	0.00		1.00
180.00	10.00	8.97	1.03	0.50	2.06	0.31	0.95

Case 5. Trichloromethane Conc. = 20 mg/L

Time (Mins)	Co (mg/L)	Ce (mg/L)	X (Co - Ce) mg/L	M (g/L)	X/M (mg/g)	log (X/M)	log (Ce)
0.00	20.00	20.00	0.00	0.50	0.00		1.30
180.00	20.00	17.47	2.53	0.50	5.07	0.70	1.24

Freundlich Isotherm Parameters for Linear Regression

X/M	Ce	fit	log Ce	log X/M	Ce Desorb
0.59	2.20	0.46	0.34	-0.23	0.62
1.19	4.40	1.10	0.64	0.08	1.16
2.06	8.97	2.43	0.95	0.31	2.20
5.07	17.47	4.92	1.24	0.71	5.11

Table B.5. Sorption and desorption data for trichloromethane with biomass from ASBR.

Solids concentration 0.5 g/L TOC

Case 1. Trichloromethane = 0 mg/L

Time (Mins)	Co (mg/L)	Ce (mg/L)	X (Co - Ce) mg/L	M (g/L)	X/M (mg/g)	log (X/M)	log (Ce)
0.00	0.00	0.00	0.00	0.50	0.00		
180.00	0.00	0.00	0.00	0.50	0.00		

Case 2. Trichloromethane Conc. = 2.5 mg/L

Time (Mins)	Co (mg/L)	Ce (mg/L)	X (Co - Ce) mg/L	M (g/L)	X/M (mg/g)	log (X/M)	log (Ce)
0.00	2.50	2.50	0.00	0.50	0.00		0.40
180.00	2.50	2.18	0.32	0.50	0.64	-0.20	0.34

Case 3. Trichloromethane Conc. = 5 mg/L

Time (Mins)	Co (mg/L)	Ce (mg/L)	X (Co - Ce) mg/L	M (g/L)	X/M (mg/g)	log (X/M)	log (Ce)
0.00	5.00	5.00	0.00	0.50	0.00		0.70
180.00	5.00	4.55	0.45	0.50	0.91	-0.04	0.66

Case 4. Trichloromethane Conc. = 10 mg/L

Time (Mins)	Co (mg/L)	Ce (mg/L)	X (Co - Ce) mg/L	M (g/L)	X/M (mg/g)	log (X/M)	log (Ce)
0.00	10.00	10.00	0.00	0.50	0.00		1.00
180.00	10.00	8.73	1.27	0.50	2.54	0.40	0.94

Case 5. Trichloromethane Conc. = 20 mg/L

Time (Mins)	Co (mg/L)	Ce (mg/L)	X (Co - Ce) mg/L	M (g/L)	X/M (mg/g)	log (X/M)	log (Ce)
0.00	20.00	20.00	0.00	0.50	0.00		1.30
180.00	20.00	18.02	1.98	0.50	3.96	0.60	1.26

Freundlich Isotherm Parameters for Linear Regression

X/M	Ce	fit	log Ce	log X/M	Ce Desorb
0.64	2.18	0.67	0.34	-0.19	0.68
0.91	4.55	1.18	0.66	-0.04	0.99
2.54	8.73	2.09	0.94	0.40	2.50
3.96	18.02	4.10	1.26	0.60	3.92

Table B.6. Sorption and desorption data for trichloromethane with biomass from pure oxygen activated sludge process.

Solids concentration 0.5 g/L TOC

Case 1. Trichloromethane = 0 mg/L

Time (Mins)	Co (mg/L)	Ce (mg/L)	X (Co - Ce) mg/L	M (g/L)	X/M (mg/g)	log (X/M)	log (Ce)
0.00	0.00	0.00	0.00	0.50	0.00		
180.00	0.00	0.00	0.00	0.50	0.00		

Case 2. Trichloromethane Conc. = 2.5 mg/L

Time (Mins)	Co (mg/L)	Ce (mg/L)	X (Co - Ce) mg/L	M (g/L)	X/M (mg/g)	log (X/M)	log (Ce)
0.00	2.50	2.50	0.00	0.50	0.00		0.40
180.00	2.50	2.20	0.30	0.50	0.59	-0.23	0.34

Case 3. Trichloromethane Conc. = 5 mg/L

Time (Mins)	Co (mg/L)	Ce (mg/L)	X (Co - Ce) mg/L	M (g/L)	X/M (mg/g)	log (X/M)	log (Ce)
0.00	5.00	5.00	0.00	0.50	0.00		0.70
180.00	5.00	4.48	0.52	0.50	1.04	0.02	0.65

Case 4. Trichloromethane Conc. = 10 mg/L

Time (Mins)	Co (mg/L)	Ce (mg/L)	X (Co - Ce) mg/L	M (g/L)	X/M (mg/g)	log (X/M)	log (Ce)
0.00	10.00	10.00	0.00	0.50	0.00		1.00
180.00	10.00	8.93	1.07	0.50	2.14	0.33	0.95

Case 5. Trichloromethane Conc. = 20 mg/L

Time (Mins)	Co (mg/L)	Ce (mg/L)	X (Co - Ce) mg/L	M (g/L)	X/M (mg/g)	log (X/M)	log (Ce)
0.00	20.00	20.00	0.00	0.50	0.00		1.30
180.00	20.00	17.62	2.38	0.50	4.76	0.68	1.25

Freundlich Isotherm Parameters for Linear Regression

X/M	Ce	fit	log Ce	log X/M	Ce Desorb
0.59	2.20	0.46	0.34	-0.23	0.66
1.03	4.48	1.08	0.65	0.01	1.00
2.14	8.93	2.30	0.95	0.33	2.09
4.76	17.62	4.68	1.25	0.68	4.82

Table B.7. Sorption and desorption data for trichlorofluoromethane with biomass from activated sludge reactor with recycle.

Solids concentration 0.5 g/L TOC

Case 1. Trichlorofluoromethane = 0 mg/L

Time (Mins)	Co (mg/L)	Ce (mg/L)	X (Co - Ce) mg/L	M (g/L)	X/M (mg/g)	log (X/M)	log (Ce)
0.00	0.00	0.00	0.00	0.50	0.00		
180.00	0.00	0.00	0.00	0.50	0.00		

Case 2. Trichlorofluoromethane Conc. = 2.5 mg/L

Time (Mins)	Co (mg/L)	Ce (mg/L)	X (Co - Ce) mg/L	M (g/L)	X/M (mg/g)	log (X/M)	log (Ce)
0.00	2.50	2.50	0.00	0.50	0.00		0.40
180.00	2.50	1.89	0.61	0.50	1.23	0.09	0.28

Case 3. Trichlorofluoromethane Conc. = 5 mg/L

Time (Mins)	Co (mg/L)	Ce (mg/L)	X (Co - Ce) mg/L	M (g/L)	X/M (mg/g)	log (X/M)	log (Ce)
0.00	5.00	5.00	0.00	0.50	0.00		0.70
180.00	5.00	3.77	1.23	0.50	2.45	0.39	0.58

Case 4. Trichlorofluoromethane Conc. = 10 mg/L

Time (Mins)	Co (mg/L)	Ce (mg/L)	X (Co - Ce) mg/L	M (g/L)	X/M (mg/g)	log (X/M)	log (Ce)
0.00	10.00	10.00	0.00	0.50	0.00		1.00
180.00	10.00	7.49	2.51	0.50	5.02	0.70	0.87

Case 5. Trichlorofluoromethane Conc. = 20 mg/L

Time (Mins)	Co (mg/L)	Ce (mg/L)	X (Co - Ce) mg/L	M (g/L)	X/M (mg/g)	log (X/M)	log (Ce)
0.00	20.00	20.00	0.00	0.50	0.00		1.30
180.00	20.00	15.43	4.57	0.50	9.15	0.96	1.19

Freundlich Isotherm Parameters for Linear Regression

X/M	Ce	fit	log Ce	log X/M	Ce Desorb
1.23	1.89	1.40	0.28	1.31	1.31
2.45	3.77	2.50	0.58	2.35	2.35
5.02	7.49	4.66	0.87	5.09	5.09
9.15	15.43	9.29	1.19	9.00	9.00

Table B.8. Sorption and desorption data for trichlorofluoromethane with biomass from ASBR.

Solids concentration 0.5 g/L TOC

Case 1. Trichlorofluoromethane = 0 mg/L

Time (Mins)	Co (mg/L)	Ce (mg/L)	X (Co - Ce) mg/L	M (g/L)	X/M (mg/g)	log (X/M)	log (Ce)
0.00	0.00	0.00	0.00	0.50	0.00		
180.00	0.00	0.00	0.00	0.50	0.00		

Case 2. Trichlorofluoromethane Conc. = 2.5 mg/L

Time (Mins)	Co (mg/L)	Ce (mg/L)	X (Co - Ce) mg/L	M (g/L)	X/M (mg/g)	log (X/M)	log (Ce)
0.00	2.50	2.50	0.00	0.50	0.00		0.40
180.00	2.50	1.82	0.68	0.50	1.35	0.13	0.26

Case 3. Trichlorofluoromethane Conc. = 5 mg/L

Time (Mins)	Co (mg/L)	Ce (mg/L)	X (Co - Ce) mg/L	M (g/L)	X/M (mg/g)	log (X/M)	log (Ce)
0.00	5.00	5.00	0.00	0.50	0.00		0.70
180.00	5.00	3.85	1.15	0.50	2.31	0.36	0.59

Case 4. Trichlorofluoromethane Conc. = 10 mg/L

Time (Mins)	Co (mg/L)	Ce (mg/L)	X (Co - Ce) mg/L	M (g/L)	X/M (mg/g)	log (X/M)	log (Ce)
0.00	10.00	10.00	0.00	0.50	0.00		1.00
180.00	10.00	7.75	2.25	0.50	4.50	0.65	0.89

Case 5. Trichlorofluoromethane Conc. = 20 mg/L

Time (Mins)	Co (mg/L)	Ce (mg/L)	X (Co - Ce) mg/L	M (g/L)	X/M (mg/g)	log (X/M)	log (Ce)
0.00	20.00	20.00	0.00	0.50	0.00		1.30
180.00	20.00	15.33	4.67	0.50	9.35	0.97	1.19

Freundlich Isotherm Parameters for Linear Regression

X/M	Ce	fit	log Ce	log X/M	Ce Desorb
1.35	1.82	1.17	0.26	1.30	1.30
2.31	3.85	2.38	0.59	2.25	2.25
4.50	7.75	4.71	0.89	4.42	4.42
9.35	15.33	9.25	1.19	9.25	9.25

Table B.9. Sorption and desorption data for trichlorofluoromethane with biomass from pure oxygen activated sludge process.

Solids concentration 0.5 g/L TOC

Case 1. Trichlorofluoromethane = 0 mg/L

Time (Mins)	Co (mg/L)	Ce (mg/L)	X (Co - Ce) mg/L	M (g/L)	X/M (mg/g)	log (X/M)	log (Ce)
0.00	0.00	0.00	0.00	0.50	0.00		
180.00	0.00	0.00	0.00	0.50	0.00		

Case 2. Trichlorofluoromethane Conc. = 2.5 mg/L

Time (Mins)	Co (mg/L)	Ce (mg/L)	X (Co - Ce) mg/L	M (g/L)	X/M (mg/g)	log (X/M)	log (Ce)
0.00	2.50	2.50	0.00	0.50	0.00		0.40
180.00	2.50	1.91	0.59	0.50	1.18	0.07	0.28

Case 3. Trichlorofluoromethane Conc. = 5 mg/L

Time (Mins)	Co (mg/L)	Ce (mg/L)	X (Co - Ce) mg/L	M (g/L)	X/M (mg/g)	log (X/M)	log (Ce)
0.00	5.00	5.00	0.00	0.50	0.00		0.70
180.00	5.00	3.87	1.13	0.50	2.25	0.35	0.59

Case 4. Trichlorofluoromethane Conc. = 10 mg/L

Time (Mins)	Co (mg/L)	Ce (mg/L)	X (Co - Ce) mg/L	M (g/L)	X/M (mg/g)	log (X/M)	log (Ce)
0.00	10.00	10.00	0.00	0.50	0.00		1.00
180.00	10.00	7.73	2.27	0.50	4.53	0.66	0.89

Case 5. Trichlorofluoromethane Conc. = 20 mg/L

Time (Mins)	Co (mg/L)	Ce (mg/L)	X (Co - Ce) mg/L	M (g/L)	X/M (mg/g)	log (X/M)	log (Ce)
0.00	20.00	20.00	0.00	0.50	0.00		1.30
180.00	20.00	15.66	4.34	0.50	8.69	0.94	1.19

Freundlich Isotherm Parameters for Linear Regression

X/M	Ce	fit	log Ce	log X/M	Ce Desorb
1.19	1.91	1.22	0.28	0.08	1.15
2.25	3.87	2.29	0.59	0.35	2.22
4.53	7.73	4.40	0.89	0.66	4.45
8.69	15.66	8.74	1.19	0.94	8.65

Table B.10. Sorption and desorption data for dichloroethane with biomass from activated sludge reactor with recycle.

Solids concentration 0.5 g/L TOC

Case 1. Dichloroethane = 0 mg/L

Time (Mins)	Co (mg/L)	Ce (mg/L)	X (Co - Ce) mg/L	M (g/L)	X/M (mg/g)	log (X/M)	log (Ce)
0.00	0.00	0.00	0.00	0.50	0.00		
180.00	0.00	0.00	0.00	0.50	0.00		

Case 2. Dichloroethane Conc. = 2.5 mg/L

Time (Mins)	Co (mg/L)	Ce (mg/L)	X (Co - Ce) mg/L	M (g/L)	X/M (mg/g)	log (X/M)	log (Ce)
0.00	2.50	2.50	0.00	0.50	0.00		0.40
180.00	2.50	2.02	0.48	0.50	0.97	-0.01	0.30

Case 3. Dichloroethane Conc. = 5 mg/L

Time (Mins)	Co (mg/L)	Ce (mg/L)	X (Co - Ce) mg/L	M (g/L)	X/M (mg/g)	log (X/M)	log (Ce)
0.00	5.00	5.00	0.00	0.50	0.00		0.70
180.00	5.00	4.13	0.87	0.50	1.74	0.24	0.62

Case 4. Dichloroethane Conc. = 10 mg/L

Time (Mins)	Co (mg/L)	Ce (mg/L)	X (Co - Ce) mg/L	M (g/L)	X/M (mg/g)	log (X/M)	log (Ce)
0.00	10.00	10.00	0.00	0.50	0.00		1.00
180.00	10.00	7.97	2.03	0.50	4.06	0.61	0.90

Case 5. Dichloroethane Conc. = 20 mg/L

Time (Mins)	Co (mg/L)	Ce (mg/L)	X (Co - Ce) mg/L	M (g/L)	X/M (mg/g)	log (X/M)	log (Ce)
0.00	20.00	20.00	0.00	0.50	0.00		1.30
180.00	20.00	16.39	3.61	0.50	7.21	0.86	1.21

Freundlich Isotherm Parameters for Linear Regression

X/M	Ce	fit	log Ce	log X/M	Ce Desorb
0.97	2.02	1.03	0.31	-0.01	0.87
1.74	4.13	1.96	0.62	0.24	1.77
4.06	7.97	3.65	0.90	0.61	4.00
7.21	16.39	7.35	1.21	0.86	7.13

Table B.11. Sorption and desorption data for dichloroethane with biomass from ASBR.

Solids concentration 0.5 g/L TOC

Case 1. Dichloroethane = 0 mg/L

Time (Mins)	Co (mg/L)	Ce (mg/L)	X (Co - Ce) mg/L	M (g/L)	X/M (mg/g)	log (X/M)	log (Ce)
0.00	0.00	0.00	0.00	0.50	0.00		
180.00	0.00	0.00	0.00	0.50	0.00		

Case 2. Dichloroethane Conc. = 2.5 mg/L

Time (Mins)	Co (mg/L)	Ce (mg/L)	X (Co - Ce) mg/L	M (g/L)	X/M (mg/g)	log (X/M)	log (Ce)
0.00	2.50	2.50	0.00	0.50	0.00		0.40
180.00	2.50	2.07	0.43	0.50	0.87	-0.06	0.32

Case 3. Dichloroethane Conc. = 5 mg/L

Time (Mins)	Co (mg/L)	Ce (mg/L)	X (Co - Ce) mg/L	M (g/L)	X/M (mg/g)	log (X/M)	log (Ce)
0.00	5.00	5.00	0.00	0.50	0.00		0.70
180.00	5.00	4.02	0.98	0.50	1.97	0.29	0.60

Case 4. Dichloroethane Conc. = 10 mg/L

Time (Mins)	Co (mg/L)	Ce (mg/L)	X (Co - Ce) mg/L	M (g/L)	X/M (mg/g)	log (X/M)	log (Ce)
0.00	10.00	10.00	0.00	0.50	0.00		1.00
180.00	10.00	8.16	1.84	0.50	3.67	0.57	0.91

Case 5. Dichloroethane Conc. = 20 mg/L

Time (Mins)	Co (mg/L)	Ce (mg/L)	X (Co - Ce) mg/L	M (g/L)	X/M (mg/g)	log (X/M)	log (Ce)
0.00	20.00	20.00	0.00	0.50	0.00		1.30
180.00	20.00	16.60	3.40	0.50	6.80	0.83	1.22

Freundlich Isotherm Parameters for Linear Regression

X/M	Ce	fit	log Ce	log X/M	Ce Desorb
0.87	2.07	1.07	0.32	-0.06	0.88
1.97	4.02	1.85	0.60	0.29	1.92
3.67	8.16	3.51	0.91	0.56	3.77
6.80	16.60	6.88	1.22	0.83	6.88

Table B.12. Sorption and desorption data for dichloroethane with biomass from pure oxygen activated sludge process.

Solids concentration 0.5 g/L TOC

Case 1. Dichloroethane = 0 mg/L

Time (Mins)	Co (mg/L)	Ce (mg/L)	X (Co - Ce) mg/L	M (g/L)	X/M (mg/g)	log (X/M)	log (Ce)
0.00	0.00	0.00	0.00	0.50	0.00		
180.00	0.00	0.00	0.00	0.50	0.00		

Case 2. Dichloroethane Conc. = 2.5 mg/L

Time (Mins)	Co (mg/L)	Ce (mg/L)	X (Co - Ce) mg/L	M (g/L)	X/M (mg/g)	log (X/M)	log (Ce)
0.00	2.50	2.50	0.00	0.50	0.00		0.40
180.00	2.50	2.04	0.46	0.50	0.92	-0.04	0.31

Case 3. Dichloroethane Conc. = 5 mg/L

Time (Mins)	Co (mg/L)	Ce (mg/L)	X (Co - Ce) mg/L	M (g/L)	X/M (mg/g)	log (X/M)	log (Ce)
0.00	5.00	5.00	0.00	0.50	0.00		0.70
180.00	5.00	4.05	0.95	0.50	1.90	0.28	0.61

Case 4. Dichloroethane Conc. = 10 mg/L

Time (Mins)	Co (mg/L)	Ce (mg/L)	X (Co - Ce) mg/L	M (g/L)	X/M (mg/g)	log (X/M)	log (Ce)
0.00	10.00	10.00	0.00	0.50	0.00		1.00
180.00	10.00	8.30	1.70	0.50	3.40	0.53	0.92

Case 5. Dichloroethane Conc. = 20 mg/L

Time (Mins)	Co (mg/L)	Ce (mg/L)	X (Co - Ce) mg/L	M (g/L)	X/M (mg/g)	log (X/M)	log (Ce)
0.00	20.00	20.00	0.00	0.50	0.00		1.30
180.00	20.00	16.13	3.87	0.50	7.74	0.89	1.21

Freundlich Isotherm Parameters for Linear Regression

X/M	Ce	fit	log Ce	log X/M	Ce Desorb
0.92	2.04	0.80	0.31	-0.04	0.91
1.90	4.05	1.77	0.61	0.28	1.90
3.40	8.30	3.81	0.92	0.53	3.37
7.74	16.13	7.58	1.21	0.89	7.70

Table B.13. Sorption and desorption data for tetrachloroethane with biomass from activated sludge reactor with recycle.

Solids concentration 0.5 g/L TOC

Case 1. Tetrachloroethane = 0 mg/L

Time (Mins)	Co (mg/L)	Ce (mg/L)	X (Co - Ce) mg/L	M (g/L)	X/M (mg/g)	log (X/M)	log (Ce)
0.00	0.00	0.00	0.00	0.50	0.00		
180.00	0.00	0.00	0.00	0.50	0.00		

Case 2. Tetrachloroethane Conc. = 2.5 mg/L

Time (Mins)	Co (mg/L)	Ce (mg/L)	X (Co - Ce) mg/L	M (g/L)	X/M (mg/g)	log (X/M)	log (Ce)
0.00	2.50	2.50	0.00	0.50	0.00		0.40
180.00	2.50	0.78	1.72	0.50	3.43	0.54	-0.11

Case 3. Tetrachloroethane Conc. = 5 mg/L

Time (Mins)	Co (mg/L)	Ce (mg/L)	X (Co - Ce) mg/L	M (g/L)	X/M (mg/g)	log (X/M)	log (Ce)
0.00	5.00	5.00	0.00	0.50	0.00		0.70
180.00	5.00	1.56	3.44	0.50	6.89	0.84	0.19

Case 4. Tetrachloroethane Conc. = 10 mg/L

Time (Mins)	Co (mg/L)	Ce (mg/L)	X (Co - Ce) mg/L	M (g/L)	X/M (mg/g)	log (X/M)	log (Ce)
0.00	10.00	10.00	0.00	0.50	0.00		1.00
180.00	10.00	3.14	6.86	0.50	13.72	1.14	0.50

Case 5. Tetrachloroethane Conc. = 20 mg/L

Time (Mins)	Co (mg/L)	Ce (mg/L)	X (Co - Ce) mg/L	M (g/L)	X/M (mg/g)	log (X/M)	log (Ce)
0.00	20.00	20.00	0.00	0.50	0.00		1.30
180.00	20.00	6.26	13.74	0.50	27.48	1.44	0.80

Freundlich Isotherm Parameters for Linear Regression

X/M	Ce	fit	log Ce	log X/M	Ce Desorb
3.43	0.78	3.43	-0.11	0.54	3.32
6.89	1.56	6.85	0.19	0.84	6.84
13.72	3.14	13.78	0.50	1.14	13.7
27.48	6.26	27.46	0.80	1.44	27.2

Table B.14. Sorption and desorption data for tetrachloroethane with biomass from ASBR.

Solids concentration 0.5 g/L TOC

Case 1. Tetrachloroethane = 0 mg/L

Time (Mins)	Co (mg/L)	Ce (mg/L)	X (Co - Ce) mg/L	M (g/L)	X/M (mg/g)	log (X/M)	log (Ce)
0.00	0.00	0.00	0.00	0.50	0.00		
180.00	0.00	0.00	0.00	0.50	0.00		

Case 2. Tetrachloroethane Conc. = 2.5 mg/L

Time (Mins)	Co (mg/L)	Ce (mg/L)	X (Co - Ce) mg/L	M (g/L)	X/M (mg/g)	log (X/M)	log (Ce)
0.00	2.50	2.50	0.00	0.50	0.00		0.40
180.00	2.50	0.78	1.72	0.50	3.43	0.54	-0.11

Case 3. Tetrachloroethane Conc. = 5 mg/L

Time (Mins)	Co (mg/L)	Ce (mg/L)	X (Co - Ce) mg/L	M (g/L)	X/M (mg/g)	log (X/M)	log (Ce)
0.00	5.00	5.00	0.00	0.50	0.00		0.70
180.00	5.00	1.51	3.49	0.50	6.97	0.84	0.18

Case 4. Tetrachloroethane Conc. = 10 mg/L

Time (Mins)	Co (mg/L)	Ce (mg/L)	X (Co - Ce) mg/L	M (g/L)	X/M (mg/g)	log (X/M)	log (Ce)
0.00	10.00	10.00	0.00	0.50	0.00		1.00
180.00	10.00	3.05	6.95	0.50	13.89	1.14	0.48

Case 5. Tetrachloroethane Conc. = 20 mg/L

Time (Mins)	Co (mg/L)	Ce (mg/L)	X (Co - Ce) mg/L	M (g/L)	X/M (mg/g)	log (X/M)	log (Ce)
0.00	20.00	20.00	0.00	0.50	0.00		1.30
180.00	20.00	6.19	13.81	0.50	27.62	1.44	0.79

Freundlich Isotherm Parameters for Linear Regression

X/M	Ce	fit	log Ce	log X/M	Ce Desorb
3.43	0.78	3.62	-0.11	0.54	3.44
6.97	1.51	6.87	0.18	0.84	7.02
13.89	3.05	13.72	0.48	1.14	13.7
27.61	6.19	27.70	0.79	1.44	27.55

Table B.15. Sorption and desorption data for tetrachloroethane with biomass from pure oxygen activated sludge process.

Solids concentration 0.5 g/L TOC

Case 1. Tetrachloroethane = 0 mg/L

Time (Mins)	Co (mg/L)	Ce (mg/L)	X (Co - Ce) mg/L	M (g/L)	X/M (mg/g)	log (X/M)	log (Ce)
0.00	0.00	0.00	0.00	0.50	0.00		
180.00	0.00	0.00	0.00	0.50	0.00		

Case 2. Tetrachloroethane Conc. = 2.5 mg/L

Time (Mins)	Co (mg/L)	Ce (mg/L)	X (Co - Ce) mg/L	M (g/L)	X/M (mg/g)	log (X/M)	log (Ce)
0.00	2.50	2.50	0.00	0.50	0.00		0.40
180.00	2.50	0.79	1.71	0.50	3.43	0.53	-0.10

Case 3. Tetrachloroethane Conc. = 5 mg/L

Time (Mins)	Co (mg/L)	Ce (mg/L)	X (Co - Ce) mg/L	M (g/L)	X/M (mg/g)	log (X/M)	log (Ce)
0.00	5.00	5.00	0.00	0.50	0.00		0.70
180.00	5.00	1.57	3.43	0.50	6.87	0.84	0.20

Case 4. Tetrachloroethane Conc. = 10 mg/L

Time (Mins)	Co (mg/L)	Ce (mg/L)	X (Co - Ce) mg/L	M (g/L)	X/M (mg/g)	log (X/M)	log (Ce)
0.00	10.00	10.00	0.00	0.50	0.00		1.00
180.00	10.00	3.09	6.91	0.50	13.83	1.14	0.49

Case 5. Tetrachloroethane Conc. = 20 mg/L

Time (Mins)	Co (mg/L)	Ce (mg/L)	X (Co - Ce) mg/L	M (g/L)	X/M (mg/g)	log (X/M)	log (Ce)
0.00	20.00	20.00	0.00	0.50	0.00		1.30
180.00	20.00	6.32	13.68	0.50	27.36	1.44	0.80

Freundlich Isotherm Parameters for Linear Regression

X/M	Ce	fit	log Ce	log X/M	Ce Desorb
3.43	0.79	3.56	-0.10	0.54	3.45
6.87	1.57	6.94	0.20	0.84	6.75
13.83	3.09	13.51	0.49	1.14	13.81
27.36	6.32	27.48	0.80	1.44	27.22

Table B.16. Sorption and desorption data for bromoethane with biomass from activated sludge reactor with recycle.

Solids concentration 0.5 g/L TOC

Case 1. Bromoethane = 0 mg/L

Time (Mins)	Co (mg/L)	Ce (mg/L)	X (Co - Ce) mg/L	M (g/L)	X/M (mg/g)	log (X/M)	log (Ce)
0.00	0.00	0.00	0.00	0.50	0.00		
180.00	0.00	0.00	0.00	0.50	0.00		

Case 2. Bromoethane Conc. = 2.5 mg/L

Time (Mins)	Co (mg/L)	Ce (mg/L)	X (Co - Ce) mg/L	M (g/L)	X/M (mg/g)	log (X/M)	log (Ce)
0.00	2.50	2.50	0.00	0.50	0.00		0.40
180.00	2.50	2.38	0.12	0.50	0.24	-0.62	0.38

Case 3. Bromoethane Conc. = 5 mg/L

Time (Mins)	Co (mg/L)	Ce (mg/L)	X (Co - Ce) mg/L	M (g/L)	X/M (mg/g)	log (X/M)	log (Ce)
0.00	5.00	5.00	0.00	0.50	0.00		0.70
180.00	5.00	4.64	0.36	0.50	0.71	-0.15	0.67

Case 4. Bromoethane Conc. = 10 mg/L

Time (Mins)	Co (mg/L)	Ce (mg/L)	X (Co - Ce) mg/L	M (g/L)	X/M (mg/g)	log (X/M)	log (Ce)
0.00	10.00	10.00	0.00	0.50	0.00		1.00
180.00	10.00	9.35	0.65	0.50	1.31	0.12	0.97

Case 5. Bromoethane Conc. = 20 mg/L

Time (Mins)	Co (mg/L)	Ce (mg/L)	X (Co - Ce) mg/L	M (g/L)	X/M (mg/g)	log (X/M)	log (Ce)
0.00	20.00	20.00	0.00	0.50	0.00		1.30
180.00	20.00	18.87	1.13	0.50	2.26	0.35	1.28

Freundlich Isotherm Parameters for Linear Regression

X/M	Ce	fit	log Ce	log X/M	Ce Desorb
0.24	2.38	0.37	0.38	-0.62	0.20
0.71	4.64	0.64	0.67	-0.15	0.65
1.31	9.35	1.19	0.97	0.12	1.25
2.26	18.87	2.32	1.28	0.35	2.25

Table B.17. Sorption and desorption data for bromoethane with biomass from ASBR.

Solids concentration 0.5 g/L TOC

Case 1. Bromoethane = 0 mg/L

Time (Mins)	Co (mg/L)	Ce (mg/L)	X (Co - Ce) mg/L	M (g/L)	X/M (mg/g)	log (X/M)	log (Ce)
0.00	0.00	0.00	0.00	0.50	0.00		
180.00	0.00	0.00	0.00	0.50	0.00		

Case 2. Bromoethane Conc. = 2.5 mg/L

Time (Mins)	Co (mg/L)	Ce (mg/L)	X (Co - Ce) mg/L	M (g/L)	X/M (mg/g)	log (X/M)	log (Ce)
0.00	2.50	2.50	0.00	0.50	0.00		0.40
180.00	2.50	2.37	0.13	0.50	0.27	-0.58	0.37

Case 3. Bromoethane Conc. = 5 mg/L

Time (Mins)	Co (mg/L)	Ce (mg/L)	X (Co - Ce) mg/L	M (g/L)	X/M (mg/g)	log (X/M)	log (Ce)
0.00	5.00	5.00	0.00	0.50	0.00		0.70
180.00	5.00	4.69	0.31	0.50	0.61	-0.21	0.67

Case 4. Bromoethane Conc. = 10 mg/L

Time (Mins)	Co (mg/L)	Ce (mg/L)	X (Co - Ce) mg/L	M (g/L)	X/M (mg/g)	log (X/M)	log (Ce)
0.00	10.00	10.00	0.00	0.50	0.00		1.00
180.00	10.00	9.37	0.63	0.50	1.26	0.10	0.97

Case 5. Bromoethane Conc. = 20 mg/L

Time (Mins)	Co (mg/L)	Ce (mg/L)	X (Co - Ce) mg/L	M (g/L)	X/M (mg/g)	log (X/M)	log (Ce)
0.00	20.00	20.00	0.00	0.50	0.00		1.30
180.00	20.00	19.06	0.94	0.50	1.89	0.28	1.28

Freundlich Isotherm Parameters for Linear Regression

X/M	Ce	fit	log Ce	log X/M	Ce Desorb
0.27	2.37	0.39	0.37	-0.57	0.25
0.62	4.69	0.61	0.67	-0.21	0.50
1.26	9.37	1.06	0.97	0.10	1.22
1.89	19.06	1.98	1.28	0.28	1.85

Table B.18. Sorption and desorption data for bromoethane with biomass from pure oxygen activated sludge process.

Solids concentration 0.5 g/L TOC

Case 1. Bromoethane = 0 mg/L

Time (Mins)	Co (mg/L)	Ce (mg/L)	X (Co - Ce) mg/L	M (g/L)	X/M (mg/g)	log (X/M)	log (Ce)
0.00	0.00	0.00	0.00	0.50	0.00		
180.00	0.00	0.00	0.00	0.50	0.00		

Case 2. Bromoethane Conc. = 2.5 mg/L

Time (Mins)	Co (mg/L)	Ce (mg/L)	X (Co - Ce) mg/L	M (g/L)	X/M (mg/g)	log (X/M)	log (Ce)
0.00	2.50	2.50	0.00	0.50	0.00		0.40
180.00	2.50	2.34	0.16	0.50	0.33	-0.48	0.37

Case 3. Bromoethane Conc. = 5 mg/L

Time (Mins)	Co (mg/L)	Ce (mg/L)	X (Co - Ce) mg/L	M (g/L)	X/M (mg/g)	log (X/M)	log (Ce)
0.00	5.00	5.00	0.00	0.50	0.00		0.70
180.00	5.00	4.78	0.22	0.50	0.44	-0.36	0.68

Case 4. Bromoethane Conc. = 10 mg/L

Time (Mins)	Co (mg/L)	Ce (mg/L)	X (Co - Ce) mg/L	M (g/L)	X/M (mg/g)	log (X/M)	log (Ce)
0.00	10.00	10.00	0.00	0.50	0.00		1.00
180.00	10.00	9.52	0.48	0.50	0.96	-0.02	0.98

Case 5. Bromoethane Conc. = 20 mg/L

Time (Mins)	Co (mg/L)	Ce (mg/L)	X (Co - Ce) mg/L	M (g/L)	X/M (mg/g)	log (X/M)	log (Ce)
0.00	20.00	20.00	0.00	0.50	0.00		1.30
180.00	20.00	18.80	1.20	0.50	2.41	0.38	1.27

Freundlich Isotherm Parameters for Linear Regression

X/M	Ce	fit	log Ce	log X/M	Ce Desorb
0.33	2.34	0.19	0.37	-0.48	0.33
0.44	4.78	0.50	0.68	-0.36	0.35
0.96	9.52	1.12	0.98	-0.02	0.95
2.41	18.80	2.33	1.27	0.38	2.30

Table B.19. Sorption and desorption data for dibromoethane with biomass from activated sludge reactor with recycle.

Solids concentration 0.5 g/L TOC

Case 1. Dibromoethane = 0 mg/L

Time (Mins)	Co (mg/L)	Ce (mg/L)	X (Co - Ce) mg/L	M (g/L)	X/M (mg/g)	log (X/M)	log (Ce)
0.00	0.00	0.00	0.00	0.50	0.00		
180.00	0.00	0.00	0.00	0.50	0.00		

Case 2. Dibromoethane Conc. = 2.5 mg/L

Time (Mins)	Co (mg/L)	Ce (mg/L)	X (Co - Ce) mg/L	M (g/L)	X/M (mg/g)	log (X/M)	log (Ce)
0.00	2.50	2.50	0.00	0.50	0.00		0.40
180.00	2.50	1.99	0.51	0.50	1.03	0.01	0.30

Case 3. Dibromoethane Conc. = 5 mg/L

Time (Mins)	Co (mg/L)	Ce (mg/L)	X (Co - Ce) mg/L	M (g/L)	X/M (mg/g)	log (X/M)	log (Ce)
0.00	5.00	5.00	0.00	0.50	0.00		0.70
180.00	5.00	4.00	1.00	0.50	1.99	0.30	0.60

Case 4. Dibromoethane Conc. = 10 mg/L

Time (Mins)	Co (mg/L)	Ce (mg/L)	X (Co - Ce) mg/L	M (g/L)	X/M (mg/g)	log (X/M)	log (Ce)
0.00	10.00	10.00	0.00	0.50	0.00		1.00
180.00	10.00	7.84	2.16	0.50	4.31	0.63	0.89

Case 5. Dibromoethane Conc. = 20 mg/L

Time (Mins)	Co (mg/L)	Ce (mg/L)	X (Co - Ce) mg/L	M (g/L)	X/M (mg/g)	log (X/M)	log (Ce)
0.00	20.00	20.00	0.00	0.50	0.00		1.30
180.00	20.00	15.92	4.08	0.50	8.15	0.91	1.20

Freundlich Isotherm Parameters for Linear Regression

X/M	Ce	fit	log Ce	log X/M	Ce Desorb
1.03	1.99	1.07	0.30	0.01	1.00
1.99	4.00	2.10	0.60	0.30	2.02
4.31	7.84	4.08	0.89	0.63	4.20
8.15	15.92	8.23	1.20	0.91	8.03

Table B.20. Sorption and desorption data for dibromoethane with biomass from ASBR.

Solids concentration 0.5 g/L TOC

Case 1. Dibromoethane = 0 mg/L

Time (Mins)	Co (mg/L)	Ce (mg/L)	X (Co - Ce) mg/L	M (g/L)	X/M (mg/g)	log (X/M)	log (Ce)
0.00	0.00	0.00	0.00	0.50	0.00		
180.00	0.00	0.00	0.00	0.50	0.00		

Case 2. Dibromoethane Conc. = 2.5 mg/L

Time (Mins)	Co (mg/L)	Ce (mg/L)	X (Co - Ce) mg/L	M (g/L)	X/M (mg/g)	log (X/M)	log (Ce)
0.00	2.50	2.50	0.00	0.50	0.00		0.40
180.00	2.50	1.98	0.52	0.50	1.05	0.02	0.30

Case 3. Dibromoethane Conc. = 5 mg/L

Time (Mins)	Co (mg/L)	Ce (mg/L)	X (Co - Ce) mg/L	M (g/L)	X/M (mg/g)	log (X/M)	log (Ce)
0.00	5.00	5.00	0.00	0.50	0.00		0.70
180.00	5.00	3.92	1.08	0.50	2.16	0.33	0.59

Case 4. Dibromoethane Conc. = 10 mg/L

Time (Mins)	Co (mg/L)	Ce (mg/L)	X (Co - Ce) mg/L	M (g/L)	X/M (mg/g)	log (X/M)	log (Ce)
0.00	10.00	10.00	0.00	0.50	0.00		1.00
180.00	10.00	8.00	2.00	0.50	4.00	0.60	0.90

Case 5. Dibromoethane Conc. = 20 mg/L

Time (Mins)	Co (mg/L)	Ce (mg/L)	X (Co - Ce) mg/L	M (g/L)	X/M (mg/g)	log (X/M)	log (Ce)
0.00	20.00	20.00	0.00	0.50	0.00		1.30
180.00	20.00	16.12	3.88	0.50	7.75	0.89	1.21

Freundlich Isotherm Parameters for Linear Regression

X/M	Ce	fit	log Ce	log X/M	Ce Desorb
1.05	1.98	1.15	0.30	0.02	1.02
2.16	3.92	2.06	0.59	0.33	2.25
4.00	8.00	3.97	0.90	0.60	3.94
7.76	16.12	7.78	1.21	0.89	7.68

Table B.21. Sorption and desorption data for dibromoethane with biomass from pure oxygen activated sludge process.

Solids concentration 0.5 g/L TOC

Case 1. Dibromoethane = 0 mg/L

Time (Mins)	Co (mg/L)	Ce (mg/L)	X (Co - Ce) mg/L	M (g/L)	X/M (mg/g)	log (X/M)	log (Ce)
0.00	0.00	0.00	0.00	0.50	0.00		
180.00	0.00	0.00	0.00	0.50	0.00		

Case 2. Dibromoethane Conc. = 2.5 mg/L

Time (Mins)	Co (mg/L)	Ce (mg/L)	X (Co - Ce) mg/L	M (g/L)	X/M (mg/g)	log (X/M)	log (Ce)
0.00	2.50	2.50	0.00	0.50	0.00		0.40
180.00	2.50	2.00	0.50	0.50	1.00	0.00	0.30

Case 3. Dibromoethane Conc. = 5 mg/L

Time (Mins)	Co (mg/L)	Ce (mg/L)	X (Co - Ce) mg/L	M (g/L)	X/M (mg/g)	log (X/M)	log (Ce)
0.00	5.00	5.00	0.00	0.50	0.00		0.70
180.00	5.00	3.83	1.17	0.50	2.35	0.37	0.58

Case 4. Dibromoethane Conc. = 10 mg/L

Time (Mins)	Co (mg/L)	Ce (mg/L)	X (Co - Ce) mg/L	M (g/L)	X/M (mg/g)	log (X/M)	log (Ce)
0.00	10.00	10.00	0.00	0.50	0.00		1.00
180.00	10.00	7.81	2.19	0.50	4.38	0.64	0.89

Case 5. Dibromoethane Conc. = 20 mg/L

Time (Mins)	Co (mg/L)	Ce (mg/L)	X (Co - Ce) mg/L	M (g/L)	X/M (mg/g)	log (X/M)	log (Ce)
0.00	20.00	20.00	0.00	0.50	0.00		1.30
180.00	20.00	15.68	4.32	0.50	8.64	0.94	1.20

Freundlich Isotherm Parameters for Linear Regression

X/M	Ce	fit	log Ce	log X/M	Ce Desorb
1.00	2.00	1.17	0.30	0.00	0.91
2.35	3.83	2.17	0.58	0.37	2.33
4.38	7.81	4.36	0.89	0.64	4.35
8.64	15.68	8.67	1.20	0.94	8.60

Table B.22. Sorption and desorption data for tribromofluoromethane with biomass from activated sludge reactor with recycle.

Solids concentration 0.5 g/L TOC

Case 1. Tribromofluoromethane = 0 mg/L

Time (Mins)	Co (mg/L)	Ce (mg/L)	X (Co - Ce) mg/L	M (g/L)	X/M (mg/g)	log (X/M)	log (Ce)
0.00	0.00	0.00	0.00	0.50	0.00		
180.00	0.00	0.00	0.00	0.50	0.00		

Case 2. Tribromofluoromethane Conc. = 2.5 mg/L

Time (Mins)	Co (mg/L)	Ce (mg/L)	X (Co - Ce) mg/L	M (g/L)	X/M (mg/g)	log (X/M)	log (Ce)
0.00	2.50	2.50	0.00	0.50	0.00		0.40
180.00	2.50	1.86	0.64	0.50	1.27	0.10	0.27

Case 3. Tribromofluoromethane Conc. = 5 mg/L

Time (Mins)	Co (mg/L)	Ce (mg/L)	X (Co - Ce) mg/L	M (g/L)	X/M (mg/g)	log (X/M)	log (Ce)
0.00	5.00	5.00	0.00	0.50	0.00		0.70
180.00	5.00	3.70	1.30	0.50	2.59	0.41	0.57

Case 4. Tribromofluoromethane Conc. = 10 mg/L

Time (Mins)	Co (mg/L)	Ce (mg/L)	X (Co - Ce) mg/L	M (g/L)	X/M (mg/g)	log (X/M)	log (Ce)
0.00	10.00	10.00	0.00	0.50	0.00		1.00
180.00	10.00	7.46	2.54	0.50	5.08	0.71	0.87

Case 5. Tribromofluoromethane Conc. = 20 mg/L

Time (Mins)	Co (mg/L)	Ce (mg/L)	X (Co - Ce) mg/L	M (g/L)	X/M (mg/g)	log (X/M)	log (Ce)
0.00	20.00	20.00	0.00	0.50	0.00		1.30
180.00	20.00	15.14	4.86	0.50	9.72	0.99	1.18

Freundlich Isotherm Parameters for Linear Regression

X/M	Ce	fit	log Ce	log X/M	Ce Desorb
1.27	1.86	1.39	0.27	0.10	-
2.59	3.70	2.55	0.57	0.41	-
5.08	7.46	4.93	0.87	0.71	-
9.72	15.14	9.79	1.18	0.99	-

Table B.23. Sorption and desorption data for tribromofluoromethane with biomass from ASBR.

Solids concentration 0.5 g/L TOC

Case 1. Tribromofluoromethane = 0 mg/L

Time (Mins)	Co (mg/L)	Ce (mg/L)	X (Co - Ce) mg/L	M (g/L)	X/M (mg/g)	log (X/M)	log (Ce)
0.00	0.00	0.00	0.00	0.50	0.00		
180.00	0.00	0.00	0.00	0.50	0.00		

Case 2. Tribromofluoromethane Conc. = 2.5 mg/L

Time (Mins)	Co (mg/L)	Ce (mg/L)	X (Co - Ce) mg/L	M (g/L)	X/M (mg/g)	log (X/M)	log (Ce)
0.00	2.50	2.50	0.00	0.50	0.00		0.40
180.00	2.50	1.88	0.62	0.50	1.25	0.10	0.27

Case 3. Tribromofluoromethane Conc. = 5 mg/L

Time (Mins)	Co (mg/L)	Ce (mg/L)	X (Co - Ce) mg/L	M (g/L)	X/M (mg/g)	log (X/M)	log (Ce)
0.00	5.00	5.00	0.00	0.50	0.00		0.70
180.00	5.00	3.72	1.28	0.50	2.56	0.41	0.57

Case 4. Tribromofluoromethane Conc. = 10 mg/L

Time (Mins)	Co (mg/L)	Ce (mg/L)	X (Co - Ce) mg/L	M (g/L)	X/M (mg/g)	log (X/M)	log (Ce)
0.00	10.00	10.00	0.00	0.50	0.00		1.00
180.00	10.00	7.72	2.28	0.50	4.56	0.66	0.89

Case 5. Tribromofluoromethane Conc. = 20 mg/L

Time (Mins)	Co (mg/L)	Ce (mg/L)	X (Co - Ce) mg/L	M (g/L)	X/M (mg/g)	log (X/M)	log (Ce)
0.00	20.00	20.00	0.00	0.50	0.00		1.30
180.00	20.00	15.15	4.85	0.50	9.70	0.99	1.18

Freundlich Isotherm Parameters for Linear Regression

X/M	Ce	fit	log Ce	log X/M	Ce Desorb
1.25	1.88	1.22	0.27	0.10	-
2.56	3.72	2.38	0.57	0.41	-
4.56	7.72	4.90	0.89	0.66	-
9.70	15.15	9.58	1.18	0.99	-

Table B.24. Sorption and desorption data for tribromofluoromethane with biomass from pure oxygen activated sludge process.

Solids concentration 0.5 g/L TOC

Case 1. Tribromofluoromethane = 0 mg/L

Time (Mins)	Co (mg/L)	Ce (mg/L)	X (Co - Ce) mg/L	M (g/L)	X/M (mg/g)	log (X/M)	log (Ce)
0.00	0.00	0.00	0.00	0.50	0.00		
180.00	0.00	0.00	0.00	0.50	0.00		

Case 2. Tribromofluoromethane Conc. = 2.5 mg/L

Time (Mins)	Co (mg/L)	Ce (mg/L)	X (Co - Ce) mg/L	M (g/L)	X/M (mg/g)	log (X/M)	log (Ce)
0.00	2.50	2.50	0.00	0.50	0.00		0.40
180.00	2.50	1.87	0.63	0.50	1.27	0.10	0.27

Case 3. Tribromofluoromethane Conc. = 5 mg/L

Time (Mins)	Co (mg/L)	Ce (mg/L)	X (Co - Ce) mg/L	M (g/L)	X/M (mg/g)	log (X/M)	log (Ce)
0.00	5.00	5.00	0.00	0.50	0.00		0.70
180.00	5.00	3.73	1.27	0.50	2.54	0.40	0.57

Case 4. Tribromofluoromethane Conc. = 10 mg/L

Time (Mins)	Co (mg/L)	Ce (mg/L)	X (Co - Ce) mg/L	M (g/L)	X/M (mg/g)	log (X/M)	log (Ce)
0.00	10.00	10.00	0.00	0.50	0.00		1.00
180.00	10.00	7.52	2.48	0.50	4.97	0.70	0.88

Case 5. Tribromofluoromethane Conc. = 20 mg/L

Time (Mins)	Co (mg/L)	Ce (mg/L)	X (Co - Ce) mg/L	M (g/L)	X/M (mg/g)	log (X/M)	log (Ce)
0.00	20.00	20.00	0.00	0.50	0.00		1.30
180.00	20.00	15.21	4.79	0.50	9.57	0.98	1.18

Freundlich Isotherm Parameters for Linear Regression

X/M	Ce	fit	log Ce	log X/M	Ce Desorb
1.27	1.87	1.36	0.27	0.10	-
2.54	3.73	2.51	0.57	0.40	-
4.96	7.52	4.86	0.88	0.70	-
9.57	15.21	9.62	1.18	0.98	-

Table B.25. Sorption and desorption data for chloropropane with biomass from activated sludge reactor with recycle.

Solids concentration 0.5 g/L TOC

Case 1. Chloropropane = 0 mg/L

Time (Mins)	Co (mg/L)	Ce (mg/L)	X (Co - Ce) mg/L	M (g/L)	X/M (mg/g)	log (X/M)	log (Ce)
0.00	0.00	0.00	0.00	0.50	0.00		
180.00	0.00	0.00	0.00	0.50	0.00		

Case 2. Chloropropane Conc. = 2.5 mg/L

Time (Mins)	Co (mg/L)	Ce (mg/L)	X (Co - Ce) mg/L	M (g/L)	X/M (mg/g)	log (X/M)	log (Ce)
0.00	2.50	2.50	0.00	0.50	0.00		0.40
180.00	2.50	2.02	0.48	0.50	0.96	-0.02	0.30

Case 3. Chloropropane Conc. = 5 mg/L

Time (Mins)	Co (mg/L)	Ce (mg/L)	X (Co - Ce) mg/L	M (g/L)	X/M (mg/g)	log (X/M)	log (Ce)
0.00	5.00	5.00	0.00	0.50	0.00		0.70
180.00	5.00	4.07	0.93	0.50	1.86	0.27	0.61

Case 4. Chloropropane Conc. = 10 mg/L

Time (Mins)	Co (mg/L)	Ce (mg/L)	X (Co - Ce) mg/L	M (g/L)	X/M (mg/g)	log (X/M)	log (Ce)
0.00	10.00	10.00	0.00	0.50	0.00		1.00
180.00	10.00	8.10	1.90	0.50	3.79	0.58	0.91

Case 5. Chloropropane Conc. = 20 mg/L

Time (Mins)	Co (mg/L)	Ce (mg/L)	X (Co - Ce) mg/L	M (g/L)	X/M (mg/g)	log (X/M)	log (Ce)
0.00	20.00	20.00	0.00	0.50	0.00		1.30
180.00	20.00	16.39	3.61	0.50	7.21	0.86	1.21

Freundlich Isotherm Parameters for Linear Regression

X/M	Ce	fit	log Ce	log X/M	Ce Desorb
0.97	2.02	1.01	0.31	-0.01	0.99
1.86	4.07	1.90	0.61	0.27	1.75
3.79	8.10	3.66	0.91	0.58	3.78
7.21	16.39	7.26	1.21	0.86	7.15

Table B.26. Sorption and desorption data for chloropropane with biomass from ASBR.

Solids concentration 0.5 g/L TOC

Case 1. Chloropropane = 0 mg/L

Time (Mins)	Co (mg/L)	Ce (mg/L)	X (Co - Ce) mg/L	M (g/L)	X/M (mg/g)	log (X/M)	log (Ce)
0.00	0.00	0.00	0.00	0.50	0.00		
180.00	0.00	0.00	0.00	0.50	0.00		

Case 2. Chloropropane Conc. = 2.5 mg/L

Time (Mins)	Co (mg/L)	Ce (mg/L)	X (Co - Ce) mg/L	M (g/L)	X/M (mg/g)	log (X/M)	log (Ce)
0.00	2.50	2.50	0.00	0.50	0.00		0.40
180.00	2.50	2.10	0.40	0.50	0.80	-0.10	0.32

Case 3. Chloropropane Conc. = 5 mg/L

Time (Mins)	Co (mg/L)	Ce (mg/L)	X (Co - Ce) mg/L	M (g/L)	X/M (mg/g)	log (X/M)	log (Ce)
0.00	5.00	5.00	0.00	0.50	0.00		0.70
180.00	5.00	4.11	0.89	0.50	1.78	0.25	0.61

Case 4. Chloropropane Conc. = 10 mg/L

Time (Mins)	Co (mg/L)	Ce (mg/L)	X (Co - Ce) mg/L	M (g/L)	X/M (mg/g)	log (X/M)	log (Ce)
0.00	10.00	10.00	0.00	0.50	0.00		1.00
180.00	10.00	8.33	1.67	0.50	3.33	0.52	0.92

Case 5. Chloropropane Conc. = 20 mg/L

Time (Mins)	Co (mg/L)	Ce (mg/L)	X (Co - Ce) mg/L	M (g/L)	X/M (mg/g)	log (X/M)	log (Ce)
0.00	20.00	20.00	0.00	0.50	0.00		1.30
180.00	20.00	16.44	3.56	0.50	7.12	0.85	1.22

Freundlich Isotherm Parameters for Linear Regression

X/M	Ce	fit	log Ce	log X/M	Ce Desorb
0.80	2.10	0.79	0.32	-0.10	0.80
1.78	4.11	1.67	0.61	0.25	1.68
3.33	8.33	3.51	0.92	0.52	3.25
7.12	16.44	7.06	1.22	0.85	7.14

Table B.27. Sorption and desorption data for chloropropane with biomass from pure oxygen activated sludge process.

Solids concentration 0.5 g/L TOC

Case 1. Chloropropane = 0 mg/L

Time (Mins)	Co (mg/L)	Ce (mg/L)	X (Co - Ce) mg/L	M (g/L)	X/M (mg/g)	log (X/M)	log (Ce)
0.00	0.00	0.00	0.00	0.50	0.00		
180.00	0.00	0.00	0.00	0.50	0.00		

Case 2. Chloropropane Conc. = 2.5 mg/L

Time (Mins)	Co (mg/L)	Ce (mg/L)	X (Co - Ce) mg/L	M (g/L)	X/M (mg/g)	log (X/M)	log (Ce)
0.00	2.50	2.50	0.00	0.50	0.00		0.40
180.00	2.50	2.04	0.46	0.50	0.92	-0.04	0.31

Case 3. Chloropropane Conc. = 5 mg/L

Time (Mins)	Co (mg/L)	Ce (mg/L)	X (Co - Ce) mg/L	M (g/L)	X/M (mg/g)	log (X/M)	log (Ce)
0.00	5.00	5.00	0.00	0.50	0.00		0.70
180.00	5.00	4.05	0.95	0.50	1.91	0.28	0.61

Case 4. Chloropropane Conc. = 10 mg/L

Time (Mins)	Co (mg/L)	Ce (mg/L)	X (Co - Ce) mg/L	M (g/L)	X/M (mg/g)	log (X/M)	log (Ce)
0.00	10.00	10.00	0.00	0.50	0.00		1.00
180.00	10.00	8.13	1.87	0.50	3.74	0.57	0.91

Case 5. Chloropropane Conc. = 20 mg/L

Time (Mins)	Co (mg/L)	Ce (mg/L)	X (Co - Ce) mg/L	M (g/L)	X/M (mg/g)	log (X/M)	log (Ce)
0.00	20.00	20.00	0.00	0.50	0.00		1.30
180.00	20.00	16.37	3.63	0.50	7.27	0.86	1.21

Freundlich Isotherm Parameters for Linear Regression

X/M	Ce	fit	log Ce	log X/M	Ce Desorb
0.92	2.04	0.99	0.31	-0.04	0.90
1.91	4.05	1.87	0.61	0.28	1.85
3.74	8.13	3.67	0.91	0.57	3.66
7.27	16.37	7.30	1.21	0.86	7.22

Table B.28. Sorption and desorption data for bromobutane with biomass from activated sludge reactor with recycle.

Solids concentration 0.5 g/L TOC

Case 1. Bromobutane = 0 mg/L

Time (Mins)	Co (mg/L)	Ce (mg/L)	X (Co - Ce) mg/L	M (g/L)	X/M (mg/g)	log (X/M)	log (Ce)
0.00	0.00	0.00	0.00	0.50	0.00		
180.00	0.00	0.00	0.00	0.50	0.00		

Case 2. Bromobutane Conc. = 2.5 mg/L

Time (Mins)	Co (mg/L)	Ce (mg/L)	X (Co - Ce) mg/L	M (g/L)	X/M (mg/g)	log (X/M)	log (Ce)
0.00	2.50	2.50	0.00	0.50	0.00		0.40
180.00	2.50	1.06	1.44	0.50	2.88	0.46	0.03

Case 3. Bromobutane Conc. = 5 mg/L

Time (Mins)	Co (mg/L)	Ce (mg/L)	X (Co - Ce) mg/L	M (g/L)	X/M (mg/g)	log (X/M)	log (Ce)
0.00	5.00	5.00	0.00	0.50	0.00		0.70
180.00	5.00	2.07	2.93	0.50	5.85	0.77	0.32

Case 4. Bromobutane Conc. = 10 mg/L

Time (Mins)	Co (mg/L)	Ce (mg/L)	X (Co - Ce) mg/L	M (g/L)	X/M (mg/g)	log (X/M)	log (Ce)
0.00	10.00	10.00	0.00	0.50	0.00		1.00
180.00	10.00	4.28	5.72	0.50	11.45	1.06	0.63

Case 5. Bromobutane Conc. = 20 mg/L

Time (Mins)	Co (mg/L)	Ce (mg/L)	X (Co - Ce) mg/L	M (g/L)	X/M (mg/g)	log (X/M)	log (Ce)
0.00	20.00	20.00	0.00	0.50	0.00		1.30
180.00	20.00	8.60	11.40	0.50	22.80	1.36	0.93

Freundlich Isotherm Parameters for Linear Regression

X/M	Ce	fit	log Ce	log X/M	Ce Desorb
2.88	1.06	3.02	0.03	0.46	2.85
5.85	2.07	5.67	0.32	0.77	5.80
11.45	4.28	11.47	0.63	1.06	11.45
22.80	8.60	22.81	0.93	1.36	22.75

Table B.29. Sorption and desorption data for bromobutane with biomass from ASBR.

Solids concentration 0.5 g/L TOC

Case 1. Bromobutane = 0 mg/L

Time (Mins)	Co (mg/L)	Ce (mg/L)	X (Co - Ce) mg/L	M (g/L)	X/M (mg/g)	log (X/M)	log (Ce)
0.00	0.00	0.00	0.00	0.50	0.00		
180.00	0.00	0.00	0.00	0.50	0.00		

Case 2. Bromobutane Conc. = 2.5 mg/L

Time (Mins)	Co (mg/L)	Ce (mg/L)	X (Co - Ce) mg/L	M (g/L)	X/M (mg/g)	log (X/M)	log (Ce)
0.00	2.50	2.50	0.00	0.50	0.00		0.40
180.00	2.50	1.08	1.42	0.50	2.85	0.45	0.03

Case 3. Bromobutane Conc. = 5 mg/L

Time (Mins)	Co (mg/L)	Ce (mg/L)	X (Co - Ce) mg/L	M (g/L)	X/M (mg/g)	log (X/M)	log (Ce)
0.00	5.00	5.00	0.00	0.50	0.00		0.70
180.00	5.00	2.14	2.86	0.50	5.73	0.76	0.33

Case 4. Bromobutane Conc. = 10 mg/L

Time (Mins)	Co (mg/L)	Ce (mg/L)	X (Co - Ce) mg/L	M (g/L)	X/M (mg/g)	log (X/M)	log (Ce)
0.00	10.00	10.00	0.00	0.50	0.00		1.00
180.00	10.00	4.26	5.74	0.50	11.49	1.06	0.63

Case 5. Bromobutane Conc. = 20 mg/L

Time (Mins)	Co (mg/L)	Ce (mg/L)	X (Co - Ce) mg/L	M (g/L)	X/M (mg/g)	log (X/M)	log (Ce)
0.00	20.00	20.00	0.00	0.50	0.00		1.30
180.00	20.00	8.44	11.56	0.50	23.12	1.36	0.93

Freundlich Isotherm Parameters for Linear Regression

X/M	Ce	fit	log Ce	log X/M	Ce Desorb
2.85	1.08	2.81	0.03	0.45	2.85
5.73	2.14	5.73	0.33	0.76	5.70
11.49	4.26	11.57	0.63	1.06	11.45
23.12	8.44	23.09	0.93	1.36	23.1

Table B.30. Sorption and desorption data for bromobutane with biomass from pure oxygen activated sludge process.

Solids concentration 0.5 g/L TOC

Case 1. Bromobutane = 0 mg/L

Time (Mins)	Co (mg/L)	Ce (mg/L)	X (Co - Ce) mg/L	M (g/L)	X/M (mg/g)	log (X/M)	log (Ce)
0.00	0.00	0.00	0.00	0.50	0.00		
180.00	0.00	0.00	0.00	0.50	0.00		

Case 2. Bromobutane Conc. = 2.5 mg/L

Time (Mins)	Co (mg/L)	Ce (mg/L)	X (Co - Ce) mg/L	M (g/L)	X/M (mg/g)	log (X/M)	log (Ce)
0.00	2.50	2.50	0.00	0.50	0.00		0.40
180.00	2.50	1.07	1.43	0.50	2.86	0.46	0.03

Case 3. Bromobutane Conc. = 5 mg/L

Time (Mins)	Co (mg/L)	Ce (mg/L)	X (Co - Ce) mg/L	M (g/L)	X/M (mg/g)	log (X/M)	log (Ce)
0.00	5.00	5.00	0.00	0.50	0.00		0.70
180.00	5.00	2.15	2.85	0.50	5.70	0.76	0.33

Case 4. Bromobutane Conc. = 10 mg/L

Time (Mins)	Co (mg/L)	Ce (mg/L)	X (Co - Ce) mg/L	M (g/L)	X/M (mg/g)	log (X/M)	log (Ce)
0.00	10.00	10.00	0.00	0.50	0.00		1.00
180.00	10.00	4.34	5.66	0.50	11.33	1.05	0.64

Case 5. Bromobutane Conc. = 20 mg/L

Time (Mins)	Co (mg/L)	Ce (mg/L)	X (Co - Ce) mg/L	M (g/L)	X/M (mg/g)	log (X/M)	log (Ce)
0.00	20.00	20.00	0.00	0.50	0.00		1.30
180.00	20.00	8.58	11.42	0.50	22.83	1.36	0.93

Freundlich Isotherm Parameters for Linear Regression

X/M	Ce	fit	log Ce	log X/M	Ce Desorb
2.86	1.07	2.80	0.03	0.46	2.82
5.70	2.15	5.67	0.33	0.76	5.62
11.33	4.34	11.49	0.64	1.05	11.35
22.83	8.58	22.76	0.93	1.36	22.5

APPENDIX C

SORPTION ISOTHERMS USING AZO DYE 151

Table C.1. Adsorption isotherm for azo dye 151 using biomass from laboratory scale activated sludge reactor with recycle, dye concentration varied.

Time (Mins)	Co (mg/L)	Ce (mg/L)	X (Co - Ce)	M (g/L)	X/M (mg/g)	log (X/M)	log (Ce)
0.00	0.00	0.00	0.00	0.10	0.00		
15.00	0.00	0.00	0.00	0.10	0.00		
30.00	0.00	0.00	0.00	0.10	0.00		
60.00	0.00	0.00	0.00	0.10	0.00		
120.00	0.00	0.00	0.00	0.10	0.00		
180.00	0.00	0.00	0.00	0.10	0.00		

Table C.2. Adsorption isotherm for azo dye 151 using biomass from laboratory scale activated sludge reactor with recycle, dye concentration varied.

Time (Mins)	Co (mg/L)	Ce (mg/L)	X (Co - Ce)	M (g/L)	X/M (mg/g)	log (X/M)	log (Ce)
0.00	2.50	2.50	0.00	0.10	0.00		0.40
15.00	2.50	1.68	0.82	0.10	8.20	0.91	0.23
30.00	2.50	1.54	0.96	0.10	9.60	0.98	0.19
60.00	2.50	1.48	1.02	0.10	10.20	1.01	0.17
120.00	2.50	1.42	1.08	0.10	10.80	1.03	0.15
180.00	2.50	1.40	1.10	0.10	11.03	1.04	0.15

Table C.3. Adsorption isotherm for azo dye 151 using biomass from laboratory scale activated sludge reactor with recycle, dye concentration varied.

Time (Mins)	Co (mg/L)	Ce (mg/L)	X (Co - Ce)	M (g/L)	X/M (mg/g)	log (X/M)	log (Ce)
0.00	5.00	5.00	0.00	0.10	0.00		0.70
15.00	5.00	3.01	1.99	0.10	19.90	1.30	0.48
30.00	5.00	2.91	2.09	0.10	20.90	1.32	0.46
60.00	5.00	2.77	2.23	0.10	22.26	1.35	0.44
120.00	5.00	2.80	2.20	0.10	22.00	1.34	0.45
180.00	5.00	2.81	2.19	0.10	21.88	1.34	0.45

Table C.4. Adsorption isotherm for azo dye 151 using biomass from laboratory scale activated sludge reactor with recycle, dye concentration varied.

Time (Mins)	Co (mg/L)	Ce (mg/L)	X (Co - Ce)	M (g/L)	X/M (mg/g)	log (X/M)	log (Ce)
0.00	10.00	10.00	0.00	0.10	0.00		1.00
15.00	10.00	7.72	2.28	0.10	22.80	1.36	0.89
30.00	10.00	7.03	2.97	0.10	29.70	1.47	0.85
60.00	10.00	6.34	3.66	0.10	36.60	1.56	0.80
120.00	10.00	5.61	4.39	0.10	43.90	1.64	0.75
180.00	10.00	5.59	4.41	0.10	44.09	1.64	0.75

Table C.5. Adsorption isotherm for azo dye 151 using biomass from laboratory scale activated sludge reactor with recycle, dye concentration varied.

Time (Mins)	Co (mg/L)	Ce (mg/L)	X (Co - Ce)	M (g/L)	X/M (mg/g)	log (X/M)	log (Ce)
0.00	20.00	20.00	0.00	0.10	0.00		1.30
15.00	20.00	12.00	8.00	0.10	80.00	1.90	1.08
30.00	20.00	12.23	7.77	0.10	77.70	1.89	1.09
60.00	20.00	12.10	7.90	0.10	79.00	1.90	1.08
120.00	20.00	11.75	8.25	0.10	82.50	1.92	1.07
180.00	20.00	11.75	8.25	0.10	82.50	1.92	1.07

Table C.6. Adsorption isotherm for azo dye 151 using biomass from laboratory scale activated sludge reactor with recycle, dye concentration varied.

X/M	Ce	Regression Fit	log Ce	log (X/M)
11.03	1.40	12.21	0.15	1.09
21.88	2.81	21.64	0.45	1.34
44.09	5.59	40.23	0.75	1.60
82.50	11.75	81.42	1.07	1.91

Table C.7. Adsorption isotherm for azo dye 151 using biomass from laboratory scale activated sludge reactor with recycle, solids concentration varied.

Time (Mins)	Co (mg/L)	Ce (mg/L)	X (Co - Ce)	M (g/L)	X/M (mg/g)	log (X/M)	log (Ce)
0.00	10.00	10.00	0.00	0.00			
15.00	10.00	10.00	0.00	0.00			
30.00	10.00	10.00	0.00	0.00			
60.00	10.00	10.00	0.00	0.00			
120.00	10.00	10.00	0.00	0.00			
180.00	10.00	10.00	0.00	0.00			

Table C.8. Adsorption isotherm for azo dye 151 using biomass from laboratory scale activated sludge reactor with recycle, solids concentration varied.

Time (Mins)	Co (mg/L)	Ce (mg/L)	X (Co - Ce)	M (g/L)	X/M (mg/g)	log (X/M)	log (Ce)
0.00	10.00	10.00	0.00	0.05	0.00		1.00
15.00	10.00	7.99	2.01	0.05	40.20	1.60	0.90
30.00	10.00	7.85	2.15	0.05	43.00	1.63	0.89
60.00	10.00	7.38	2.62	0.05	52.40	1.72	0.87
120.00	10.00	7.24	2.76	0.05	55.20	1.74	0.86
180.00	10.00	7.24	2.76	0.05	55.17	1.74	0.86

Table C.9. Adsorption isotherm for azo dye 151 using biomass from laboratory scale activated sludge reactor with recycle, solids concentration varied.

Time (Mins)	Co (mg/L)	Ce (mg/L)	X (Co - Ce)	M (g/L)	X/M (mg/g)	log (X/M)	log (Ce)
0.00	10.00	10.00	0.00	0.10	0.00		1.00
15.00	10.00	6.28	3.72	0.10	37.20	1.57	0.80
30.00	10.00	6.15	3.85	0.10	38.50	1.59	0.79
60.00	10.00	5.98	4.02	0.10	40.20	1.60	0.78
120.00	10.00	5.66	4.34	0.10	43.40	1.64	0.75
180.00	10.00	5.65	4.35	0.10	43.53	1.64	0.75

Table C.10. Adsorption isotherm for azo dye 151 using biomass from laboratory scale activated sludge reactor with recycle, solids concentration varied.

Time (Mins)	Co (mg/L)	Ce (mg/L)	X (Co - Ce)	M (g/L)	X/M (mg/g)	log (X/M)	log (Ce)
0.00	10.00	10.00	0.00	0.50	0.00		1.00
15.00	10.00	3.01	6.99	0.50	13.98	1.15	0.48
30.00	10.00	2.35	7.65	0.50	15.30	1.18	0.37
60.00	10.00	2.12	7.88	0.50	15.76	1.20	0.33
120.00	10.00	2.06	7.94	0.50	15.88	1.20	0.31
180.00	10.00	2.04	7.96	0.50	15.92	1.20	0.31

Table C.11. Adsorption isotherm for azo dye 151 using biomass from laboratory scale activated sludge reactor with recycle, solids concentration varied.

Time (Mins)	Co (mg/L)	Ce (mg/L)	X (Co - Ce)	M (g/L)	X/M (mg/g)	log (X/M)	log (Ce)
0.00	10.00	10.00	0.00	1.00	0.00		1.00
15.00	10.00	2.21	7.79	1.00	7.79	0.89	0.34
30.00	10.00	1.73	8.27	1.00	8.27	0.92	0.24
60.00	10.00	1.18	8.82	1.00	8.82	0.95	0.07
120.00	10.00	1.14	8.86	1.00	8.86	0.95	0.06
180.00	10.00	1.14	8.86	1.00	8.86	0.95	0.06

Table C.12. Adsorption isotherm for azo dye 151 using biomass from laboratory scale activated sludge reactor with recycle, solids concentration varied.

X/M	Ce	Regression Fit	log Ce	log (X/M)
55.17	7.24	55.37	0.86	1.74
43.54	5.65	43.28	0.75	1.64
15.92	2.04	15.84	0.31	1.20
8.86	1.14	9.00	0.06	0.95

APPENDIX D

CONNECTIVITY INDEXES OF THE AX CLASS

Table D.1. Molecular connectivity indexes calculated using GRAPH III©.

Compound name	Molecular Connectivity Indexes							
	${}^0\chi$	${}^1\chi$	${}^2\chi$	${}^3\chi$	${}^0\chi^v$	${}^1\chi^v$	${}^2\chi^v$	${}^3\chi^v$
CH ₃ Cl	2.000	1.000	0.000	0.000	2.132	1.132	0.000	0.000
CH ₂ Cl ₂	2.707	1.414	0.707	0.000	2.972	1.601	0.907	0.000
CHCl ₃	3.577	1.732	1.732	0.000	3.974	1.961	2.221	0.000
CHCl ₂ F	3.577	1.732	1.732	0.000	3.220	1.526	1.234	0.000
CHClF ₂	3.577	1.732	1.732	0.000	2.466	1.090	0.577	0.000
CCl ₄	4.500	2.000	3.000	0.000	5.029	2.265	3.846	0.000
CCl ₃ F	4.500	2.000	3.000	0.000	4.275	1.887	2.565	0.000
CCl ₂ F ₂	4.500	2.000	3.000	0.000	3.520	1.510	1.568	0.000
CH ₃ Br	2.000	1.000	0.000	0.000	2.961	1.961	0.000	0.000
CH ₃ -CH ₂ Cl	2.707	1.414	0.707	0.000	2.839	1.508	0.801	0.000
CHCl-CH ₂ Cl	3.414	1.914	1.000	0.500	3.679	2.101	1.132	0.641
CH ₂ Br-CH ₂ Cl	3.414	1.914	1.000	0.500	4.378	2.449	1.263	0.907
CH ₂ Cl-CHCl ₂	4.284	2.270	1.802	0.816	4.681	2.516	2.127	1.047
CH ₃ -CCl ₃	4.500	2.000	3.000	0.000	4.897	2.198	3.621	0.000
CHCl ₂ -CHCl ₂	5.207	2.561	2.914	1.061	5.606	2.641	3.231	1.110
CHCl ₂ -CCl ₃	6.077	2.943	3.521	1.732	6.739	3.925	4.298	2.221
CCl ₃ -CCl ₃	7.000	3.250	4.500	2.250	7.794	3.647	5.545	2.885
CCl ₂ F-CClF ₂	7.000	3.250	4.500	2.250	5.531	2.515	2.701	1.247
CH ₂ Br-CH ₂ Br	3.414	1.914	1.000	0.500	5.207	2.927	1.601	1.570
CH ₃ -CHCl ₂	3.577	1.732	1.732	0.000	3.842	1.885	2.048	0.000
CClF ₂ -CClF ₂	7.000	3.250	4.500	2.250	4.776	2.138	1.943	0.891
CH ₃ -CHCl-CH ₂ Cl	4.284	2.270	1.802	0.816	4.419	2.218	1.742	0.805

Table D.1. Molecular connectivity indexes calculated using GRAPH III© (continued).

Compound name	Molecular Connectivity Indexes							
	${}^0\chi$	${}^1\chi$	${}^2\chi$	${}^3\chi$	${}^0\chi^v$	${}^1\chi^v$	${}^2\chi^v$	${}^3\chi^v$
CH ₂ Cl-CHCl-CH ₂ Cl	4.992	2.808	1.922	1.394	5.259	2.850	1.915	1.485
CH ₃ -CH ₂ -CH ₂ F	3.414	1.914	1.000	0.500	2.792	1.474	0.689	0.189
CH ₂ F-CH ₂ -CH ₂ F	4.121	2.414	1.354	0.707	2.877	1.535	0.732	0.267
CH ₃ -CF ₂ -CH ₃	4.500	2.000	3.000	0.000	3.256	1.378	1.327	0.000
CH ₂ Cl-CHCl-CHCl ₂	5.862	3.181	2.630	1.782	6.391	3.503	3.033	2.179
CH ₂ F-CF ₂ -CH ₂ Cl	5.914	3.121	2.871	1.914	4.180	2.153	1.390	0.781
CH ₃ -CF ₂ -CH ₂ Cl	5.207	2.561	2.914	1.061	4.095	2.032	1.471	0.703
CH ₃ -CH ₂ Br	2.707	1.414	0.707	0.000	3.668	2.094	1.387	0.000
CHBr ₃	3.577	1.732	1.732	0.000	6.461	3.397	6.662	0.000
CH ₃ -CH ₂ F	2.707	1.414	0.707	0.000	2.085	0.974	0.267	0.000
CH ₃ -CHBr ₂	3.577	1.732	1.732	0.000	5.500	2.842	4.485	0.000
CBr ₂ ClF	4.500	2.000	3.000	0.000	5.933	2.716	5.099	0.000
CH ₂ Br ₂	2.707	1.414	0.707	0.000	4.500	2.265	2.221	0.000
CH ₃ I	2.000	1.000	0.000	0.000	3.500	2.500	0.000	0.000
CH ₂ BrCl	2.707	1.414	0.707	0.000	3.671	1.786	1.282	0.000
CBrF ₃	4.500	2.000	3.000	0.000	3.595	1.548	1.326	0.000
CBr ₃ F	4.500	2.000	3.000	0.000	6.761	3.131	6.881	0.000
CH ₂ Br-CH ₂ F	3.414	1.914	1.000	0.000	3.753	2.154	1.170	0.371
CH ₃ -CHF ₂	3.577	1.732	1.732	0.000	2.333	1.014	0.519	0.000
CH ₃ -CH ₂ I	2.707	1.414	0.707	0.000	4.207	2.475	1.768	0.000
CH ₂ Br-CH ₂ -CH ₂ Br	4.121	2.414	1.354	0.707	5.914	3.427	2.070	1.132
CH ₂ Br-CH ₂ -CH ₂ F	4.121	2.414	1.354	0.707	4.460	2.654	1.523	0.827
CH ₃ -CH ₂ -CH ₂ Br	3.414	1.914	1.000	0.500	4.375	2.594	1.481	0.981
CH ₃ -CHBr-CH ₃	3.577	1.732	1.732	0.000	4.539	2.287	2.842	0.000
CH ₃ -CH ₂ -CH ₂ Cl	3.414	1.914	1.000	0.500	3.546	2.008	1.066	0.566
CH ₃ -CHCl-CH ₃	3.577	1.732	1.732	0.000	3.710	1.808	1.885	0.000

Table D.1. Molecular connectivity indexes calculated using GRAPH III© (contd.).

Compound name	Molecular Connectivity Indexes							
	${}^0\chi$	${}^1\chi$	${}^2\chi$	${}^3\chi$	${}^0\chi^v$	${}^1\chi^v$	${}^2\chi^v$	${}^3\chi^v$
CH ₃ -CH ₂ -CH ₂ I	3.414	1.914	1.000	0.500	4.914	2.975	1.750	1.250
CH ₃ -CHI-CH ₃	3.577	1.732	1.732	0.000	5.077	2.598	3.464	0.000
CH ₂ Br-CH ₂ -CH ₂ -CH ₂ Br	4.828	2.914	1.707	0.957	6.621	3.927	2.423	1.464
CH ₃ -CH ₂ -CH ₂ -CH ₂ Br	4.121	2.414	1.354	0.707	5.082	3.094	1.834	1.047
[CH ₃] ₃ -CBr	4.121	2.414	1.354	0.707	5.082	3.094	1.834	1.047
CH ₃ -CH ₂ -CH ₂ -CH ₂ Cl	4.121	2.414	1.354	0.707	4.254	2.508	1.420	0.754
[CH ₃] ₃ -CCl	4.121	2.414	1.354	0.707	4.254	2.508	1.420	0.754
CH ₃ -CH ₂ -CH ₂ -CH ₂ I	4.121	2.414	1.354	0.707	5.621	3.475	2.104	1.237
[CH ₃] ₃ -Cl	4.121	2.414	1.354	0.707	5.621	3.475	2.104	1.237
CH ₃ -CH ₂ -CHI-CH ₃	4.284	2.270	1.802	0.816	5.784	3.136	3.280	1.429

REFERENCES

1. Anderson, T. W. (1984). An Introduction to Multivariate Statistical Analysis. 2nd Edition, John Wiley and Sons, New York.
2. APHA. (1989). Standard Methods for the Examination of Water and Wastewater, 17th edition, APHA, AWWA and WPCF, Washington D.C.
3. Balmat, J. L. (1957). "Biochemical Oxidation of Various Particulate Fractions of Sewage," *Sewage and Industrial Wastes*, vol. 29, pp. 757-761.
4. Banerjee, S., Howard, P. H., Rosenberg, A. M., Dombrowski, A. E., Sikka, A. and Tullis, D. L. (1984). "Development of a General Kinetic Model for Biodegradation and Its Application to Chlorophenols and Related Compounds," *Environmental Science and Technology*, vol.18, pp. 6-13.
5. Bell, J. P. and Tsezos, M. (1987). "Removal of Hazardous Organic Pollutants by Biomass Adsorption," *Journal of Water Pollution Control Federation*, vol. 59, pp. 191-198.
6. Bell, J. P. and Tsezos, M. (1988). "The Selectivity of Biosorption of Hazardous Organics by Microbial Biomass," *Water Research*, 22, 1245-1251, 1988.
7. Bintein, S. and Devillers, J. (1994). "QSAR for Organic Chemical Sorption in Soils and Sediments," *Chemosphere*, vol. 28, no. 6, pp. 1171-1188.
8. Boethling, R. S. and Sabljic, A. (1989). "Screening-Level Model for Aerobic Biodegradability Based on a Survey of Expert Knowledge," *Environmental Science and Technology*, vol. 23, no. 6, pp. 672-679.
9. Boethling, R. S., Howard, P., Meylan, W., Stitler, W., Beauman, J. and Tirado, N. (1994). "Group Contribution Method for Predicting Probability and Rate of Aerobic Biodegradation," *Environmental Science and Technology*, vol. 28, no. 6, pp. 459-465.
10. Brock, T. D. and Madigan, M. T. (1991). Biology of Microorganisms, Sixth Edition. Prentice Hall, NJ.
11. Brusseau, M. L. (1993). "Using QSAR to Evaluate Phenomenological Models for Sorption of Organic Compounds by Soil," *Environmental Toxicology and Chemistry*, vol. 12, pp. 1835-1846.

12. Canton, J. H., van Esch G. H., Greeve, P. A. and van Hellemond, A. B. A. M. (1977). "Accumulation and elimination of α -hexachlorocyclohexane (α -HCH) by the Marine Algae *Chlamydomonas* and *Dunaliella*," Water Research, vol. 11, pp. 111-115.
13. Crittenden, J. C., Berrigan, J. K. and Hand, D. (1986). "Design of Rapid Small - Scale Adsorption Tests For a Constant Diffusivity," Journal of the Water Pollution Control Federation, vol. 58, no. 4, pp. 312-319.
14. Curl, R. L. and Keolelan, G. A. (1984). "Implicit Adsorbate Model for Apparent Anomalies with Organic Adsorption on Natural Sediments," Environmental Science and Technology, vol. 18, no. 12, pp. 916-922.
15. Dammel, E. E. and Schroeder, E. D. (1991). "Density of Activated Sludge Solids," Water Research, vol. 25, no. 7, pp. 841-846.
16. Dennis, R. W. and Irvine, R. L. (1979). "Effect of Fill:React Ratio on Sequencing Batch Biological Reactors," Journal of the Water Pollution Control Federation, vol. 51, no. 2, pp. 255-263.
17. Desai, S. M., Govind, R. and Tabak, H. H. (1990). "Development of Quantitative Structure - Activity Relationships for Predicting Biodegradation Kinetics," Environmental Toxicology and Chemistry, vol. 9, pp. 473-477.
18. Dick, R. I. (1992). "Comment on Density of Activated Sludge Solids," Water Research, vol. 26, no. 11, pp. 1555-1558.
19. Dobbs, R. A., Jelus, M. and Cheng, K. Y. (1986). "Partitioning of Toxic Organic Compounds on Municipal Wastewater Treatment Plant Solids," Proceedings of the International Conference on Innovative Biological Treatment of Toxic Wastewaters, Virginia, pp. 585-601.
20. Dobbs, R. A., Shan, Y., Wang, L. and Govind, R. (1995). "Sorption on Wastewater Solids: Elimination of Biological Activity," Water Environment Research, vol. 67, pp. 327-329.
21. Dobbs, R. A., Wang, L., Govind, R. (1989). "Sorption of Toxic Organic Compounds on Wastewater Solids: Correlation with Fundamental Properties," Environmental Science and Technology, vol. 23, pp. 1092-1097.
22. Droste, R. L. and Sanchez, W. A. (1983). "Microbial Activity in Aerobic Sludge Digestion," Water Research, vol. 17, no. 9, pp. 975-983.
23. Dunnivant, F. M. and Eizerman, A. W. (1992). "Quantitative Structure - Property Relationships for Aqueous Solubilities and Henry's Law Constants of Polychlorinated Biphenyls," Environmental Science and Technology, vol. 26, pp.8.

24. Eriksson, L., Jonsson, J., Hellberg, S., Lindgren, F., Skagerberg, B., Sjostrom, M., Wold, S., and Berglind, R. (1990). "A Strategy for Ranking Environmentally Occurring Chemicals. Part III: Multivariate Quantitative -Structure Activity Relationship for Halogenated Aliphatics," *Environmental Toxicology and Chemistry*, vol. 9, pp. 1339-1351.
25. Eriksson, L., Jonsson, J., Sjostrom, M. and Wold, S. (1989). "A Strategy for Ranking Environmentally Occurring Chemicals. Part II. An Illustration with Two Data Sets of Chlorinated Aliphatics and Aliphatic Alcohols," *Chemometrics and Intelligent Laboratory Systems*, vol. 7, pp. 131-141.
26. Govers, H., Ruepert, C. and Aiking, H. (1984). "Quantitative Structure Activity Relationships for Polycyclic Aromatic Hydrocarbons: Correlation Between Molecular Connectivity, Physico-Chemical Properties, Bioconcentration, and Toxicity in *Daphnia Pulex*," *Chemosphere*, vol. 13, no. 2, pp. 227-236.
27. Govind, R., Flaherty, P. A. and Dobbs, R. A. (1991). "Fate and Effects of Semivolatile Organic Pollutants During Anaerobic Digestion of Sludge," *Water Research*, vol. 25, no. 5, pp. 547-556.
28. Gschwend, P. M. and Wu, S. C. (1985). "On the Constancy of Sediment-Water Partition Coefficients of Hydrophobic Organic Pollutants," *Environmental Science and Technology*, vol. 19, pp. 90-96.
29. Gupta, S. P. (1987). "QSAR Studies on Enzyme Inhibitors," *Chemical Reviews*, vol. 87, pp. 1183-1253.
30. Hannah, S. A., Austern, B. M., Erlap, A. E. and Dobbs, R. A. (1988). "Communication: Removal of Organic Pollutants By Trickling Filter and Activated Sludge," *Journal of the Water Pollution Control Federation*, vol. 60, no. 7, pp. 1281-1283.
31. Hannah, S. A., Austern, B. M., Erlap, A. E. and Wise, R. H. (1986). "Comparative Removal of Toxic Pollutants by Six Wastewater Treatment Processes," *Journal of the Water Pollution Control Federation*, vol. 58, no. 1, pp. 27-34.
32. Hassett, J. P. and Anderson, M. A. (1982). "Effects of Dissolved Organic Matter on Adsorption of Hydrophobic Organic Compounds by River and Sewage-Borne Particles," *Water Research*, vol. 16, pp. 681-686.
33. Herbes, S. E. (1977). "Partitioning of Polycyclic Aromatic Hydrocarbons between Dissolved and Particulate Phases in Natural Waters," *Water Research*, vol. 11, pp. 493-496.

34. Ho, C. C. and Tan, Y. K. (1983). "Centrifugal Fractionation Studies on the Particulates of Palm Oil Mill Effluent," *Water Research*, vol. 17, no. 6, pp. 613-618.
35. Hoepker, E. C. and Schroeder, E. D. (1979). "The Effect of Loading Rate on Batch-Activated Sludge Effluent Quality," *Journal of the Water Pollution Control Federation*, vol. 51, no. 2, pp. 264-272.
36. Howard, P. H., Boethling, R. S., Stiteler, W. M., Meylan, W. M., Hueber, A. E., Beauman, J. A. and Larosche, M. E. (1992). "Predictive Model for Aerobic Biodegradability Developed From a File of Evaluated Biodegradation Data," *Environmental Toxicology and Chemistry*, vol. 11, pp. 593-603.
37. Irvine, R. L. and Busch, A. W. (1979). "Sequencing Batch Biological Reactors - An Overview," *Journal of the Water Pollution Control Federation*, vol. 51, pp. 2.
38. Irvine, R. L., Miller, G. and Bhamrah, A. S. (1979). "Sequencing Batch Treatment of Wastewater in Rural Areas," *Journal of the Water Pollution Control Federation*, vol. 51, no. 2, pp. 235-243.
39. Jacobsen, B. N., Nyholm, N., Pedersen, B. M., Poulsen, O. and Ostefltdt, P. (1993). "Removal of Organic Micropollutants In Laboratory Activated Sludge Reactors Under Various Operating Conditions: Sorption," *Water Research*, vol. 27, no. 10, pp. 1505.
40. Jolliffe, I. T. (1986). Principal Component Analysis. Springer-Verlag Inc., New York.
41. Jonsson, J., Eriksson, L., Sjostrom, M., Wold, S. and Tosato, M. (1989). "A Strategy for Ranking Environmentally Occurring Chemicals," *Chemometrics and Intelligent Laboratory Systems*, vol. 5, pp. 169-186.
42. Jorgensen, K. P. (1984). "Determination of the Enzyme Activity of Activated Sludge by Methylene Blue Reduction," *Journal of the Water Pollution Control Federation*, vol. 56, pp.1-5.
43. Karickhoff, S. W. (1985). "Sorption Dynamics of Hydrophobic Pollutants in Sediment Suspensions," *Environmental Toxicology and Chemistry*, vol. 4, pp. 469-479.
44. Karr, P. R. and Keinath, T. M. (1984). "Influence of Particle Size on Sludge Dewaterability," *Journal of the Water Pollution Control Federation*, vol. 50, pp. 1911-1930.
45. Kier, B. L. and Hall, L. H. (1986) Molecular Connectivity in Structure-Activity Analysis. Research Studies Press Ltd., Hertfordshire, England.

46. Kirschner, G. L. and Kowalski, B. R. (1979) Drug Design, Ariens, E. J. (Ed.) Medicinal Chemistry, Vol. 8, 73, Academic Press, New York.
47. Knocke, W. R. (1992). "Comment on Density of Activated Sludge Solids," Water Research, vol. 26, no. 11, pp. 1559-1562.
48. Kumar, S., Dhanaraj, P. S., Bhatnagar, P. (1989). "Bioconcentration and Effects of Dieldrin, Dimethoate, and Permethrin on *Sacchromyces cerivisiae*," Bulletin of Environmental Contamination and Toxicology, vol. 43, pp. 246-253.
49. Levine A. D., Tchobanoglous, G. and Asano, T. (1991). "Size Distributions of Particulate Contaminants in Wastewater and their Impact on Treatability," Water Research, vol. 25, pp. 911-922.
50. Levine, A. D., Tchobanoglous, G. and Asano, T. (1985). "Characterization of the Size Distribution of Contaminants in Wastewater: Treatment and Reuse Implications," Journal of Water Pollution Control Federation, vol. 57, pp. 805-816.
51. Levine, A. D., Tchobanoglous, G. and Asano. (1991). "Particulate Contaminants in Wastewater: A Comparison of Measurement Techniques and Reported Particle Size Distributions," Fluid/Particle Separation Journal, vol. 4, pp. 2.
52. Lewandowski, G. A. and Baltziz, B. C. (1992). "Analysis of Sequencing Batch Reactors in Large Scale Denitrifying Applications," Chemical Engineering Science, vol. 47, no. 9-11, pp. 2389-2394.
53. Lewi, P. J. (1976). Drug Design, Ariens, E. J. (Ed.) Medicinal Chemistry, 7, 209, Academic Press, New York.
54. Lewi, P. J. (1980). Drug Design, Ariens, E. J. (Ed.) Medicinal Chemistry, 10, 308, Academic Press, New York.
55. Lindqvist, R. and Enfield, C. G. (1992). "Biosorption of Dichlorodiphenyltrichloroethane and Hexachlorobenzene in Groundwater and Its Implications for Facilitated Transport," Applied and Environmental Microbiology, vol. 58, pp. 2211-2218.
56. Mager P. J. (1980). Drug Design, Ariens, E. J. (Ed.) Medicinal Chemistry, 9, 187, Academic Press, New York.
57. Mager P. J. (1980). Drug Design, Ariens, E. J. (Ed.) Medicinal Chemistry, 10, 343, Academic Press, New York, New York.

58. Mani, S. V., Connell, D. W. and Braddock, R. D. (1991). "Structure Activity Relationships for the Prediction of Biodegradability of Environmental Pollutants," *Critical Reviews in Environmental Control*, vol. 21, no. 3/4, pp. 217-236.
59. Manley, B. F. J. (1986). Multivariate Statistical Methods: A Primer. Chapman and Hall, New York, New York.
60. McKinley, J. P. and Jenne, A. (1991). "Experimental Investigation and Review of the 'Solids Concentration' Effect in Adsorption Studies," *Environmental Science and Technology*, vol. 25, pp. 2082-2087.
61. Meylan, W. and Howard, P. H. (1992). "Molecular Topology/Fragment Contribution Method for Predicting Soil Sorption Coefficients," *Environmental Science and Technology*, vol. 26, no. 8, pp. 1560-1567.
62. Michaels, G. B. and Lewis, D. L. (1985). "Sorption and Toxicity of Azo and Triphenylmethane Dyes to Aquatic Microbial Populations," *Environmental Toxicology and Chemistry*, vol. 4, pp. 45-50.
63. Moore, A. S., Pope, J. D., Barnett, J. T. and Suarez, L. A. (1989). "Structure Activity Relationships and Estimation Techniques for Biodegradation of Xenobiotics," EPA/600/3-89/080. Environmental Research Laboratory, USEPA, Athens, GA.
64. Moretti, C. J. and Neufeld, R. D. (1989). "PAH Partitioning Mechanisms with Activated Sludge," *Water Research*, vol. 23, pp. 93-102.
65. Mukherjee, S. R. (1992). "Chemical Solubilization of Particulate Organics as a Pretreatment Approach," M. S. Thesis, Dept. of Civil and Construction Eng., Iowa State University, Ames, IA.
66. Mukherjee, S. R. and Levine, A. D. (1992). "Chemical Solubilization of Particulate Organics as a Pretreatment Approach," *Water Science and Technology*, vol. 5, pp. 2289-2292.
67. Niemi, G. J., Basak, S. C. and Veith, G. D. (1992). "Prediction of Octanol/Water Partition Coefficient (K_{ow}) with Algorithmically Derived Variables," *Environmental Toxicology and Chemistry*, vol. 11, pp. 893-900.
68. Nirmalakhandan, N. N. and Speece, R. E. (1988). "Prediction of Aqueous Solubility of Organic Chemicals Based on Molecular Structure," *Environmental Science and Technology*, vol. 22, no. 3, pp. 328-338.
69. Nirmalakhandan, N. N. and Speece, R. E. (1989). "Prediction of Aqueous Solubility of Organic Chemicals Based on Molecular Structure. 2. Application to PNAs, PCBs, PCDDs, etc," *Environmental Science and Technology*, vol. 23, pp. 708-713.

70. Nirmalakhandan, N. N. and Speece, R. E. (1988). "QSAR Model for Predicting Henry's Constant," *Environmental Science and Technology*, vol. 22, no. 11 pp. 1349-1357.
71. Patterson, J. W. and Kodukala, P. S. (1981). "Biodegradation of Hazardous Organic Pollutants," *Chemical Engineering Progress*, vol. 77, pp. 48-54.
72. Petrasek, A. C., Kugelman, J. I., et al. (1983). "Fate of Toxic Organic Compounds in Wastewater Treatment Plants," *Journal of Water Pollution Control Federation*, vol. 55, pp. 1296-1286.
73. Pignatello, J. A. (1990). "Slowly Reversible Sorption of Aliphatic Halocarbons in Soils. I. Formation of Residual Fractions," *Environmental Toxicology and Chemistry*, vol. 9, pp. 1107-1115.
74. Pignatello, J. A. (1990). "Slowly Reversible Sorption of Aliphatic Halocarbons in Soils. II. Mechanistic Aspects," *Environmental Toxicology and Chemistry*, vol. 9, pp. 1115-1126.
75. Pujol, R. and Canler, J. P. (1992). "Biosorption and Dynamics of Bacterial Populations in Activated Sludge," *Water Research*, vol. 26, no. 2, pp. 209-212.
76. Randic, M. (1975). "On Characterization of Molecular Branching," *Journal of the American Chemical Society*, vol. 97, no. 23, pp. 6609-6615
77. Reddy, K. N. and Locke, M. A. (1994). "Relationships Between Molecular Properties and Log P and Soil Sorption (K_{oc}) of Substituted Phenylrears: QSAR Models," *Chemosphere*, vol. 28, no. 11, pp. 1929-1941.
78. Rogers, H. R., Campbell, J. A., Crathorne, B. and Dobbs, A. J. (1989). "The Occurrence of Chlorobenzenes and Permethrins in Twelve U.K. Sewage Sludges," *Water Research*, vol. 23, no. 7, pp. 913-922.
79. Sabljic, A. (1987). "On the Prediction of Soil Sorption Coefficients of Organic Pollutants from Molecular Structure: Application of Molecular Topology Model," *Environmental Science and Technology*, vol. 21, pp. 358-366.
80. Sabljic, A. and Piver, W. T. (1992). "Quantitative Modeling of Environmental Fate and Impact of Commercial Chemicals," *Environmental Toxicology and Chemistry*, vol. 11, pp. 961-972.
81. Sabljic, A., Gusten, H., Verhaar, H. and Hermens, J. (1995). "QSAR Modelling of Soil Sorption. Improvements and Systematics of log K_{oc} vs. Log K_{ow} Correlations," *Chemosphere*, vol. 31, no. 11/12, pp. 4489-4514.

82. Sabljic, A. (1989). "Quantitative Modeling of Soil Sorption for Xenobiotic Chemicals," *Environmental Health Perspectives*, vol. 83, pp. 179-190.
83. Sabljic, A. and Horvatic, D. (1993). "A Computer Program for Calculating Molecular Connectivity Indexes on Microcomputers," *Journal of Chemical Information and Computer Science*, vol. 33, pp. 292-295.
84. Sawyer C.N., McCarty, P. L. and Parkin, G. F. (1994). Chemistry for Environmental Engineering. 4th edition, McGraw Hill Inc., New York, NY.
85. Scharp, S. M., Vries, P. J., Opperhuizen, A. (1994). "Experimental Problems in Determining Sorption Coefficients of Organic Chemicals; An Example for Chlorobenzenes," *Chemosphere*, vol. 28, no. 5, pp. 931-945.
86. Selvakumar, A. (1988). "Adsorption of Organic Compounds by Microbial Biomass," D. Eng. Sc. Thesis, New Jersey Institute of Technology, Newark, NJ.
87. Servos, M. R. and Muir, C. G. (1989). "Notes: Effect of Suspended Sediment Concentration on the Sediment to Water Partition Coefficient for 1,3,6,8-Tetrachlorodibenzo-p-dioxin," *Environmental Science and Technology*, vol. 23, pp. 1302-1306.
88. Shimizu, Y., Takei, N. and Terashima, Y. (1992). "Sorption of Organic Pollutants from Vapor Phase: The Effect of Natural Solids Characteristics and Moisture Content," *Proceedings of Water Quality International, Water Science and Technology*, vol. 26, pp. 79-87.
89. Speece, R.R. E. (1990). "Comment on : Prediction of Aqueous Solubility of Organic Chemicals Based on Molecular Structure. 2. Application to PNAs, PCBs, PCDDs, etc," *Environmental Science and Technology*, vol. 24, pp. 6.
90. Sugiura, K., Sato, S. and Goto, M. (1975). "Mechanistic Aspects of Sorption of Toxic Organic Pollutants to Bacteria," *Chemosphere*, vol. 4, pp. 189-192.
91. Tang, N. H., Blum, D. J., Nirmalakhandan, N. and Speece, R. E. (1992). "QSAR Parameters for Toxicity of Organic Chemicals to *Nitrobacter*," *Journal of Environmental Engineering*, vol. 118, pp. 17-37.
92. Tchobanoglous, G. and Schroeder, E. D. (1985). Water Quality. Addison-Wesley Publishing Company, California.
93. Topliss, J. G. (1983). Quantitative Structure-Activity Relationships of Drugs. Academic Press, New York, New York.

94. Tosato, M., Marchini, S., Passerini, L., Pino, A., Eriksson, L., Jonsson, J., Hellberg, S., Lindgren, F., Skagerberg, B., Sjostrom, M. and Wold, S. (1990). "QSARs Based on Statistical Design and Their Use for Identifying Chemicals for Further Biological Testing," *Environmental Toxicology and Chemistry*, vol. 9, pp. 265-277.
95. Tsezos, M. and Bell, J. P. (1989). "Comparison of the Biosorption and Desorption of Hazardous Organic Pollutants by Live and Dead Biomass," *Water Research*, vol. 23, pp. 561-568.
96. Tsezos, M. and Bell, J. P. (1991). "A Mechanistic Study on the Fate of Malathion Following Interaction With Microbial Biomass," *Water Research*, vol. 25, pp. 1039-1046.
97. Tsezos, M. and Bell, J. P. (1988). "Significance of Biosorption of the Hazardous Organics Removal of a biological Reactor," *Water Research*, vol. 22, pp. 391-394.
98. Tsezos, M. and Seto, W. (1986). "The Adsorption of Chloroethanes by Microbial Biomass," *Water Research*, vol. 20, no. 7, pp. 851-858.
99. Tsezos, M. and Wang, X. (1991). "Study on the Kinetics of Hazardous Pollutant Adsorption and Desorption by Biomass: Mechanistic Considerations," *Journal of Chemical Technology and Biotechnology*, vol. 50, pp. 507-521.
100. U.S. EPA. (1982). "Fate of Priority Toxic Pollutants in Publicly-Owned Treatment Works," EPA-440/1-82-303, Vol. I and II. Office of Water Regulation and Standards, US Environmental Protection Agency, Washington, D.C., Sept.
101. U.S. EPA. (1982). "Test Methods for Evaluating Solid Wastes. Volume: 1, 2, 3 and 4, USEPA SW - 846," Office of Solid Waste and Emergency Response. United States Environmental Protection Agency, Washington, D.C., Sept.
102. Vaishnav, D. D., Boethling, R. S. and Babeu, L. (1987). "Quantitative Structure - Biodegradability Relationships for Alcohols, Ketones and Alicyclic Compounds," *Chemosphere*, vol. 16, no. 4, pp. 695-703.
103. Voice, T. C., and Weber, W. J. (1985). "Sorbent Concentration Effects in Liquid/Solid Partitioning," *Environmental Science and Technology*, vol. 19, pp. 789-796.
104. Wang, K., Rott, B. and Korte, F. (1982). "Uptake and Bioaccumulation of Three PCBs by *Chlorella fusca*," *Chemosphere*, vol. 11, pp. 525-530.
105. Wang, L., Govind, R. and Dobbs, R. A. (1993). "Sorption of Toxic Organic Compounds on Wastewater Solids: Mechanism and Modeling," *Environmental Science and Technology*, vol. 27, pp. 152-158.

106. Wang, X. (1993). "The Effects of Biosorption on the Biodegradation of Di-n-Butyl Phthalate," Ph. D Dissertation, Dept. of Environmental Eng., Clemson University, Clemson, SC.
107. Wang, X. and Grady, C. P. L. Jr. (1993). "The Effects of Biosorption on the Biodegradation of Di-n-Butyl Phthalate," Proceedings of the 66th Annual Conference of Water Environment Federation, Anaheim, California, pp. 61-72.
108. Wanner, J. and Novak, L. (1990). "The Influence of a Particulate Substrate on Filamentous Bulking and Phosphorous Removal in Activated Sludge Systems" Water Research, vol. 24, pp. 553-581.
109. Wilczak, A. (1988). "Sorption of Heavy Metal Cations on Activated Carbon," Ph. D Dissertation, Dept. of Environmental Eng., Clemson University, Clemson, SC.
110. Wilmanski, K. and van Breemen A. N. (1990). "Competitive Adsorption of Trichloroethylene and Humic Substances from Groundwater on Activated Carbon," Water Research, vol. 24, no. 6, pp. 773-779.
111. Wold, S. (1976). *Experientia Supplementum*, Lecture Proceedings, International Protoplast Symposium, vol. 23, pp. 87-94.